



This is to certify that the

thesis entitled

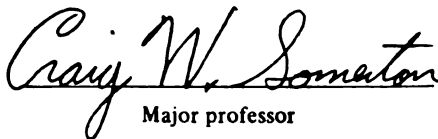
ANALYSIS OF THE EFFECT OF AXIAL CONDUCTION ON THE
PERFORMANCE OF A COUNTERFLOW HEAT EXCHANGER

presented by

KEVIN J. DOWDING

has been accepted towards fulfillment
of the requirements for

MASTERS degree in MECHANICAL ENGINEERING


Major professor

Date 3/31/93

LIBRARY
Michigan State
University

PLACE IN RETURN BOX to remove this checkout from your record.
 TO AVOID FINES return on or before date due.

DATE DUE	DATE DUE	DATE DUE
SEP 25 1992	_____	_____
_____	_____	_____
_____	_____	_____
_____	_____	_____
_____	_____	_____
_____	_____	_____
_____	_____	_____

MSU Is An Affirmative Action/Equal Opportunity Institution

c:\circ\datedue.pm3-p.1

**ANALYSIS OF THE EFFECT OF AXIAL
CONDUCTION ON THE PERFORMANCE OF A
COUNTERFLOW HEAT EXCHANGER**

By

Kevin J Dowding

A THESIS

**Submitted to
Michigan State University
in partial fulfillment of the requirements
for the degree of**

MASTER OF SCIENCE

Department of Mechanical Engineering

1993

CO

An inv
within the wa
exact solution
while includi
within the wa

The eff
exchanger wa
effect. The re
to 45% under
small ratio of
capacity ratio
exchanger de
presence of a
parameter cal
duction was n
conduction, w

ABSTRACT

ANALYSIS OF THE EFFECT OF AXIAL CONDUCTION ON THE PERFORMANCE OF A COUNTERFLOW HEAT EXCHANGER

By

Kevin J Dowding

An investigation into the effect of axial (longitudinal) conduction within the wall of a counterflow heat exchanger has been completed. The exact solution was obtained for the temperature fields of the wall and fluids while including the possibility of heat flow in the direction of the fluid flow within the wall of the heat exchanger, so-called axial conduction.

The effect of axial conduction on the performance of the heat exchanger was quantified by comparison to a solution that neglects this effect. The results showed that the effectiveness could be over-estimated up to 45% under certain conditions. These conditions were a small Biot number, small ratio of the heat exchanger wall length to thickness, and large flow heat capacity ratios. The severity of the effect on the performance of the heat exchanger depended on the magnitudes of these conditions. Predicting the presence of axial conduction was shown to depend on a dimensionless parameter called the Mondt number. For magnitudes less than .01, axial conduction was negligible; while magnitudes greater displayed a nonzero axial conduction, which grew larger as the Mondt number increased.

to my parents, Roger and Mary Ann Dowding

I am
his guidance
gained in t
sions conce

The
Beck and S
tive. Additi
was comple

The I
continued g
erton and F

Final
my education
appreciated
could have n
understandin

ACKNOWLEDGMENTS

I am grateful for the opportunity to work with Professor Somerton; for his guidance and encouragement conducting this research and the experience gained in the undergraduate teaching laboratory. Also, his open, frank discussions concerning professorial life were enlightening and appreciated.

The commitment of the remaining committee members, Professors Beck and Schock, is also recognized. Their comments and input were instructive. Additional thanks to Professor Beck for his patience while this research was completed.

The Department of Mechanical Engineering is acknowledged for the continued generous support. Special thanks are extended to Professors Somerton and Foss for the involvement in their teaching laboratories.

Finally, I would like to thank my family, who have endured through my education and given love and encouragement. My Mother and Dad are appreciated for their endless unassuming support, without which this point could have never been reached. While I am eternally grateful for the patience, understanding, and support of my wife Tracey.

List of Tables

List of Figures

Nomenclature

1 Introduction

1.0 History

1.1 Introduction

2 Description

2.0 Introduction

2.1 Introduction

TABLE OF CONTENTS

List of Tables *ix*

List of Figures *x*

Nomenclature *xiv*

Chapter

1 Introduction 1

1.0 Heat Exchanger Analysis.....4

1.0.1 Basic Analysis.....4

1.0.2 Dimensionless Analysis.....6

1.1 Literature Review9

2 Describing Equations and Boundary Conditions 11

2.0 Dimensional Equations..... 11

2.0.1 Wall Conduction Equation.....11

2.0.2 Fluid Energy Balance Equations.....12

2.1 Dimensionless Equations..... 14

2.1.1 Nondimensionalization of Lengths.....14

2.2

2.3

3 Meth

3.0

3.1

3.2

3.3

3.4

2.1.2 Nondimensionalization of Temperature.....	15
2.2 Dimensionless Parameters	16
2.3 Heat Exchanger Performance Analysis	18
3 Method of Solution.....	20
3.0 General Method	20
3.1 General Solution of the Wall Conduction Equation	22
3.1.1 General Solution for Nonhomogeneous Boundary Condition at $x = L$	23
3.1.2 General Solution for Nonhomogeneous Boundary Condition on y	27
3.2 Solution of the Fluid Energy Balance Equations.....	28
3.2.1 Hot Fluid Formulation	28
3.2.2 Hot Fluid Solution	29
3.2.3 Cold Fluid Solution.....	31
3.3 Application of Nonhomogeneous Boundary Conditions	33
3.3.1 Application of Boundary Condition at $x = L$	34
3.3.2 Application of Boundary Condition at $y = 0$	36
3.3.3 Application of Boundary Condition at $y = \delta$	38
3.3.4 Summary of Applying Orthogonality	40
3.4 Computer Program AXCOND.....	44

4 Results

4.0

4.1

4.2

4

4

4

4 Results and Discussion.....	47
4.0 Identification of Input Parameters	47
4.0.1 Presentation of Results.....	50
4.1 Influence of Axial Conduction at a Constant NTU	52
4.1.1 Influence of the Wall Aspect Ratio	52
4.1.2 Influence of the Wall End Biot Numbers	63
4.1.3 Influence of the Fluid Biot Numbers	69
4.1.4 Summary of Investigation with a Constant NTU	74
4.2 Characterization of Axial Conduction as a Function of NTU	77
4.2.1 Ineffectiveness- NTU Results	83
4.2.1.1 Heat Capacity Ratio of 1	83
4.2.1.2 Heat Capacity Ratio of .75	85
4.2.1.3 Heat Capacity Ratio of .50	87
4.2.1.4 Heat Capacity Ratio of .25	89
4.2.1.5 Discussion of Results	91
4.3 Predicting the Presence of Axial Conduction with the Mondt number	96
4.4 Application of Results	102
4.5 Comparison to Published Results	108

5 Conclu

List of Re

Appendic

App

App

App

App

App

App

App

App

App

App

5 Conclusions and Recommendations for Future Work ..	112
<i>List of References</i>	<i>114</i>
<i>Appendices</i>	<i>116</i>
Appendix A.1: General Solution of the Wall Conduction Equation	116
Appendix B.1: Solution of Hot Fluid Energy Balance	125
Appendix B.2: Solution of Cold Fluid Energy Balance	130
Appendix B.3: Summary of Energy Balance Solutions	136
Appendix C.1: Application of Nonhomogeneous Boundary Conditions	138
Appendix C.2: Summary of Applying Nonhomogeneous Boundary Conditions	156
Appendix D.1: Solution for Constants	157
Appendix E.1: Derivation of Effectiveness- <i>NTU</i> Relationship for a Counterflow Heat Exchanger Neglecting Axial Conduction	163
Appendix E.2: Solution of Fluid Temperatures for a Counterflow Heat Exchanger Neglecting Axial Conduction	167
Appendix F: Listing of Computer Program AXCOND	173

TABLE 4.1

TABLE 4.2

TABLE 4.3

TABLE 4.4

TABLE 4.5

TABLE 4.6

TABLE 4.7

LIST OF TABLES

TABLE 4.1: Input variables and dependencies for determining heat exchanger performance	49
TABLE 4.2: Relationship between the slope of the hot and cold fluids temperature profile and heat capacity ratio	55
TABLE 4.3: Ineffectiveness as a function of the fluid Biot numbers from Figure 4.14	69
TABLE 4.4: Classification of effects seen as the NTU varied	95
TABLE 4.5: Relationship among the Mondt number, wall aspect ratio, <i>NTU</i> , and fluid Biot numbers	96
TABLE 4.6: Magnitude of dividing Mondt number as a function of the heat capacity ratio	99
TABLE 4.7: Operating conditions for axial conduction to exist	105

FIGURE

FIGURE

FIGURE

FIGURE

FIGURE

FIGURE 3

FIGURE 3

FIGURE 4

FIGURE 4

FIGURE 4.

FIGURE 4.4

FIGURE 4.5

FIGURE 4.6

LIST OF FIGURES

FIGURE 1.1: Possible heat flow paths for wall of a heat exchanger	2
FIGURE 1.2: Generic heat exchanger, nonspecific design exchanging energy between two fluids	4
FIGURE 1.3: Thermal circuit for a heat exchanger wall neglecting any fouling	5
FIGURE 2.1: Heat exchanger geometry studied	11
FIGURE 2.2: Thermal circuit for heat exchanger wall	19
FIGURE 3.1: Flowchart of solution procedure	21
FIGURE 3.2: Flowchart of FORTRAN program AXCOND used to compute solution	46
FIGURE 4.1: Ineffectiveness as a function of the wall aspect ratio for $NTU = 7$ and $C_R = 1$	59
FIGURE 4.2: Ineffectiveness as a function of the wall aspect ratio for $NTU = 7$ and $C_R = .75$	59
FIGURE 4.3: Ineffectiveness as a function of the wall aspect ratio for $NTU = 7$ and $C_R = .50$	60
FIGURE 4.4: Ineffectiveness as a function of the wall aspect ratio for $NTU = 7$ and $C_R = .25$	60
FIGURE 4.5: Median dimensionless wall temperature as a function of dimensionless position and Biot number for $NTU = 7$, $L^* = 100$, and $C_R = 1$	61
FIGURE 4.6: Ineffectiveness as a function of the wall aspect ratio and heat capacity ratio for $NTU = 7$ and all Biot numbers equal .001	61

FIGURE 4.

FIGURE 4.

FIGURE 4.

FIGURE 4.

FIGURE 4.

FIGURE 4.

FIGURE 4.

FIGURE 4.

FIGURE 4.

FIGURE 4.

FIGURE 4.

FIGURE 4.

FIGURE 4.

FIGURE 4.7: Median dimensionless wall temperature as a function of dimensionless position and heat capacity ratio for $NTU = 7$, $L^* = 100$, and all Biot numbers .001	62
FIGURE 4.8: Median dimensionless wall and fluid temperature as a function of dimensionless position and heat capacity ratio for $NTU = 7$, $L^* = 100$, and all Biot numbers equal .001	62
FIGURE 4.9: Ineffectiveness as a function of the end Biot numbers for $NTU = 7$, $L^* = 100$, and $C_R = 1$	66
FIGURE 4.10: Ineffectiveness as a function of the end Biot numbers for $NTU = 7$, $L^* = 100$, and $C_R = .75$	67
FIGURE 4.11: Ineffectiveness as a function of the end Biot numbers for $NTU = 7$, $L^* = 100$, and $C_R = .50$	67
FIGURE 4.12: Ineffectiveness as a function of the end Biot numbers for $NTU = 7$, $L^* = 100$, and $C_R = .25$	68
FIGURE 4.13: Ineffectiveness as a function of the end Biot numbers and heat capacity ratio for $NTU = 7$, $L^* = 100$, and fluid Biot numbers equal .001	68
FIGURE 4.14: Ineffectiveness as a function of the fluid Biot numbers for $NTU = 7$, $L^* = 100$, and $C_R = 1$	72
FIGURE 4.15: Ineffectiveness as a function of the fluid Biot numbers for $NTU = 7$, $L^* = 100$, and $C_R = .75$	72
FIGURE 4.16: Ineffectiveness as a function of the fluid Biot numbers for $NTU = 7$, $L^* = 100$, and $C_R = .50$	73
FIGURE 4.17: Ineffectiveness as a function of the fluid Biot numbers for $NTU = 7$, $L^* = 100$, and $C_R = .25$	73
FIGURE 4.18: Ineffectiveness as a function of the hot fluid Biot number and heat capacity ratio for $NTU = 7$, $L^* = 100$, and a cold fluid Biot number equal .001	74
FIGURE 4.19: Ineffectiveness as a function of the NTU , wall aspect ratio, and maximum fluid Biot number for $Bi_{min} = 0.0001$ and $C_R = 1$	78

FIGURE

FIGURE

FIGURE

FIGURE

FIGURE

FIGURE

FIGURE

FIGURE

FIGURE 4

FIGURE 4

FIGURE 4

FIGURE 4

FIGURE 4.3

FIGURE 4.3

FIGURE 4.20: Ineffectiveness as a function of the NTU and heat capacity ratio for $Bi_{min} = 0.0001$, $Bi_{max} = 0.001$, and $L^* = 100$	81
FIGURE 4.21: Ineffectiveness as a function of the NTU and wall aspect ratio for $Bi_{min} = 0.0001$ and $C_R = 1$	83
FIGURE 4.22: Ineffectiveness as a function of the NTU and wall aspect ratio for $Bi_{min} = 0.001$ and $C_R = 1$	83
FIGURE 4.23: Ineffectiveness as a function of the NTU and wall aspect ratio for $Bi_{min} = 0.01$ and $C_R = 1$	84
FIGURE 4.24: Ineffectiveness as a function of the NTU and wall aspect ratio for $Bi_{min} = 0.1$ and $C_R = 1$	84
FIGURE 4.25: Ineffectiveness as a function of the NTU and wall aspect ratio for $Bi_{min} = 0.0001$ and $C_R = .75$	85
FIGURE 4.26: Ineffectiveness as a function of the NTU and wall aspect ratio for $Bi_{min} = 0.001$ and $C_R = .75$	85
FIGURE 4.27: Ineffectiveness as a function of the NTU and wall aspect ratio for $Bi_{min} = 0.01$ and $C_R = .75$	86
FIGURE 4.28: Ineffectiveness as a function of the NTU and wall aspect ratio for $Bi_{min} = 0.1$ and $C_R = .75$	86
FIGURE 4.29: Ineffectiveness as a function of the NTU and wall aspect ratio for $Bi_{min} = 0.0001$ and $C_R = .50$	87
FIGURE 4.30: Ineffectiveness as a function of the NTU and wall aspect ratio for $Bi_{min} = 0.001$ and $C_R = .50$	87
FIGURE 4.31: Ineffectiveness as a function of the NTU and wall aspect ratio for $Bi_{min} = 0.01$ and $C_R = .50$	88
FIGURE 4.32: Ineffectiveness as a function of the NTU and wall aspect ratio for $Bi_{min} = 0.1$ and $C_R = .50$	88
FIGURE 4.33: Ineffectiveness as a function of the NTU and wall aspect ratio for $Bi_{min} = 0.0001$ and $C_R = .25$	89

FIGUR

FIGUR

FIGUR

FIGURE

FIGURE

FIGURE

FIGURE 4

FIGURE 4.

FIGURE 4.4

FIGURE 4.34: Ineffectiveness as a function of the NTU and wall aspect ratio for $Bi_{min} = 0.001$ and $C_R = .25$	89
FIGURE 4.35: Ineffectiveness as a function of the NTU and wall aspect ratio for $Bi_{min} = 0.01$ and $C_R = .25$	90
FIGURE 4.36: Ineffectiveness as a function of the NTU and wall aspect ratio for $Bi_{min} = 0.1$ and $C_R = .25$	90
FIGURE 4.37: Predicted region affected by axial conduction in terms of the NTU , Mondt number, wall aspect ratio and minimum fluid Biot number	98
FIGURE 4.38: Magnitude of pertinent heat exchanger operating conditions as a function of wall thermal conductivity, which is needed for axial conduction to exist	104
FIGURE 4.39: Comparison of present results to past result of Pan, Welch, and Head [15] and Rohsenow [17]. Ineffectiveness as a function of the NTU and wall aspect ratio for $Bi_{min} = 0.0001$ and $C_R = 1$.	110
FIGURE 4.40: Comparison of present results to past result of Pan, Welch, and Head [15] and Rohsenow [17]. Ineffectiveness as a function of the NTU and wall aspect ratio for $Bi_{min} = 0.001$ and $C_R = 1$	110
FIGURE 4.41: Comparison of present results to past result of Pan, Welch, and Head [15] and Rohsenow [17]. Ineffectiveness as a function of the NTU and wall aspect ratio for $Bi_{min} = 0.01$ and $C_R = 1$	111
FIGURE 4.42: Comparison of present results to past result of Pan, Welch, and Head [15] and Rohsenow [17]. Ineffectiveness as a function of the NTU and wall aspect ratio for $Bi_{min} = 0.1$ and $C_R = 1$	111

Arabic

A

A_n, B_n, C_n

Bi

C_p

C

H

h

h

K_w

L

L^{}*

m

N

NTU

P

q

q^{}*

R

t

T

U

w

NOMENCLATURE

Arabic

A	area [m^2]
A_n, B_n, C_n	constants
Bi	Biot number
C_p	specific heat [$\frac{J}{kgK}$]
C	heat capacity [W/K]
\dot{H}	enthalpy [J]
\hat{h}	specific enthalpy [$\frac{J}{kg}$]
h	convective heat transfer coefficient [$\frac{W}{m^2K}$]
K_w	thermal conductivity [$\frac{W}{mK}$]
L	length of heat exchanger [m]
L^*	wall aspect ratio ($L^* = \frac{L}{\delta}$)
\dot{m}	mass flow rate [$\frac{kg}{sec}$]
N	number of terms in series solutions
NTU	number of transfer units
P	perimeter [m]
q	heat [W]
q''	heat flux [$\frac{W}{m^2}$]
R	thermal resistance [$\frac{K}{W}$]
t	time [sec]
T	temperature [C or K]
U	thermal conductance [$\frac{W}{m^2K}$]
w	heat exchanger wall width [m]

x, y

Greek

ϵ

δ

δ_{ij}

θ

Θ

μ, α

Subscri

C

H

in

L

min

max

o

out

R

w

Superscr

$+$

x, y Cartesian coordinates [m]

Greek

ε effectiveness
 δ wall thickness [m]
 δ_{ij} kronecker delta function
 θ scaled temperature [C or K]
 Θ dimensionless temperature
 μ, α eigenvalues

Subscripts

C cold fluid wall side
 H hot fluid wall side
 in inlet
 L $x = L$ or $x^+ = 1$ wall end
 min minimum
 max maximum
 o $x = 0$ wall end
 out outlet
 R ratio
 w wall

Superscripts

$+$ dimensionless variable

Heat
fluids. The
cessing, he
ognizable
exchanger
tion. There
characteris
form of a h
exchanger.
moving fluid
moving in t
site direction

Design
heat transfer
energy need
the heat exch
heat transfer
transfer yet m
obtained by e
transfer conve
an increase in
resulting in an
increase the co
There is a trade
ria is usually at
established.

Focusing c
has two fluid stre

Chapter 1

Introduction

Heat exchangers provide for the transfer of heat between two moving fluids. These devices are used in power generation, chemical and food processing, heating and air conditioning, and motor vehicles. It is the most recognizable heat transfer device and one of the most widely used. Heat exchangers are classified based on flow arrangement and type of construction. There are many types of heat exchanger designs, each type with its own characteristics that make it suitable for a particular application. The simplest form of a heat exchanger would be a double pipe (or concentric tube) heat exchanger. The construction of this type of heat exchanger consists of two moving fluids separated via a wall parallel to the fluid motion; with the fluids moving in the same direction for a parallel flow heat exchanger and in opposite directions in a counterflow heat exchanger.

Design of heat exchangers in general, requires consideration of the heat transfer occurring between the two fluids in addition to the mechanical energy needed to overcome the frictional forces to move the fluids through the heat exchanger. These two design criteria can be generally classified as heat transfer and pressure drop. It is typically desired to achieve large heat transfer yet maintain a small pressure drop. Large heat transfer rates can be obtained by either having a larger heat transfer area or having a larger heat transfer convection coefficient. Unfortunately, both of these conditions cause an increase in the pressure drop, since a larger area gives more frictional area resulting in an increase in the pressure drop and the larger flow rate to increase the convection coefficient would likewise increase the pressure drop. There is a trade-off in these two design criteria; a beneficial gain in one criteria is usually at the expense of the other criteria and a compromise must be established.

Focusing on the heat transfer, consider a simplistic heat exchanger that has two fluid streams separated by an infinitesimally thin wall. The analysis

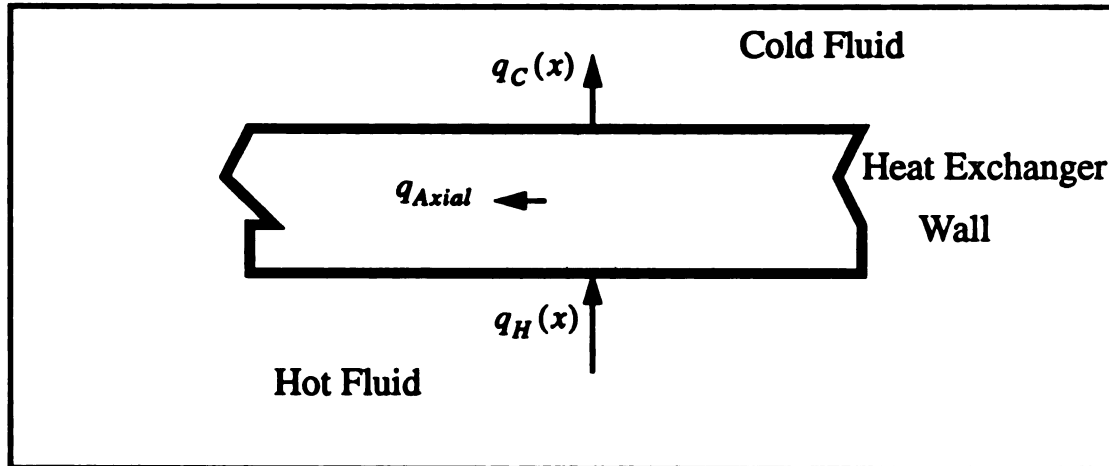


Figure 1.1. Possible heat flow paths for the wall of a heat exchanger

of this heat exchanger could be accomplished by considering the energy balances of the two fluids since the wall has negligible thickness. In reality, the wall will be required to have some thickness to perform its function of separating the two fluids. As the thickness of the wall becomes nonnegligible, some resistance to the flow of heat between the two fluids is added and now the wall must be considered in the analysis. In addition, an alternate path for the heat to flow is provided. Figure 1.1 shows the heat flow paths: q_H is the heat convected from the hot fluid to the wall, q_{Axial} is the heat conducted along the wall, and q_C is the heat conducted to the cold fluid from the wall. When the wall is very thin, it is unlikely that heat transferred to the wall from the fluid will flow parallel to the wall and the energy exchanged will balance locally ($q_H(x) = q_C(x)$). This may not be the case when the wall thickness is increased; some of the heat may flow along the wall. This effect is called axial (longitudinal) conduction, and when axial conduction is nonzero ($q_{Axial} \neq 0$) the fluid streams may have a local energy imbalance ($q_H(x) \neq q_C(x)$). The energy is conserved, however.

Axial conduction of heat is typically neglected in the analysis of the heat transfer in a heat exchanger. This assumption may be appropriate for most cases, but under certain circumstances the effect of axial conduction can become important. These circumstances depend on more than the wall thickness, which was used to introduce the effect. In general, axial conduction depends on the material and physical dimensions of the wall and the proper-

ties and flo
be the focu
quantified
ble identifi
heat excha

The
heat excha
tions and b
two, while
three. Chap
sponding d
in chapter f

ties and flow rate of the fluids. Assessing the effect of axial conduction will be the focus of this thesis. Specifically, the effect of axial conduction will be quantified and the conditions of the wall and fluids for which it is nonnegligible identified. Also, the adverse effect on the performance of a counterflow heat exchanger will be determined.

The remaining sections of this chapter will review the analysis of a heat exchanger and conclude with a literature review. The describing equations and boundary conditions for the problem will be addressed in chapter two, while the methods employed to solve the problem are shown in chapter three. Chapter four will present the results of the investigation with corresponding discussion. A summary and the resulting conclusions will be given in chapter five, in addition to recommendations for future work.

1

1

n

e

h

tr

(v

b

w

ci

an

As

ne

T_H

-

$T_{C,i}$

-

m_C

F

1.0 Heat Exchanger Analysis

1.0.1 Basic Analysis

Figure 1.2 shows a heat exchanger that transfers energy between two moving fluids through a wall; the geometry and construction of this heat exchanger may be considered arbitrary. A general thermal analysis of this heat exchanger will be performed. First, taking the heat exchanger as a control volume and applying an overall energy balance, assuming no interactions (work or heat) with the surroundings and steady state, results in an enthalpy balance (\dot{H})

$$\dot{H}_{in} = \dot{H}_{out} \quad (1.1)$$

which can be written in terms of the inlet and exiting conditions using specific enthalpy and mass flow rate as

$$\dot{m}_H \hat{h}_H|_{in} + \dot{m}_C \hat{h}_C|_{in} = \dot{m}_H \hat{h}_H|_{out} + \dot{m}_C \hat{h}_C|_{out} \quad (1.2)$$

and rearranged to group the fluids

$$\dot{m}_H (\hat{h}_H|_{in} - \hat{h}_H|_{out}) = \dot{m}_C (\hat{h}_C|_{out} - \hat{h}_C|_{in}) \quad (1.3)$$

Assuming the fluid behaves as an incompressible liquid or an ideal gas and a negligible pressure change, the change in enthalpy can be expressed as

$$d\hat{h} = C_p dT \quad (1.4)$$

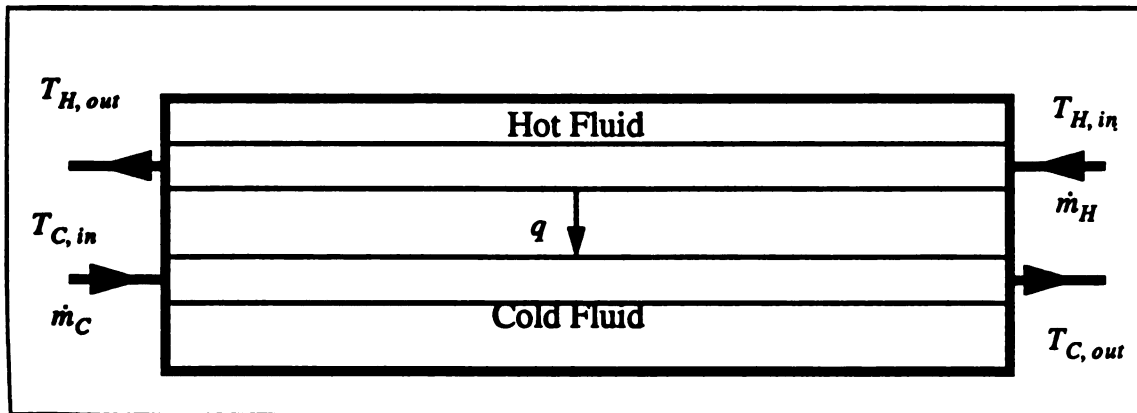


Figure 1.2. Generic heat exchanger, nonspecific design exchanging energy between the two fluids

which can be approximated by differences ($d\hat{h} = \hat{h}_2 - \hat{h}_1$). Using the approximate form of equation (1.4) in equation (1.3), the results for the overall energy balance

are

$$q = \dot{m}_H C_{p,H} (T_{H,in} - T_{H,out}) = \dot{m}_C C_{p,C} (T_{C,out} - T_{C,in}) \quad (1.5)$$

Introducing the heat capacity

$$C \equiv \dot{m} C_p \quad (1.6)$$

equation (1.5) can be rewritten as

$$q = C_H (T_{H,in} - T_{H,out}) = C_C (T_{C,out} - T_{C,in}) \quad (1.7)$$

In general, the heat transfer between the two fluid streams is a function of the following six parameters:

$$q = f\left(\underbrace{\dot{m}_H, \dot{m}_C, T_{H,in}, T_{C,in}}_{\text{given}}, \underbrace{T_{C,out}, T_{H,out}}_{\text{unknown}}\right) \quad (1.8)$$

where the first four are typically given design parameters and the last two are desired results. Thus, in order to obtain a solution more information is needed. The additional information will come from the heat transfer analysis of the wall separating the two fluids.

A circuit describing the thermal communication of the two fluids is shown in Figure 1.3. This circuit shows the resistance that impedes the heat flow, neglecting any fouling on the heat exchanger wall. The total resistance of the series circuit is the sum of the individual resistances

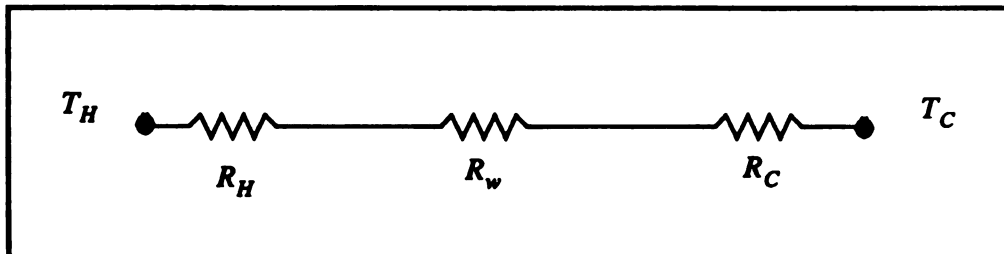


Figure 1.3. Thermal circuit for a heat exchanger wall neglecting any fouling

$$R_{tot} = R_H + R_w + R_C \quad (1.9)$$

Also, the overall conductance of the heat exchanger wall, that will give the total amount of heat transferred if the temperature difference is known, is

$$UA = \frac{1}{R_{tot}} \quad (1.10)$$

These terms are analogous to an electrical circuit, with the temperature difference as the voltage potential and the heat flow as the current. The heat transfer over a differential element of length dx is

$$dq = UP [T_H(x) - T_C(x)] dx \quad (1.11)$$

The heat transfer over the entire length of the heat exchanger is the sum of these differentials elements over the total length

$$q = \int_0^L dq = UP \int_0^L [T_H(x) - T_C(x)] dx \quad (1.12)$$

The product UP was assumed constant and thus could be taken out of the integral, but $(T_H - T_C)$ depends on x and cannot be removed from the integral. Because this integral is not known in general, we will define the mean temperature difference as

$$(\Delta T)_m = \frac{1}{L} \int_0^L [T_H(x) - T_C(x)] dx \quad (1.13)$$

Substituting equation (1.13) into equation (1.12), the total heat transfer can be written as

$$q = UA (\Delta T)_m \quad (1.14)$$

For a double pipe heat exchanger, equation (1.13) can be evaluated. The result is the log mean temperature difference. However, for geometries that are more complicated, evaluating equation (1.13) is difficult if not impossible. This suggests that another approach may be necessary to remain a general analysis.

1.0.2 Dimensionless Analysis

To introduce another approach, consider the parameters that the mean temperature difference is a function of

$$(\Delta T)_m = f(T_{H,in}, T_{C,in}, C_C, C_H, UA) \quad (1.15)$$

It depends on the inlet temperatures and heat capacities of the fluids and the wall conductance. The number of independent parameters can be reduced by considering a second function times the temperature difference at the inlet

$$(\Delta T)_m = g(C_C, C_H, UA) (T_{H,in} - T_{C,in}) \quad (1.16)$$

substituting equation (1.16) into equation (1.14) the functional dependence for the heat transfer is given by

$$q = UA g(C_C, C_H, UA) (T_{H,in} - T_{C,in}) \quad (1.17)$$

As typical in heat transfer, scaling will be introduced to provide dimensionless parameters. Define the maximum possible heat transfer as

$$q_{max} = C_{min} (T_{H,in} - T_{C,in}) \quad (1.18)$$

where $C_{min} = \min(C_H, C_C)$. Dividing equation (1.17) by equation (1.18)

$$\frac{q}{q_{max}} = \frac{UA}{C_{min}} g(C_C, C_H, UA) \quad (1.19)$$

and introducing another function that is in terms of the scaled independent variables gives

$$\frac{q}{q_{max}} = \frac{UA}{C_{min}} g'(C_R, \frac{UA}{C_{min}}) \quad (1.20)$$

where

$$C_R = \frac{C_{min}}{C_{max}} \quad (1.21)$$

Finally, noting that equation (1.20) can be written for a final function as

$$\frac{q}{q_{max}} = h(C_R, \frac{UA}{C_{min}}) \quad (1.22)$$

This demonstrates that the performance of a heat exchanger can be expressed in terms of three dimensionless variables. The first was given previously in equation (1.21) as the ratio of the heat capacities. The second is the effectiveness

$$\varepsilon = \frac{q}{q_{max}} = \frac{q}{C_{min} (T_{H,in} - T_{C,in})} \quad (1.23)$$

which is the
maximum po
last dimension

which is a rat
mum fluid's a

The pro
moderately si
analysis of the
sider a double
describing the
in Appendix K

for the case of

This is the usu
heat exchange
dimensionless
different heat e
performance o

The deri
ligible axial flo
tion is true for
thesis. Further
assuming axial

which is the ratio of the actual heat transfer given by equation (1.7) to the maximum possible heat transfer. The number of transfer units (NTU) is the last dimensionless parameter

$$NTU = \frac{UA}{C_{min}} \quad (1.24)$$

which is a ratio of the heat exchangers ability to transfer energy to the minimum fluid's ability to retain energy.

The previously mentioned dimensionless parameters, at least for the moderately simple heat exchanger geometry, can result during the analytical analysis of the heat transfer occurring in a heat exchanger. For example, consider a double pipe counterflow heat exchanger arrangement. The correlation describing the performance of this heat exchanger, whose derivation is shown in Appendix E, is

$$\varepsilon = \frac{1 - e^{-NTU(1-C_R)}}{1 - C_R e^{-NTU(1-C_R)}} \quad (1.25)$$

for the case of $C_R \neq 1$. If $C_R = 1$, equation (1.25) reduces to

$$\varepsilon = \frac{NTU}{1 + NTU} \quad (1.26)$$

This is the usual form used in evaluating or presenting the performance of a heat exchanger, as a function describing the relationship between the three dimensionless parameters. These functional relations are tabulated for many different heat exchanger geometries and are the basis for easily predicting the performance of a heat exchanger design.

The derivation of these functional relationships typically assumes negligible axial flow of heat in the wall. The conditions for which this assumption is true for a counterflow heat exchanger geometry is the focus of this thesis. Furthermore, the amount that the performance is over-estimated by assuming axial conduction is negligible will be addressed.

1.1 Literature Review.

The counterflow heat exchanger theory previously presented was for the idealization of no axial conduction (in the flow direction) of heat in the wall or fluids. It is not apparent under what conditions this assumption is not valid, but the consequences can be an over-estimation of the effectiveness for a given NTU by as much as 45%, as shown by Rosenhow [17].

Some of the earliest work performed in analyzing the effect of axial conduction was done by Mondt [9]. By inspecting the finite difference equations for a solution that includes axial conduction, he proposed using a conduction parameter to correlate the results. This conduction parameter was

$$\lambda = \frac{K_w A_w}{L \dot{m} C_p} \quad (1.27)$$

and he showed that to accurately predict the convection from a surface at low Reynolds numbers requires consideration of longitudinal conduction.

In later works, the investigation was less specific and looked to predict the influence of axial conduction on the performance of the heat exchanger. Landau and Hlinka [8] and Pan and Welch [11] developed exact solutions to predicting the performance of a counterflow heat exchanger while including the effect of axial conduction. The solutions were in the form of finite series and were algebraically involved. A general investigation was difficult, if not impossible, with the availability of the computing power at the time.

However, Pan, Welch and Head [10], were able to improve on their earlier work [11] and predicted analytically the effect of axial conduction on the performance of the heat exchanger as a function of the NTU and a “modified-conduction-flowrate-ratio”

$$N_K = \frac{K_w A_w}{\dot{m} C_p} \frac{h A}{L \dot{m} C_p} \quad (1.28)$$

Using the exact solution, the existence of axial conduction was predicted for a counterflow heat exchanger with balanced symmetric flow, that is equal mass flow rates and convective heat transfer coefficients for both fluids. Although more general than their past work, the balanced symmetric flow was still rather restrictive.

T
addresse
incorpor
tion para
Mondt n

He then s
Mondt nu
worst and
mance of
large Mon
nant.

This
and solution
flow heat e
([8], [10],
not needed
required thi
tion to desc
differential
to solve the
easily evalu
tions to obta
of the heat e
cated in com
tion of the he

The most recent work was performed by Rohsenow [17], who addressed reasons that laminar flow heat exchangers perform poorly. He incorporated a similar formulation as [8], [10], and [11], but used the conduction parameter above in equation (1.27), from Mondt [9], which he called the Mondt number

$$M_o = \frac{K_w A_w}{L \dot{m} C_p} \quad (1.29)$$

He then solved for the performance of the heat exchanger at the limits of the Mondt number, zero and infinity. The extremes of the Mondt number provide worst and best case scenarios. A Mondt number of zero gives the performance of the heat exchanger when axial conduction is negligible; while a large Mondt number gives the performance when axial conduction is dominant.

This investigation shall differ from previous work in the formulation and solution of the problem. All previous investigations involving a counter-flow heat exchanger have neglected temperature gradients normal to the wall ([8], [10], [11], [17]). Although this assumption does seem reasonable it is not needed for this investigation to obtain a solution; whereas past studies required this assumption. This difference results in a partial differential equation to describe the wall temperature for this study, instead of the ordinary differential equation obtained for past studies. However, the techniques used to solve the partial differential equation will allow for a solution that is more easily evaluated; while past solution techniques required special flow conditions to obtain a solution. Therefore, by considering the two-dimensionality of the heat exchanger wall the problem was more mathematically complicated in comparison to past studies, but allowed for a more general investigation of the heat exchanger design parameters.

Chapter 2

Describing Equations and Boundary Conditions

2.0 Dimensional Equations

2.0.1 Wall Conduction Equation

The geometry is shown in Figure 2.1, a two dimensional wall with hot fluid entering at one end and cold fluid entering at the other. The problem was formulated as a boundary value problem on the wall assuming steady state and constant properties. The differential equation and boundary conditions corresponding to the plane geometry with the given assumptions are

$$\frac{\partial^2 T_w}{\partial x^2} + \frac{\partial^2 T_w}{\partial y^2} = 0 \quad (2.1)$$

$$K_w \frac{\partial T_w}{\partial x} \bigg|_{x=0} = h_o [T_w(0, y) - T_o] \quad (2.2a)$$

$$-K_w \frac{\partial T_w}{\partial x} \bigg|_{x=L} = h_L [T_w(L, y) - T_L] \quad (2.2b)$$

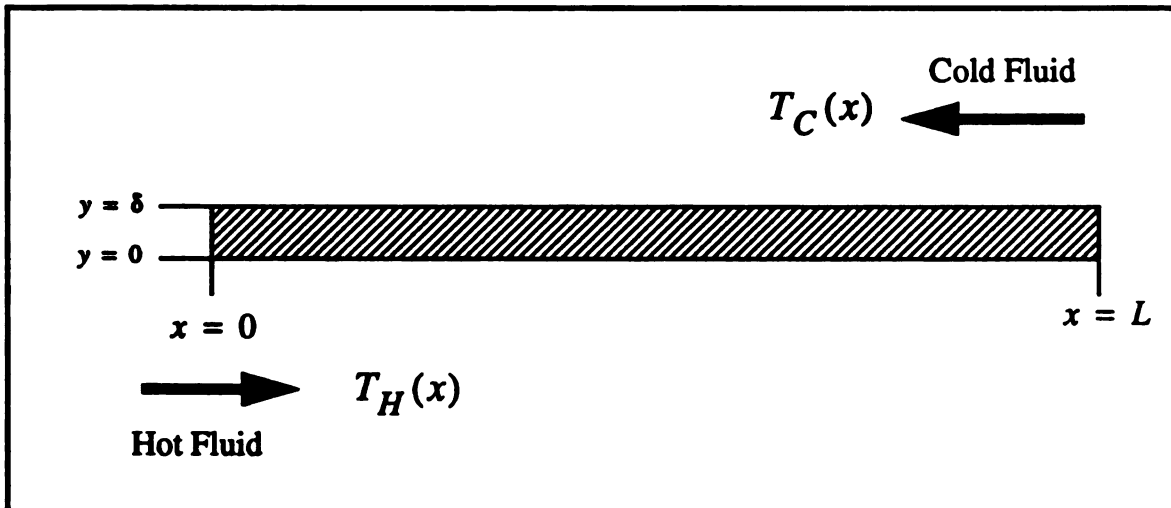


Figure 2.1. Heat exchanger geometry studied. Note, the analysis was performed on a per unit width basis.

$$-K_w \frac{\partial T_w}{\partial y} \Big|_{y=0} = h_H [T_H(x) - T_w(x, 0)] \quad (2.2c)$$

$$-K_w \frac{\partial T_w}{\partial y} \Big|_{y=\delta} = h_C [T_w(x, \delta) - T_C(x)] \quad (2.2d)$$

where boundary conditions of the third kind were used to represent the most general case and still allow for boundary conditions of the first and second kind by adjusting the magnitudes of the constants $(K_w, h_o, h_L, h_H, h_C)$.

2.0.2 Fluid Energy Balance Equations

The describing equations for the fluids were formulated using an energy balance on a differential length element of the heat exchanger. For the hot fluid the energy balance on a differential element of length Δx can be written

$$\dot{H}|_x = \dot{H}|_{x+\Delta x} + q''_{wall} P_H \Delta x \quad (2.3)$$

Substituting mass flow rates and the specific enthalpy and rearranging gives

$$\frac{\dot{m}\hat{h}|_{x+\Delta x} - \dot{m}\hat{h}|_x}{\Delta x} + q''_{wall} P_H = 0 \quad (2.4)$$

Taking the limit as $\Delta x \rightarrow 0$ and assuming the fluid behaves as an ideal gas or an incompressible liquid ($C_p dT = d\hat{h}$) gives

$$(\dot{m}_H C_{p,H}) \frac{dT_H}{dx} + q''_{wall} P_H = 0 \quad (2.5)$$

The heat flux from the wall from Newton's law of cooling is

$$q''_{wall} = h_H [T_H(x) - T_w(x, 0)] \quad (2.6)$$

substituting into equation (2.5) and rearranging, results in the final describing equation for the hot fluid

$$\frac{dT_H}{dx} + \frac{h_H P_H}{\dot{m}_H C_{p,H}} [T_H(x) - T_w(x, 0)] = 0 \quad (2.7)$$

Prescribing a constant temperature at the inlet gives the initial condition

$$T_H(0) = T_{H,in} \quad (2.8)$$

Using a similar analysis, the describing equation for the cold fluid and corresponding initial condition are

$$\frac{dT_C}{dx} + \frac{h_C P_C}{\dot{m}_C C_{p_c}} [T_w(x, \delta) - T_C(x)] = 0 \quad (2.9)$$

$$T_C(L) = T_{C,in} \quad (2.10)$$

2.1 Dimensionless Equations

2.1.1 Nondimensionalization of lengths

To remove any dimensional length dependence on the formulation of the problem the length scales were nondimensionalized using the characteristic lengths of the wall

$$x^+ = \frac{x}{L} \quad (2.11)$$

$$y^+ = \frac{y}{\delta} \quad (2.12)$$

Applying this nondimensionalization to the previously presented equations for the wall and fluid temperatures results in equations that only have units of temperature, which were made dimensionless after solving (to be shown later) for algebraic ease and for the physical insight available with units of temperature. The wall conduction equation and boundary conditions are

$$\frac{\partial^2 T_w}{\partial x^{+2}} + \frac{L^2}{\delta^2} \frac{\partial^2 T_w}{\partial y^{+2}} = 0 \quad (2.13)$$

$$-\left. \frac{\partial T_w}{\partial x^+} \right|_{x^+ = 0} + Bi_o T_w(0, y^+) = Bi_o T_o \quad (2.14a)$$

$$\left. \frac{\partial T_w}{\partial x^+} \right|_{x^+ = 1} + Bi_L T_w(1, y^+) = Bi_L T_L \quad (2.14b)$$

$$-\left. \frac{\partial T_w}{\partial y^+} \right|_{y^+ = 0} + Bi_H T_w(x^+, 0) = Bi_H T_H(x^+) \quad (2.14c)$$

$$\left. \frac{\partial T_w}{\partial y^+} \right|_{y^+ = 1} + Bi_C T_w(x^+, 1) = Bi_C T_C(x^+) \quad (2.14d)$$

where dimensionless parameters introduced in the equations are defined in the next section.

Similarly, nondimensionalization of the equations for the hot and cold fluids gives

$$\frac{dT_H}{dx^+} + N_H [T_H(x^+) - T_w(x^+, 0)] = 0 \quad (2.15)$$

$$T_H(0) = T_{H,in} \quad (2.16)$$

$$\frac{dT_C}{dx^+} + N_C [T_w(x^+, 1) - T_C(x^+)] = 0 \quad (2.17)$$

$$T_C(1) = T_{C,in} \quad (2.18)$$

2.1.2 Nondimensionalization of Temperature

The problem was solved as presented in equations (2.13-2.18), giving the solution with units of temperature only. The following equations were used to present the results in a dimensionless form:

$$\Theta_w(x^+, y^+) = \frac{T_w(x^+, y^+) - T_{C,in}}{T_{H,in} - T_{C,in}} \quad (2.19)$$

$$\Theta_H(x^+) = \frac{T_H(x^+) - T_{C,in}}{T_{H,in} - T_{C,in}} \quad (2.20)$$

$$\Theta_C(x^+) = \frac{T_C(x^+) - T_{C,in}}{T_{H,in} - T_{C,in}} \quad (2.21)$$

2.2 Dim

Th
alization
mational m
wall cond
thickness

As this pa
tion must
must be is
likely the
duction is

The dir
the wall, e

These paran
axial condu
equations (2
ends of the v
a surface of
insight into
pared to the
For large Bic
ature gradien
convecting fl

2.2 Dimensionless Parameters

The dimensionless parameters that resulted during the nondimensionalization of lengths in the equations will provide a link between the mathematical model and the physical problem. The dimensionless parameter in the wall conduction equation, equation (2.13), is a ratio of the wall length to thickness

$$L^* = \frac{L}{\delta} \quad (2.22)$$

As this parameter is increased, the change in heat conduction in the x -direction must also increase. Therefore axial conduction must increase; or the wall must be isothermal in the y -direction (normal to the wall). The later is most likely the dominant effect, but there may be values of L^* for which axial conduction is the dominant effect.

The dimensionless parameters that appear in the boundary conditions on the wall, equations (2.14a-d), are Biot numbers

$$Bi_o = \frac{h_o L}{K_w} \quad (2.23)$$

$$Bi_L = \frac{h_L L}{K_w} \quad (2.24)$$

$$Bi_H = \frac{h_H \delta}{K_w} \quad (2.25)$$

$$Bi_C = \frac{h_C \delta}{K_w} \quad (2.26)$$

These parameters are expected to have the most influence on the solution and axial conduction. The Biot numbers on the hot and cold sides of the wall, equations (2.25-26), should be more influential than the Biot numbers at the ends of the wall. Biot numbers, in general, give a ratio of the convection from a surface of the body to the conduction through the body. This provides insight into the temperature difference that will exist across the body compared to the temperature difference between the surface and convecting fluid. For large Biot numbers the convection dominates, resulting in a large temperature gradient across the body and a surface temperature that is close to the convecting fluid temperature. Conversely, for small Biot numbers the con-

duction v
and a larg

Th
of transfe
ters are

where the

Using equ
ten in term

which relat

duction will dominate, giving a small temperature gradient across the body and a large difference between the surface and convecting fluid temperatures.

The dimensionless parameters for the fluids are similar to the number of transfer units (NTU), but based on the pertinent fluid only. These parameters are

$$N_H = \frac{h_H A_H}{\dot{m}_H C_{p_H}} = \frac{h_H A_H}{C_H} \quad (2.27)$$

$$N_C = \frac{h_C A_C}{\dot{m}_C C_{p_C}} = \frac{h_C A_C}{C_C} \quad (2.28)$$

where the area in equations (2.27-28) is

$$A_H = A_C = Lw \quad (2.29)$$

Using equation (2.29) with the heat capacity, equations (2.27-28) can be written in terms of the corresponding Biot number

$$N_H = \frac{Bi_H K_w L^* w}{C_H} \quad (2.30)$$

$$N_C = \frac{Bi_C K_w L^* w}{C_C} \quad (2.31)$$

which relates the wall parameters to the fluid parameters.

2.3 Heat Exchanger

Solution
ture fields
wall. But the
heat exchanger
mance from
lation neglect
terms of the
These dimensions
eters from the
exchanger's

Effectively
considered
may be considered
imbalance between
energy balance

and the effective

The definition
the inclusion of
parameters used
evaluating the
thermal circuit
lar to the previous
ual resistance
the circuit is
exchanger was

2.3 Heat Exchanger Performance Analysis

Solution of the equations presented up to this point provides the temperature fields for the wall and fluids, without neglecting axial conduction in the wall. But the temperature as a function of the position along the length of the heat exchanger is not the desired result. It is desired to compare the performance from this solution with one that neglects axial conduction. The correlation neglecting axial conduction was presented in equations (1.25-26) in terms of the effectiveness, number of transfer unit, and heat capacity ratio. These dimensionless parameters must be related to the dimensionless parameters from the mathematical solution to make the comparison in the heat exchanger's performance when axial conduction is included.

Effectiveness, defined in equation (1.23), will depend upon which fluid is considered when axial conduction is included because some of the energy may be conducted out the ends of the heat exchanger and result in an energy imbalance between the fluids. Thus, when including axial conduction the energy balance on the fluids are, from equation (1.5)

$$q_H = C_H (T_{H, in} - T_{H, out}) \neq q_C = C_C (T_{C, out} - T_{C, in}) \quad (2.32)$$

and the effectiveness must be defined as a function of the fluid

$$\varepsilon_H = \frac{q_H}{q_{max}} \quad (2.33)$$

$$\varepsilon_C = \frac{q_C}{q_{max}} \quad (2.34)$$

The definition of NTU is given in equation (1.24) and will not depend on the inclusion of axial conduction, but must be related to the dimensionless parameters used to model the physical problem. This was accomplished by evaluating the thermal circuit that describes the heat exchanger wall. The thermal circuit, neglecting any fouling, is shown in Figure 2.2, which is similar to the previously presented thermal circuit (except values for the individual resistances are shown for the geometry studied). The total resistance of the circuit is evaluated using equation (1.9). The conductance for the heat exchanger wall given by equation (1.10) is

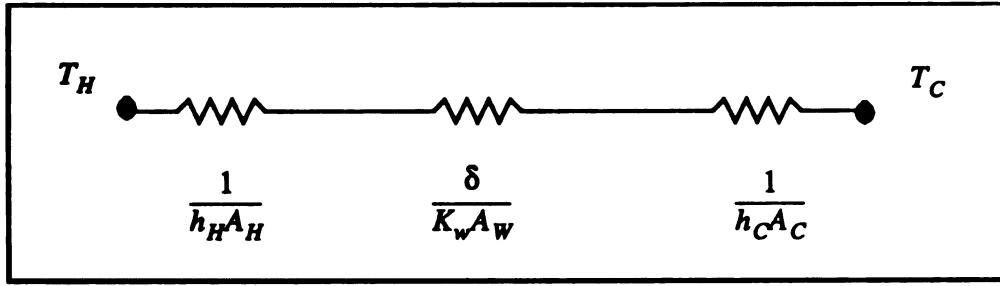


Figure 2.2. Thermal circuit for heat exchanger wall

$$UA = \frac{1}{R_{tot}} = \left[\frac{1}{h_H A_H} + \frac{\delta}{K_w A_w} + \frac{1}{h_C A_C} \right]^{-1} \quad (2.35)$$

and NTU easily follows:

$$NTU = \frac{UA}{C_{min}} = \frac{1}{C_{min}} \left[\frac{1}{h_H A_H} + \frac{\delta}{K_w A_w} + \frac{1}{h_C A_C} \right]^{-1} \quad (2.36)$$

Relating equation (2.36) to the mathematical formulation was accomplished through equations (2.27-28); substituting these equations into equation (2.36) gives

$$NTU = \frac{1}{C_{min}} \left[\frac{1}{N_H C_H} + \frac{\delta}{K_w A_w} + \frac{1}{N_C C_C} \right]^{-1} \quad (2.37)$$

Noting that $A_w = Lw$, equation (2.37) can be rewritten as a function of dimensionless parameters and the wall thermal conductivity using equations (2.30-31), after some arranging it becomes

$$NTU = \frac{K_w w L^*}{C_{min}} \left[\frac{Bi_H Bi_C}{Bi_H + Bi_H Bi_C + Bi_C} \right] \quad (2.38)$$

The equations to be solved for the temperature fields of the wall and fluids are given in equations (2.13-2.18). Using the solution, the performance of the heat exchanger can be presented with equations (2.33), (2.34), and (2.38) in terms of heat exchanger dimensionless parameters, which can be compared to solutions neglecting axial conduction to quantify the effect of axial conduction.

Chapter 3

Method of Solution

3.0 General Method

The problem presented in equations (2.13-18) is a system consisting of a second order homogenous partial differential equation (PDE) with four nonhomogeneous boundary conditions coupled with two first order nonhomogeneous ordinary differential equations (ODE). The coupling occurs through the boundary conditions of the PDE and in the nonhomogeneous term for the ODEs. Thus, if a general solution can be obtained for the PDE without evaluating all boundary conditions, that is in terms of a product of unknown constants and functions, the solution can be substituted into the ODEs and the ODEs solved as a function of the unknown constants. The ODEs solution's can then be substituted back into the boundary conditions of the PDE and the unknown constants evaluated. With the constants specified, the explicit solutions for all differential equations can be generated. This is the general procedure used to solve the set of differential equations and is shown schematically in Figure 3.1.

This section is intended to present the methods that were applied to solve the problem. However, when the same methods were applied more than once they are not shown in detail after the first application. Also, some methods contain details that are not necessary in understanding a method, and whose inclusion would overburden this section. For these reasons, the reader is referred to the Appendices (A-D) for additional details about the solution.

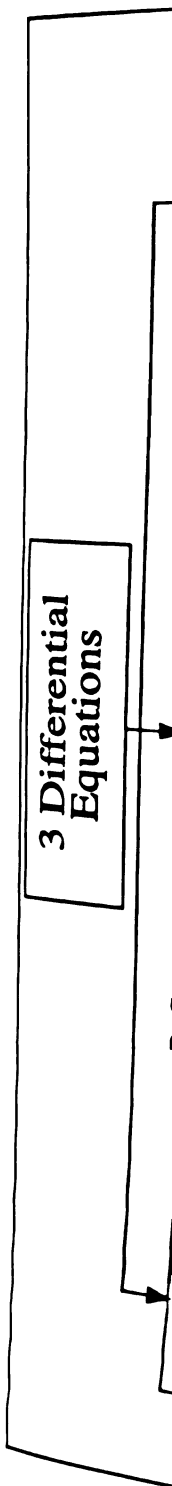


FIGURE 3.1. Flowc

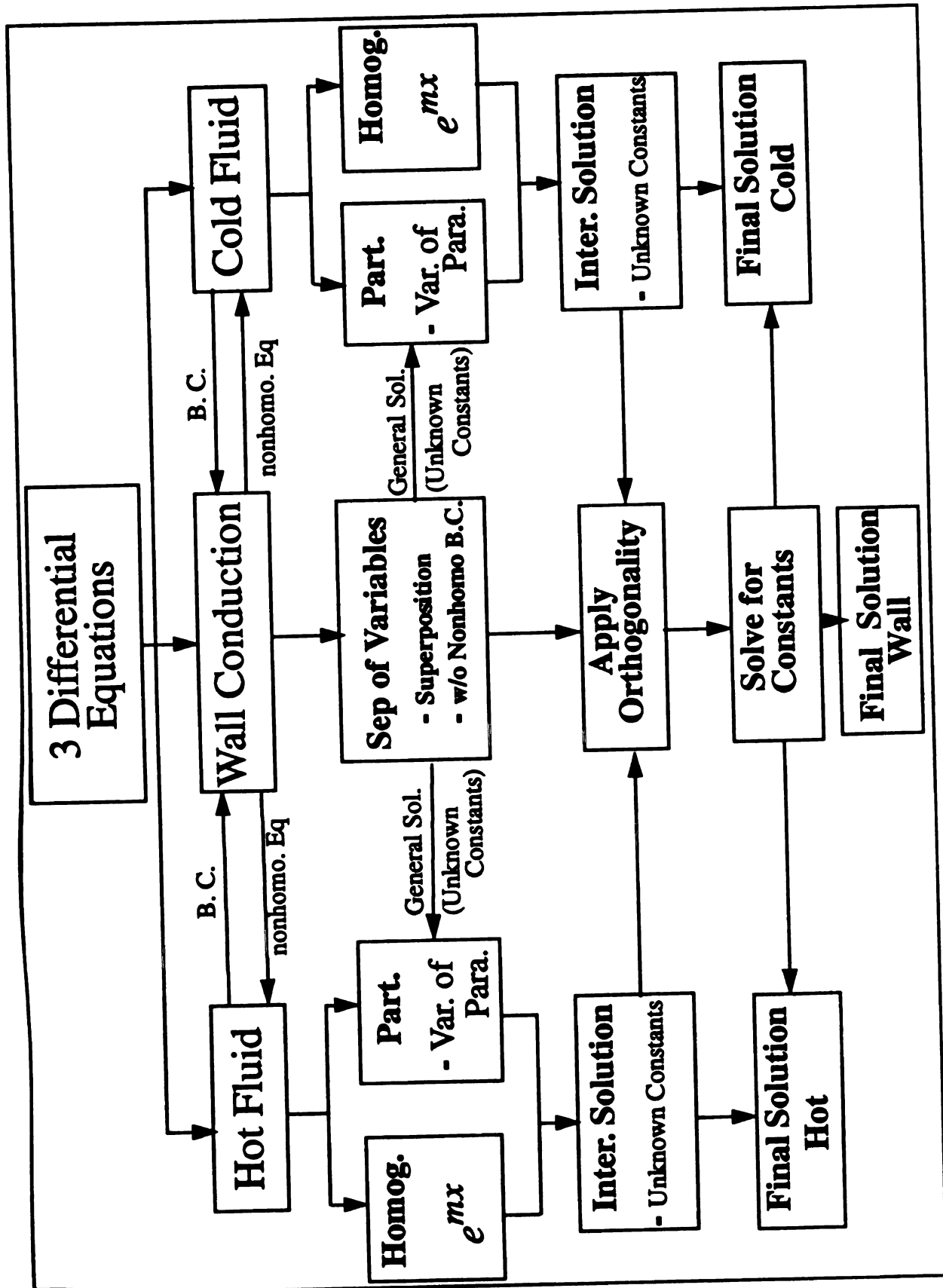


FIGURE 3.1. Flowchart of solution procedure

3.1 General

Since
ferent math
separation
of this met
ferential eq
lem has for
introducing

one of the
mathematical for

Three nonhom
Since the prob
problem is par
mogeneous bo
ables technique
application of s
sented by three
boundary condi
lows:

3.1 General Solution of the Wall Conduction Equation

Since the problem is linear, the PDE could be solved using many different mathematical approaches; Fourier transforms, Green's functions, or separation of variables. The method chosen was separation of variables. Use of this method requires that only one nonhomogeneous term exist in the differential equation or boundary conditions. As presently formulated the problem has four nonhomogeneous boundary conditions equations (2.14a-d). By introducing scaling on the temperature

$$\theta_w(x^+, y^+) = T_w(x^+, y^+) - T_o \quad (3.1)$$

one of the nonhomogeneous boundary conditions is eliminated. The mathematical formulation with the scaled temperature becomes

$$\frac{\partial^2 \theta_w}{\partial x^{+2}} + L^{*2} \frac{\partial^2 \theta_w}{\partial y^{+2}} = 0 \quad (3.2)$$

$$-\frac{\partial \theta_w}{\partial x^+} \Big|_{x^+=0} + Bi_o \theta_w(0, y^+) = 0 \quad (3.3a)$$

$$\frac{\partial \theta_w}{\partial x^+} \Big|_{x^+=1} + Bi_L \theta_w(1, y^+) = Bi_L (T_L - T_o) \quad (3.3b)$$

$$-\frac{\partial \theta_w}{\partial y^+} \Big|_{y^+=0} + Bi_H \theta_w(x^+, 0) = Bi_H [T_H(x^+) - T_o] \quad (3.3c)$$

$$\frac{\partial \theta_w}{\partial y^+} \Big|_{y^+=1} + Bi_C \theta_w(x^+, 1) = Bi_C [T_C(x^+) - T_o] \quad (3.3d)$$

Three nonhomogeneous boundary conditions, equations (3.3b-d), still exist. Since the problem is linear the principle of superposition may be applied. The problem is partitioned into a set of simpler problems that contain one nonhomogeneous boundary condition, and can be solved using separation of variables techniques. Then the solution to equations (3.2-3) is obtained by application of superposition. The problem in equations (3.2-3) can be represented by three simpler problems, since there are three nonhomogeneous boundary conditions. Using superposition the solutions are related as follows:

where θ_i is

where $i = 1,$

It can be shown
the originally

3.1.1 General

The se
solution for θ

Substituting in
(3.5-6), yields

$$\theta_w(x^+, y^+) = \sum_{i=1}^3 \theta_i(x^+, y^+) \quad (3.4)$$

where θ_i is the solution to the problem given mathematically as

$$\frac{\partial^2 \theta_i}{\partial x^{+2}} + L^{*2} \frac{\partial^2 \theta_i}{\partial y^{+2}} = 0 \quad (3.5)$$

$$-\frac{\partial \theta_i}{\partial x^+} \Big|_{x^+=0} + Bi_o \theta_i(0, y^+) = 0 \quad (3.6a)$$

$$\frac{\partial \theta_i}{\partial x^+} \Big|_{x^+=1} + Bi_L \theta_i(1, y^+) = \delta_{1i} Bi_L (T_L - T_o) \quad (3.6b)$$

$$-\frac{\partial \theta_i}{\partial y^+} \Big|_{y^+=0} + Bi_H \theta_i(x^+, 0) = \delta_{2i} Bi_H [T_H(x^+) - T_o] \quad (3.6c)$$

$$\frac{\partial \theta_i}{\partial y^+} \Big|_{y^+=1} + Bi_C \theta_i(x^+, 1) = \delta_{3i} Bi_C [T_C(x^+) - T_o] \quad (3.6d)$$

where $i = 1, 2, 3$ and

$$\delta_{ji} = \text{kroncker delta} = \begin{cases} 0 & i \neq j \\ 1 & i = j \end{cases} \quad (3.7)$$

It can be shown by adding the three problems ($i = 1, 2, 3$) stated above that the originally posed problem in equations (3.2-3) is obtained.

3.1.1 General Solution for Nonhomogeneous Boundary Condition at $x = L$

The separation of variables technique begins by assuming a product solution for θ_1 of the form

$$\theta_1 = F(x^+) G(y^+) \quad (3.8)$$

Substituting into the differential equation and boundary conditions, equations (3.5-6), yields

$$F_{x^+x^+} G + L^{*2} G_{y^+y^+} F = 0 \quad (3.9)$$

$$-GF_{x^+} \Big|_{x^+=0} + Bi_o GF(0) = 0 \quad (3.10a)$$

where the f

Rearranging
tion (3.10) p

where a con
(3.12). Since
only a func
stant. This
tial differen
equation (3
sign is cho
homogenou
have a gene
sian coordi
nary differ
appropriate

$$GF_{x^+}|_{x^+=1} + Bi_o GF(1) = Bi_L(T_L - T_o) \quad (3.10b)$$

$$-FG_{y^+}|_{y^+=0} + Bi_H FG(0) = 0 \quad (3.10c)$$

$$FG_{y^+}|_{y^+=1} + Bi_H FG(1) = 0 \quad (3.10d)$$

where the following convention for representing derivatives was used:

$$\frac{\partial^2 F}{\partial x^{+2}} \equiv F_{x^+x^+} \quad (3.11)$$

Rearranging equation (3.9) to group similar variables and simplifying equation (3.10) gives

$$\frac{1}{L^{*2}} \frac{F_{x^+x^+}}{F} = -\frac{G_{y^+y^+}}{G} = \pm\mu^2 \quad (3.12)$$

$$-F_{x^+}|_{x^+=0} + Bi_o F(0) = 0 \quad (3.13a)$$

$$GF_{x^+}|_{x^+=1} + Bi_o GF(1) = Bi_L(T_L - T_o) \quad (3.13b)$$

$$-G_{y^+}|_{y^+=0} + Bi_H G(0) = 0 \quad (3.13c)$$

$$G_{y^+}|_{y^+=1} + Bi_H G(1) = 0 \quad (3.13d)$$

where a constant, $\pm\mu^2$ (the eigenvalue), has been introduced in equation (3.12). Since the left hand side is only a function of x^+ and the right hand side only a function of y^+ , to obtain equality both sides must be equal to this constant. This key result allows for separation of the variables, reducing the partial differential equation to two ordinary differential equations. Before equation (3.12) can be separated a sign must be chosen for the constant. This sign is chosen to produce an eigenvalue problem for the function that has two homogenous boundary conditions to evaluate. The eigenvalue problem will have a general solution in terms of *sine* and *cosine* functions for this Cartesian coordinate system. After choosing the sign on the eigenvalue, two ordinary differential equations can be written from equation (3.12) with the appropriate boundary conditions from equation (3.13)

$$F_{x^+x^+} - L^{*2}\mu^2 F = 0 \quad (3.14)$$

Note that eq
(3.16) has tw
tion (3.13b),
to either fun
tion. Thus, t
complete so

Equat
The general

Applying th
the two con

which can b
tion

The solution

Applying th
ship between

Substituting

$$-F_{x^+} \Big|_{x^+=0} + Bi_o F(0) = 0 \quad (3.15a)$$

$$G_{y^+ y^+} + \mu^2 G = 0 \quad (3.16)$$

$$-G_{y^+} \Big|_{y^+=0} + Bi_H G(0) = 0 \quad (3.17a)$$

$$G_{y^+} \Big|_{y^+=1} + Bi_H G(1) = 0 \quad (3.17b)$$

Note that equation (3.14) only has one boundary condition, whereas equation (3.16) has two boundary conditions. The reason for this can be seen in equation (3.13b), which depends on both functions F and G and cannot be applied to either function singularly. This is the nonhomogeneous boundary condition. Thus, this boundary condition must be applied after assembling the complete solution.

Equations (3.14) and (3.16) have easily obtainable general solutions. The general solution for equation (3.14) is

$$F(x^+) = A_1 \cosh(\mu L^* x^+) + A_2 \sinh(\mu L^* x^+) \quad (3.18)$$

Applying the boundary condition, equation (3.15a), gives a relationship for the two constants

$$A_2 = \frac{Bi_o}{\mu L^*} A_1 \quad (3.19)$$

which can be substituted into equation (3.18) and rearranged giving the solution

$$F(x^+) = A_2 [\mu L^* \cosh(\mu L^* x^+) + Bi_o \sinh(\mu L^* x^+)] \quad (3.20)$$

The solution of equation (3.16) is

$$G(y^+) = A_3 \cos(\mu y^+) + A_4 \sin(\mu y^+) \quad (3.21)$$

Applying the boundary conditions in equation (3.17a) solves for the relationship between the constants

$$A_4 = \frac{Bi_H A_3}{\mu} \quad (3.22)$$

Substituting into equation (3.21) and rearranging gives

Applying t
any inform
equation. F
equation si

To meet the
satisfied fo
it has an in
solved to d
is then

with μ_n give

Subst
vide the sol
to equation
solution. Al
one constant
dition, equat
rate and was

$\theta_1(\lambda)$

and the eigen

For eas
defined:

X_1

and the solution

$$G(y^+) = A_4 [\mu \cos(\mu y^+) + Bi_H \sin(\mu y^+)] \quad (3.23)$$

Applying the final boundary condition, equation (3.17b), does not provide any information about the constant A_4 because the constant cancels from the equation. However, it does provide information about the eigenvalue (μ). The equation simplifies to

$$\tan(\mu_n) = \frac{(Bi_H + Bi_C) \mu_n}{(\mu_n^2 - Bi_H Bi_C)} \quad (3.24)$$

To meet the boundary condition in equation (3.17b), equation (3.24) must be satisfied for all values of μ_n . Equation (3.24) is a transcendental equation and it has an infinite number of solutions, hence the subscript on μ . It will be solved to determine the possible values of μ_n . The solution for the function G is then

$$G(\mu_n, y^+) = A_2 [\mu_n \cos(\mu_n y^+) + Bi_H \sin(\mu_n y^+)] \quad (3.25)$$

with μ_n given by the solution of equation (3.24).

Substituting equations (3.25) and (3.20) into equation (3.8) will provide the solution. However, since there exist an infinite number of solutions to equation (3.25) all possible solutions will be summed to obtain the final solution. Also, the undetermined constants, A_2 and A_4 , will be grouped into one constant that will be determined later by applying the last boundary condition, equation (3.6c), which was the boundary condition that did not separate and was not evaluated. The solution for problem one is

$$\theta_1(x^+, y^+) = \sum_{n=0}^{\infty} A_n [\mu_n L^* \cosh(\mu_n L^* x^+) + Bi_o \sinh(\mu_n L^* x^+)] * [\mu_n \cos(\mu_n y^+) + Bi_H \sin(\mu_n y^+)] \quad (3.26)$$

and the eigenvalues are found from the solution of equation (3.24).

For ease in presenting these large solutions, the following functions are defined:

$$X_1(\mu_n, x^+) \equiv \mu_n L^* \cosh(\mu_n L^* x^+) + Bi_o \sinh(\mu_n L^* x^+) \quad (3.27)$$

$$Y_1(\mu_n, y^+) \equiv \mu_n \cos(\mu_n y^+) + Bi_H \sin(\mu_n y^+) \quad (3.28)$$

and the solution can be rewritten as

3.1.2 General

The solution of the previous section. The results are repeated here for problems of the form

$$\theta$$

$$\theta_3(x)$$

The eigenvalue

Defining the following

$$Y_2$$

allows the solution

$$\theta$$

$$\theta$$

$$\theta_1(x^+, y^+) = \sum_{n=0}^{\infty} A_n X_1(\mu_n, x^+) Y_1(\mu_n, y^+) \quad (3.29)$$

3.1.2 General Solution for Nonhomogeneous Boundary Conditions on y

The solution for $i=2, 3$ apply a similar procedure as used in the previous section. The details of which are shown in Appendix A and will not be repeated here. Applying these procedures results in the following solutions for problems two and three:

$$\theta_2(x^+, y^+) = \sum_{n=0}^{\infty} B_n \left[\cosh\left(\frac{\alpha_n}{L^*} y^+\right) - \zeta_n \sinh\left(\frac{\alpha_n}{L^*} y^+\right) \right]^* \quad (3.30)$$

$$[\alpha_n \cos(\alpha_n x^+) + Bi_o \sin(\alpha_n x^+)]$$

$$\theta_3(x^+, y^+) = \sum_{n=0}^{\infty} C_n \left[\frac{\alpha_n}{L^*} \cosh\left(\frac{\alpha_n}{L^*} y^+\right) + Bi_H \sinh\left(\frac{\alpha_n}{L^*} y^+\right) \right]^* \quad (3.31)$$

$$[\alpha_n \cos(\alpha_n x^+) + Bi_o \sin(\alpha_n x^+)]$$

The eigenvalues are given by the positive roots of the transcendental equation

$$\tan(\alpha_n) = \frac{(Bi_o + Bi_L) \alpha_n}{(\alpha_n^2 - Bi_L Bi_o)} \quad (3.32)$$

Defining the following variables:

$$X_2(\alpha_n, x^+) \equiv \alpha_n \cos(\alpha_n x^+) + Bi_o \sin(\alpha_n x^+) \quad (3.33)$$

$$Y_2(\alpha_n, y^+) \equiv \cosh\left(\frac{\alpha_n}{L^*} y^+\right) - \zeta_n \sinh\left(\frac{\alpha_n}{L^*} y^+\right) \quad (3.34)$$

$$Y_3(\alpha_n, y^+) \equiv \frac{\alpha_n}{L^*} \cosh\left(\frac{\alpha_n}{L^*} y^+\right) + Bi_H \sinh\left(\frac{\alpha_n}{L^*} y^+\right) \quad (3.35)$$

allows the solutions to be presented in a compact form

$$\theta_2(x^+, y^+) = \sum_{n=0}^{\infty} B_n Y_2(\alpha_n, y^+) X_2(\alpha_n, x^+) \quad (3.36)$$

$$\theta_3(x^+, y^+) = \sum_{n=0}^{\infty} C_n Y_3(\alpha_n, y^+) X_2(\alpha_n, x^+) \quad (3.37)$$

3.2 Solution

3.2.1 Hot Fluid

The
hot fluid, p
equation in
 $T_w(x^+, 0)$ i
from equat

$$T_w(x^+, 0) =$$

where the la
(3.36) and (2.15) and a

$$\frac{dT_H}{dx^+} + N_H T_H$$

with the initi

This equation
solution may
lar solution. T

and a particular

3.2 Solution of the Fluid Energy Balances Equations

3.2.1 Hot Fluid Formulation

The ordinary differential equation describing the temperature of the hot fluid, presented in equations (2.15-16), is coupled to the wall conduction equation in the differential equation itself. This is seen by the presence of $T_w(x^+, 0)$ in the differential equation. The value of this term can be obtained from equations (3.1), (3.4), (3.29), (3.36), and (3.37) as

$$T_w(x^+, 0) = \theta_w(x^+, 0) + T_o = T_o + \sum_{n=0}^{\infty} A_n X_1(\mu_n, x^+) Y_1(\mu_n, 0) + \sum_{n=0}^{\infty} [B_n Y_2(\alpha_n, 0) + C_n Y_3(\alpha_n, 0)] X_2(\alpha_n, x^+) \quad (3.38)$$

where the last term in equation (3.38) is obtained from combining equations (3.36) and (3.37). Substituting this into the differential equation in equation (2.15) and arranging gives

$$\frac{dT_H}{dx^+} + N_H T_H = N_H \left\{ T_o + \sum_{n=0}^{\infty} A_n X_1(\mu_n, x^+) Y_1(\mu_n, 0) + \sum_{n=0}^{\infty} [B_n Y_2(\alpha_n, 0) + C_n Y_3(\alpha_n, 0)] X_2(\alpha_n, x^+) \right\} \quad (3.39)$$

with the initial condition from equation (2.16a)

$$T_H(0) = T_{H, in} \quad (3.40a)$$

This equation is a linear nonhomogeneous ordinary differential equation. Its solution may be written as the sum of a homogeneous solution and a particular solution. The homogenous problem is given as

$$\frac{dT_{H,h}}{dx^+} + N_H T_{H,h} = 0 \quad (3.41)$$

and a particular problem is

$$\frac{dT_{H,p}}{dx^*} + N_H$$

The particu
pler proble
eral solution

where $T_{H,h}$

$$\frac{dT_{H,pi}}{dx^*} + N_H$$

($i = 1, 2, 3$)

3.2.2 Hot Flu

The h

where D_1 is a
solution as sh

The pa
parameter tec
form similar t
the unknown
tion ($i=1$) the

Substituting eq
gives

$$\begin{aligned} \frac{dT_{H,p}}{dx^+} + N_H T_{H,p} = N_H \{ T_o + \sum_{n=0}^{\infty} A_n X_1(\mu_n, x^+) Y_1(\mu_n, 0) \\ + \sum_{n=0}^{\infty} [B_n Y_2(\alpha_n, 0) + C_n Y_3(\alpha_n, 0)] X_2(\alpha_n, x^+) \} \end{aligned} \quad (3.42)$$

The particular problem in equation (3.42) was further divided into three simpler problems for each term on the right hand side of the equation. The general solution for equation (3.39) in terms of the simpler problem's solutions is

$$T_H(x^+) = T_{H,h}(x^+) + \sum_{i=1}^3 T_{H,pi}(x^+) \quad (3.43)$$

where $T_{H,h}$ is the solution to equation (3.41) and $T_{H,pi}$ is the solution to

$$\begin{aligned} \frac{dT_{H,pi}}{dx^+} + N_H T_{H,pi} = N_H \{ \delta_{1i} T_o + \delta_{2i} \sum_{n=0}^{\infty} A_n X_1(\mu_n, x^+) Y_1(\mu_n, 0) \\ + \delta_{3i} \sum_{n=0}^{\infty} [B_n Y_2(\alpha_n, 0) + C_n Y_3(\alpha_n, 0)] X_2(\alpha_n, x^+) \} \end{aligned} \quad (3.44)$$

($i = 1, 2, 3$) and δ_{ji} is the kronecker delta function as defined in equation (3.7)

3.2.2 Hot Fluid Solution

The homogeneous problem in equation (3.41) is solved giving

$$T_{H,h}(x^+) = D_1 \exp(-N_H x^+) \quad (3.45)$$

where D_1 is a constant that will be evaluated after assembling the complete solution as shown in equation (3.43).

The particular solution was obtained by using standard variation of parameter techniques. This method utilizes a general solution of functional form similar to the nonhomogeneous term in the problem and then solves for the unknown constants in this general solution. For the first particular solution ($i=1$) the general solution would be a constant

$$T_{H,p1}(x^+) = k = \text{constant} \quad (3.46)$$

Substituting equation (3.46) into equation (3.44) and solving for the constant gives

The second
 $x_1(x^+)$, sin

$$T_{H,p2}(x)$$

Substituting
 constants, b_n

$$T_{H,p2}$$

Finally, the th

$$T_{H,p3}(x)$$

which after su
 stants can be v

$$T_{H,p3}(x)$$

Assembling th
 (3.49), and (3.5
 balance is

$$T_{H,p1}(x^+) = T_o \quad (3.47)$$

The second particular solution ($i=2$) would be of the same functional form as $X_1(x^+)$, since all other terms in this summation are constants

$$T_{H,p2}(x^+) = f(X_1(x^+)) = \sum_{n=0}^{\infty} b_n \cosh(\mu_n L^* x^+) + c_n \sinh(\mu_n L^* x^+) \quad (3.48)$$

Substituting equation (3.48) into equation (3.44) and solving for the unknown constants, b_n and c_n , equation (3.48) can be written as

$$T_{H,p2}(x^+) = \sum_{n=0}^{\infty} A_n \left\{ \mu_n^2 L^* \left[1 - \frac{(Bi_o N_H - \mu_n^2 L^{*2})}{(N_H^2 - \mu_n^2 L^{*2})} \right] \cosh(\mu_n L^* x^+) \right. \\ \left. + N_H \mu_n \left[\frac{(Bi_o N_H - \mu_n^2 L^{*2})}{(N_H^2 - \mu_n^2 L^{*2})} \right] \sinh(\mu_n L^* x^+) \right\} \quad (3.49)$$

Finally, the third particular solution is of the functional form

$$T_{H,p3}(x^+) = f(X_2(\alpha_n, x^+)) = \sum_{n=0}^{\infty} a_n \cos(\alpha_n x^+) + d_n \sin(\alpha_n x^+) \quad (3.50)$$

which after substituting into the differential equation and solving for the constants can be written as

$$T_{H,p3}(x^+) = \sum_{n=0}^{\infty} \left(B_n + \frac{\alpha_n}{L^*} C_n \right) \left\{ \alpha_n \left[1 - \frac{(Bi_o N_H + \alpha_n^2)}{(N_H^2 + \alpha_n^2)} \right] \cos(\alpha_n x^+) \right. \\ \left. + N_H \left[\frac{Bi_o N_H + \alpha_n^2}{N_H^2 + \alpha_n^2} \right] \sin(\alpha_n x^+) \right\} \quad (3.51)$$

Assembling the solutions to the simpler problems, equations (3.45), (3.47), (3.49), and (3.51), using equation (3.43) the solution for the hot fluid energy balance is

$$T_H(x^+) = T$$

Applying the

3.2.3 Cold Flow

For the
perature is sl
ated at $(y^+ =$
procedurally
only the final
found in App

The sol

$$\begin{aligned}
T_H(x^+) = & T_o + D_1 \exp(-N_H x^+) \\
& + \sum_{n=0}^{\infty} A_n \left\{ \mu_n^2 L^* \left[1 - \frac{(Bi_o N_H - \mu_n^2 L^{*2})}{(N_H^2 - \mu_n^2 L^{*2})} \right] \cosh(\mu_n L^* x^+) \right. \\
& \quad \left. + N_H \mu_n \left[\frac{(Bi_o N_H - \mu_n^2 L^{*2})}{(N_H^2 - \mu_n^2 L^{*2})} \right] \sinh(\mu_n L^* x^+) \right\} \\
& + \sum_{n=0}^{\infty} \left(B_n + \frac{\alpha_n}{L^*} C_n \right) \left\{ \alpha_n \left[1 - \frac{(Bi_o N_H + \alpha_n^2)}{(N_H^2 + \alpha_n^2)} \right] \cos(\alpha_n x^+) \right. \\
& \quad \left. + N_H \left[\frac{Bi_o N_H + \alpha_n^2}{N_H^2 + \alpha_n^2} \right] \sin(\alpha_n x^+) \right\} \quad (3.52)
\end{aligned}$$

Applying the boundary condition, equation (3.40a), gives the constant

$$\begin{aligned}
D_1 = & T_{H, in} - T_o - \sum_{n=0}^{\infty} A_n \mu_n^2 L^* \left[1 - \frac{(Bi_o N_H - \mu_n^2 L^{*2})}{(N_H^2 - \mu_n^2 L^{*2})} \right] \\
& - \sum_{n=0}^{\infty} \left(B_n + \frac{\alpha_n}{L^*} C_n \right) \alpha_n \left[1 - \frac{(Bi_o N_H + \alpha_n^2)}{(N_H^2 + \alpha_n^2)} \right] \quad (3.53)
\end{aligned}$$

3.2.3 Cold Fluid Solution

For the cold fluid the ordinary differential equation describing the temperature is slightly more involved due to the wall temperature being evaluated at $(y^+ = 1)$. This adds algebraic difficulty to the problem, but procedurally the solution is obtained exactly as the hot fluid. For this reason, only the final solution will be shown. All the details for this solution can be found in Appendix B.

The solution for the cold fluid energy balance equation is

$$T_C(x^+)$$

where the i

$$E_1 = \exp(\cdot)$$

and the follow

$$\begin{aligned}
T_C(x^+) &= T_o + E_1 \exp(N_C x^+) \\
&+ \sum_{n=0}^{\infty} A_n' \left\{ \mu_n L^* \left[1 + \frac{N_C Bi_o + \mu_n^2 L^{*2}}{N_C^2 - \mu_n^2 L^{*2}} \right] \cosh(\mu_n L^* x^+) \right. \\
&\quad \left. + N_C \left[\frac{N_C Bi_o + \mu_n^2 L^{*2}}{N_C^2 - \mu_n^2 L^{*2}} \right] \sinh(\mu_n L^* x^+) \right\} \\
&+ \sum_{n=0}^{\infty} (B_n' + C_n') \left\{ \alpha_n \left[1 + \frac{N_C Bi_o - \alpha_n^2}{N_C^2 + \alpha_n^2} \right] \cos(\alpha_n x^+) \right. \\
&\quad \left. + N_C \left[\frac{N_C Bi_o - \alpha_n^2}{N_C^2 + \alpha_n^2} \right] \sin(\alpha_n x^+) \right\} \quad (3.54)
\end{aligned}$$

where the integration constant is

$$\begin{aligned}
E_1 &= \exp(-N_C) \left[(T_{C,in} - T_o) - \sum_{n=0}^{\infty} A_n' \left\{ \mu_n L^* \left[1 + \frac{N_C Bi_o + \mu_n^2 L^{*2}}{N_C^2 - \mu_n^2 L^{*2}} \right] \cosh(\mu_n L^*) \right. \right. \\
&\quad \left. \left. + N_C \left[\frac{N_C Bi_o + \mu_n^2 L^{*2}}{N_C^2 - \mu_n^2 L^{*2}} \right] \sinh(\mu_n L^*) \right\} \right. \\
&\quad \left. - \sum_{n=0}^{\infty} (B_n' + C_n') \left\{ \alpha_n \left[1 + \frac{N_C Bi_o - \alpha_n^2}{N_C^2 + \alpha_n^2} \right] \cos(\alpha_n) \right. \right. \\
&\quad \left. \left. + N_C \left[\frac{N_C Bi_o - \alpha_n^2}{N_C^2 + \alpha_n^2} \right] \sin(\alpha_n) \right\} \right] \quad (3.55)
\end{aligned}$$

and the following constants were introduced to simplify the expressions:

$$A_n' = A_n [\mu_n \cos(\mu_n) + Bi_H \sin(\mu_n)] \quad (3.56)$$

$$B_n' = B_n \left[\cosh\left(\frac{\alpha_n}{L^*}\right) - \zeta_n \sinh\left(\frac{\alpha_n}{L^*}\right) \right] \quad (3.57)$$

$$C_n' = C_n \left[\frac{\alpha_n}{L^*} \cosh\left(\frac{\alpha_n}{L^*}\right) + Bi_H \sinh\left(\frac{\alpha_n}{L^*}\right) \right] \quad (3.58)$$

3.3 Appl

Ha
boundary
conditions
conditions
to be appl
equation (
neous bou

The difficu
an infinite s
(3.37), are

This means t
determined. C
than an infini
the series con
vidual terms a
point and futur
for the series t
assumed large.

3.3 Application of Nonhomogeneous Boundary Conditions

Having obtained the solution for the temperature of the fluids, the final boundary conditions (nonhomogeneous) can now be applied. The boundary conditions that need to be applied are the three nonhomogeneous boundary conditions given in equations (3.6b-d). These boundary conditions only need to be applied to the respective θ_i solution, (i.e. equation (3.6b) applied to θ_1 , equation (3.6c) to θ_2 and equation (3.6d) to θ_3). These three nonhomogeneous boundary conditions are

$$\left. \frac{\partial \theta_1}{\partial x^+} \right|_{x^+=1} + Bi_L \theta_1(1, y^+) = Bi_L (T_L - T_o) \quad (3.59)$$

$$-\left. \frac{\partial \theta_2}{\partial y^+} \right|_{y^+=0} + Bi_H \theta_2(x^+, 0) = Bi_H [T_H(x^+) - T_o] \quad (3.60)$$

$$\left. \frac{\partial \theta_3}{\partial y^+} \right|_{y^+=1} + Bi_C \theta_3(x^+, 1) = Bi_C [T_C(x^+) - T_o] \quad (3.61)$$

The difficulty with equations (3.59-61) is that the relationships are in terms of an infinite series for θ_i . These series, from equations (3.29), (3.36), and (3.37), are

$$\theta_1(x^+, y^+) = \sum_n^{\infty} A_n X_1(\mu_n, x^+) Y_1(\mu_n, y^+) \quad (3.62)$$

$$\theta_2(x^+, y^+) = \sum_n^{\infty} B_n Y_2(\alpha_n, y^+) X_2(\alpha_n, x^+) \quad (3.63)$$

$$\theta_3(x^+, y^+) = \sum_n^{\infty} C_n Y_3(\alpha_n, y^+) X_2(\alpha_n, x^+) \quad (3.64)$$

This means that theoretically an infinite number of constants will need to be determined. Of course, experience with series solutions has shown that less than an infinite number of terms (and constants) need to be considered since the series converges after a finite number of terms; beyond which, the individual terms are zero or negligible in comparison to the summation up to that point and future terms decay further. However, the number of terms needed for the series to converge is not known and must remain arbitrary and assumed large.

The procedure used to determine the constants that will satisfy the nonhomogeneous boundary conditions involves applying orthogonality. Using the orthogonality of the eigenfunctions, the constants will be determined. An appropriate mathematical statement of this property is

$$\int_0^1 w_{xy} Y_1(\mu_n, y^+) Y_1(\mu_m, y^+) dy^+ = \begin{cases} 0 & m \neq n \\ N(\mu_m) & m = n \end{cases} \quad (3.65)$$

or

$$\int_0^1 w_{xy} X_2(\alpha_n, x^+) X_2(\alpha_m, x^+) dx^+ = \begin{cases} 0 & m \neq n \\ N(\alpha_m) & m = n \end{cases} \quad (3.66)$$

where w_{xy} is a weighting constant, which for the Cartesian coordinate system is equal to one. After substituting expressions for the temperatures and derivatives of temperatures into the boundary condition in equations (3.59-61), the equations will be multiplied by a second eigenfunction and integrated over the boundary. Since the eigenfunctions have the property shown in equations (3.65-66), the equations will be simplified and the unknown constants can be determined.

3.3.1 Application of Boundary Condition at $x = L$

Beginning with the solution for θ_1 in equation (3.26) and taking the derivative with respect to x^+ and evaluating both expressions at the boundary gives

$$\theta_1(1, y^+) = \sum_{n=0}^{\infty} A_n [\mu_n L^* \cosh(\mu_n L^*) + Bi_o \sinh(\mu_n L^*)] * [\mu_n \cos(\mu_n y^+) + Bi_H \sin(\mu_n y^+)] \quad (3.67)$$

$$\frac{\partial \theta_1}{\partial x^+}(1, y^+) = \sum_{n=0}^{\infty} A_n [\mu_n^2 L^{*2} \sinh(\mu_n L^*) + Bi_o \mu_n L^* \cosh(\mu_n L^*)] * [\mu_n \cos(\mu_n y^+) + Bi_H \sin(\mu_n y^+)] \quad (3.68)$$

Substituting these expressions into the boundary condition, equation (3.59), produces

$$\begin{aligned}
& \sum_{n=0}^{\infty} A_n [\mu_n^2 L^{*2} \sinh(\mu_n L^*) + Bi_o \mu_n L^* \cosh(\mu_n L^*)] * \\
& \quad [\mu_n \cos(\mu_n y^+) + Bi_H \sin(\mu_n y^+)] \\
& + Bi_L \sum_{n=0}^{\infty} A_n [\mu_n L^* \cosh(\mu_n L^*) + Bi_o \sinh(\mu_n L^*)] * \\
& \quad [\mu_n \cos(\mu_n y^+) + Bi_H \sin(\mu_n y^+)] \\
& = Bi_L (T_L - T_o) \tag{3.69}
\end{aligned}$$

The orthogonality of the eigenfunctions is used to determine the constants. The eigenfunction for this problem is

$$Y(\mu_n, y^+) = \mu_n \cos(\mu_n y^+) + Bi_H \sin(\mu_n y^+) \tag{3.70}$$

and these eigenfunctions have the property shown in equation (3.65). Therefore, equation (3.69) will be multiplied by a second eigenfunction $Y(\mu_m, y^+)$ and integrated over the boundary. Because this integral is only nonzero for $m=n$, only this term will remain from the summations. The integrals of each term in equation (3.69) after multiplying by a second eigenfunction are shown in Appendix C.

After applying orthogonality, equation (3.69) reduces to

$$\begin{aligned}
& A_m [\mu_m^2 L^{*2} \sinh(\mu_m L^*) + Bi_o \mu_m L^* \cosh(\mu_m L^*)] N(\mu_m) + \\
& A_m Bi_L [\mu_m L^* \cosh(\mu_m L^*) + Bi_o \sinh(\mu_m L^*)] N(\mu_m) = \\
& Bi_L (T_L - T_o) \left[\sin(\mu_m) - \frac{Bi_H}{\mu_m} \cos(\mu_m) + \frac{Bi_H}{\mu_m} \right] \tag{3.71}
\end{aligned}$$

where all summations that were present in equation (3.69) have been reduced to a single term through the application of orthogonality. Equation (3.71) can now be solved for the unknown constant

$$A_m = \frac{Bi_L (T_L - T_o) \left[\sin(\mu_m) - \frac{Bi_H}{\mu_m} \cos(\mu_m) + \frac{Bi_H}{\mu_m} \right]}{[(\mu_m^2 L^{*2} + Bi_o Bi_L) \sinh(\mu_m L^*) + (Bi_o + Bi_L) \mu_m L^* \cosh(\mu_m L^*)] N(\mu_m)} \tag{3.72}$$

The functional relationship for $N(\mu_m)$ is

$$N(\mu_m) = \frac{1}{2} \left[(\mu_m^2 + Bi_o^2) \left(1 + \frac{Bi_L}{(\mu_m^2 + Bi_L^2)} \right) + Bi_o \right] \quad (3.73)$$

This completes the solution of problem one, equation (3.62) could be evaluated since A_n is known from equation (3.72), noting that m is a dummy variable.

3.3.2 Application of Boundary Condition at $y = 0$

The difficulty in applying the boundary condition in equation (3.60) is recognized by noticing that the right hand side contains the temperature of the hot fluid. Using the solution for θ_2 from equation (3.30) and taking the derivative with respect to y^+ and evaluating both at the boundary gives

$$\theta_2(x^+, 0) = \sum_{n=0}^{\infty} B_n [\alpha_n \cos(\alpha_n x^+) + Bi_o \sin(\alpha_n x^+)] \quad (3.74)$$

$$\frac{\partial \theta_2}{\partial y^+}(x^+, 0) = - \sum_{n=0}^{\infty} B_n \frac{\alpha_n}{L^*} \zeta_n [\alpha_n \cos(\alpha_n x^+) + Bi_o \sin(\alpha_n x^+)] \quad (3.75)$$

In addition, the hot fluid temperature is, from equation (3.52)

$$\begin{aligned} T_H(x^+) = & T_o + D_1 \exp(-N_H x^+) \\ & + \sum_{n=0}^{\infty} A_n \left\{ \mu_n^2 L^* \left[1 - \frac{(Bi_o N_H - \mu_n^2 L^{*2})}{(N_H^2 - \mu_n^2 L^{*2})} \right] \cosh(\mu_n L^* x^+) \right. \\ & \quad \left. + N_H \mu_n \left[\frac{(Bi_o N_H - \mu_n^2 L^{*2})}{(N_H^2 - \mu_n^2 L^{*2})} \right] \sinh(\mu_n L^* x^+) \right\} \\ & + \sum_{n=0}^{\infty} \left(B_n + \frac{\alpha_n}{L^*} C_n \right) \left\{ \alpha_n \left[1 - \frac{(Bi_o N_H + \alpha_n^2)}{(N_H^2 + \alpha_n^2)} \right] \cos(\alpha_n x^+) \right. \\ & \quad \left. + N_H \left[\frac{Bi_o N_H + \alpha_n^2}{N_H^2 + \alpha_n^2} \right] \sin(\alpha_n x^+) \right\} \quad (3.76) \end{aligned}$$

Putting these three expressions into equation (3.60) yields

$$\begin{aligned}
& \sum_{n=0}^{\infty} B_n \frac{\alpha_n}{L^*} \zeta_n [\alpha_n \cos(\alpha_n x^+) + Bi_o \sin(\alpha_n x^+)] \\
& + Bi_H \sum_{n=0}^{\infty} B_n [\alpha_n \cos(\alpha_n x^+) + Bi_o \sin(\alpha_n x^+)] = \\
& Bi_H [D_1 \exp(-N_H x^+) \\
& + \sum_{n=0}^{\infty} A_n \left\{ \mu_n^2 L^* \left[1 - \frac{(Bi_o N_H - \mu_n^2 L^{*2})}{(N_H^2 - \mu_n^2 L^{*2})} \right] \cosh(\mu_n L^* x^+) \right. \\
& \quad \left. + N_H \mu_n \left[\frac{(Bi_o N_H - \mu_n^2 L^{*2})}{(N_H^2 - \mu_n^2 L^{*2})} \right] \sinh(\mu_n L^* x^+) \right\} \\
& + \sum_{n=0}^{\infty} \left(B_n + \frac{\alpha_n}{L^*} C_n \right) \left\{ \alpha_n \left[1 - \frac{(Bi_o N_H + \alpha_n^2)}{(N_H^2 + \alpha_n^2)} \right] \cos(\alpha_n x^+) \right. \\
& \quad \left. + N_H \left[\frac{Bi_o N_H + \alpha_n^2}{N_H^2 + \alpha_n^2} \right] \sin(\alpha_n x^+) \right\} \quad (3.77)
\end{aligned}$$

for which orthogonality will be applied. Each term in equation (3.77) will be multiplied by the eigenfunction

$$X(\alpha_n, x^+) = \alpha_n \cos(\alpha_n x^+) + Bi_o \sin(\alpha_n x^+) \quad (3.78)$$

evaluated at term m , and integrated over the boundary. The eigenfunction has the same property as discussed earlier, which is given in equation (3.66).

After applying orthogonality, equation (3.77) becomes

$$B_m \lambda_m = -\omega_m D_1 - \sum_{n=0}^{\infty} A_n (\rho_{mn,1} + \rho_{mn,2} + \rho_{mn,3} + \rho_{mn,4}) - \sum_n \left(B_n + C_n \frac{\alpha_n}{L^*} \right) \psi_{mn} \quad (3.79)$$

where the order of the terms in the two equations, equation (3.77) and equation (3.79), has been maintained, except the first two terms in equation (3.77) have been combined into a single term in equation (3.79). Additional variables were introduced to represent the results of the integration, the variable definitions and integration details are shown in Appendix C.

The complexity added by the hot fluid being the nonhomogeneous term in the boundary condition is seen in equation (3.79), where summations

are present
cation of
Because
perature
term. Also
ally two s
equation,
temperature
the other h

3.3.3 Appli

The
very simila
expression
both at the

and the temp

are present after applying orthogonality. This was not the case for the application of orthogonality to θ_1 , where all summations reduced to a single term. Because the summations in equation (3.77) that represent the hot fluid temperature do not contain eigenfunctions, they were not reduced to a single term. Also, equation (3.79) is a function of all three unknown constants (actually two since A_n was just obtained). Nevertheless, the dependence of this equation, which would only be a function of the constant B_n if the hot fluid temperature were not present in the boundary condition, is now coupled to the other boundary condition, equation (3.61), through the constant C_n .

3.3.3 Application of Boundary Condition at $y = \delta$

The evaluation of the boundary condition given in equation (3.61) is very similar to the previously discussed method for θ_2 . Starting with the expression for θ_3 in equation (3.31) and taking the derivative and evaluating both at the boundary gives

$$\theta_3(x^+, 1) = \sum_{n=0}^{\infty} C_n \left[\frac{\alpha_n}{L^*} \cosh\left(\frac{\alpha_n}{L^*}\right) + Bi_H \sinh\left(\frac{\alpha_n}{L^*}\right) \right] * [\alpha_n \cos(\alpha_n x^+) + Bi_o \sin(\alpha_n x^+)] \quad (3.80)$$

$$\frac{\partial \theta_3}{\partial y^+}(x^+, 1) = \sum_{n=0}^{\infty} C_n \frac{\alpha_n}{L^*} \left[\frac{\alpha_n}{L^*} \sinh\left(\frac{\alpha_n}{L^*}\right) + Bi_H \cosh\left(\frac{\alpha_n}{L^*}\right) \right] * [\alpha_n \cos(\alpha_n x^+) + Bi_o \sin(\alpha_n x^+)] \quad (3.81)$$

and the temperature of the cold fluid, from equation (3.54), is

$$T_C(x^+) =$$

Putting the

$$\sum_{n=0}^{\infty} C_n \frac{\alpha}{L} + Bi_C \sum_{n=0}^{\infty}$$

$$Bi_C [E_1 \exp$$

$$\begin{aligned}
T_C(x^+) &= T_o + E_1 \exp(N_C x^+) \\
&+ \sum_{n=0}^{\infty} A_n' \left\{ \mu_n L^* \left[1 + \frac{(Bi_o N_C + \mu_n^2 L^{*2})}{(N_C^2 - \mu_n^2 L^{*2})} \right] \cosh(\mu_n L^* x^+) \right. \\
&\quad \left. + N_C \left[\frac{(Bi_o N_C + \mu_n^2 L^{*2})}{(N_C^2 - \mu_n^2 L^{*2})} \right] \sinh(\mu_n L^* x^+) \right\} \\
&+ \sum_{n=0}^{\infty} (B_n' + C_n') \left\{ \alpha_n \left[1 + \frac{(Bi_o N_C - \alpha_n^2)}{(N_C^2 + \alpha_n^2)} \right] \cos(\alpha_n x^+) \right. \\
&\quad \left. + N_C \left[\frac{Bi_o N_C - \alpha_n^2}{N_C^2 + \alpha_n^2} \right] \sin(\alpha_n x^+) \right\} \quad (3.82)
\end{aligned}$$

Putting these temperatures into equation (3.61) gives

$$\begin{aligned}
&\sum_{n=0}^{\infty} C_n \frac{\alpha_n}{L^*} \left[\frac{\alpha_n}{L^*} \sinh\left(\frac{\alpha_n}{L^*}\right) + Bi_H \cosh\left(\frac{\alpha_n}{L^*}\right) \right] [\alpha_n \cos(\alpha_n x^+) + Bi_o \sin(\alpha_n x^+)] \\
&+ Bi_C \sum_{n=0}^{\infty} C_n \left[\frac{\alpha_n}{L^*} \cosh\left(\frac{\alpha_n}{L^*}\right) + Bi_H \sinh\left(\frac{\alpha_n}{L^*}\right) \right] * \\
&[\alpha_n \cos(\alpha_n x^+) + Bi_o \sin(\alpha_n x^+)] =
\end{aligned}$$

$$Bi_C [E_1 \exp(N_C x^+)$$

$$\begin{aligned}
&+ \sum_{n=0}^{\infty} A_n' \left\{ \mu_n L^* \left[1 + \frac{(Bi_o N_C + \mu_n^2 L^{*2})}{(N_C^2 - \mu_n^2 L^{*2})} \right] \cosh(\mu_n L^* x^+) \right. \\
&\quad \left. + N_C \left[\frac{(Bi_o N_C + \mu_n^2 L^{*2})}{(N_C^2 - \mu_n^2 L^{*2})} \right] \sinh(\mu_n L^* x^+) \right\} \\
&+ \sum_{n=0}^{\infty} (B_n' + C_n') \left\{ \alpha_n \left[1 + \frac{(Bi_o N_C - \alpha_n^2)}{(N_C^2 + \alpha_n^2)} \right] \cos(\alpha_n x^+) \right. \\
&\quad \left. + N_C \left[\frac{(Bi_o N_C - \alpha_n^2)}{(N_C^2 + \alpha_n^2)} \right] \sin(\alpha_n x^+) \right\} \quad (3.83)
\end{aligned}$$

for which
multiplied

evaluated at
the same pro
After applying

$$C_m \phi_m = \Omega_m$$

where the or
tion (3.83) an
(3.83) have b
ilar procedure
to represent th
details of this

Notice
(3.61) had the
Summations e
to equation (3.

3.3.4 Summary

After ap
was obtained f

$$A_n = \frac{1}{[\mu_n]}$$

where

$$N(n)$$

Note that the sub
shown since it is

for which orthogonality will be applied. Each term in equation (3.83) will be multiplied by the eigenfunction

$$X(\alpha_n, x^+) = \alpha_n \cos(\alpha_n x^+) + Bi_o \sin(\alpha_n x^+) \quad (3.84)$$

evaluated at term m and integrated over the boundary. The eigenfunction has the same property as discussed earlier, which is given in equation (3.66).

After applying orthogonality, equation (3.83) becomes

$$C_m \Phi_m = \Omega_m E_1 + \sum_n A_n' (P_{mn,1} + P_{mn,2} + P_{mn,3} + P_{mn,4}) + \sum_n (B_n' + C_n') \Psi_{mn} \quad (3.85)$$

where the order of the terms has been maintained for the two equations, equation (3.83) and equation (3.85), except that the first two terms of equation (3.83) have been combined into a single term in equation (3.85). Using a similar procedure as the last boundary condition, new variables were introduced to represent the results of the integration when orthogonality was applied. All details of this step are shown in Appendix C.

Notice that the presence of the cold fluid temperature in equation (3.61) had the same effect as the hot fluid in the previous boundary condition. Summations exist after applying orthogonality and equation (3.85) is coupled to equation (3.79).

3.3.4 Summary of Applying Orthogonality

After applying orthogonality to equation (3.59) a closed form solution was obtained for the θ_1 constant, from equation (3.72)

$$A_n = \frac{Bi_L (T_L - T_o) \left[\sin(\mu_n) - \frac{Bi_H}{\mu_n} \cos(\mu_n) + \frac{Bi_H}{\mu_n} \right]}{[\mu_n^2 L^{*2} \sinh(\mu_n L^*) + (Bi_o + Bi_L) \mu_n L^* \cosh(\mu_n L^*)] N(\mu_n)} \quad (3.86)$$

where

$$N(\mu_n) = \frac{1}{2} \left[(\mu_n^2 + Bi_o^2) \left(1 + \frac{Bi_L}{(\mu_n^2 + Bi_L^2)} \right) + Bi_o \right] \quad (3.87)$$

Note that the subscript n was substituted for m in the form of the equations shown since it is a dummy subscript.

Applica
the simple alge
The difference
tion (3.59) this
a function (infin
present two pro
the series will n
Secondly, they c
in equations (3.
pled equations g
ranging, are

$$B_m \lambda_m + \sum_n (B_n +$$

$$C_m \phi_m - \sum_n (B_n'$$

These equ
for the unknown
exist in the equat
number of terms
two equations; h
hence the subscri
series ($m = N$), t
stants.

The unknow
($n = 1, 2, \dots, N$). T
of B_n and C_n , nee
Also, D_1 and E_1
substituted. From

D_1

Application of orthogonality to equations (3.60-61) did not result in the simple algebraic equation with one unknown as it did for equation (3.59). The difference is the terms on the right hand side of the equations. For equation (3.59) this term is a constant, whereas for equations (3.60-61) the term is a function (infinite series). These functions are $T_H(x^+)$ and $T_C(x^+)$, and they present two problems. First, they are not orthogonal functions; and therefore, the series will not be reduced to a single term after orthogonality is applied. Secondly, they contain both unknown constants, B_n and C_n , which will result in equations (3.60-61) being coupled after applying orthogonality. The coupled equations given in equation (3.79) and equation (3.85), after some rearranging, are

$$B_m \lambda_m + \sum_n \left(B_n + C_n \frac{\alpha_n}{L^*} \right) \Psi_{mn} + \omega_m D_1 = - \sum_n A_n (\rho_{mn,1} + \rho_{mn,2} + \rho_{mn,3} + \rho_{mn,4}) \quad (3.88)$$

$$C_m \Phi_m - \sum_n (B_n' + C_n') \Psi_{mn} - \Omega_m E_1 = \sum_n A_n' (P_{mn,1} + P_{mn,2} + P_{mn,3} + P_{mn,4}) \quad (3.89)$$

These equations represent a set of simultaneous equations to be solved for the unknown constants B_n and C_n ($n = 1, 2, 3, \dots$). Because summations exist in the equations it is now required to truncate the series after a finite number of terms ($n = N$). This gives $2N$ constants to be determined from the two equations; however, both equations can be written for each eigenvalue, hence the subscript m . Since there are as many eigenvalues as terms in the series ($m = N$), this totals $2N$ equations to solve for the same number of constants.

The unknowns in equations (3.88) and (3.89) are B_n and C_n ($n = 1, 2, \dots, N$). The primed constants in equation (3.89), which are functions of B_n and C_n , need to be substituted for, giving a new variable for that term. Also, D_1 and E_1 are function of the unknown constants and will need to be substituted. From equations (3.53) and (3.55), D_1 and E_1 are respectively

$$D_1 = T_{H,in} - T_o - \sum_{n=0}^{\infty} A_n \mu_n^2 L^* \left[1 - \frac{(Bi_o N_H - \mu_n^2 L^{*2})}{(N_H^2 - \mu_n^2 L^{*2})} \right] - \sum_{n=0}^{\infty} \left(B_n + \frac{\alpha_n}{L^*} C_n \right) \alpha_n \left[1 - \frac{(Bi_o N_H + \alpha_n^2)}{(N_H^2 + \alpha_n^2)} \right] \quad (3.90)$$

$$E_1 = \exp$$

Introducing
(3.91) and
reduced to

$$E_1 =$$

where all ne
 E_1 from equ
defining new

$$B_m \lambda_m + \sum_n B_n$$

$$\sum_n [\Omega_m \sigma_n - (\Psi$$

$$\Omega_m \exp(-N$$

These eq
unknown const
to the left of the
ods were employ

$$\begin{aligned}
E_1 = \exp(-N_C) & \left[(T_{C,in} - T_o) - \sum_{n=0}^{\infty} A_n' \left\{ \mu_n L^* \left[1 + \frac{N_C Bi_o + \mu_n^2 L^{*2}}{N_C^2 - \mu_n^2 L^{*2}} \right] \cosh(\mu_n L^*) \right. \right. \\
& \left. \left. + N_C \left[\frac{N_C Bi_o + \mu_n^2 L^{*2}}{N_C^2 - \mu_n^2 L^{*2}} \right] \sinh(\mu_n L^*) \right\} \right. \\
& - \sum_{n=0}^{\infty} (B_n' + C_n') \left\{ \alpha_n \left[1 + \frac{N_C Bi_o - \alpha_n^2}{N_C^2 + \alpha_n^2} \right] \cos(\alpha_n) \right. \\
& \left. \left. + N_C \left[\frac{N_C Bi_o - \alpha_n^2}{N_C^2 + \alpha_n^2} \right] \sin(\alpha_n) \right\} \right] \quad (3.91)
\end{aligned}$$

Introducing variables to represent the large terms in equations (3.90) and (3.91) and converting B_n' and C_n' to B_n and C_n allows these equations to be reduced to

$$D_1 = (T_{H,in} - T_o) - \sum_{n=0}^{\infty} A_n \beta_n - \sum_{n=0}^{\infty} \left(B_n + C_n \frac{\alpha_n}{L^*} \right) \gamma_n \quad (3.92)$$

$$E_1 = \exp(-N_C) (T_{C,in} - T_o) - \sum_{n=0}^{\infty} A_n' v_n - \sum_{n=0}^{\infty} (B_n \sigma_n + C_n \tau_n) \quad (3.93)$$

where all new variables are defined in Appendix D. Substituting for D_1 and E_1 from equations (3.92) and (3.93) into equations (3.88) and (3.89) and defining new variables to convert the primed constants gives

$$\begin{aligned}
B_m \lambda_m + \sum_n B_n (\psi_{mn} - \gamma_n \omega_m) + \sum_n C_n \frac{\alpha_n}{L^*} (\psi_{mn} - \gamma_n \omega_m) = \\
- \omega_m (T_{H,in} - T_o) - \sum_n A_n (\rho_{mn,1} + \rho_{mn,2} + \rho_{mn,3} + \rho_{mn,4} - \omega_m \beta_n) \quad (3.94)
\end{aligned}$$

$$\begin{aligned}
\sum_n [\Omega_m \sigma_n - (\Psi B)_{mn}] B_n + C_m \Phi_m + \sum_n [\Omega_m \tau_n - (\Psi C)_{mn}] C_n = \\
\Omega_m \exp(-N_C) (T_{C,in} - T_o) + \sum_n A_n' (P_{mn,1} + P_{mn,2} + P_{mn,3} + P_{mn,4} - \Omega_m v_n) \quad (3.95)
\end{aligned}$$

These equations are now in the form that they were solved for the unknown constants. The equations are organized with functions of unknowns to the left of the equal sign and known quantities to the right. Standard methods were employed to solve the set of simultaneous equations described by

equations (3.94-95) and these methods are addressed in Appendix D. In short, the two equations were separated into coefficient of B_n and C_n for each eigenvalue and equation. These terms were put into a matrix and then solved for the unknown constants using a partial pivoting scheme with the Gauss method. Once the constants were determined, all solutions could be evaluated.

3.4

ana
of s
on
the
frar
the
wer

1. D

2. A

3. E

4. C

listin
of th
subr
tines
OUT
mari
the s
were

impo
data
while
optio
to be
param
anoth
param
ied.

equatic
the fun

3.4 Computer Program AXCOND

The development of the solution to this problem has been completely analytical up to this point. A closed form solution is not possible since a set of simultaneous equations must be solved for series constants, which depend on a truncation of the general series solutions obtained for the temperature of the wall and fluids, as discussed in the previous section. With the solution framework complete a computer program needed to be developed to perform the evaluation of the analytical solution. The main functions of the program were to:

1. Determine the eigenvalues from the transcendental equations.
2. Assemble the set of simultaneous equations and solve for B_n and C_n .
3. Evaluate the series to calculate the temperatures of the wall and fluids.
4. Check that the boundary conditions are satisfied and that energy is conserved.

A FORTRAN program was developed to perform these functions and a listing of the program is given in Appendix F. In addition, a general flowchart of the program is shown in Figure 3.2. It contains a main program that calls subroutines to perform each of the individual tasks. There are nine subroutines in the program: INPUT0, INPUT1, ROOT, BUILD, GAUSS, PROFIL, OUT0, OUT1, and OUPUT. Each of these will be briefly discussed to summarize its function. In the program, variables were named to coincide with the solution shown herein, and deviations from the variables in the solution were noted.

The first two subroutines INPUT0 and INPUT1, as their names imply, import the data needed for a particular run. The former reads dimensional data in and computes the dimensionless parameters needed for computation; while the latter reads in the dimensionless parameters, depending on the option selected. In addition, INPUT1 allowed for a particular input parameter to be varied, with the first call to the subroutine reading in the data and the parameter to vary and subsequent calls updating the selected parameter for another computation. This option allowed for assessing the effect of various parameters on the solution by observing the results as one parameter is varied.

Subroutine ROOT is used to locate positive roots of the transcendental equation. It employs a marching scheme that searches for a change in sign of the function then backs up to locate the zero crossing, i.e. the root. A great

deal of time
the large c
tion and no

Ass
constants A
obtaining a
partial pivo

Term
solutions in
the derivat
lated. The
ated in the
and $x=L$) t

Equation (3
series. Usin
the fluid en
ditions on t
enabled a t
two checks
used to sele
ity of the so

The
tines OUTC
The main d
while OUT
the varied p
tine OUTPUT
tion if desir
file and ther
in the input
the results to

deal of time was spent to make this subroutine sufficiently robust to handle the large changes in magnitude of the parameters in the transcendental equation and not skip roots of the equation.

Assembling the matrix of simultaneous equation to be solved for the constants B_n and C_n was done in subroutine BUILD. This was the key step in obtaining a solution. After building the matrix, the subroutine GAUSS used a partial pivoting scheme to solve for the constants.

Temperatures for the wall and fluids were generated from the series solutions in the subroutine PROFIL. In addition to computing temperatures the derivatives of the temperatures with respect to the coordinates are calculated. The derivatives of the analytical series solutions were taken then evaluated in the subroutine. Also, to calculate heat loss from the wall ends ($x=0$ and $x=L$) the integral of the heat flux over the ends was taken

$$q|_{end} = \int_0^1 K_w \frac{\partial T_w}{\partial x^+} \Big|_{end} dy^+ \quad (3.96)$$

Equation (3.96) was determined analytically and programmed to evaluate the series. Using the derivatives of temperature it was possible to check whether the fluid energy balances equations were being met and if the boundary conditions on the wall were being satisfied. The heat losses from the ends enabled a total energy balance to be performed insuring conservation. These two checks, conserving energy and satisfying the boundary conditions, were used to select the number of terms to truncate the series and insure the validity of the solution.

The final three subroutines generate the output file for a run. Subroutines OUT0 and OUT1 correspond to the option listed earlier for the input. The main difference is that OUT0 produces the results of one computed run while OUT1 varies a particular parameter giving the results as a function of the varied parameter, but not listing the unchanged parameters again. Subroutine OUTPUT can write the fluid and wall temperatures as a function of position if desired. These temperature are only written if a flag is set in the input file and there are separate flags for the fluids and wall. Likewise, another flag in the input file can check that the boundary conditions are satisfied and write the results to the output file.

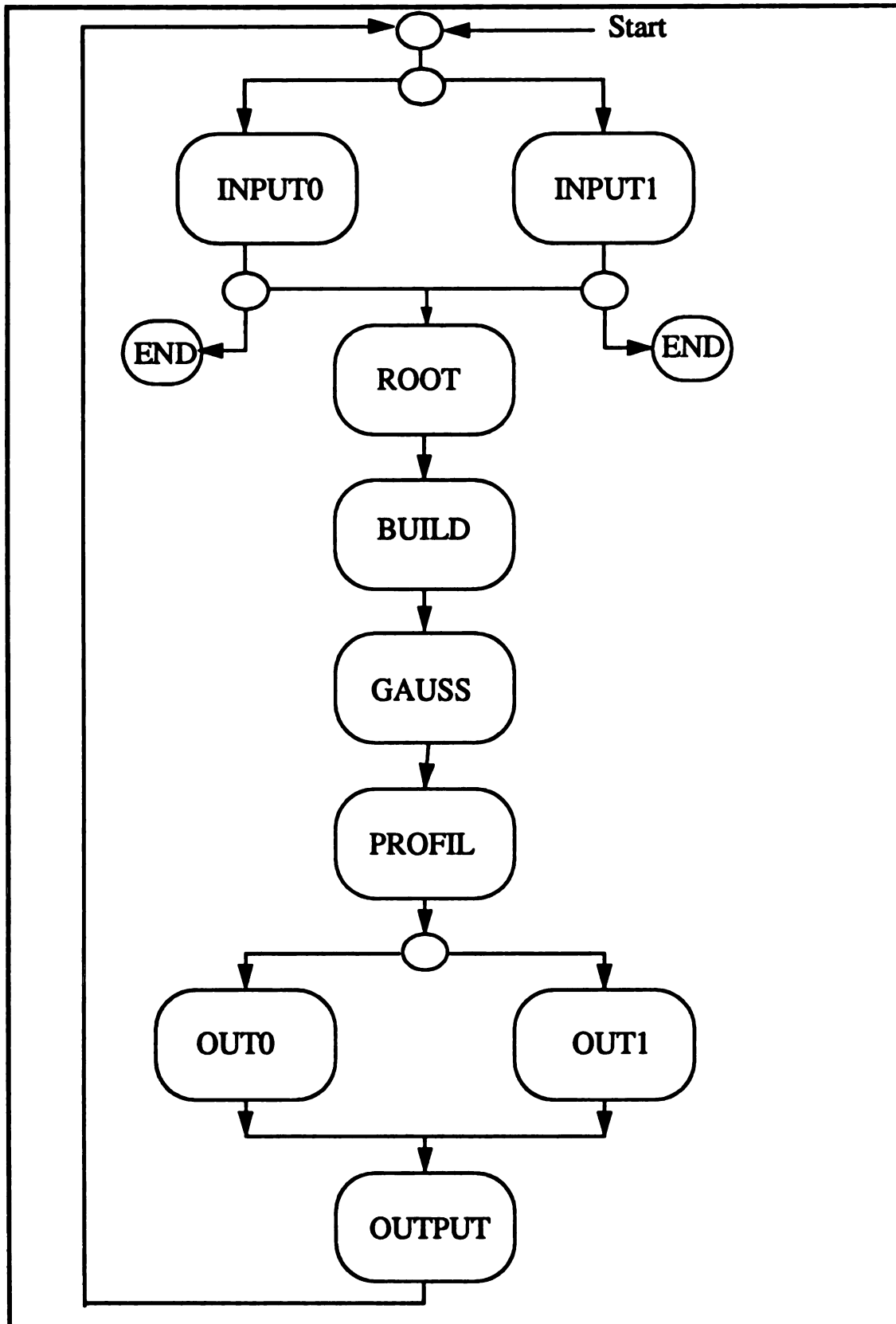


FIGURE 3.2. Flowchart of the FORTRAN program used compute a solution

4.0 Identifi

In the
dimensionless
form a link be
dimensionless
the wall aspect

and Biot numb

The parameters

In addition to the
wall ends (T_o and
 $T_{c,in}$) need to be
model can be so

Chapter 4

Results and Discussion

4.0 Identification of Input Parameters

In the formulation of the mathematical model for this problem certain dimensionless groups appeared (Chapter 2). These dimensionless parameters form a link between the mathematical model and the physical problem. The dimensionless parameters needed to solve the wall conduction equation are the wall aspect ratio

$$L^* = \frac{L}{\delta} \quad (4.1)$$

and Biot numbers for each surface of the wall

$$Bi_o = \frac{h_o L}{K_w} \quad (4.2)$$

$$Bi_L = \frac{h_L L}{K_w} \quad (4.3)$$

$$Bi_H = \frac{h_H \delta}{K_w} \quad (4.4)$$

$$Bi_C = \frac{h_C \delta}{K_w} \quad (4.5)$$

The parameters needed in the fluid energy balance equations were

$$N_H = \frac{h_H A_H}{C_H} = \frac{Bi_H K_w L^* w}{C_H} \quad (4.6)$$

$$N_C = \frac{h_C A_C}{C_C} = \frac{Bi_C K_w L^* w}{C_C} \quad (4.7)$$

In addition to these dimensionless parameters the ambient temperatures at the wall ends (T_o and T_L) and the initial or inlet condition for the fluids ($T_{H,in}$ and $T_{C,in}$) need to be specified. With these eleven parameters the mathematical model can be solved for the wall and fluid temperatures as functions of posi-

tic
co
pa
cu
ax
ne

de
ass
ne
enc
geo

This
the
mo
the
defi
mal
puti
para
phy

inde
com
tion.
tains
solu
capa
mum
tions.
signif

tion. There are then eleven independent variables that may influence axial conduction as the problem was formulated. The investigation of all eleven parameters to determine their influence on axial conduction presents a difficult task. To reduce the number of independent variables, quantification of axial conduction will be shown by evaluating the solution using effectiveness- NTU relationships.

Presenting the solution in terms of the effectiveness eliminates the dependence of the solution on any of the ambient or fluid temperatures, assuming a constant ambient temperature ($T_o = T_L$); because the effectiveness is based on temperature differences and scaled by the temperature difference at the fluid inlets. The NTU , which represents the physical and thermal geometry of the heat exchanger, was earlier shown in Section 2.3 as

$$NTU = w \frac{K_w}{C_{min}} L^* \left[\frac{Bi_H Bi_C}{Bi_H + Bi_H Bi_C + Bi_C} \right] \quad (4.8)$$

This equation introduces the need for specifying the thermal conductivity of the wall and the minimum heat capacity; whereas for the mathematical model, the thermal conductivity was accounted for in the Biot numbers and the heat capacity accounted for in N_C and N_H and did not need to be explicitly defined. It was decided that since the additional parameters of the wall thermal conductivity and minimum heat capacity need to be specified for computing NTU , they could also be used to compute N_C and N_H from the other parameters, as shown in equations (4.6) and (4.7). This allows for the more physical parameter of heat capacity to be input.

The wall thermal conductivity and minimum heat capacity do not independently affect the solution because they appear only as a ratio used to compute the NTU in equation (4.8) and the parameters N_H and N_C in equations (4.6) and (4.7). It does not matter that the ratio in equations (4.6-7) contains the individual heat capacities rather than the minimum. Since the solution depends on the heat capacity ratio and the magnitudes of the heat capacity will be set by the ratio of the wall thermal conductivity and minimum heat capacity, the ratio will be accounted for in at least one of the equations. Therefore, the individual magnitude of these variables is not significant.

The
 mum heat c
 cific proper
 dimensionle
 adjusted to
 these variab
 group of ten
 variable wil

where the w
 definition. S

The Mondt
 After specif
 number is se
 number can
 is important.

TABLE 4.1. I

Input Param
L
Bi_o
Bi_L
Bi_C
Bi_H
K_w
C_C
C_H
$T_{H, in}$
$T_{C, in}$
T_o
T_L

The appearance of the ratio of the thermal conductivity to the minimum heat capacity provides some additional flexibility to this study. The specific properties of the wall and fluids do not need to be specified, and a dimensionless analysis can be performed. Furthermore, this ratio can be adjusted to provide the desired magnitude of NTU . To present the ratio of these variables, a new dimensionless variable will be defined to represent the group of terms that are not dimensionless in the NTU in equation (4.8). This variable will be the Mondt number, from Rohsenow [17]

$$M_o \equiv \frac{K_w w}{C_{min} L^*} \quad (4.9)$$

where the wall aspect ratio was included to be consistent with Rohsenow's definition. Substituting the Mondt number into equation (4.8) gives

$$NTU = M_o L^{*2} \left[\frac{Bi_H Bi_C}{Bi_H + Bi_H Bi_C + Bi_C} \right] \quad (4.10)$$

The Mondt number will be used as the adjustable parameter in this study. After specifying the fluid Biot numbers and wall aspect ratio, the Mondt number is set to provide the desired NTU . The magnitudes of the Mondt number can be looked at to correlate the conditions in which axial conduction is important.

TABLE 4.1. Input variables and dependency for determining heat exchanger performance

Input Parameters	Mathematical Model	NTU	Effectiveness
L^*	L^*	L^*	L^*
Bi_o	Bi_o	Bi_C	Bi_o
Bi_L	Bi_L	Bi_H	Bi_L
Bi_C	Bi_C	M_o	Bi_C
Bi_H	Bi_H		Bi_H
K_w	N_C		C_R
C_C	N_H		M_o
C_H	$T_{H,in}$		
$T_{H,in}$	$T_{C,in}$		
$T_{C,in}$	T_o		
T_o	T_L		
T_L			

Present
number of ind
obtain a soluti
were used to c
and *NTU* show
allows for the
with this soluti
tiveness, will d
of Table 4.1.

An addit
terms needed b
vious discussio
overlooked in t
the series soluti
ary conditions
fied. Since these
applying this cr
verge. Another
tion. This check
from the hot flu
tion from the w
of the results, u
validity of the s

The influ
solution would
However, the b
considered; but
a smaller numbe
simplified expre

4.0.1 Presentation

It was ant
strated through
(shown in Table
their influence o

Presenting the results in an effectiveness- NTU format will reduce the number of independent variables. The input parameters that were specified to obtain a solution are shown in the first column of Table 4.1. These parameters were used to calculate the information needed for the mathematical model and NTU shown in columns two and three in Table 4.1. This information allows for the mathematical model to be solved and a NTU to be associated with this solution. However, the solution, which will be in the form of effectiveness, will depend only on the seven parameters shown in the last column of Table 4.1.

An additional input that is not listed in Table 4.1 was the number of terms needed before the series is truncated, N . It was not included in the previous discussion because it lacks any physical significance, but it was not overlooked in the analysis. The value of N must be sufficiently large to allow the series solutions to converge. Taking this criteria a step further, the boundary conditions on the wall were checked to ensure that they were being satisfied. Since these boundary conditions involve the wall and fluid temperatures, applying this criteria is equivalent to having all three series solutions converge. Another check performed was an overall energy balance of the solution. This checked that the solution conserved energy, i.e. the energy lost from the hot fluid was accounted for in the cold fluid and/or lost by convection from the wall ends. Although magnitudes of N will not be shown in any of the results, using those two criteria the value of N was chosen and the validity of the solution assured for all results reported.

The influence of N was not investigated in any detail. In general, the solution would converge based on an energy balance within 10-20 terms. However, the boundary conditions would not be met until more terms were considered; but the solution ($\epsilon - NTU$) did not change from the values seen at a smaller number of terms. These results suggest it may be possible to obtain simplified expressions for the solution, but this point was not pursued further.

4.0.1 Presentation of Results

It was anticipated that the effect of axial conduction could be demonstrated through the seven variables upon which the effectiveness depends (shown in Table 4.1). These variables were to be investigated to determine their influence on the performance of the heat exchanger. In order to present

these results it is useful to introduce a final variable that will describe the degradation in the performance of a heat exchanger. It is called the ineffectiveness, and it represents the amount that a heat exchanger's performance is reduced due to the effect of axial conduction. It is defined by

$$i_C = \frac{\epsilon_{Neg} - \epsilon_C}{\epsilon_{Neg}} \quad (4.11)$$

$$i_H = \frac{\epsilon_{Neg} - \epsilon_H}{\epsilon_{Neg}} \quad (4.12)$$

where ϵ_{Neg} is the effectiveness calculated neglecting axial conduction using equation (1.25), which assumes one-dimensional heat flow. The ineffectiveness must be defined for both hot and cold fluids since the energy balances may differ due to heat lost from the wall ends. For the case that there is negligible heat loss from the ends of the wall, the two values for ineffectiveness are equal

$$i_C = i_H \equiv i \text{ for } \epsilon_C = \epsilon_H \quad (4.13)$$

Note that when the ineffectiveness is zero there is no degradation in the performance of the heat exchanger due to axial conduction, indicating that axial conduction is negligible. In addition to showing when axial conduction is not negligible, the ineffectiveness gives the magnitude that the effectiveness would be over-estimated or in some special cases under-estimated, using a standard effectiveness- NTU relationship which neglects axial conduction. It is the percentage of error introduced from assuming that axial conduction is negligible.

4.1 Influence of Axial Conduction at a Constant NTU

To begin this parametric study the NTU will be held constant as other parameters are varied. Through some initial computer runs it was seen that a larger degradation in effectiveness was seen at higher values of NTU . Hence, a NTU of seven was chosen for the study. This allows the identification of the more important parameters and will give insight into the conditions under which axial conduction should not be neglected.

While maintaining a constant NTU , the Biot numbers are varied over a range from .0001 to .1, the heat capacity ratios of 1, .75, .50, and .25 are investigated, and the wall aspect ratio is also varied. Variation of the Biot numbers will be done by grouping all four or grouping the ends and the hot and cold side. Although grouping all the Biot numbers may be unrealistic, it will provide insight for future more realistic cases.

4.1.1 Influence of the Wall Aspect Ratio (L^*)

A natural choice to begin this parameter study is with the wall aspect ratio, which will address the physical dimensions for which axial conduction should not be assumed negligible and may need further investigation. Also, by beginning with the wall aspect ratio some bounds can be established on the other parameters that need to be investigated. This is achieved by eliminating ranges of the other parameters for which axial conduction only occurs under unrealistic physical dimensions. All four wall Biot numbers were set equal, and the magnitudes were varied beginning with .1 and decreasing an order of magnitude each run to the final value of .0001. The results, showing ineffectiveness as a function of the wall aspect ratio, are presented for the different Biot numbers in Figures 4.1-4.4 with each figure depicting a different heat capacity ratio.

Examination of the data, prior to plotting figures, showed a negligible difference in the effectiveness based on the cold fluid and the effectiveness based on the hot fluid ($\epsilon_C = \epsilon_H$). For this reason, only one ineffectiveness was plotted in Figures 4.1-4.4. There was a slight deviation from the two effectivenesses being equal for very low magnitudes of the wall aspect ratio ($L^* < 40$). Because this effect is not related to axial conduction and merely demonstrates the effect of the wall aspect ratio becoming very small, it was not included in Figures 4.1-4.4.

The ϵ represents a nonzero. Due to the effect of the degradation, the maximum heat transfer numbers through the characteristic values

The ϵ can be explained by the exchanger value

For a plane value

It can then be seen that the resistance becomes smaller and will lead to a larger degradation

In conclusion, the effectiveness of the heat exchanger is expected. Due to the effective heat transfer, the definition of the

The results indicate that as the aspect ratio decreases, which physically represents a thick wall or short heat exchanger, the ineffectiveness becomes nonzero. Depending on the heat capacity ratio (C_R), one finds a degradation in the effectiveness from 20% at small C_R to nearly 50% at C_R equal to one. The degradation is further enhanced as the wall Biot numbers decrease. A maximum Biot number of .1 is shown in the figures, since for larger Biot numbers the ineffectiveness only departs from zero for very small and unrealistic values of the wall aspect ratio.

The trend of increasing ineffectiveness with decreasing aspect ratio can be explained by considering the thermal resistances across the heat exchanger wall in the two principal directions

$$R_{Streamwise} = \frac{L}{K_w A_x} \quad (4.14)$$

$$R_{normal} = \frac{\delta}{K_w A_y} \quad (4.15)$$

For a plane wall $A_x = w\delta$ and $A_y = wL$ giving

$$R_{Streamwise} = \frac{L^*}{K_w w} \quad (4.16)$$

$$R_{normal} = \frac{1}{K_w w L^*} \quad (4.17)$$

It can then be noted that as L^* becomes small, the streamwise thermal resistance becomes small while the normal thermal resistance becomes large. This will lead to a greater energy flow in the streamwise direction and ultimately a larger degradation of the effectiveness.

In considering the influence of the Biot number on the degradation of the effectiveness, the increase in ineffectiveness with decreasing Biot number is expected. Decreasing the Biot number results in a reduction in the convective heat transfer at the surface of wall and/or an enhancement of the conductive heat transfer within the wall, which is shown by considering the definition of the Biot number

$$Bi \equiv \frac{R_{normal}}{R_{convection}} = \frac{\delta/K_w A_y}{1/h A_y} = \frac{\delta h}{K_w} \quad (4.18)$$

also
fun
me
cap
rati
par
lui
nu
xc

Both these trends lessen the influence of axial conduction since energy moves more freely from the surface while encountering more difficulty conducting within the heat exchanger wall. This is further seen by observing the temperature profile along the wall. These results are shown in Figure 4.5. Notice that the temperature profile along the wall flattens as the Biot numbers decrease, that is, the temperature at the ends of the heat exchanger becomes closer to the temperature at the center of the heat exchanger as the Biot numbers decrease. This is the effect of axial conduction moving energy along the length of the heat exchanger wall. Coupling the effect of the Biot numbers to the wall aspect ratio follows.

As the Biot numbers decrease, the alternate path of heat flow along the wall becomes more influential. At the smaller Biot numbers the wall aspect ratio has less influence because the convective resistance is so high. Therefore, the wall aspect ratio requires a larger magnitude to reduce the normal resistance or increase the streamwise resistance to the point that axial conduction will not occur. Hence the smoothing of the curves in Figures 4.1-4.4 as the Biot numbers decreased.

The final dependency that can be observed in Figures 4.1-4.4 is the influence of the heat capacity ratio. To aid in this comparison, Figure 4.6 was generated, which illustrates how the heat capacity affects the solution for a Biot number of .001. This figure does not provide any new information, it instead combines a curve from Figures 4.1 through 4.4 into a single figure. In Figure 4.6 it is seen that, at a particular Biot number, the ineffectiveness increases as the heat capacity ratio increases. This trend is not a physically obvious result.

To better understand the effect, the dimensionless temperature profile along the heat exchanger at a wall aspect ratio of 100 was generated as a function of heat capacity ratio and is shown in Figure 4.7. In this figure the median wall temperature shows little or no variation in shape with heat capacity ratio, the curves increase a constant amount as the heat capacity ratio decreased. This can be explained through the existence of a greater disparity in the amount of energy per degree of temperature between the two fluid streams as the heat capacity ratio decreases. The stream with the maximum heat capacity will undergo a smaller temperature change in the heat exchanger than the fluid with the minimum heat capacity. Thus, the fluid with

the maximum
with the minimum
change, as the
energy to raise the
temperature as the
wall does not
examination

For maximum
dimensionless temperature
dimensionless
capacity ratio
effect of axial
heat exchange
energy balance

However, in the
energy exchange

for $C_H \geq C_C$

TABLE 4.2
heat capacity

C_R
1.0
.75
.50
.25

the maximum heat capacity can cause a larger temperature change in the fluid with the minimum heat capacity while experiencing less of a temperature change, as the heat capacity ratio decreases. Therefore, there exists more energy to raise the temperature of the wall which results in a larger wall temperature as the heat capacity ratio decreases. The elevated temperature of the wall does not explain the decreased ineffectiveness, however; and further examination is needed.

For more insight into the effect of the heat capacity ratio the dimensionless temperature profiles of the hot and cold fluids were added to the dimensionless wall temperatures and are shown in Figure 4.8, with a heat capacity ratio of .75 omitted for clarity. This figure clearly demonstrates the effect of axial conduction, which moves the energy along the length of the heat exchanger within the wall. The magnitude of which can be gauged by an energy balance on the fluids. For negligible axial conduction

$$C_H \frac{d\Theta_H}{dx^+} = C_C \frac{d\Theta_C}{dx^+} \quad (4.19)$$

However, if axial conduction is present there exist a local imbalance in the energy exchange between the fluids and equation (4.19) becomes

$$\left(\frac{d\Theta_H}{dx^+} - C_R \frac{d\Theta_C}{dx^+} \right) \propto q_{Axial} \quad (4.20)$$

for $C_H \geq C_C$, which can be rearranged to give

TABLE 4.2. Relationship between the slope of the hot and cold fluid's temperature profile and the heat capacity ratio

C_R	$\frac{d\Theta_H/dx^+}{C_R (d\Theta_C/dx^+)}$		
	$x^+ = 0$	$x^+ = 0.5$	$x^+ = 1$
1.0	15.68	1.00	1/15.63
.75	15.53	1.28	1/11.58
.50	14.29	1.81	1/7.75
.25	13.5	2.67	1/4.95

Using
excha
the ho
show
and a
for ne
when

decre
excha
shows
 $x^+ =$
Figure
ture p
heat a
onstra
ratio.

ing a
There
the ca
There
on op
the h
temp

nitue
cold
on th
the H
the v

$$\left(\frac{d\Theta_H/dx^+}{C_R(d\Theta_C/dx^+)} - 1 \right) \propto q_{Axial} \quad (4.21)$$

Using equation (4.21), axial conduction at different locations along the heat exchanger can be assessed. To help quantify the differences in the slope of the hot and cold fluid temperature profiles Table 4.2 was created, which shows the ratio on the left hand side of equation (4.21) at various locations and as a function of the heat capacity ratio. This ratio should be nearly one for negligible axial conduction and considerably smaller or larger than one when axial conduction is appreciable.

The data in Table 4.2 demonstrates that as the heat capacity ratio decreases, axial conduction shows a local decrease at the ends of the heat exchanger; while it increases near the center. Comparison of the magnitudes shows the dominant effect at the $x^+ = 1$ end of the heat exchanger, while the $x^+ = 0$ end and center show less significant change. This can also be seen in Figure 4.8, more qualitatively, by a comparison of the slopes of the temperature profiles. The net effect on the heat exchanger is that axially conducted heat and ineffectiveness decrease as the heat capacity ratio decreases, as demonstrated in Figure 4.6 where ineffectiveness decreases with heat capacity ratio.

The difficulty with interpreting this case is that both solutions, including and neglecting axial conduction, change with the heat capacity ratio. Therefore, it is required to analyze why the solution more closely resembles the case of neglecting axial conduction as the heat capacity ratio decreases. There are two related reasons. The first is the change in the available energy on opposite sides of the wall. Second is the change in the driving potential on the hot side of the wall, which is the difference between the fluid and wall temperatures.

The smaller heat capacity ratios were obtained by increasing the magnitude of the hot fluid heat capacity while maintaining the heat capacity of the cold fluid. Providing more energy per degree on the hot side of the wall than on the cold side and this disparity in energy across the wall becomes larger as the heat capacity ratio decreases. This situation was earlier shown to increase the wall temperature.

from
obse

The
has b
pote
ture.
incre
cons

ener
to th
Beca
ratio
its te

on th
Figur
figur
it inc
capa
effec
the i
the r

whic
this
desi
bers
mai
heat
Ref

The increased driving potential on the hot fluid side of the wall results from the increase in the heat capacity of this fluid, which can be shown by observing the describing equations for the hot fluid, from equation (2.15)

$$C_H \frac{dT_H}{dx^+} + Bi_H K_w L^* w [T_H(x^+) - T_w(x^+, 0)] = 0 \quad (4.22)$$

The dimensionless parameter previously introduced in this equation (N_H) has been separated into components to isolate the heat capacity. The driving potential balances the product of the heat capacity and slope of the temperature. Therefore, when the heat capacity increases, the driving potential must increase to balance the equation since the slope of the temperature remains constant.

The outcome of these two effects is that the cold fluid acquires more energy at or near its inlet, due to the hot fluid having more energy to transfer to the cold fluid and the increased driving potential to move more energy. Because both these effects become more pronounced as the heat capacity ratio decreases, the cold fluid will depend less on axial conduction to provide its temperature rise and the ineffectiveness will decrease.

Having an understanding of the overall effect of the heat capacity ratio on the performance of the heat exchanger, it is now possible to refer back to Figure 4.6 and the influence of the wall aspect ratio can be addressed. In this figure it is seen that the wall aspect ratio reduces the ineffectiveness to zero as it increases, and the convergence to zero is more pronounced at lower heat capacity ratios. The increased convergence to zero is a consequence of the effect of axial conduction already reduced by the heat capacity ratio, and then the influence of the wall aspect ratio requires a smaller magnitude to decrease the normal resistance and eliminate axial conduction.

The product of $M_o L^{*2}$ is shown in the legend of Figures 4.1-4.4, from which the Mondt number can be calculated. The use of the Mondt number in this study was as a variable parameter, which could be adjusted to provide the desired NTU as the other parameters were varied. In general, as the Biot numbers and wall aspect ratio increased; the Mondt number was decreased to maintain a constant NTU , while the Mondt number was independent of the heat capacity ratio because the minimum heat capacity remained constant. Referring to equation (4.8) for NTU , as the wall aspect ratio and Biot num-

bers were increased
by the ratio K
unit width.

The tre
reaction to ch
essence, the
properties to
the Mondt nu
increase since
be available.
by only the n

bers were increased, the noted trend in the Mondt number was accomplished by the ratio K_w / C_{min} becoming smaller because the analysis was based on a unit width.

The trends seen in the Mondt number to maintain a constant NTU are a reaction to changes made in the wall aspect ratio and Biot numbers. In essence, the Mondt number is compensating the wall (K_w) and fluid (C_{min}) properties to match the conditions (Bi_H, Bi_C, L^*). Therefore, it is fitting that the Mondt number decreases as the wall aspect ratio and fluid Biot numbers increase since more energy can be transferred for these conditions and must be available. This outcome suggest that axial conduction may be described by only the magnitude of the Mondt number. A point to be investigated later.

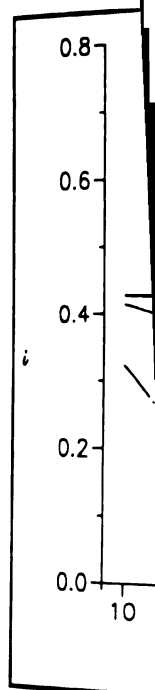


FIGURE 4.1. Inc

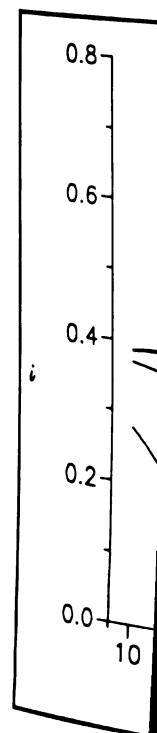


FIGURE 4.2. Inc

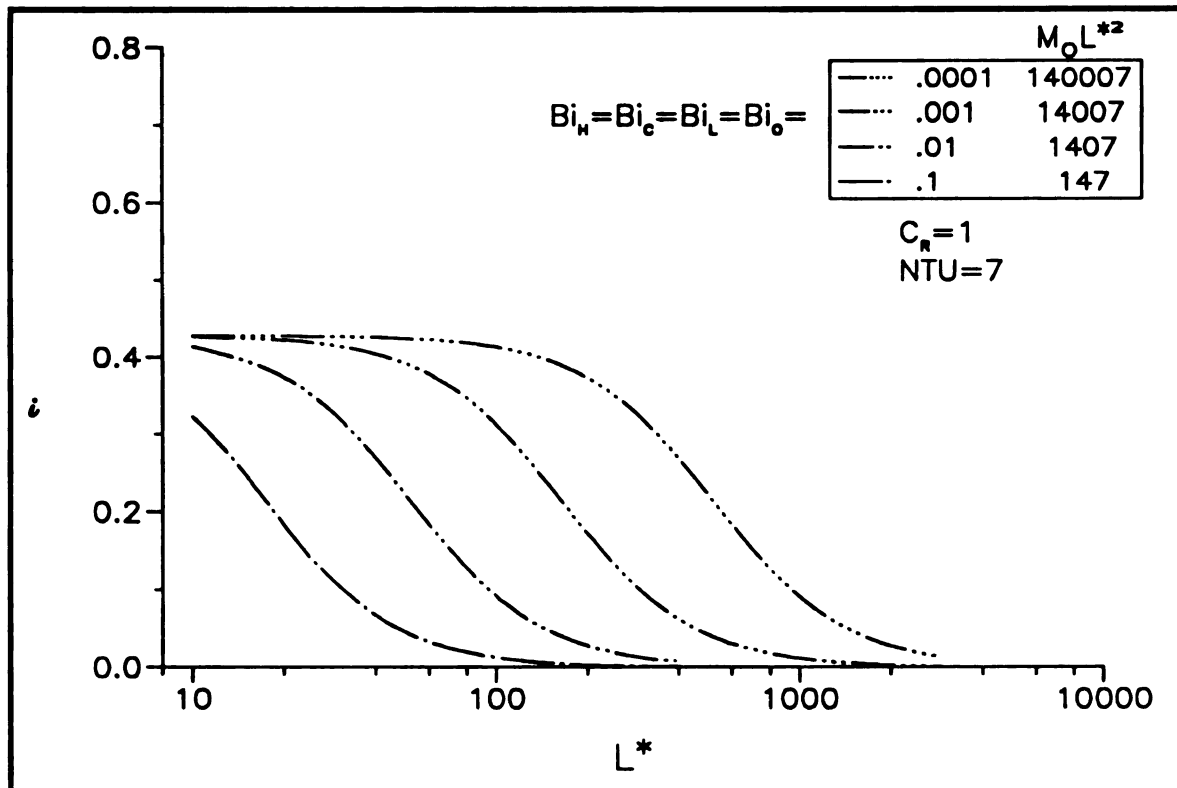


FIGURE 4.1. Ineffectiveness as a function of the wall aspect ratio for $NTU = 7$ and $C_R = 1$

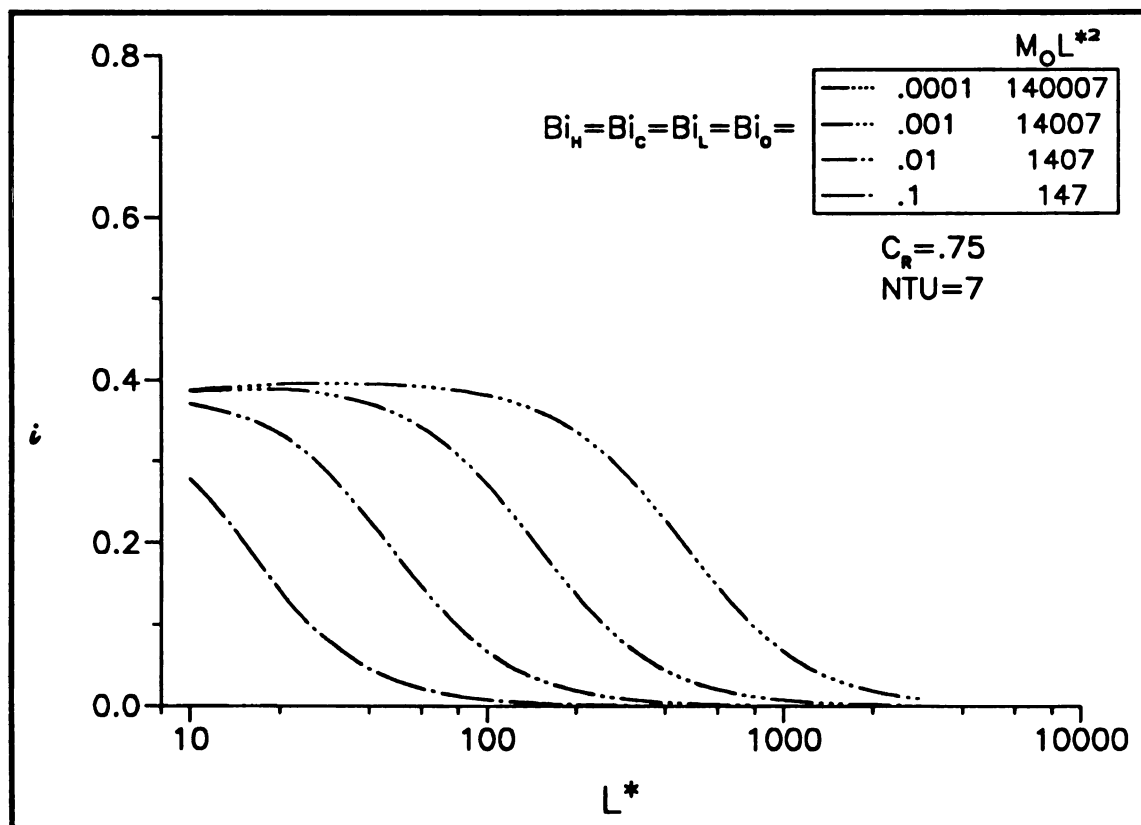


FIGURE 4.2. Ineffectiveness as a function of the wall aspect ratio for $NTU = 7$ and $C_R = .75$

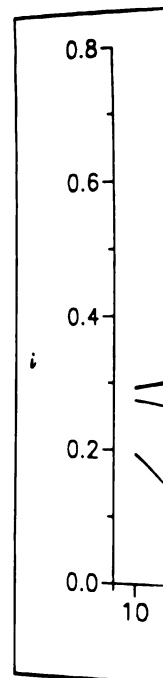


FIGURE 4.3. Inc

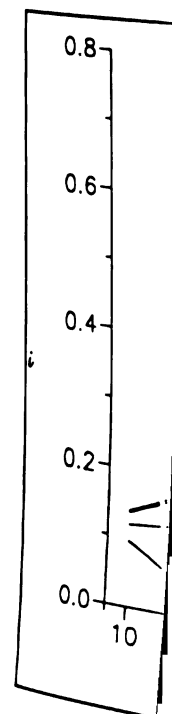


FIGURE 4.4. Inc

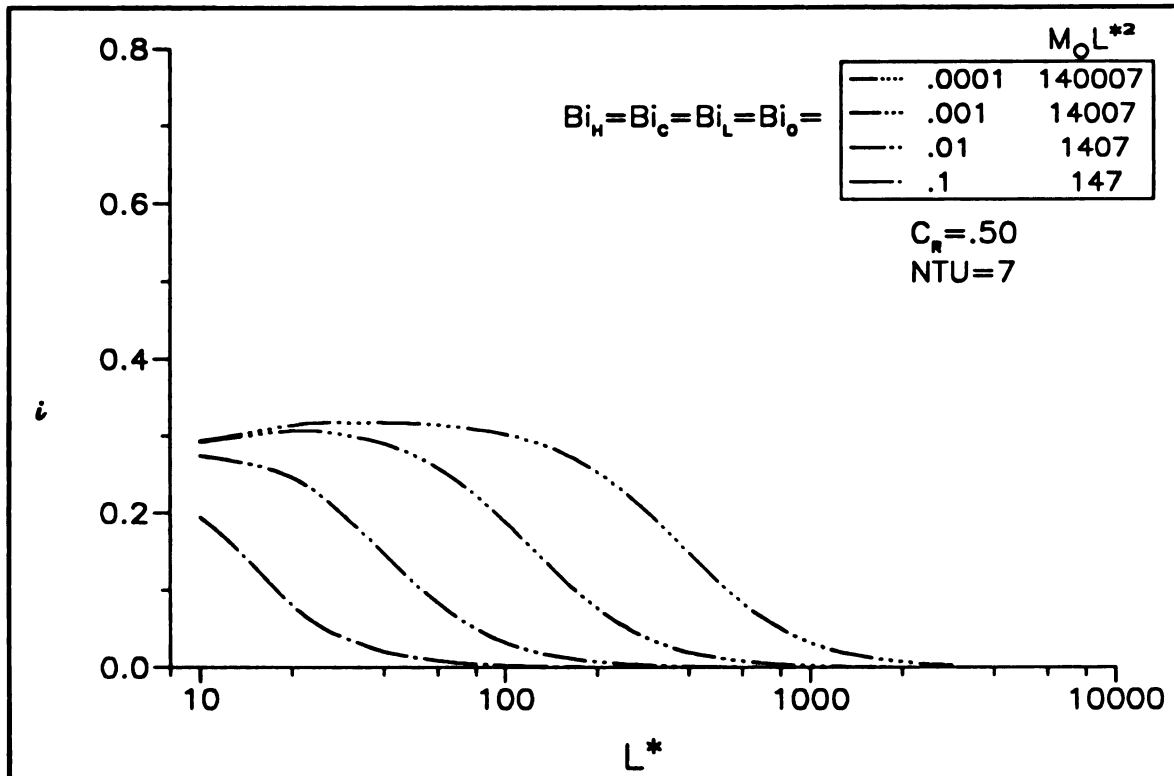


FIGURE 4.3. Ineffectiveness as a function of the wall aspect ratio for $NTU = 7$ and $C_R = .50$

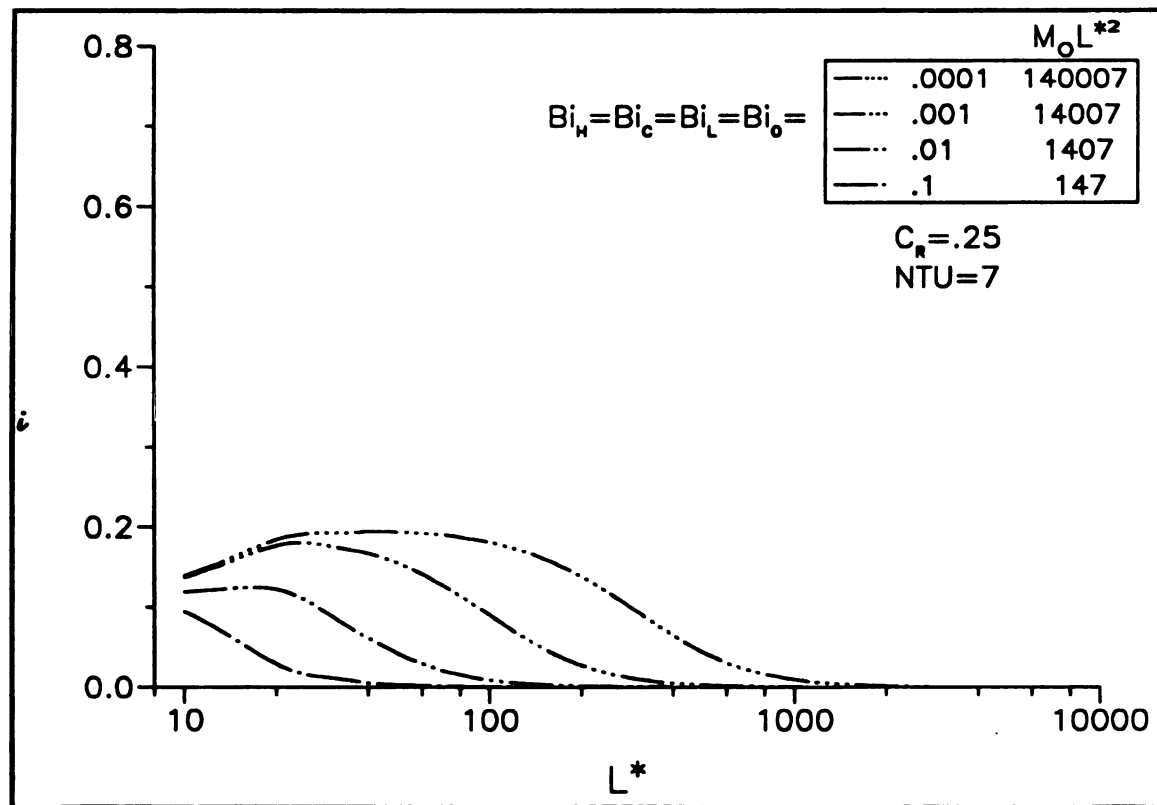


FIGURE 4.4. Ineffectiveness as a function of the wall aspect ratio for $NTU = 7$ and $C_R = .25$

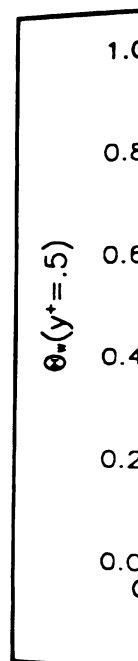


FIGURE 4.3
Biot number

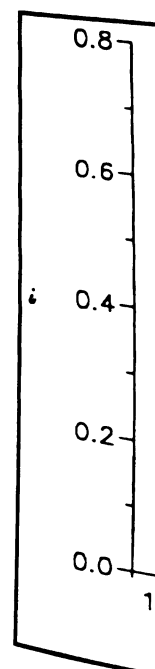


FIGURE 4.4
NTU = 7

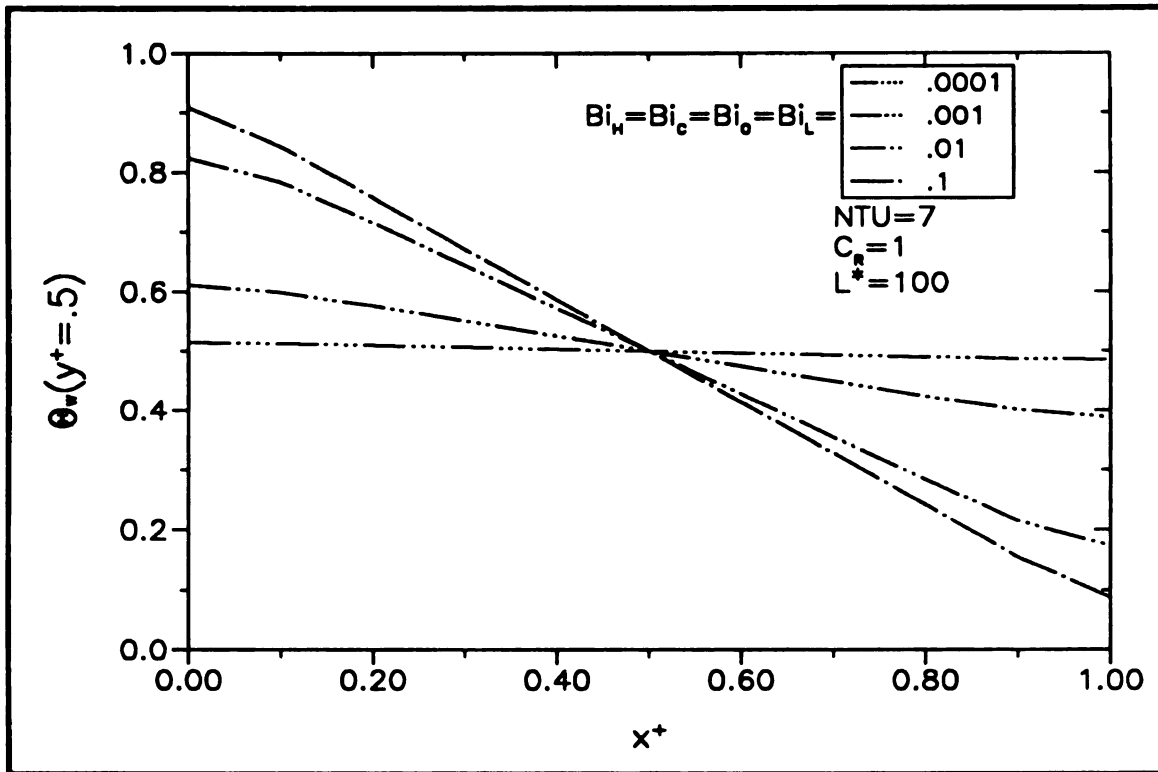


FIGURE 4.5. Median dimensionless wall temperature as a function of dimensionless position and Biot numbers for $NTU = 7$, $L^* = 100$, and $C_R = 1$

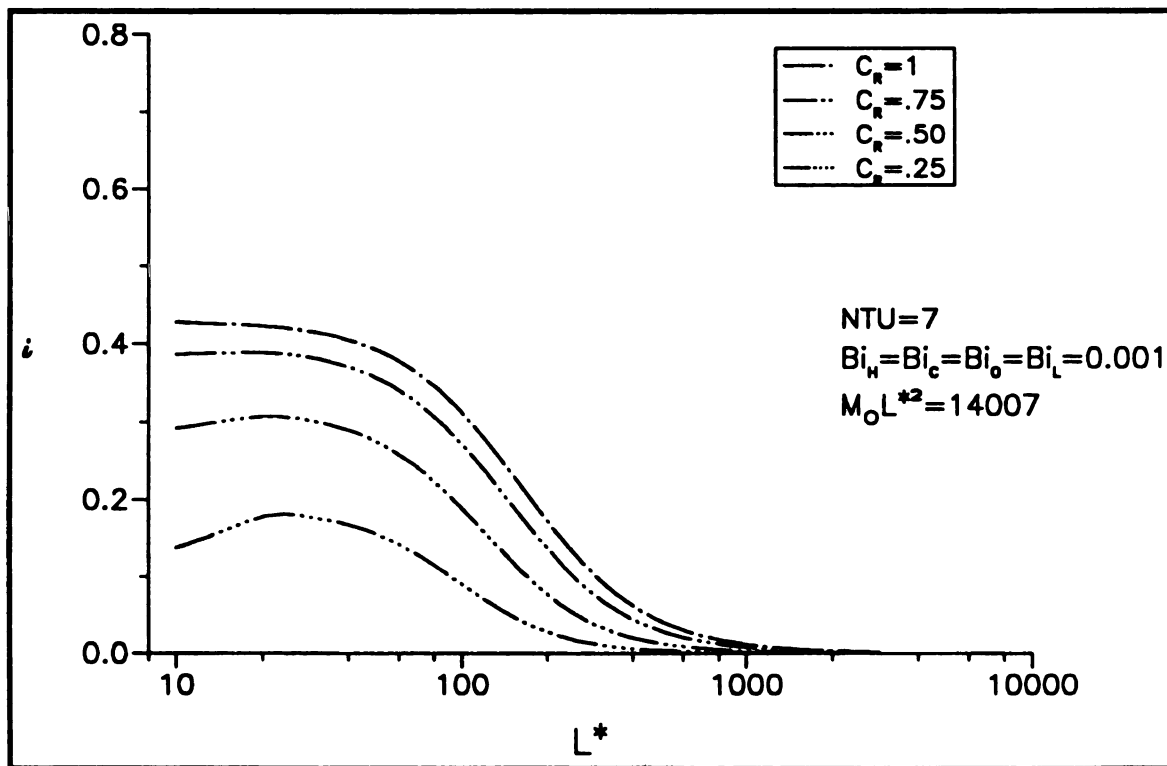


FIGURE 4.6. Ineffectiveness as a function of the wall aspect ratio and heat capacity ratio for $NTU = 7$, $L^* = 100$, and all Biot numbers equal .001

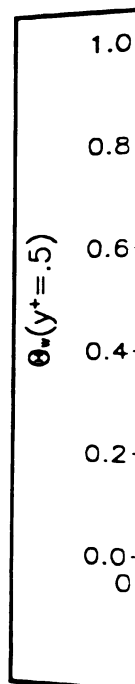


FIGURE 4.
heat capacity

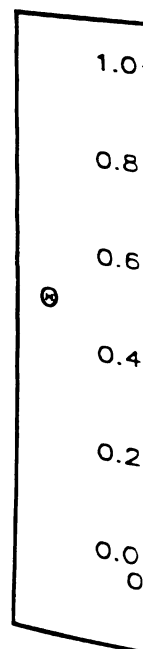


FIGURE 4J
position and

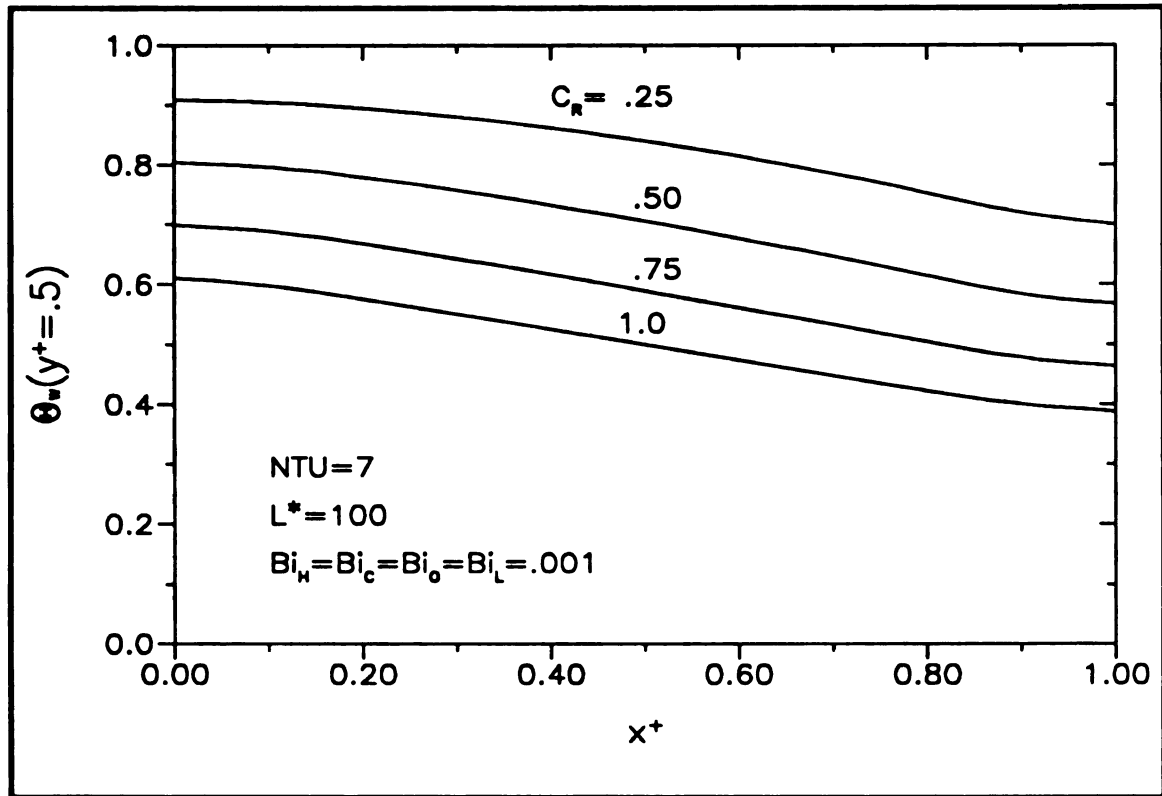


FIGURE 4.7. Median dimensionless wall temperature as a function of dimensionless position and heat capacity ratio for $NTU = 7$, $L^* = 100$, and all Biot numbers equal .001

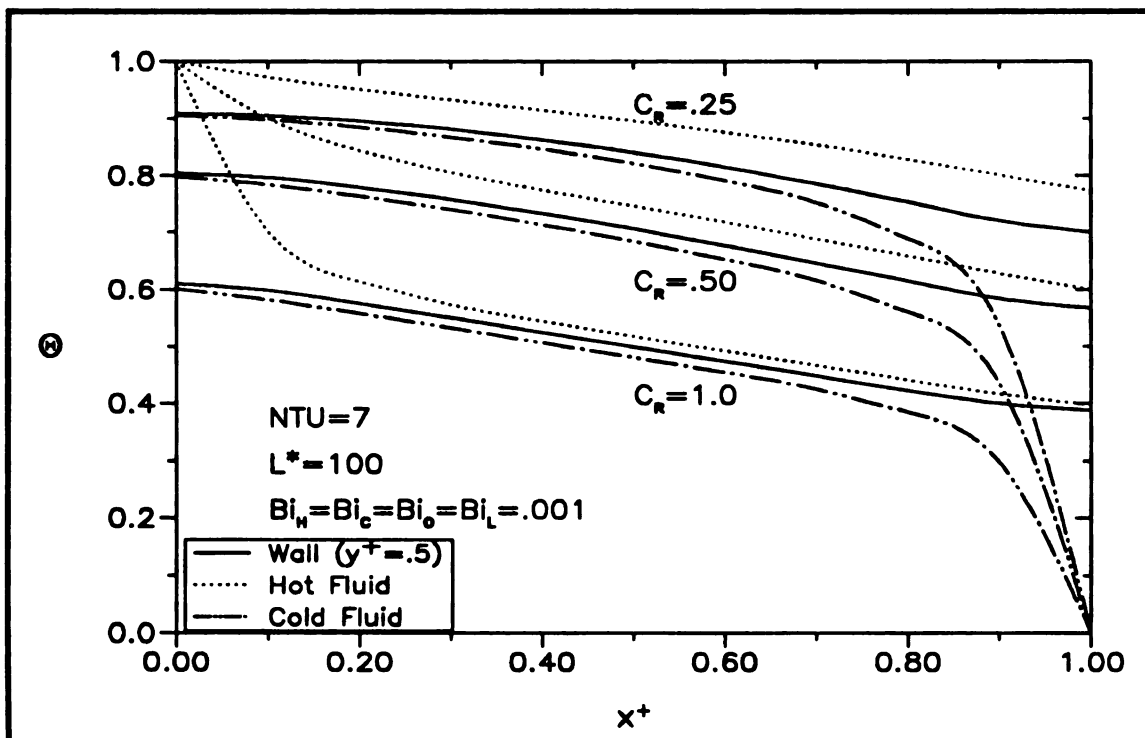


FIGURE 4.8. Median dimensionless wall and fluid temperature as a function of dimensionless position and heat capacity ratio for $NTU = 7$, $L^* = 100$, and all Biot numbers equal .001

4.1.

con
end
col
cas
cas
as i
as t
nitu
Bio
tran
tic l

hel
the
ity
fun
tion
Not
zer
two
and
alw

the
nun
incr
form
bers
incr
ence

be n
the h

4.1.2 Influence of the Wall End Biot Numbers (Bi_o and Bi_L)

During the investigation of the wall aspect ratio it was determined that convective losses from the ends of the heat exchanger wall are negligible if the end Biot numbers are less than or equal to the fluid Biot numbers (hot and cold side Biot numbers). This dependence will be further investigated for cases that have end Biot numbers greater than the fluid Biot numbers. These cases are physically possible since the end Biot numbers have the wall length as its characteristic length and the fluid Biot numbers have the wall thickness as the characteristic length, as shown in equations (4.2)-(4.5). Thus, the magnitude of the end Biot numbers being greater than the magnitude of the fluid Biot numbers does not require the same dependence on the convective heat transfer coefficients, a case that would be unrealistic, because the characteristic lengths proportionately increase the end Biot numbers.

Following a similar procedure as the previous section the NTU will be held at seven while the end Biot numbers are varied. The same magnitudes of the hot and cold side Biot number will be investigated at the four heat capacity ratios for a prescribed wall aspect ratio of 100. The ineffectiveness as a function of the end wall Biot numbers ($Bi_o = Bi_L$) are shown for these conditions in Figures 4.9-4.12, with a different heat capacity ratio in each figure. Notice for these figures that each curve has a starting point at approximately a zero end Biot number, then is double valued for larger end Biot numbers. The two values at each end Biot number are the ineffectiveness based on the hot and cold fluids. For a specified end Biot number, the cold ineffectiveness is always greater than or equal to the hot ineffectiveness in absolute magnitude.

Observing Figure 4.9, which shows the ineffectiveness as a function of the end Biot number for a heat capacity of one, the effect of the end Biot number is seen. As the end Biot numbers increase i_H decreases while i_C increases, for all fluid Biot numbers investigated. This divergence of the performance based on the hot and cold fluids is expected as the end Biot numbers increase because the heat lost by convection from the ends similarly increases resulting in an energy imbalance between the fluids and a difference in the ineffectiveness based on the hot or cold fluid.

Recalling that an ineffectiveness of zero implies axial conduction can be neglected, it is seen for smaller fluid Biot numbers that the performance of the heat exchanger is actually enhanced, as noted by the ineffectiveness based

on the hot fluid being negative. That is, the effectiveness calculated based on the hot fluid is greater than the effectiveness calculated neglecting axial conduction. However, this enhancement of the performance based on the hot fluid is at the cost of the performance based on the cold fluid, as seen by the hot ineffectiveness being negative while the cold ineffectiveness approaches one. This outcome exists because the heat that is acquired from the hot fluid is lost from the wall ends and is not transferred to the cold fluid. The appropriateness of this result depends on the use of the heat exchanger. For removing heat from the hot fluid this outcome is beneficial, but for adding energy to the cold fluid the results are discouraging. In systems which have one stream as a waste stream, such as an automobile cooling system, this could be a useful result.

The fluid Biot numbers affect both the starting point of the curve and the amount that the ineffectiveness calculated based on the hot fluid diverges from the ineffectiveness based on the cold fluid. Figure 4.9 shows that the curves begin at a higher ineffectiveness and diverge a greater amount between the two ineffectivenesses as the fluid Biot numbers decrease. Further, the divergence of the two ineffectivenesses as the end Biot number increases occurs at a faster rate at smaller magnitudes of the fluid Biot number. There are three relevant observations to be made as the fluid Biot numbers decrease 1) the starting ineffectiveness increases, 2) the magnitude of the divergence of the two ineffectivenesses increases, and 3) the rate of the divergence with respect to the end Biot number increases. These points will be addressed in subsequent paragraphs.

The higher starting ineffectiveness of the curves is a consequence of the effect of axial conduction increasing as the fluid Biot numbers decrease. The basis of this outcome was addressed in the previous section.

The magnitude of the divergence of the ineffectivenesses increasing as the fluid Biot numbers decrease is also due to the effect of axial conduction increasing as the fluid Biot numbers decrease. Since energy is more likely to proceed along the heat exchanger as the fluid Biot numbers decrease, it follows that increasing end Biot numbers will result in more energy being removed. The additional energy removed results in an increase in the magnitude of the divergence as the fluid Biot numbers decrease, which correspondingly grows with the end Biot numbers.

Finally, addressing the rate of the divergence with respect to the end Biot numbers, which increases with the decreasing fluid Biot numbers, is again linked to the increased effect of axial conduction at lower fluid Biot numbers. With axial conduction being more prevalent at lower fluid Biot numbers it is expected that the sensitivity to the end Biot numbers will be greater at the lower fluid Biot numbers. With axial conduction more prevalent, a change in the end Biot number will have more effect than when axial conduction is less and the effect of the end Biot number is diminished. This sensitivity to the end Biot number is seen by the change in ineffectiveness as the end Biot numbers change, which explains the change in rate of divergence as the fluid Biot numbers decrease.

The influence of the heat capacity ratio requires a comparison of information from Figures 4.9-4.12. To aid in visualizing this information Figure 4.13 combines the curve for a fluid Biot number of .001 from each of the four figures, onto a single figure. In this figure the ineffectiveness is seen to increase as the heat capacity ratio increases, which was covered in an initial discussion of the heat capacity ratio, where this trend was also seen. However, as the heat capacity ratio varied; the end Biot number showed more influence on the hot ineffectiveness.

At a heat capacity ratio of one the curve for ineffectiveness based on the hot and cold fluids is symmetric. As the heat capacity ratio decreased, the curve for the ineffectiveness becomes asymmetric, sloping more on the lower leg. This leg of the curve represents the ineffectiveness based on the hot fluid. The change with heat capacity ratio represents the performance of the heat exchanger actually improving, as seen by the curving sloping more negative. The effect is due to the increased driving force, or larger difference between the hot fluid and wall temperature, on the hot side resulting in more energy available to the wall. This additional energy is then lost from the wall ends through convection.

For this case the Mondt number depends only on the hot and cold Biot numbers, and therefore was constant with respect to the end Biot numbers. For this reason little can be learned about the Mondt number by varying the end Biot numbers.

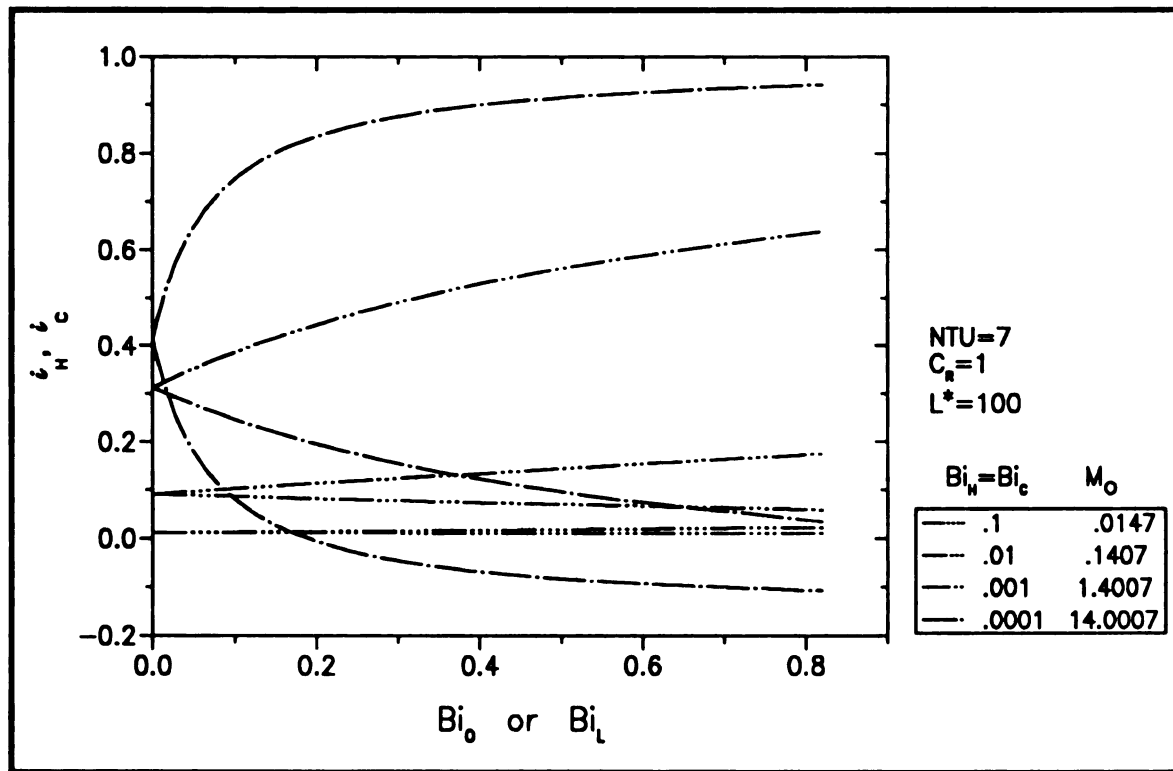


FIGURE 4.9. Ineffectiveness as a function of the end Biot numbers for $NTU = 7$, $L^* = 100$, and $C_R = 1$

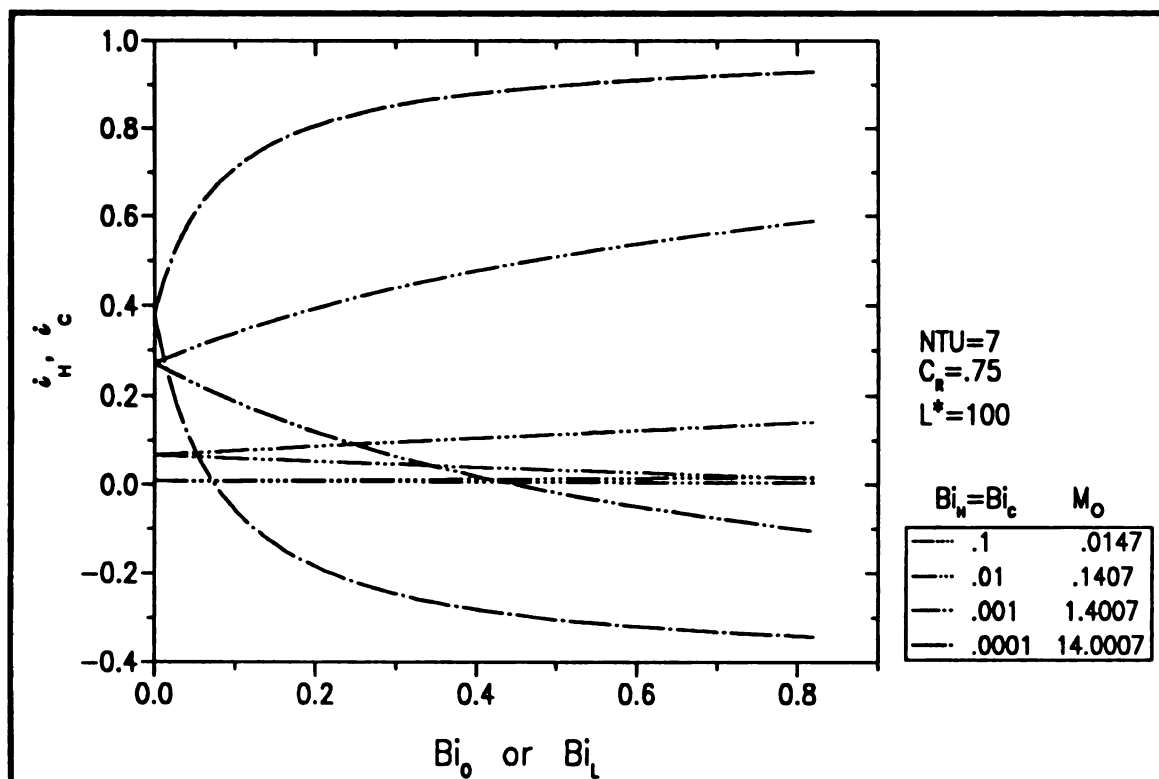


FIGURE 4.10. Ineffectiveness as a function of the end Biot numbers for $NTU = 7$, $L^* = 100$, and $C_R = .75$

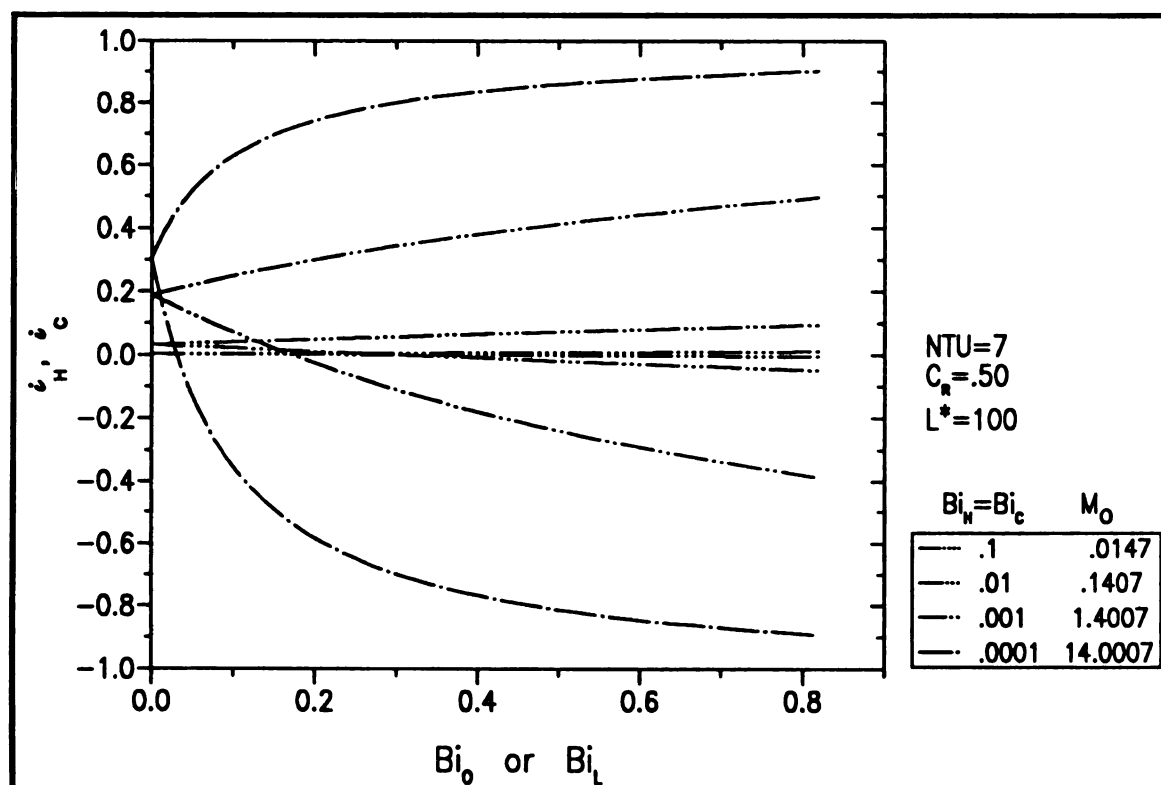


FIGURE 4.11. Ineffectiveness as a function of the end Biot numbers for $NTU = 7$, $L^* = 100$, and $C_R = .50$

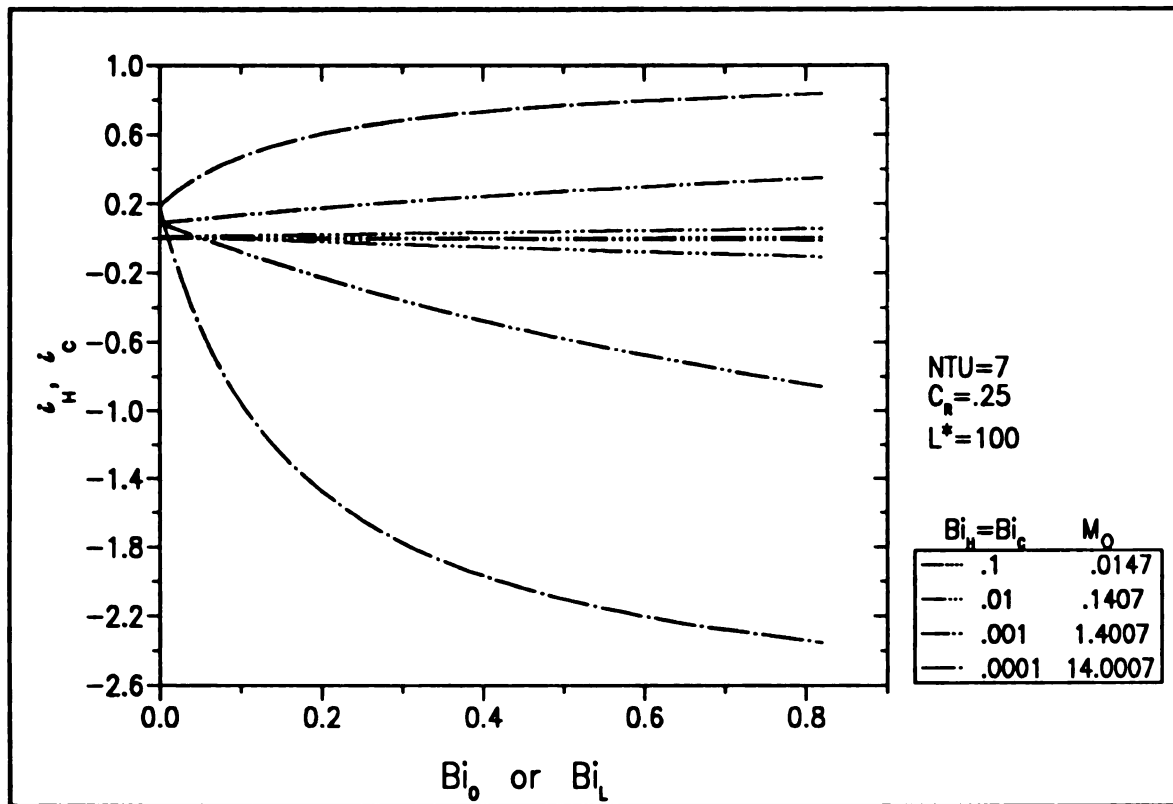


FIGURE 4.12. Ineffectiveness as a function of the end Biot numbers for $NTU = 7$, $L^* = 100$, and $C_R = .25$

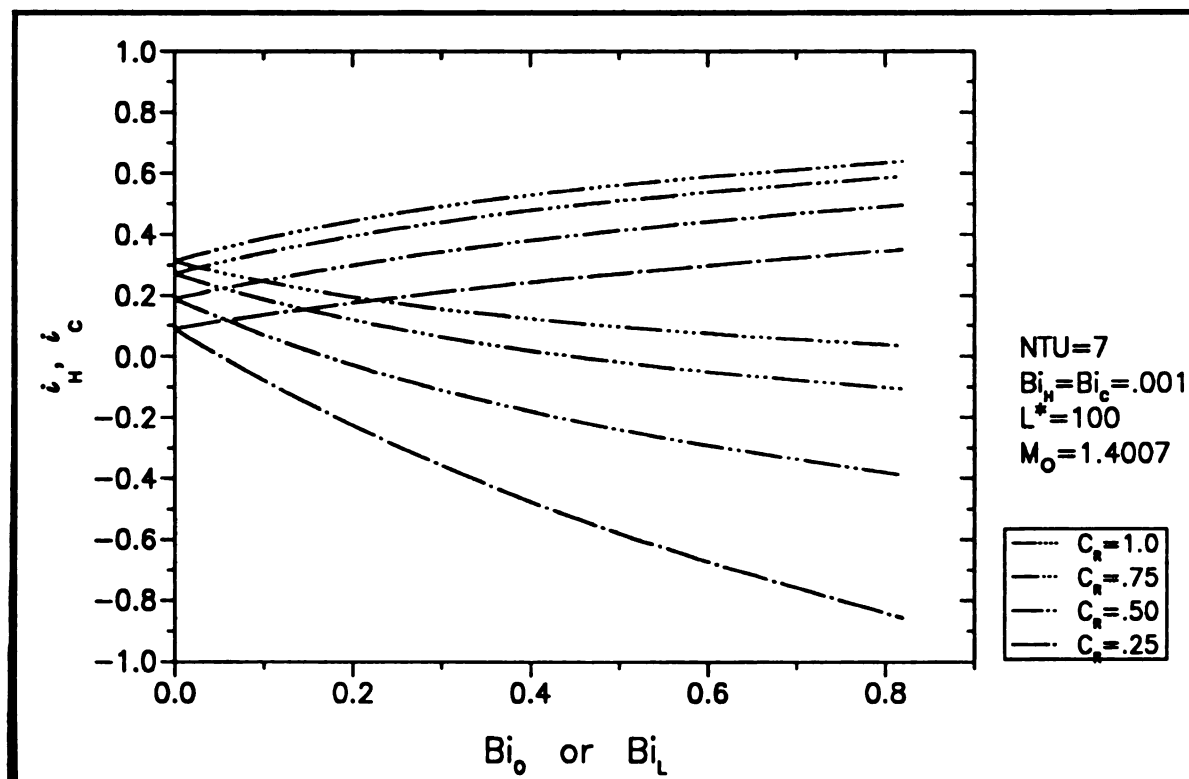


FIGURE 4.13. Ineffectiveness as a function of the end Biot numbers and heat capacity ratio for $NTU = 7$, $L^* = 100$, and fluid Biot numbers equal .001

4.1.3 Influence of the Fluid Biot Numbers (Bi_H and Bi_C)

To change the end Biot numbers requires the least effort without altering the operating conditions (flow rates or inlet temperatures) of the heat exchanger. Assuming that the end Biot numbers can be reduced to the minimum Biot number by reducing the convective heat transfer coefficient, the fluid Biot numbers will be investigated. These Biot numbers should represent the core of this study because the end effects require some unusual circumstances to become appreciable; and it is these fluid Biot numbers and the wall aspect ratio that should characterize axial conduction.

Setting the NTU at seven with the end Biot numbers equal at a magnitude of .0001, the fluid Biot numbers are varied. The cold Biot number was set and the hot Biot number varied over the range of interest. The cold Biot number was then increased, and the hot Biot number varied over the same range. This procedure was repeated for the four heat capacity ratios. Figures 4.14-4.17 shows the ineffectiveness as a function of the hot and cold Biot numbers at each heat capacity ratio. With such small end Biot numbers chosen, negligible end effects were seen and the ineffectivenesses based on either fluid were equal ($i_H = i_C = i$).

Examining the results for a heat capacity ratio of one, Figure 4.14, the insensitivity of the ineffectiveness to the hot Biot number is seen at larger magnitudes of the hot Biot number. This result shows that beyond a certain magnitude of the hot side Biot number the performance of the heat exchanger depends minimally on this Biot number. This implies that the effect of axial conduction depends on the minimum fluid Biot number and increasing the other fluid Biot number does not improve matters significantly. To determine the magnitude of the hot Biot number beyond which the ineffectiveness does

TABLE 4.3. Ineffectiveness as a function of fluid Biot numbers from Figure 4.14

	Bi_H										
Bi_C	.0001	.0002	.0016	.0032	.0128	.0256	.0512	.1024	.2048	.4096	.8192
.0001	.413	.408	.402	.402	.402	.402	.401	.401	.401	.401	.401
.001	.403	.383	.294	.276	.260	.257	.256	.255	.255	.255	.255
.01	.402	.378	.216	.155	.084	.069	.062	.058	.056	.055	.055
.1	.401	.377	.206	.136	.048	.028	.017	.012	.009	.008	.007

not change, Table 4.3 was created. This table shows the ineffectiveness as a function of the fluid Biot numbers from Figure 4.14. In Table 4.3 it is seen that for magnitudes of the hot Biot number less than the cold Biot number the ineffectiveness shows a dependence on the hot Biot number. However, for magnitudes of the hot Biot number greater than the cold Biot number the ineffectiveness changes a maximum of 5% after the point of equal fluid Biot numbers. If more accuracy is desired, it is possible to be within 1%, for Biot numbers separated by one order of magnitude or more. These results show that axial conduction is weakly dependent on the larger fluid Biot number.

This outcome is explained by realizing that an increase of one fluid Biot number will improve the heat transfer between the wall and that fluid. However, the increased thermal communication between the fluid with the higher Biot number and the wall will not significantly affect the performance of the heat exchanger because of conditions on the other side of the wall. On the side where the Biot number is unchanged, any additional energy that could be acquired by the increased Biot number cannot be handled on this side. There can be some change in the amount of energy transferred between the wall and the fluid with the minimum Biot number; through an increase in the wall temperature, but the magnitude of this increase will be much less than the energy change due to the increased Biot number on the other side. To summarize, the wall is unable to transfer more energy between the fluids when one Biot number is increased because it cannot increase the energy transfer at the other side of the wall. The outcome is the wall not acquiring any more energy even though one fluid Biot number is increased.

To assess the influence of the heat capacity ratio, Figure 4.18 was created, which combines a curve from Figures 4.14-17 on to a single figure for a cold Biot number of .001. In Figure 4.18 the affect of the heat capacity ratio is seen. The ineffectiveness increased as heat capacity ratio increased. However, little change in the shape of the curves is seen as the hot side Biot number varies. An interesting result, considering that the heat capacity was seen to increase the driving temperature differential, as the heat capacity ratio decreased, on the fluid with the maximum heat capacity, which was the hot fluid for this case. Even with the increased driving force it is not possible to move more energy while increasing only one fluid Biot number.

For this case, each pair of hot and cold Biot numbers had a corresponding Mondt number. Requiring a different Mondt number for each point on the figures. Because the case of a constant NTU and $L^* = 100$ is rather restrictive, the influence of the Mondt number will be left for a more general case.

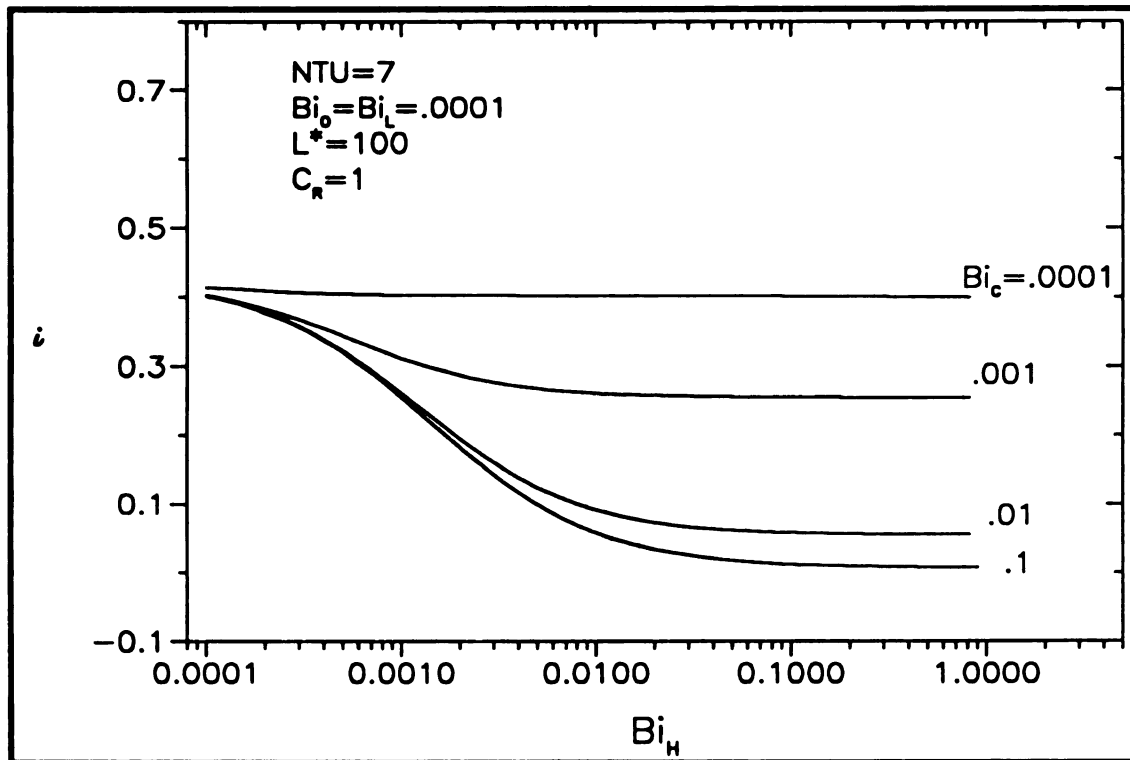


FIGURE 4.14. Ineffectiveness as a function of the fluid Biot numbers for $NTU = 7$, $L^* = 100$, and $C_R = 1$

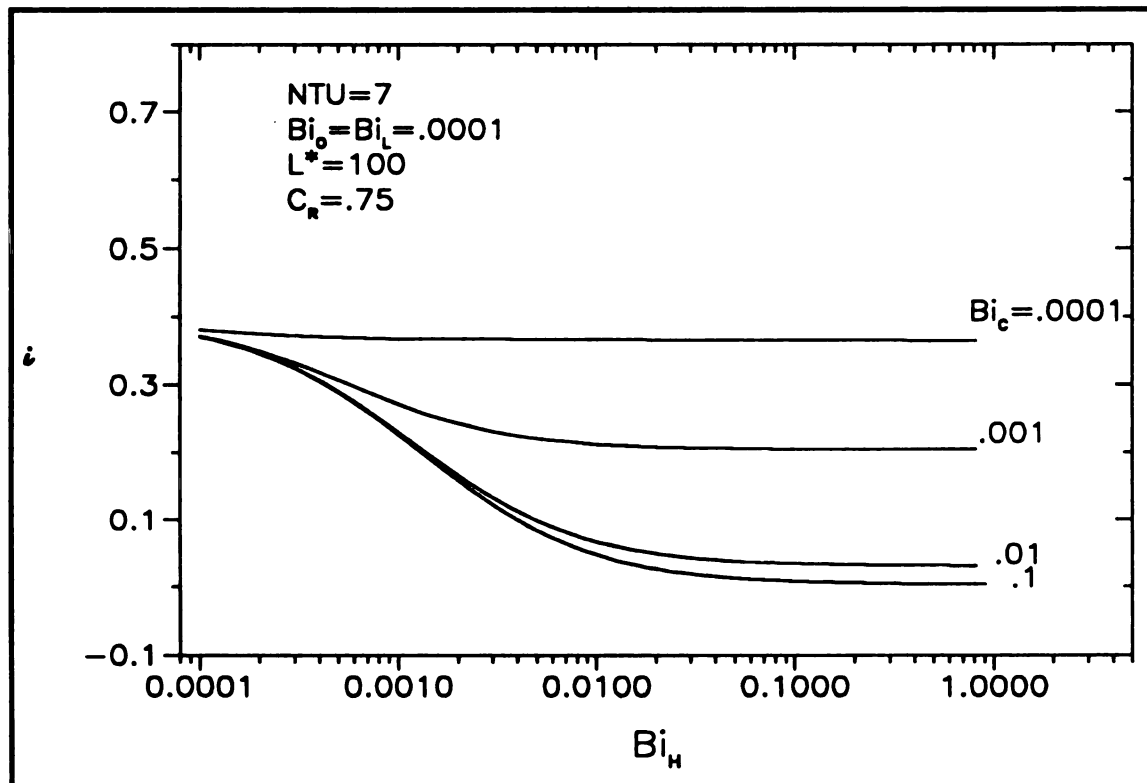


FIGURE 4.15. Ineffectiveness as a function of the fluid Biot numbers for $NTU = 7$, $L^* = 100$, and $C_R = .75$

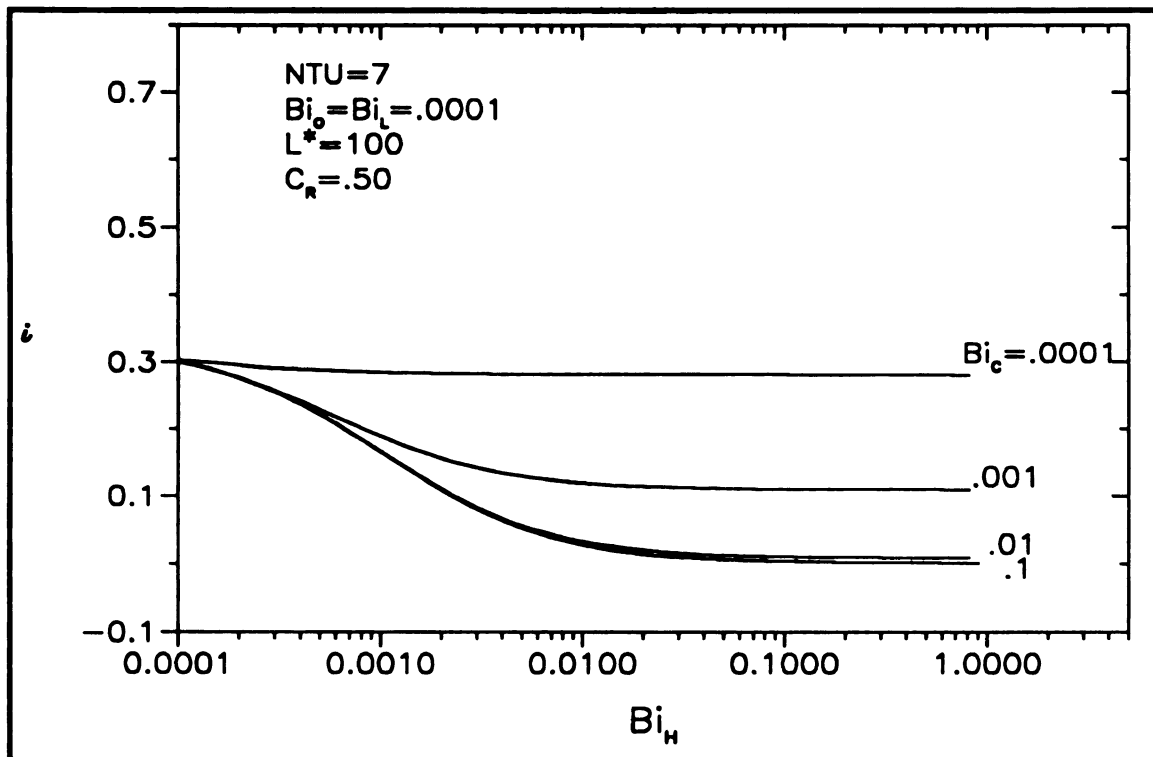


FIGURE 4.16. Ineffectiveness as a function of the fluid Biot numbers for $NTU = 7$, $L^* = 100$, and $C_R = .50$

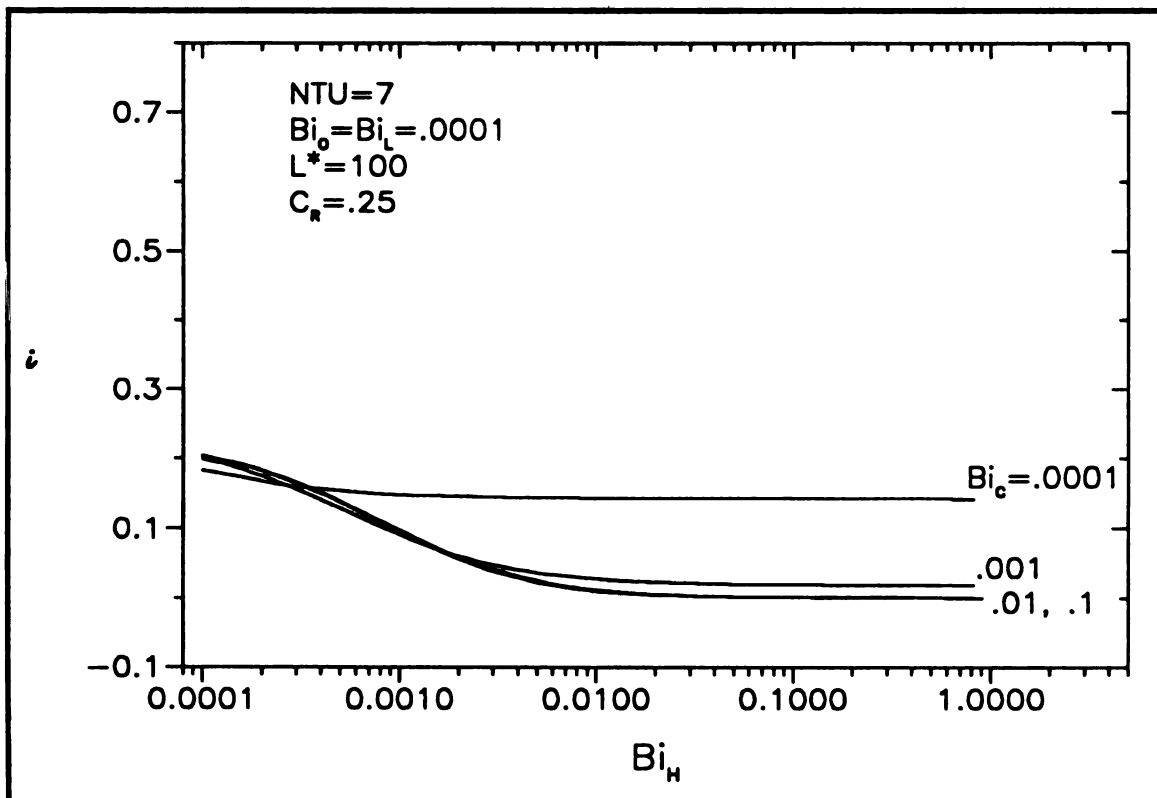


FIGURE 4.17. Ineffectiveness as a function of the fluid Biot numbers for $NTU = 7$, $L^* = 100$, and $C_R = .25$

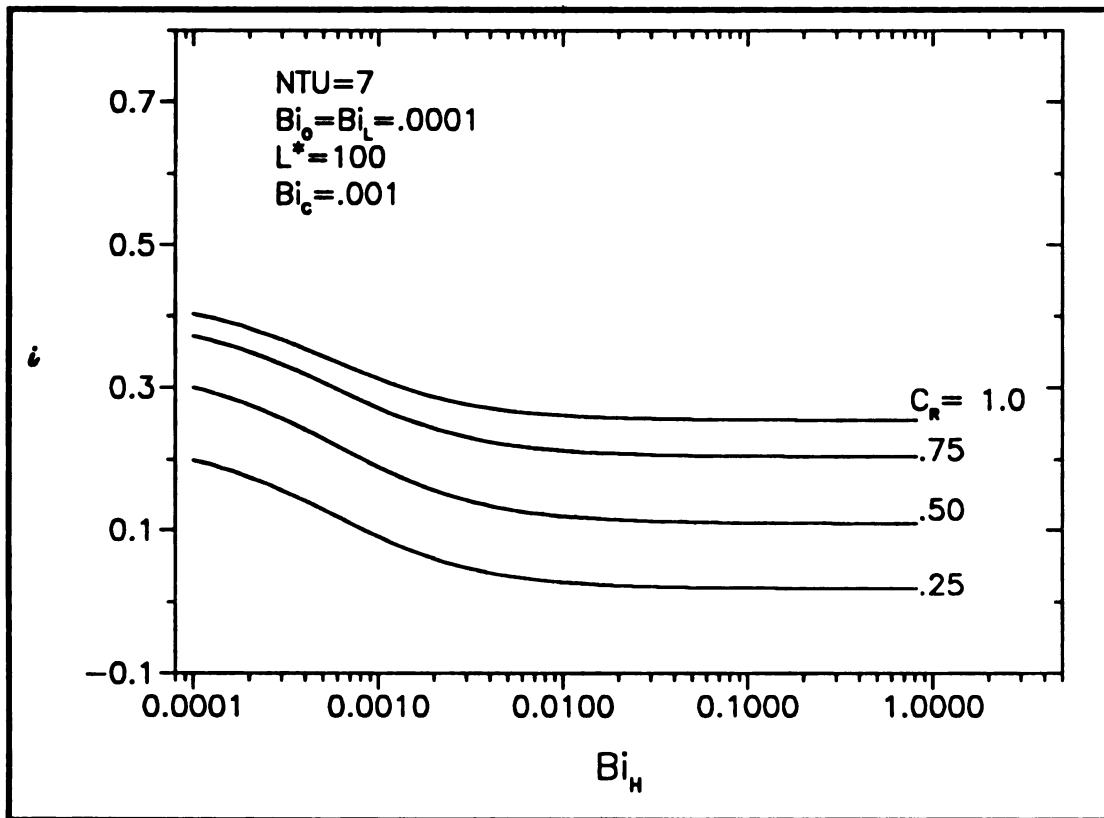


FIGURE 4.18. Ineffectiveness as a function of the hot fluid Biot number and heat capacity ratio for $NTU = 7$, $L^* = 100$, and a cold fluid Biot numbers of .001

4.1.4 Summary of Investigation with a Constant NTU

Examination of the effect of axial conduction at a constant, relatively high NTU has provided insight into the parameters that characterize conditions that axial conduction will arise. There were also some possible simplifications that arose. These issues are now discussed.

The wall aspect ratio is an important parameter in describing axial conduction. This parameter represents the physical dimensions of the heat exchanger; and it was seen that for large values of the wall aspect ratio axial conduction could be neglected, almost regardless of the Biot numbers. It was still possible for axial conduction to exist at the larger wall aspect ratios, but only for very small Biot numbers. A case simulating a nearly insulated wall

($h \approx 0$) or an infinite wall thermal conductivity ($K_w \gg h$), both physically trivial cases.

Having investigated the physical dimensions that axial conduction was important, a wall aspect ratio was set to exhibit axial conduction; and the influence of the wall Biot numbers could be investigated. The Biot numbers on the ends and for the hot and cold fluids were grouped separately. This permitted setting one group while varying the other, which reduces the possible combinations to study.

The end Biot numbers cause energy losses from the wall ends through convection and an energy imbalance between the fluids. However, this effect was not significant for magnitudes of the end Biot numbers less than or equal to the magnitude of the fluid Biot numbers. When the end Biot numbers exceeded the fluid Biot numbers some interesting results were seen, with the performance based on the hot fluid actually larger than the performance calculated neglecting axial conduction. This was at the cost of the performance based on the cold fluid, however.

Although the scaling used in the Biot numbers can result in the end Biot numbers being larger than the fluid Biot numbers, the proportionate amount that the scaling changes the Biot numbers, in comparison to the convective heat transfer coefficients, is the wall aspect ratio. Making the end Biot numbers greater than the fluid Biot numbers, in most cases, would require a very large wall aspect ratio, based on the expected magnitude difference in the convection coefficients; a case shown to result in negligible axial conduction. In addition, the effect of the end Biot numbers improves the effectiveness in certain situations, and may not have any affect on axial conduction. For these reasons, the end Biot numbers will be assumed negligible and not a factor in further investigation.

With the end Biot numbers eliminated from further scrutiny, they were set to the minimum magnitude of the Biot number, the focus turned to the fluid Biot numbers. Physically, the fluid Biot number can be thought of as the fluid operating conditions. Describing the interface convection between the fluid and the wall. As the fluid Biot numbers were varied, it was seen that the results were fairly insensitive to the larger Biot number. This outcome simplifies the task of characterizing axial conduction, which now may be shown to be a function of the wall aspect ratio and the minimum fluid Biot number.

The heat capacity ratio plays a role in the effect of axial conduction on the performance of the heat exchanger. The heat capacity ratio was varied during the investigation of all other parameters. It can alter axial conduction by influencing the interaction between the fluid and wall. The effect of axial conduction is smaller as the heat capacity decreases. Therefore, to reduce axial conduction the heat capacity ratio can be decreased.

Although the Mondt number was not covered for all cases it was shown to be influential. The Mondt number was adjusted as other parameters were varied to maintain a constant NTU . As the wall aspect ratio and Biot number became larger the Mondt number became smaller and the effect of axial conduction decreases, which is interpreted as the Mondt number adjusting the properties of the fluids and wall to match the operating conditions. This parameter may be useful to describe the condition when axial conduction will be seen.

In closing, this section has allowed the characterization of axial conduction to be reduced to a function of four variables; which includes the wall aspect ratio, minimum fluid Biot number, the heat capacity ratio, and Mondt number. These variables will provide approximate estimates when axial conduction needs to be considered and to what extent the performance will be altered if it is assumed negligible. Approximate, because only one variable is considered for the fluid Biot numbers. In the next section these results will be used to produce ineffectiveness curves as a function of NTU for the parameters of interest.

4.2 Characterization of Axial Conduction as a Function of NTU

Setting the NTU constant and varying the parameters revealed some possible simplifications in the parameters needed to characterize the conditions that axial conductions will arise. At the beginning of this chapter it was shown that it requires eleven parameters to mathematically model this problem. Of the number of parameters needed to mathematically represent the problem the solution presented in dimensionless form would be a function of seven of these parameters. Which includes four Biot numbers, a wall aspect ratio, the fluid heat capacity ratio, and Mondt number. Using the results of the previous section the number of independent variables will be reduced.

The effect of the end Biot numbers was only seen for end Biot number magnitudes greater than that of the fluid Biot numbers. Although this is possible, it is not seen as a plausible operating condition. Therefore, the end Biot numbers will be assumed to be the lowest possible magnitude and play no role. This reduces the parameters needed to characterize axial conduction to five.

Another simplification that can be considered is the dependence of axial conduction on the fluid Biot numbers. For a constant NTU it was shown that the ineffectiveness depends mainly on the magnitude of the smaller of the two fluid Biot numbers. However, these results were for a constant NTU and wall aspect ratio of 100 and the dependence, or lack of, may differ with these parameters variable. To explore this point, data were generated to produce ineffectiveness- NTU plots for a heat capacity ratio of one, which are shown in Figure 4.19. The plots are shown as a function of the wall aspect ratio and the maximum fluid Biot number, while the minimum fluid Biot number remained constant. The minimum and maximum fluid Biot numbers are

$$Bi_{min} = \min(Bi_H, Bi_C) \quad (4.22)$$

$$Bi_{max} = \max(Bi_H, Bi_C) \quad (4.23)$$

In Figure 4.19 the results of the previous section are supported for a wall aspect ratio of 100 with less than a 1% change in the ineffectiveness as the maximum fluid Biot number increased three orders of magnitude. However, for larger wall aspect ratios the ineffectiveness shows a dependence on the maximum fluid Biot number with as high as a 45% reduction in the ineffec-

tiveness. This reduction was at a maximum Biot number one order of magnitude larger than the minimum Biot number, for further increases in the maximum Biot number the ineffectiveness was not changed significantly.

Although Figure 4.19 shows a greater absolute change in the ineffectiveness at a wall aspect ratio of 500 than it does at a wall aspect ratio of 1000, the relative change in the ineffectiveness, which gauges the magnitude of axial conduction, is larger for a wall aspect ratio of 1000 with a 45% reduction in the ineffectiveness.

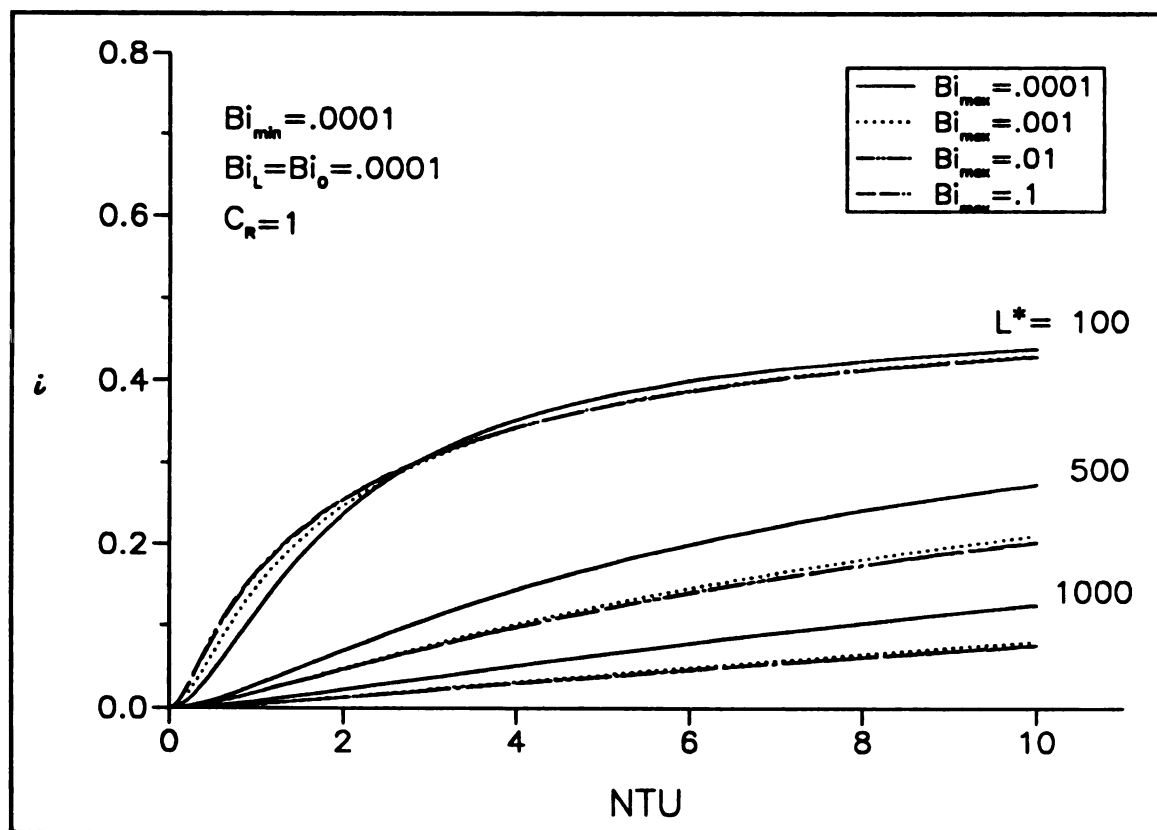


FIGURE 4.19. Ineffectiveness as a function of the NTU, wall aspect ratio, and maximum fluid Biot number for $Bi_{min} = 0.0001$ and $C_R = 1$

It was shown earlier that axial conduction was greater for smaller wall aspect ratios and fluid Biot numbers. For this reason, at lower wall aspect ratio, the ineffectiveness is less sensitive to the fluid Biot numbers because both parameters are at magnitudes that promote axial conduction. As the wall aspect ratio increases, the solution becomes more sensitive to the fluid Biot numbers because this parameter is more influential in promoting axial conduction with the wall aspect ratio larger. This results in the ineffectiveness decreasing significantly as the maximum fluid Biot number is increased at larger wall aspect ratios. However, the maximum fluid Biot number can only improve the operating conditions so much, due to the limiting nature of the conditions on the opposite side of the wall where the minimum fluid Biot number remains unchanged. The outcome is less degradation in the performance of the heat exchanger as the maximum fluid Biot number is initially increased, but further change in the maximum fluid Biot number produces no improvement.

A final observation that can be made concerning Figure 4.19 is the increased ineffectiveness at lower values of NTU as the maximum fluid Biot number increased for a wall aspect ratio of 100, a result contrary to all other cases, where ineffectiveness decreased as the maximum fluid Biot number was increased. This is only seen for values of NTU less than three, where there is a crossing point and previous trends are seen, and only for this particular wall aspect ratio. This is due to the wall aspect ratio and minimum fluid Biot number both being at magnitudes that promote axial conduction.

Increasing the maximum fluid Biot number is expected to decrease the ineffectiveness because of the increased convection on one side of the wall. In addition to increasing the maximum Biot number the Mondt number will decrease to maintain the same NTU that existed when the fluid Biot numbers were equal. The lower Mondt number also would be expected to decrease axial conduction. But it is the decrease in the Mondt number that actually causes the increase in the ineffectiveness at low NTU .

To decrease the Mondt number the ratio (K_w/C_{min}) must be decreased. At lower values of the NTU , the magnitude of the minimum heat capacity is relatively larger and decreasing the ratio K_w/C_{min} will make it even larger. Therefore, the limiting factor on the energy transfer will be the magnitude of the wall aspect ratio and fluid Biot numbers. When the maximum fluid Biot

number is increased, the corresponding increase in the Mondt number results in the ineffectiveness increasing because the additional energy can not be moved across the wall.

For larger NTU the heat capacity is relatively small and it becomes the limiting factor on the energy transfer. For this case, the result is the ineffectiveness decreases as the maximum fluid Biot number is increased.

The results in Figure 4.19 show, contrary to the previous section, that in addition to the minimum fluid Biot number the maximum fluid Biot number must also be considered for magnitudes of the maximum fluid Biot number within one order of magnitude of the minimum fluid Biot number. Increasing the maximum fluid Biot number further produces negligible change in the results and does not need to be considered.

Because unequal fluid Biot numbers must be considered the relative magnitudes of the heat capacities on the streams will also play a role. For example, at a particular heat capacity ratio and for unequal fluid Biot numbers the results obtained when the fluid with the minimum heat capacity has the minimum fluid Biot number will differ from the results obtained when the minimum heat capacity is for the fluid with the maximum fluid Biot number. To verify this point Figure 4.20 was created, which shows ineffectiveness- NTU curves at various heat capacity ratios with the minimum heat capacity associated with the minimum fluid Biot number and maximum fluid Biot number. At lower magnitudes of the NTU the two cases vary greatly, while at larger values of the NTU the two cases converge toward a common result and the convergence occurs at a lower NTU for larger heat capacity ratios.

The two noted dependencies are due to the magnitude of the heat capacities at the referenced NTU . At lower values of NTU the minimum heat capacity is relatively larger in comparison to the amount of energy that the wall can transfer. For an opposite pairing of the extremes of heat capacity and fluid Biot numbers the amount of energy transferred is dictated mainly by the fluid Biot numbers. The larger heat capacity is limited by the smaller Biot number on one side of the wall and similarly the larger Biot number is limited by the smaller heat capacity on the other side of the wall. Producing an insensitivity to the heat capacity ratio. However, if the pairing is changed to associate extremes, the magnitudes of the heat capacity and fluid Biot number

will not oppose each other and a dependence on the heat capacity ratio exists.

For larger values of NTU the minimum heat capacity is smaller in comparison to the possible energy transfer through the wall; and the energy transferred is dictated mainly by the heat capacity ratios. The insensitivity to the Biot number is shown by the two cases approaching the same result at larger values of the NTU . The smaller heat capacity ratios requires a larger magnitudes of the NTU to converge to the same result because the larger differences in the heat capacity across the wall make the result more sensitive to the Biot numbers, which requires a larger NTU to insure that heat capacity is the limiting parameter on the heat transfer and not the fluid Biot numbers.

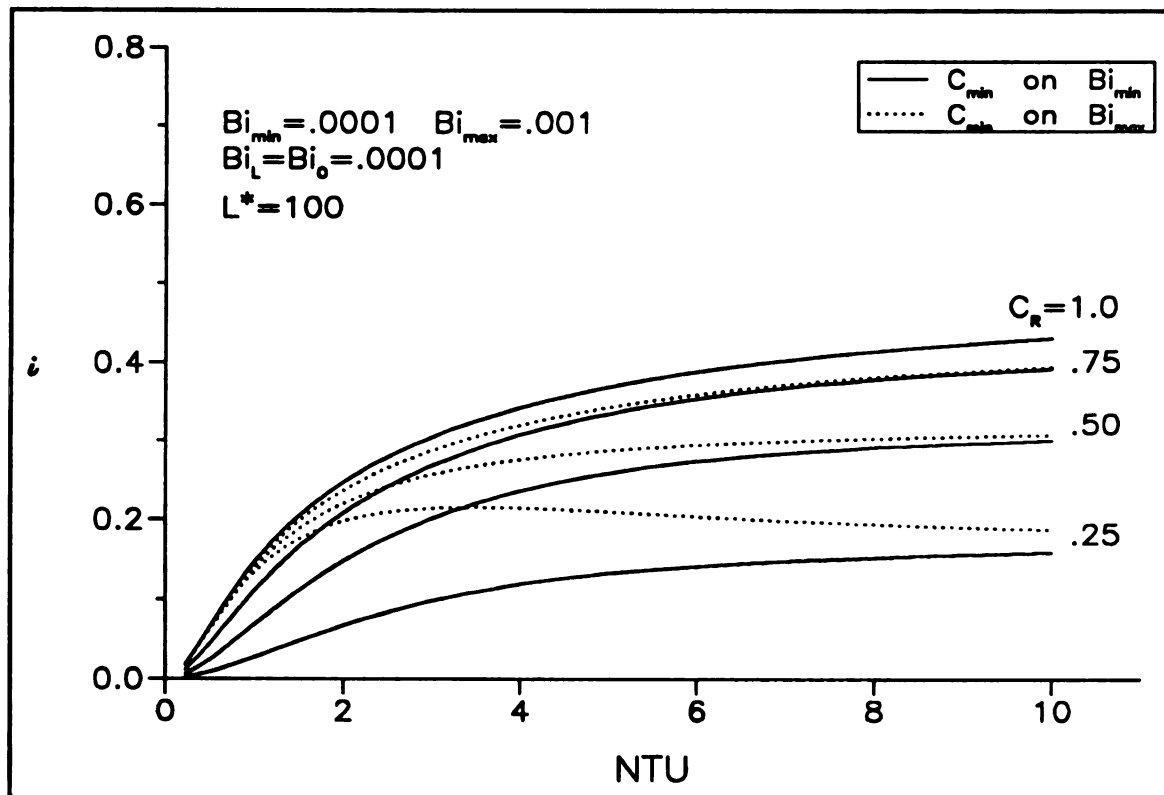


FIGURE 4.20. Ineffectiveness as a function of the NTU and heat capacity ratio for $Bi_{min} = 0.0001$, $Bi_{max} = 0.001$, and $C_R = 1$

Between the limiting cases of a small NTU (where the heat transfer is limited by the fluid Biot numbers) and a large NTU (where heat transfer is limited by the heat capacity ratio) both parameters are important. In this region a combination of the outcomes is seen.

The results of Figures 4.19 and 4.20 have shown that axial conduction can now be characterized for all fluid Biot number combinations with minimal error by two cases; the fluid Biot numbers equal ($Bi_{max} = Bi_{min}$) or the maximum fluid Biot number an order of magnitude larger than the minimum ($Bi_{max} = 10Bi_{min}$). For the case of unequal fluid Biot numbers, the minimum heat capacity ratio must be considered to exist on the fluid with the minimum fluid Biot number ($C_{min} - Bi_{min}$) and with the maximum fluid Biot number ($C_{min} - Bi_{max}$) separately, since the results will differ.

Encompassing the previous results, the operating conditions that axial conduction will arise can now be identified with five parameters. A minimum and maximum fluid Biot number, the wall aspect ratio, the heat capacity ratio, and Mondt number. However, for the fluid Biot numbers only one order of magnitude larger than the minimum needs to be considered for the maximum fluid Biot number, greatly reducing the possibilities.

It is now possible to produce figures, which can be used to predict the possibility of axial conduction affecting the performance of the heat exchanger. To do this requires considering four minimum fluid Biot numbers at four heat capacity ratios, giving sixteen figures. On each figure, two cases for the fluid Biot number will be shown, fluid Biot numbers equal and maximum fluid Biot number ten times the minimum fluid Biot number. Furthermore, for unequal fluid Biot numbers both maximum and minimum Biot numbers will be associated with minimum heat capacity. All of these cases shall be shown at different wall aspect ratios.

4.2.1 Ineffectiveness- NTU Results

4.2.1.1 Heat Capacity Ratio of 1

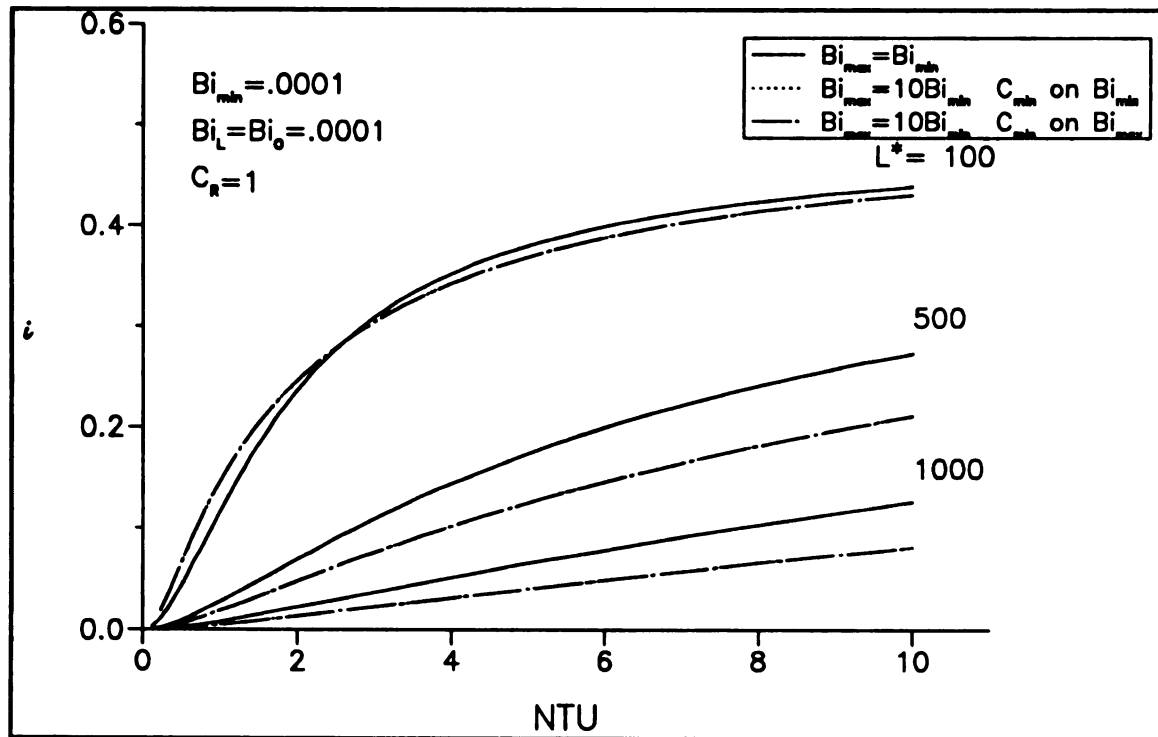


FIGURE 4.21. Ineffectiveness as a function of the NTU and wall aspect ratio for $Bi_{min} = 0.0001$ and $C_R = 1$

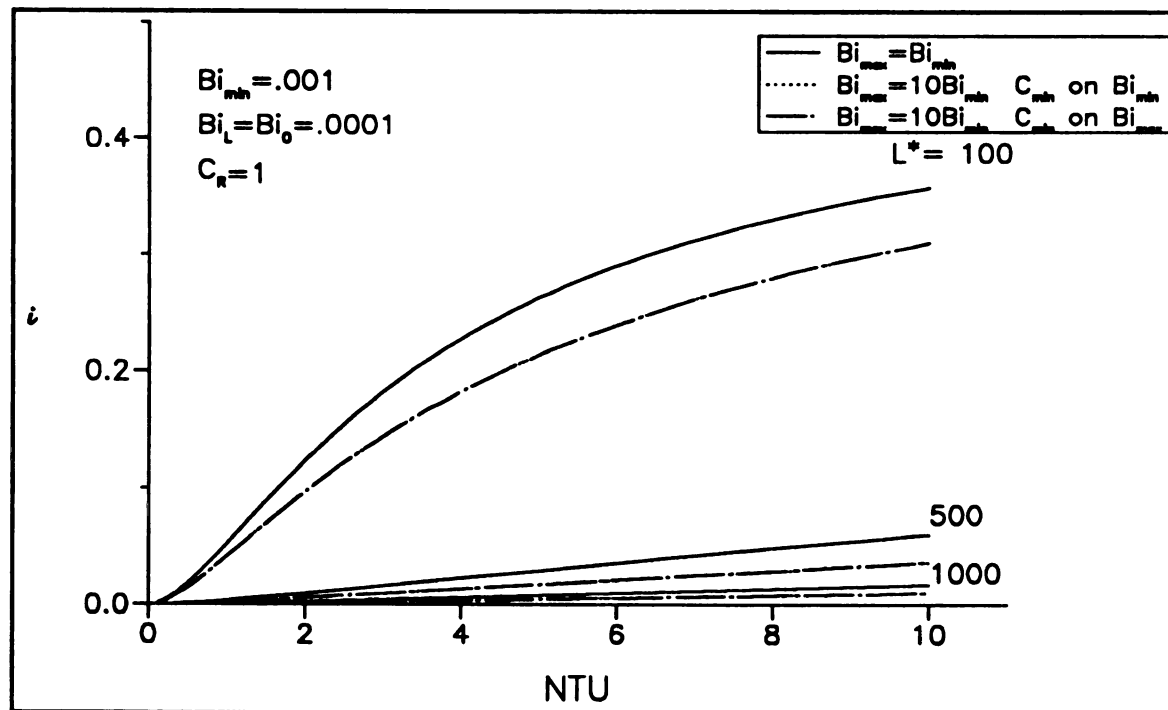


FIGURE 4.22. Ineffectiveness as a function of the NTU and wall aspect ratio for $Bi_{min} = 0.001$ and $C_R = 1$

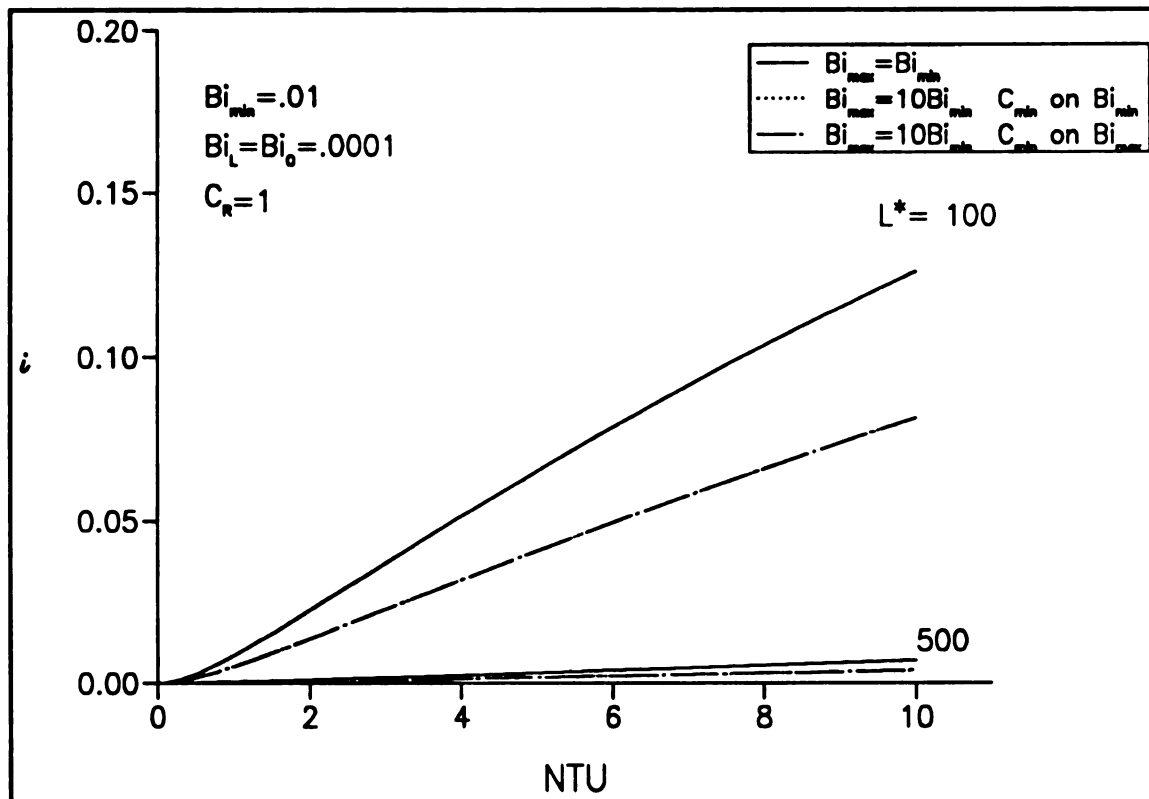


FIGURE 4.23. Ineffectiveness as a function of the NTU and wall aspect ratio for $Bi_{min} = 0.01$ and $C_R = 1$

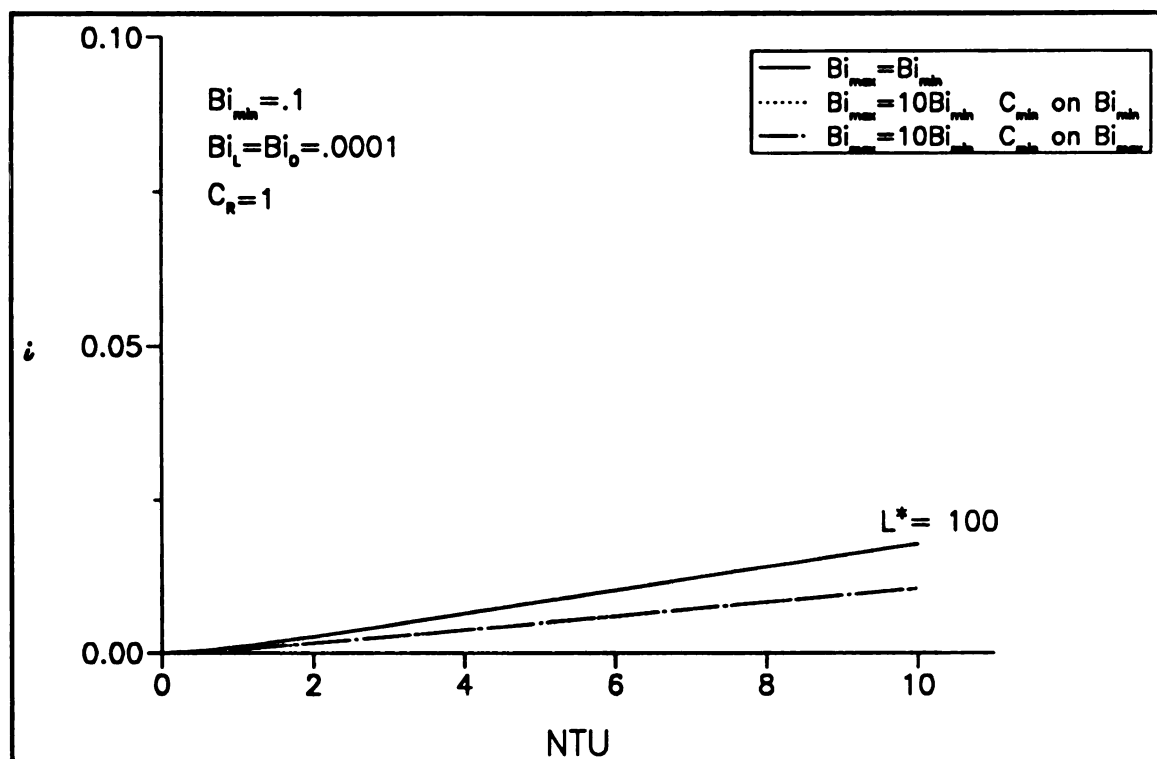


FIGURE 4.24. Ineffectiveness as a function of the NTU and wall aspect ratio for $Bi_{min} = 0.1$ and $C_R = 1$

4.2.1.2 Heat Capacity Ratio of .75

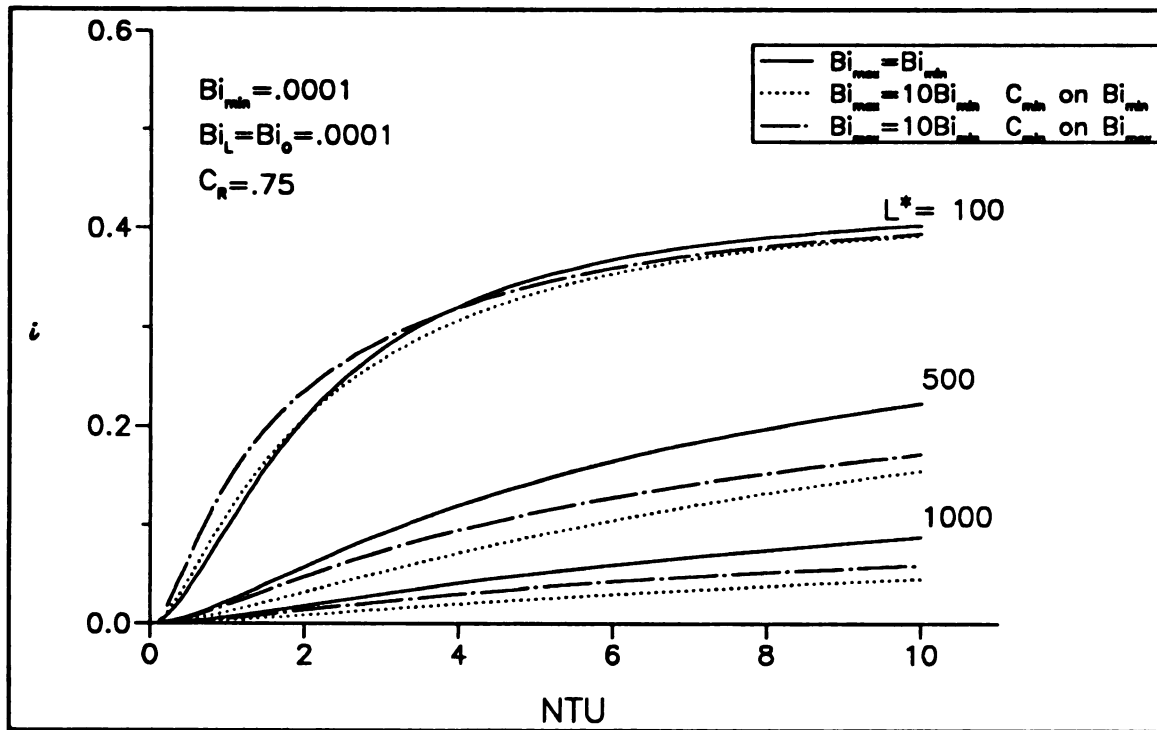


FIGURE 4.25. Ineffectiveness as a function of the NTU and wall aspect ratio for $Bi_{min} = 0.0001$ and $C_R = .75$

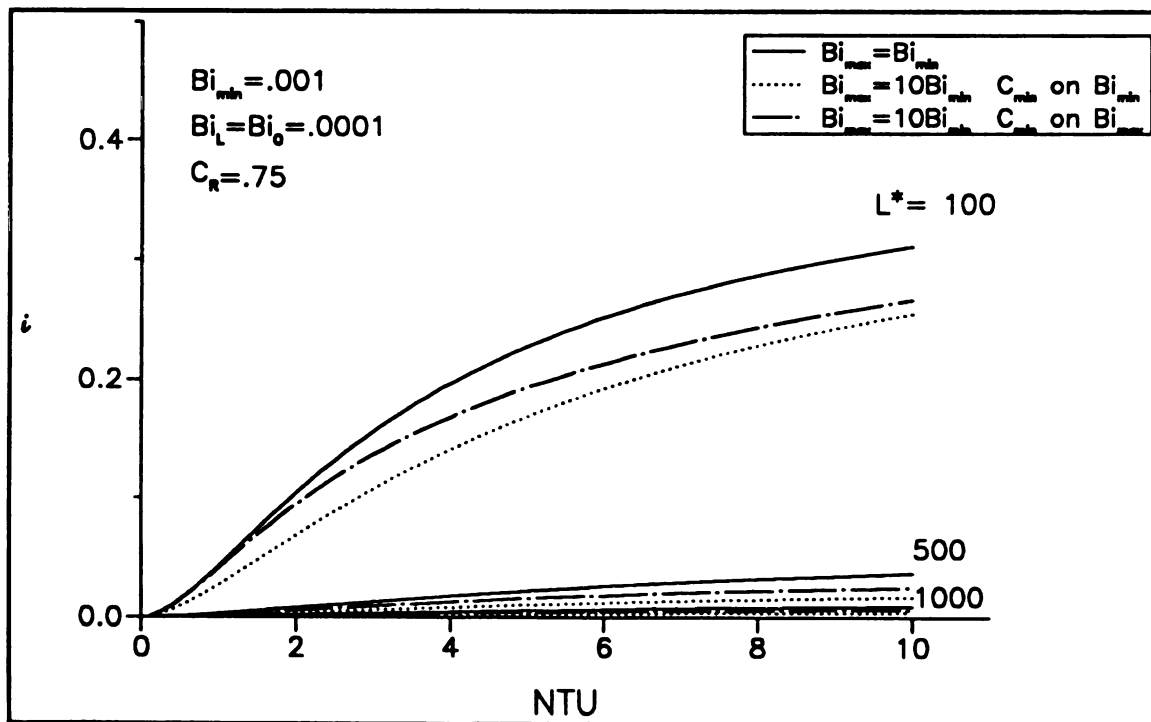


FIGURE 4.26. Ineffectiveness as a function of the NTU and wall aspect ratio for $Bi_{min} = 0.001$ and $C_R = .75$

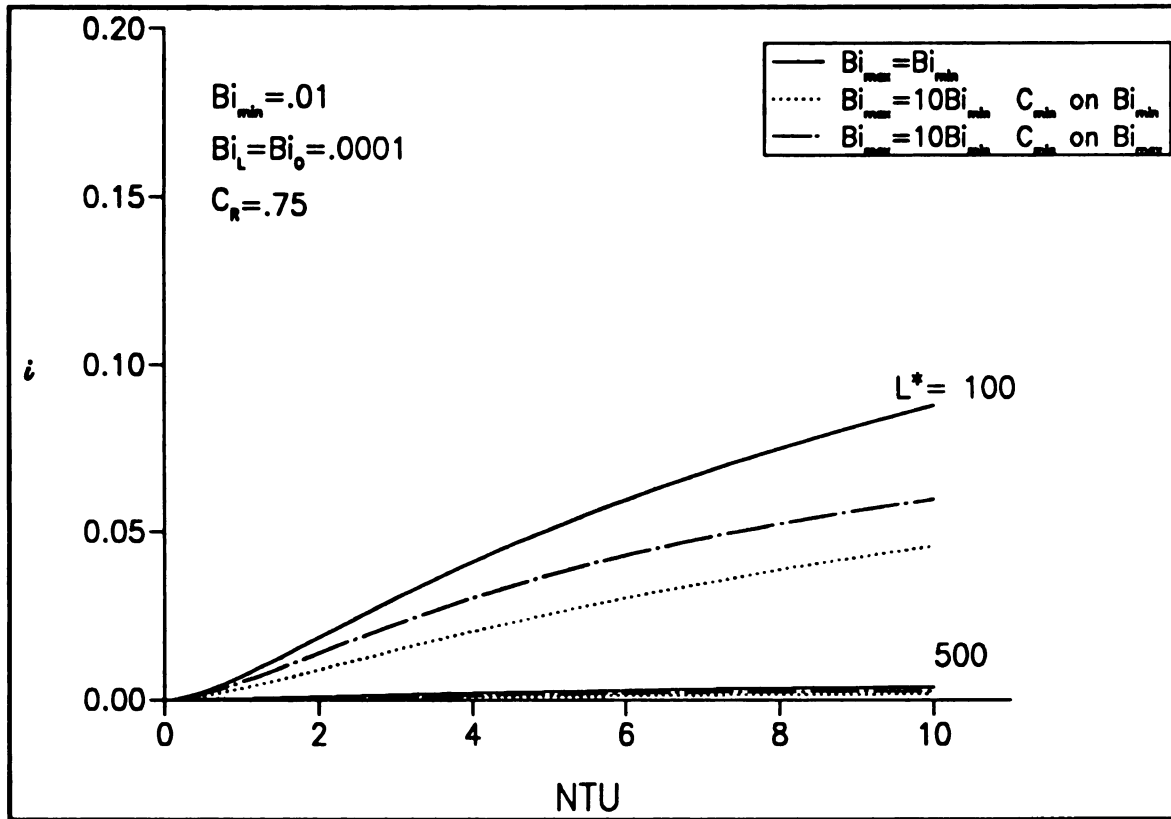


FIGURE 4.27. Ineffectiveness as a function of the NTU and wall aspect ratio for $Bi_{min} = 0.01$ and $C_R = .75$

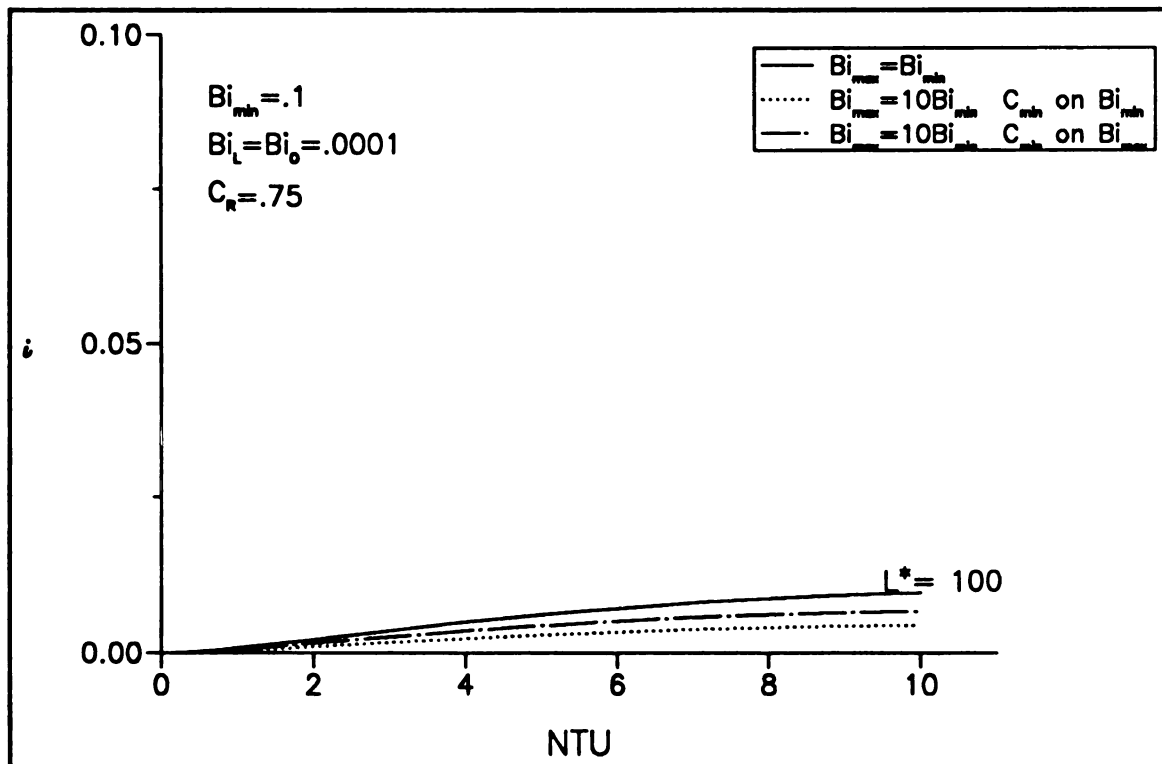


FIGURE 4.28. Ineffectiveness as a function of the NTU and wall aspect ratio for $Bi_{min} = 0.1$ and $C_R = .75$

4.2.1.3 Heat Capacity Ratio of .50

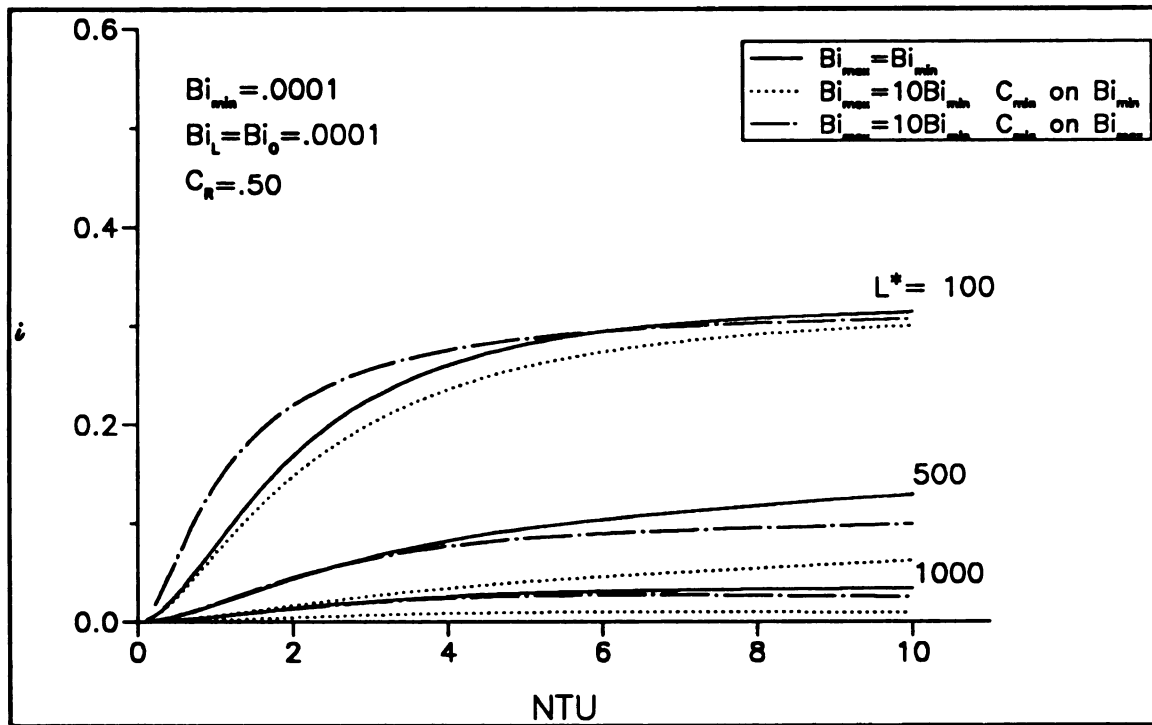


FIGURE 4.29. Ineffectiveness as a function of the NTU and wall aspect ratio for $Bi_{min} = 0.0001$ and $C_R = .50$

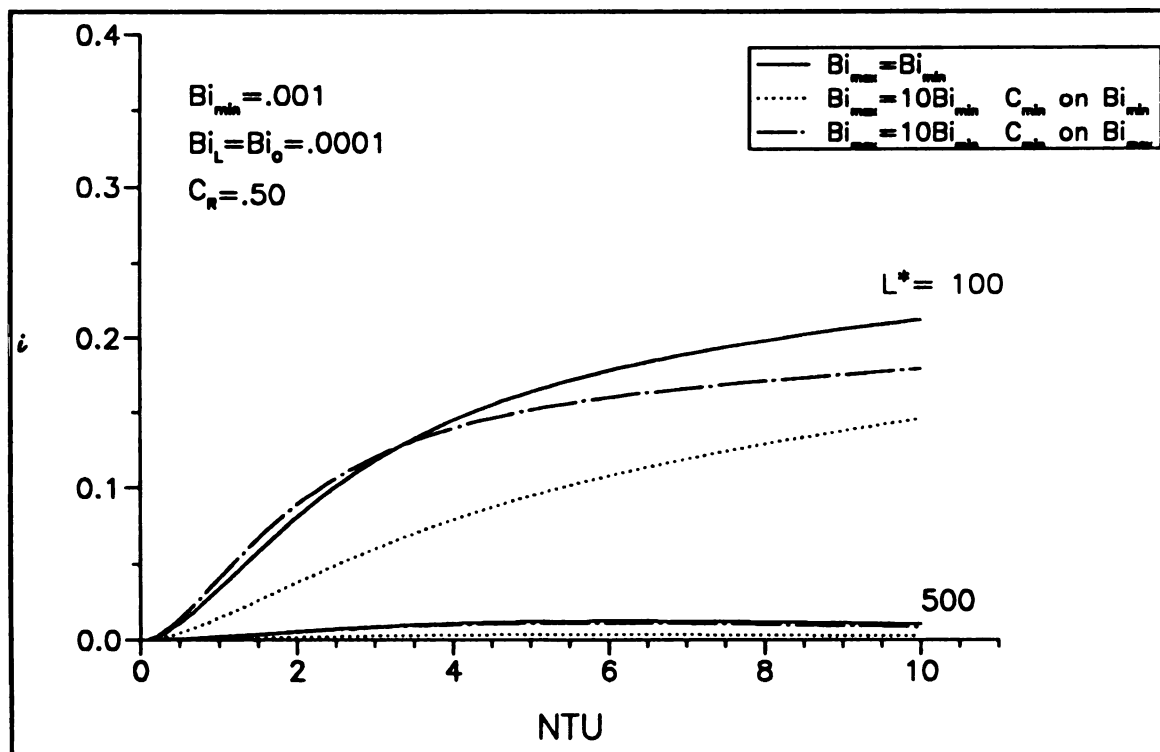


FIGURE 4.30. Ineffectiveness as a function of the NTU and wall aspect ratio for $Bi_{min} = 0.001$ and $C_R = .50$

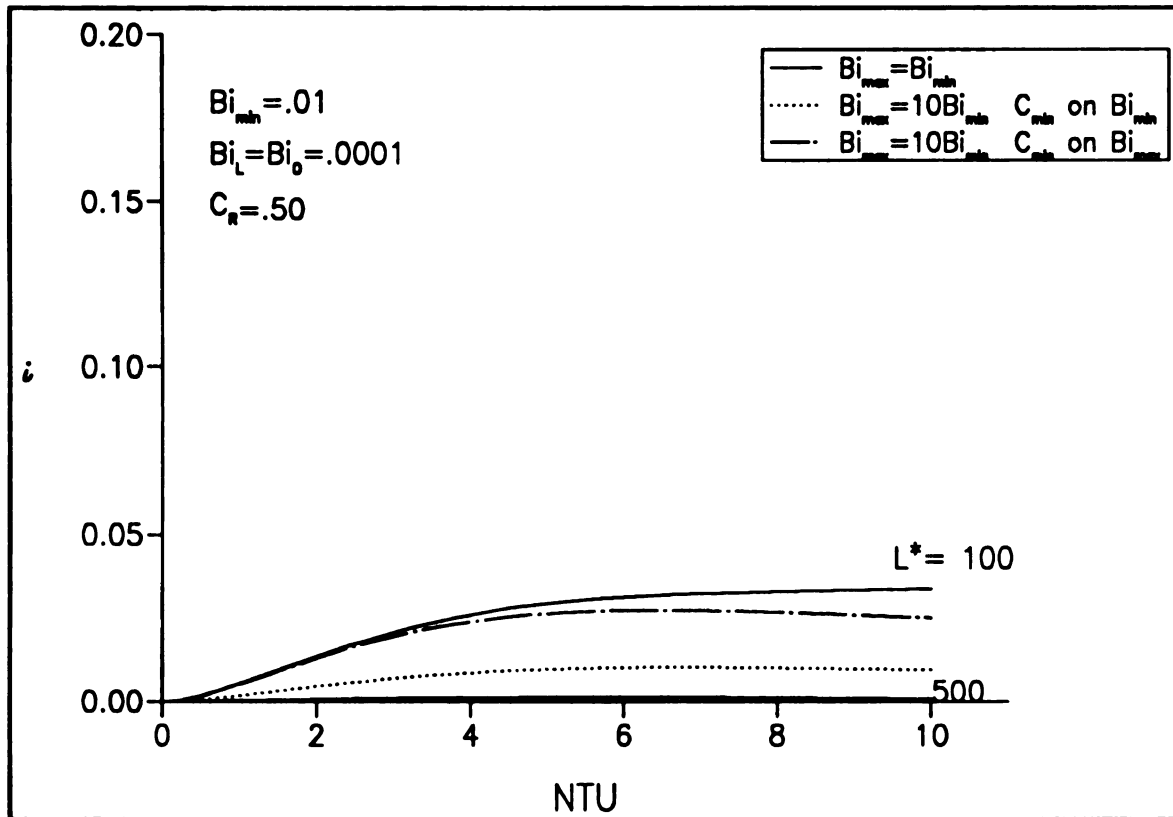


FIGURE 4.31. Ineffectiveness as a function of the NTU and wall aspect ratio for $Bi_{min} = 0.01$ and $C_R = .50$

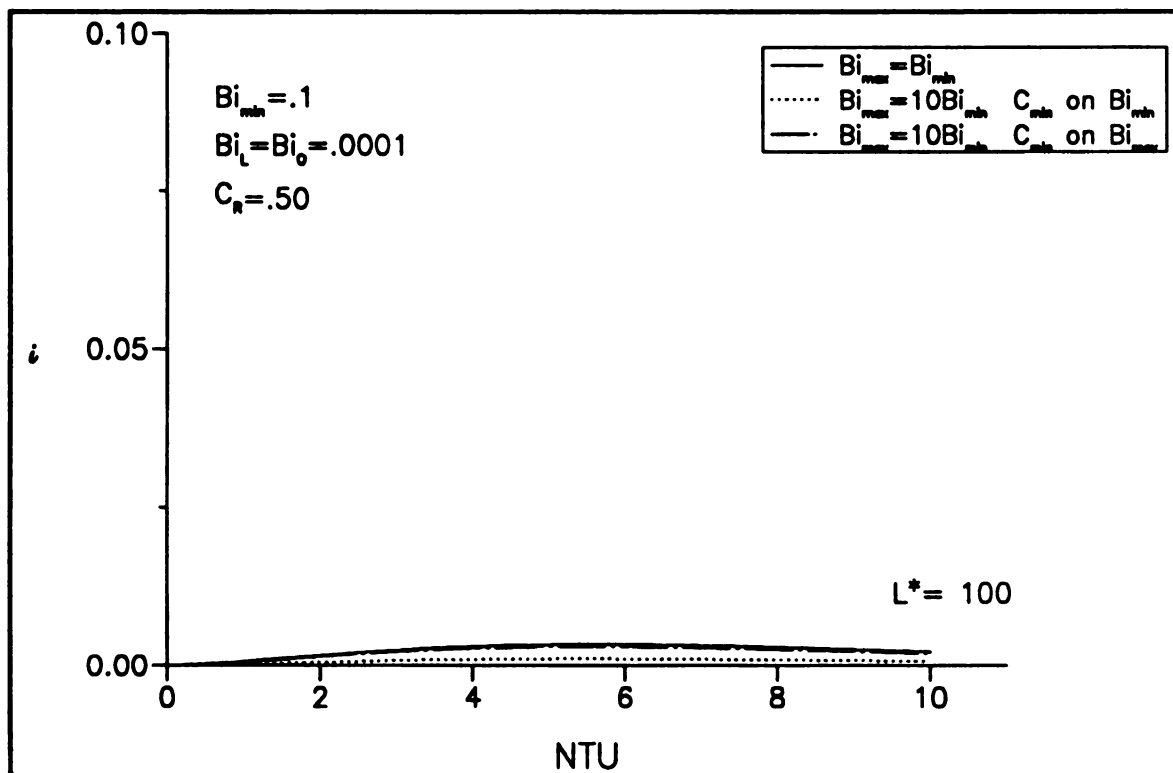


FIGURE 4.32. Ineffectiveness as a function of the NTU and wall aspect ratio for $Bi_{min} = 0.1$ and $C_R = .50$

4.2.1.4 Heat Capacity Ratio of .25

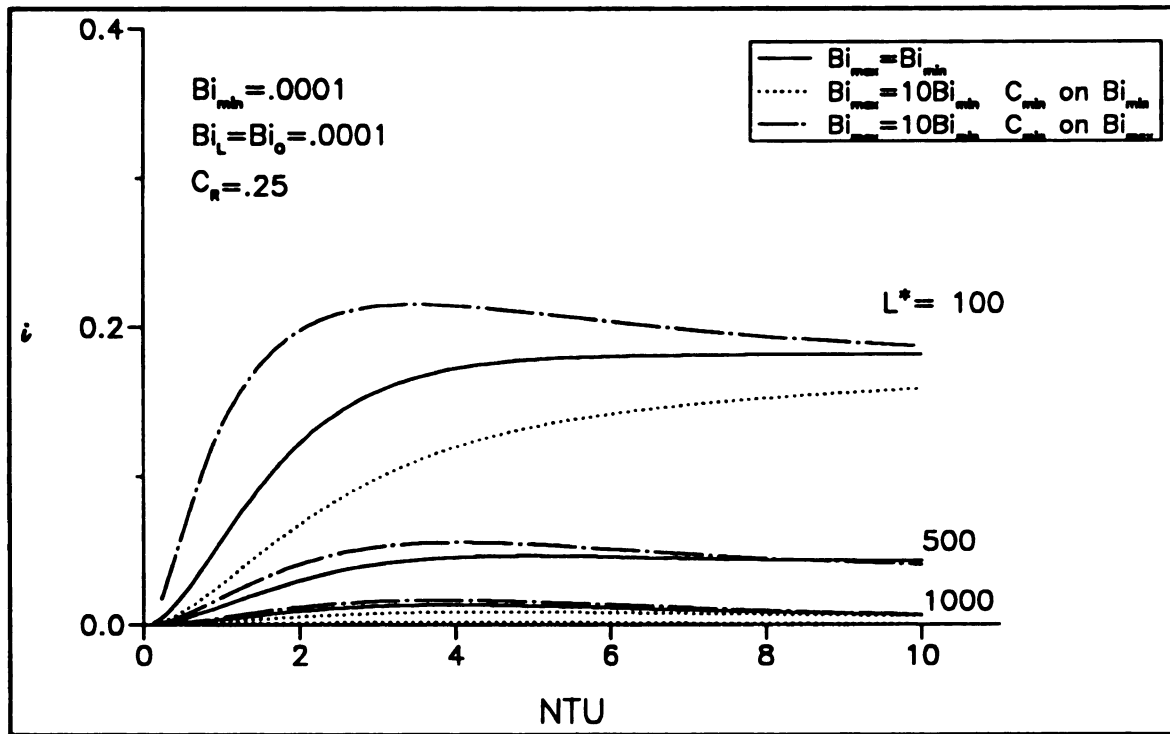


FIGURE 4.33. Ineffectiveness as a function of the NTU and wall aspect ratio for $Bi_{min} = 0.0001$ and $C_R = .25$

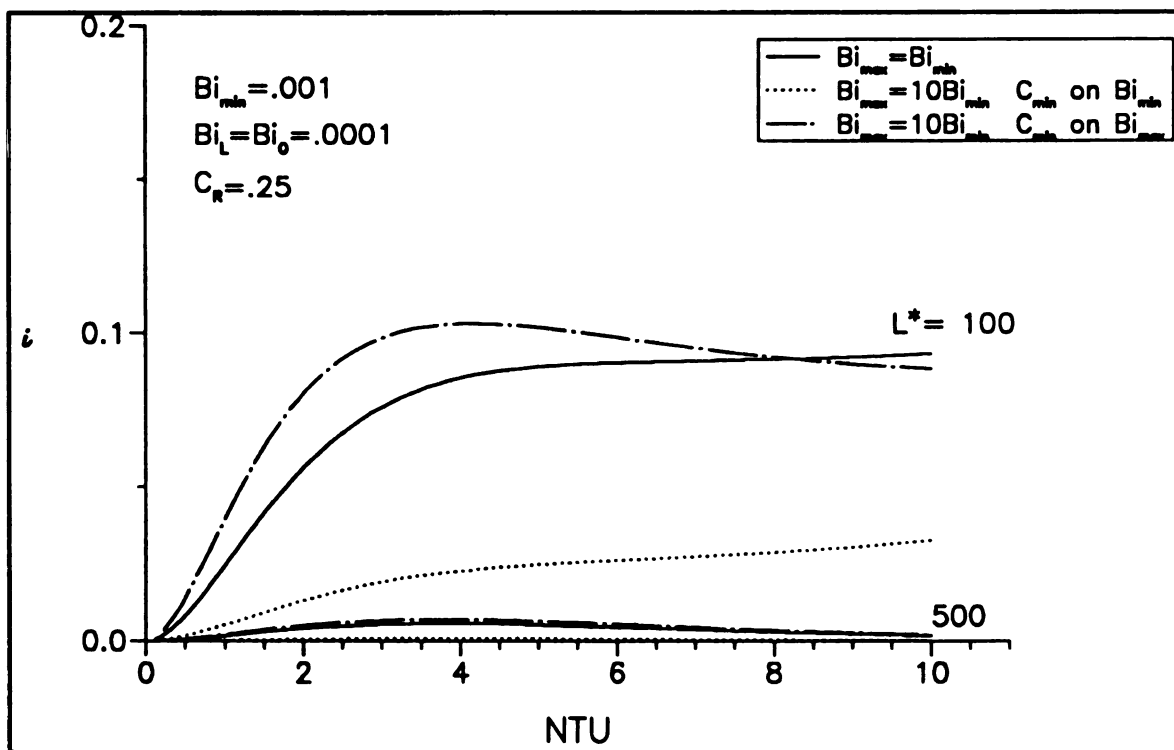


FIGURE 4.34. Ineffectiveness as a function of the NTU and wall aspect ratio for $Bi_{min} = 0.001$ and $C_R = .25$

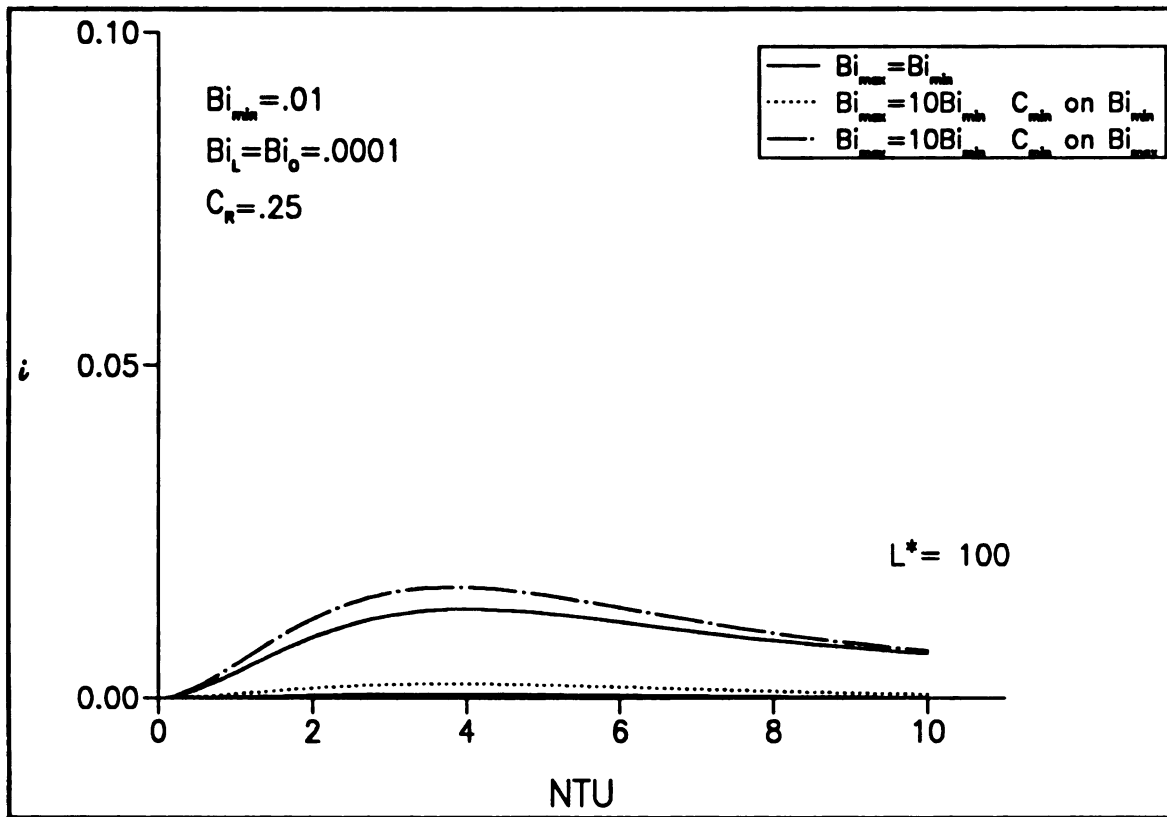


FIGURE 4.35. Ineffectiveness as a function of the NTU and wall aspect ratio for $Bi_{min} = 0.01$ and $C_R = 0.25$

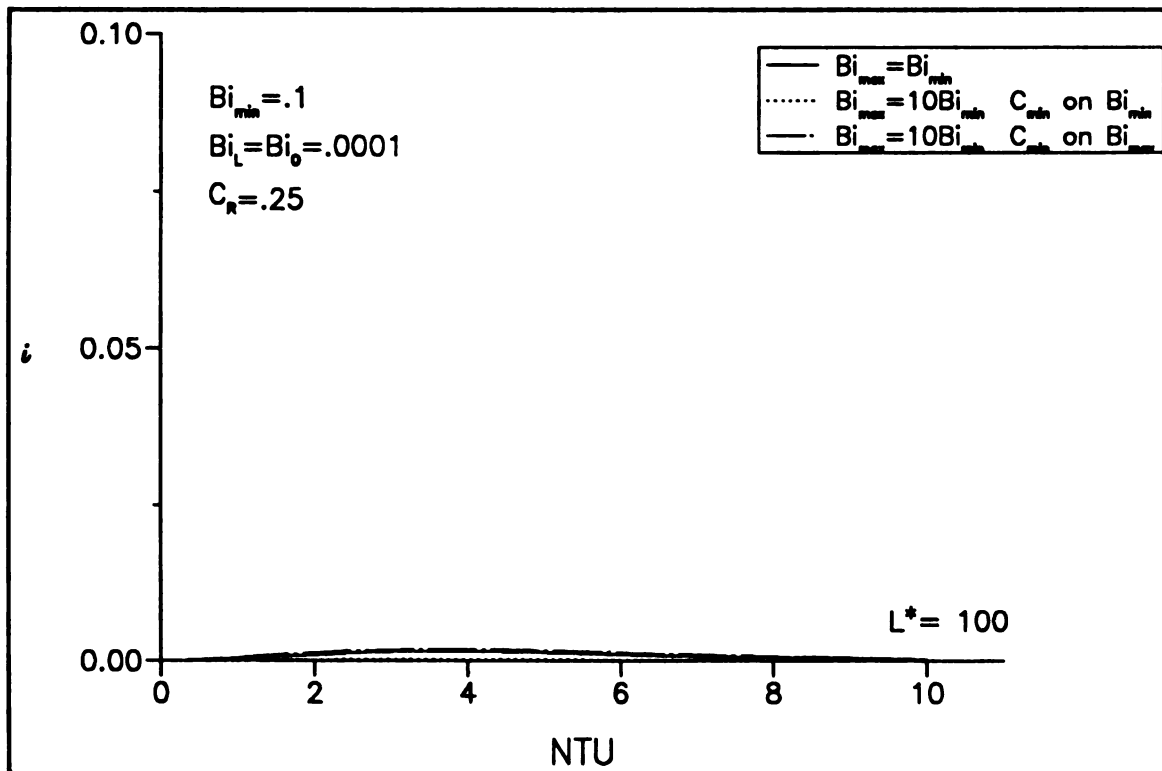


FIGURE 4.36. Ineffectiveness as a function of the NTU and wall aspect ratio for $Bi_{min} = 0.1$ and $C_R = 0.25$

4.2.1.5 Discussion of Results

In Sections (4.2.1.1-4.2.1.4) results were presented to give an indication of the operating conditions when axial conduction will exist and the extent to which the performance of the heat exchanger will be affected. Much of the information pertaining to the underlying physics was covered when the NTU was held constant and therefore will not be covered in detail in this section. Instead, the general trends in Figures 4.21-4.36 will be discussed. Because the scope of this study was intended to be general, all magnitudes of the describing parameters were considered for which axial conduction was nonzero. However, only the figures that best demonstrate the trends will be discussed.

The Mondt number is the only describing parameter that is not shown on the figures because it was the adjustable parameter in this study. Equation (4.10) shows that NTU is a function of the fluid Biot numbers, wall aspect ratio, and the Mondt number. To vary the NTU the fluid Biot numbers and wall aspect ratio was set and an appropriate magnitude of the Mondt number selected to provide the desired NTU , which is analogous to adjusting the flow rate of the fluids since the remaining terms in the Mondt number depend on the properties of the wall and fluid. Thus, the NTU is indicative of the Mondt number, and the two variables are linearly related for specified a wall aspect ratio and fluid Biot numbers. Although the influence of the Mondt number will be discussed in this section the real power of this variable is to predict the presence of axial conduction, which is covered in the next section.

The wall aspect ratio and fluid Biot numbers display a similar influence on axial conduction. At smaller magnitudes of these parameters the effect of axial conduction is more prominent. This is demonstrated in Figures 4.21 and 4.24. In Figure 4.21 for $L^* = 100$ and $Bi_{min} = Bi_{max} = 0.0001$ the ineffectiveness is over 40%, maintaining the same fluid Biot numbers the ineffectiveness decreases to a maximum of 10% at a wall aspect ratio of 1000. In Figure 4.24 the fluid Biot numbers are increased to .1 while maintaining the wall aspect ratio at 100 and the ineffectiveness decreases to 2%. These trends are seen for the wall aspect ratio regardless of the fluid Biot number and for equal fluid Biot numbers ($Bi_{max} = Bi_{min}$), but are not as universally true for unequal fluid Biot numbers. Since the maximum fluid Biot

number introduces secondary effects as it is increased, a point to be discussed later.

On a physical basis the smaller wall aspect ratios and fluid Biot numbers represent less thermal communication between the fluids because the smaller wall aspect ratios increase the wall thickness or decreases the wall length while the smaller Biot numbers decrease the convection between the wall and the fluid. These changes result in a greater amount of energy flow along the wall because the resistance to the energy flow in this direction is less than the resistance to the flow across the wall, which increased due to the changes in the wall aspect ratio and fluid Biot numbers.

In general, increasing the maximum fluid Biot number reduces the effect of axial conduction. This is shown by the ineffectiveness decreasing by as much as 40% in Figure 4.21 when the maximum fluid Biot number was increased at a wall aspect ratio of 1000, which is explained by the resistance to convection decreasing at the larger maximum fluid Biot number and axial conduction having less influence with the lower resistance. An exception to this outcome is seen for a combination of small magnitudes of the NTU , wall aspect ratio, and fluid Biot numbers, where the ineffectiveness increased at the larger maximum fluid Biot number, as shown in Figure 4.21 for $L^* = 100$ and $NTU < 2.5$. This is a result of the energy transfer switching from being limited by the thermodynamic parameter (C_{min}) to the heat transfer parameters (Bi_{max} , Bi_{min} , L^*). To show this, the effect of the Mondt number must first be considered.

The Mondt number varies with NTU , fluid Biot numbers, and the wall aspect ratio. To maintain a constant NTU at the larger maximum fluid Biot numbers the Mondt number is smaller than it was for equal fluid Biot numbers, which means the minimum heat capacity must become larger with the maximum fluid Biot number since all other parameters are constant in the Mondt number for a specified wall and fluids. In addition, at small NTU the Mondt number is relatively small in comparison to its magnitude at larger values of the NTU . Therefore, the minimum heat capacity is larger for small magnitudes of the NTU , and larger yet at the increased maximum fluid Biot number; due to the reciprocal relationship between the Mondt number and minimum heat capacity.

With these arguments, at the small values of the NTU the energy transfer is limited mainly by the minimum Biot number and wall aspect ratio since the minimum heat capacity is large. Then increasing the maximum fluid Biot number increases the ineffectiveness because the additional energy cannot be moved across the wall. While at larger NTU the energy transfer is limited mainly by the magnitude of the minimum heat capacity and when the maximum fluid Biot number is increased the additional energy can be moved across the wall ineffectiveness decreases. Note that at larger minimum fluid Biot numbers and wall aspect ratios this effect is not seen because the conditions are not as limiting on the energy transfer, as shown in Figure 4.21 at $L^* = 500$ and 1000 and for all wall aspect ratios at $Bi_{min} = 0.001$ in Figure 4.22.

Because unequal fluid Biot numbers needed to be investigated, the association between the magnitude of the heat capacity and fluid Biot numbers became an issue. Both possibilities are shown on all figures: minimum heat capacity with maximum fluid Biot number and with minimum fluid Biot numbers. The outcome of these two cases is straightforward. When like extremes of the heat capacity and fluid Biot numbers are associated an increase in the maximum fluid Biot number will improve conditions more so than when opposite extremes are associated. Since similar capabilities of energy transfer are being matched in the former case, largest heat transfer parameter with largest thermodynamic parameter. While for the later case the opposite extremes limit the energy transfer because the heat transfer parameter restricts the thermodynamic parameter or the thermodynamic parameter limits the heat transfer parameter. The outcome is, associating like extremes of heat capacity and fluid Biot numbers always has an equal or lower ineffectiveness compared to the case of opposite extremes associated.

The heat capacity ratio reduces the effect of axial conduction as it decreases. Considering a wall aspect ratio of 100 and equal fluid Biot numbers of magnitude .0001, at $C_R = 0.25$ the ineffectiveness is less than one-half the ineffectiveness at $C_R = 1.0$, in Figures 4.33 and 4.21 respectively. The heat capacity ratio decreases the effect of axial conduction because there is more energy available on one side of the wall and this increased amount of energy causes a larger driving temperature potential between the wall and the fluid. The improved energy transfer and larger amount of available energy

reduces the effect of axial conduction and hence decreases the ineffectiveness.

The heat capacity ratio also has some secondary effects that are related to the maximum fluid Biot number and the association between the magnitudes of the heat capacity and fluid Biot numbers. For the minimum fluid heat capacity associated with the maximum fluid Biot number the ineffectiveness was shown to increase as the maximum fluid Biot number increased for small magnitudes of the NTU , wall aspect ratio, and minimum fluid Biot number. Comparing the results of Figures 4.21, 4.25, 4.29, and 4.33 at $L^* = 100$ shows that the heat capacity ratio magnifies the amount that ineffectiveness increases at the larger maximum fluid Biot number in comparison to the ineffectiveness at equal fluid Biot numbers. Also, the magnitude of NTU at which the crossing point is seen and the ineffectiveness decreases for larger maximum fluid Biot numbers moves to larger NTU as the heat capacity ratio decreases.

Recalling that the larger ineffectiveness seen for small NTU as the maximum fluid Biot number increases was due to the energy transfer being limited by the magnitude of the wall aspect ratio and minimum fluid Biot number. The larger maximum fluid Biot number resulted in additional energy available, which could not be moved across the wall and hence the ineffectiveness increased. This was seen until at larger NTU the minimum heat capacity was smaller and the energy transfer limited by the available energy. In which case the ineffectiveness decreased at the larger maximum fluid Biot number.

As the heat capacity ratio decreases, the energy disparity across the wall grows. With opposite extremes of the heat capacity ratio and fluid Biot numbers paired, the growing energy disparity results in a larger increase in the ineffectiveness at the larger maximum fluid Biot number in comparison to the ineffectiveness at equal fluid Biot numbers. In Figure 4.29 for $L^* = 100$ the ineffectiveness increases nearly 10% for $C_R = 0.5$ at the larger maximum fluid Biot number and small NTU , while similar conditions produce an increase of only 5% for $C_R = 0.75$ in Figure 4.25. Note that the magnitude of the ineffectiveness is greater at $C_R = 0.75$ than it is at $C_R = 0.5$ for similar conditions, but the change seen in the ineffectiveness as the maximum fluid Biot number increased is larger for $C_R = 0.5$.

To summarize the results, the effects seen can be separated into two groups: primary effects and secondary effects. The primary effects occur due to changes in the wall aspect ratio, fluid Biot numbers, or heat capacity ratio. Secondary effects occur due to changes in the Mondt number and minimum heat capacity to maintain a constant NTU after varying the wall aspect ratio or fluid Biot numbers. These effects are shown in Table 4.4.

The primary effects occur as a direct result of a change in the amount of axial conduction. Table 4.4 shows that these effects decrease the amount of axial conduction and the ineffectiveness. However, when the conditions reach certain magnitudes; the secondary effects occur.

The secondary effects are the result of varying the NTU and show the status of the interaction between the heat transfer and thermodynamics. For small magnitudes of the NTU the minimum heat capacity is relatively large, and the amount of energy transferred is dictated mainly by the heat transfer. Whereas for larger magnitudes of the NTU , the minimum heat capacity is relatively small; and the amount of energy transfer dictated by the thermodynamics or available energy. Therefore, at small NTU the larger ineffectiveness seen as the parameters were varied is not due to an increase in axial conduction, instead it reflects that the limit of the energy transfer based on the heat transfer parameters has been reached or exceeded. This produces a larger ineffectiveness because the available energy increased as the parameters were varied but no additional energy could be transferred; due to the magnitude of heat transfer parameters (Bi_{max} , Bi_{min} , L^*). The secondary effects demonstrate interactions between the heat transfer and thermodynamics that are quite complex to analyze.

TABLE 4.4. Classification of effects seen as the NTU was varied

Primary Effect	Secondary Effect
Ineffectiveness decreases at larger L^* , Bi_{min} , and Bi_{max} .	Ineffectiveness increases for small magnitudes of NTU , L^* , and Bi_{min} when Bi_{max} is increased.
Ineffectiveness decreases at smaller C_R .	Ineffectiveness increases for small magnitudes of NTU , L^* , Bi_{min} , when Bi_{max} is increased and the amount of the increase grows as C_R is decreased.

4.3 Predicting the Presence of Axial Conduction with the Mondt number

Having shown that axial conduction can indeed adversely affect the performance of the heat exchanger, the conditions at which this will occur will now be analyzed. These operating conditions are represented in dimensionless form by the minimum and maximum fluid Biot numbers, wall aspect ratio, heat capacity ratio, NTU , and the Mondt number. Note that not all of these condition can be independently specified, as seen in equation (4.10). The first five parameters are defined on all figures in Section 4.2.1. The Mondt number however, is not shown on these figures because its magnitude was calculated to provide the desired NTU . Hence, as the minimum and maximum fluid Biot numbers and wall aspect ratio were varied the Mondt number was changed. However, using the equation for NTU the Mondt number can be calculated from the information on the figures

$$M_o = \frac{NTU}{L^{*2}} \left[\frac{Bi_{max} + Bi_{max}Bi_{min} + Bi_{min}}{Bi_{min}Bi_{max}} \right] \quad (4.24)$$

Using equation (4.24) the information in Table 4.5 was created allowing the Mondt number to be easily calculated as a function of the fluid Biot numbers, wall aspect ratio and NTU . Note that the Mondt number, which was defined earlier, is

$$M_o = \frac{K_w w}{C_{min} L^*} \quad (4.25)$$

and equation (4.24) is used to calculate the magnitude of the Mondt number for a particular operating condition, not define it.

TABLE 4.5. Relationship among Mondt number, wall aspect ratio, NTU , and Fluid Biot numbers

	$\frac{M_o L^{*2}}{NTU}$				
	Bi_{max}				
Bi_{min}	.0001	.001	.01	.1	1
.0001	20001	11001	10101	10011	10002
.001		2001	1101	1011	1002
.01			201	111	102
.1				21	12

Now the magnitude of the Mondt number as a function of the other parameters can be investigated. This was done for equal minimum and maximum fluid Biot numbers. The results are shown in Figure 4.37 for the Mondt number as a function of the NTU while varying the minimum fluid Biot number and wall aspect ratio. The legend identifies the correspondence between the minimum fluid Biot number and line pattern and to the right of the legend the wall aspect ratio for each curve is shown. Following upwards from a curve the corresponding wall aspect ratio for that curve can be found then moving horizontally from the wall aspect ratio the associated minimum fluid Biot number can be identified. The legend also allows the minimum Biot number to be identified directly from the curve, but when the curves overlap this is difficult and the alternate method may be used. Also, the trends in the magnitude of the wall aspect ratio can be visualized at the various minimum fluid Biot numbers.

The information concerning the relationship among the Mondt number, NTU , fluid Biot number, and wall aspect ratio by itself is not very useful. Using the information from Section 4.2.1 it was possible to draw the line depicting the dividing line between axial conduction being present and negligible. Ineffectiveness is negligible for parameters to the left of the line and nonzero for parameters to the right. The significance of this line is that it identifies the regions in terms of all the influencing parameters when axial conduction needs to be considered, albeit for a heat capacity ratio of one and equal fluid Biot numbers. After addressing the limitations on Figure 4.37 the basis for axial conduction depending mainly on the Mondt number is discussed.

As noted, the line identifying where axial conduction becomes nonzero is restricted to equal minimum and maximum fluid Biot numbers. However, as shown earlier, only a maximum fluid Biot number one order of magnitude larger than the minimum fluid Biot number needs to be considered since further increases in the maximum Biot number do not result in significant changes. Because the Mondt number changes with the maximum fluid Biot number, this requires a shifting of the curve for a particular wall aspect ratio and minimum fluid Biot number. The individual curve on Figure 4.37 needs to be shifted an amount equal to the ratio of the values in Table 4.5.

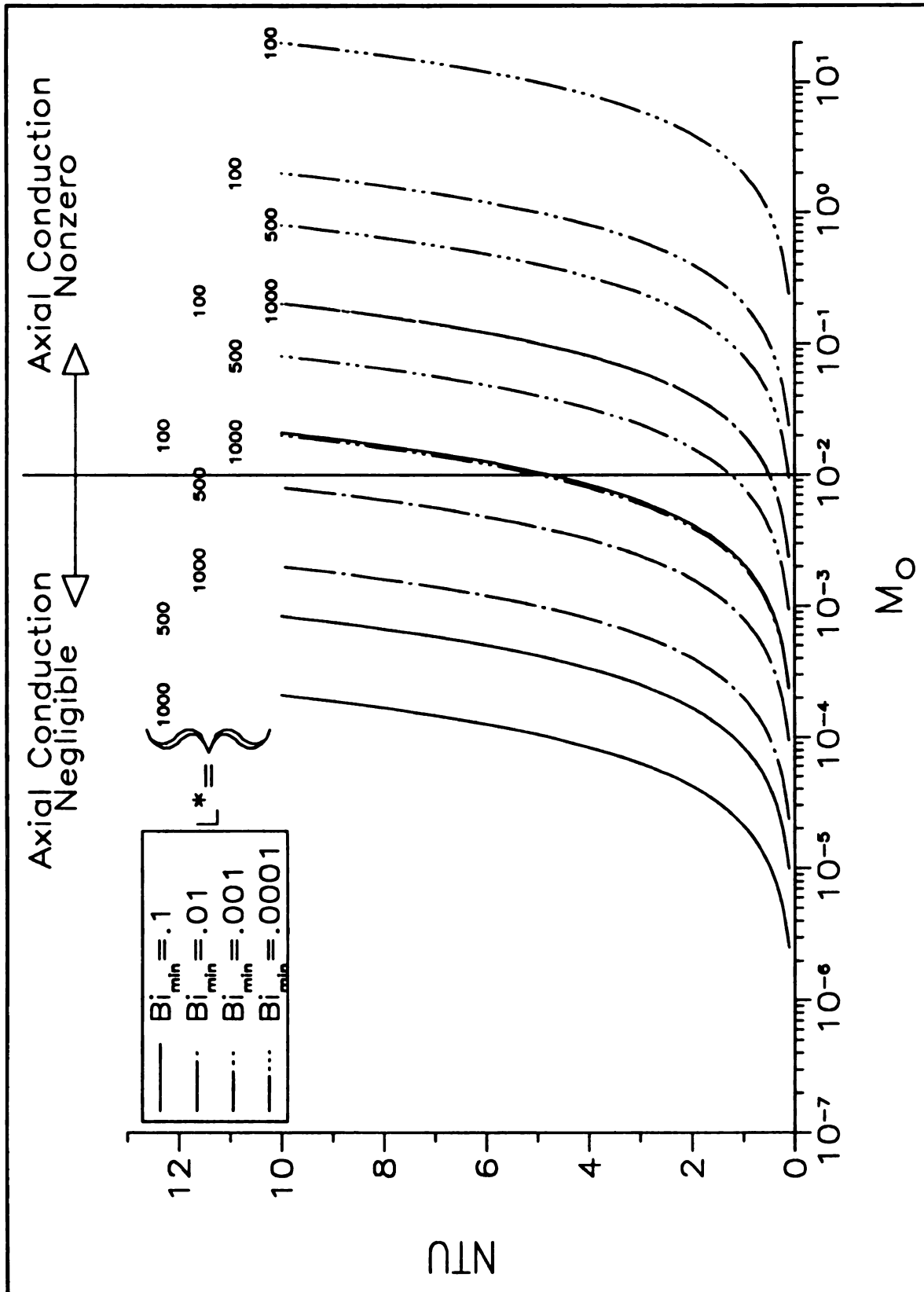


FIGURE 4.37. Predicted region affected by axial conduction in terms of the NTU, Mondt number, wall aspect ratio, and minimum fluid Biot number

To use the curves for equal fluid Biot numbers in Figure 4.37 when fluid Biot numbers are not equal requires the Mondt number or NTU read from the figure to be corrected. The Mondt number for unequal fluid Biot numbers is

$$M_o(Bi_{max} > Bi_{min}) = M_o(Bi_{max} = Bi_{min}) \left(\frac{\frac{M_o L^*{}^2}{NTU} (Bi_{max} > Bi_{min})}{\frac{M_o L^*{}^2}{NTU} (Bi_{max} = Bi_{min})} \right) \quad (4.26a)$$

while the NTU is

$$NTU(Bi_{max} > Bi_{min}) = NTU(Bi_{max} = Bi_{min}) \left(\frac{\frac{M_o L^*{}^2}{NTU} (Bi_{max} = Bi_{min})}{\frac{M_o L^*{}^2}{NTU} (Bi_{max} > Bi_{min})} \right) \quad (4.26b)$$

where $M_o(Bi_{max} = Bi_{min})$ in equation (4.26a) and $NTU(Bi_{max} = Bi_{min})$ in equation (4.26b) are read from Figure 4.37 and the ratio on the right hand side is obtained from Table 4.5 at the corresponding maximum and minimum fluid Biot numbers. Equation (4.26a) corrects the Mondt number to correlate to the NTU in Figure 4.37 for unequal fluid Biot number and equation (4.26b) corrects the NTU to correlate to the Mondt number in Figure 4.37 for unequal fluid Biot numbers. Only one of the variables (NTU or M_o) needs to be corrected; the other can be read from the figure directly.

A final restriction to the dividing line in Figure 4.37 is that it applies for a heat capacity ratio of one. Because this heat capacity ratio is the most adversely affected, these results will be correct in predicting when axial conduction is negligible for smaller heat capacity ratios. However, the results may indicate axial conduction is nonzero when in fact it is negligible at smaller heat capacity ratios. To alleviate this restriction, the dividing line can

TABLE 4.6. Magnitude of dividing Mondt number as a function of the heat capacity ratio

C_R	M_o
1.0	.010
.75	.015
.50	.030
.25	.070

be shifted for smaller heat capacity ratios, where the effect of axial conduction is less, if all other conditions are the same. Table 4.6 gives the approximate Mondt numbers that divide axial conduction as a function of the heat capacity ratio. Because the line does not shift very much, the additional lines were not added to Figure 4.37.

The Mondt number varies with the wall aspect ratio, NTU and fluid Biot numbers, as seen in equation (4.24). The Mondt number can be interpreted as the parameter that matches the properties of the wall and fluids (K_w and C_{min}) to the operating conditions (Bi_{max} , Bi_{min} , L^* , NTU). Figure 4.37 in conjunction with the results of Section 4.2.1 shows that as the Mondt number approaches zero the effect of axial conduction is negligible, while at larger values axial conduction is present.

The smaller Mondt number results in less axial conduction because to become smaller the product of the streamwise resistance and minimum heat capacity must get larger, which is shown using equations (4.25) and (4.16)

$$M_o = \frac{K_w w}{C_{min} L^*} = \frac{1}{C_{min} R_{streamwise}} \quad (4.27)$$

A larger minimum heat capacity means the fluid retains its energy better, and the energy that is transferred to the wall is hindered from conducting axially by the large resistance in that direction. However, for larger Mondt numbers the heat capacity is small, and the fluid gives up its energy easily. This energy can then be conducted down the wall because of the smaller streamwise resistance.

Physically the Mondt number represents the capabilities of the fluids and wall, the fluid's ability to carry energy and the walls ability to move energy in the axial direction. Because the Mondt number varies with fluid Biot number, wall aspect ratio and NTU it will reflect any changes seen in these variables, which explains why it is possible to base the presence of axial conduction on this parameter

The results in Figure 4.37 are intended to serve as a design guide to predict if axial conduction will exist. A certain amount of caution must be exercised in applying the results in Figure 4.37 and Table 4.6, however. The line presented on the figure for a heat capacity ratio of one was estimated by observing the ineffectiveness- NTU plots presented earlier, as were the magni-

tudes listed in Table 4.6. The criteria was an ineffectiveness less than 1% was negligible. For the regions near the dividing line, it is recommended to check the magnitudes of the ineffectiveness on the appropriate figure in Section 4.2.1.

The corrections allowing Figure 4.37 to be applied for unequal fluid Biot numbers in equations (4.26a) and (4.26b) will be in error for small values of the NTU , wall aspect ratio, and fluid Biot numbers if the relationship between the heat capacity and fluid Biot numbers associates the opposite extremes ($C_{min} - Bi_{max}$). This is due to the influence of the secondary effects when the thermodynamic energy becomes large. Even though the Mondt number is getting smaller the ineffectiveness increases, and this outcome reaches larger values of the NTU as the heat capacity ratio decreases. It is recommended not to use the corrections for this association of the fluid Biot numbers and heat capacity ratio.

4.4 Application of the Results

Up to this point, all operating conditions of the heat exchanger have been in terms of the Biot numbers, wall aspect ratio, heat capacity ratio, and Mondt number. Also the material properties of the wall or fluids have not been an issue since they were absorbed into dimensionless parameters. In this section the dimensional variables will be presented to show specific operating conditions (i.e. flow rates, fluid types, and wall material) when the previously presented results will apply. The results of this section could be used to establish experiments to verify the analytical solution.

The parameters that will be addressed in dimensional terms are the wall aspect ratio

$$L^* = \frac{L}{\delta} \quad (4.28)$$

minimum and maximum fluid Biot numbers

$$Bi_{min} = \min(Bi_C, Bi_H) \quad (4.29)$$

$$Bi_{max} = \max(Bi_C, Bi_H) \quad (4.30)$$

where

$$Bi_C = \frac{h_C \delta}{K_w} \quad (4.31)$$

$$Bi_H = \frac{h_H \delta}{K_w} \quad (4.32)$$

heat capacity ratio

$$C_R = \frac{C_{min}}{C_{max}} \quad (4.33)$$

where

$$C_{min} = \min(C_C, C_H) \quad (4.34)$$

$$C_{max} = \max(C_C, C_H) \quad (4.35)$$

and the Mondt number

$$M_o = \frac{K_w w}{C_{min} L^*} \quad (4.36)$$

which were all defined earlier, but are shown again for discussion purposes. The NTU is then

$$NTU = M_o L^*{}^2 \left[\frac{Bi_{min} Bi_{max}}{Bi_{max} + Bi_{min} Bi_{max} + Bi_{min}} \right] \quad (4.37)$$

In the previous section it was shown for a Mondt number less than .01 axial conduction was negligible. Consequently, the Mondt number must be larger to see axial conduction, and this is the parameter to begin the investigation of the dimensional quantities. Figure 4.38 gives an indication of the conditions required on the wall and fluids ($C_{min} L^* / w$) as a function of the wall thermal conductivity, that are needed to provide the required Mondt number. Also, for the given wall thermal conductivity the product of the convective heat transfer coefficient and wall thickness, calculated from equations (4.29-32), are given as a function of the minimum fluid Biot number by the additional labelled axes.

The results in Figure 4.38 give insight into the magnitudes and trends of the basic heat exchanger parameters required for axial conduction to exist. The thermal conductivity that intuitively would improve the performance if it were larger actually increases the possibility of axial conduction because the value of ($C_{min} L^* / w$) becomes larger as the thermal conductivity increases, as does the product $h\delta$. The larger these two groups of parameters are the more likely the chance they will be seen in a typical application. Noting that typical magnitudes of the wall aspect ratio and minimum heat capacity are at minimum $10^2 - 10^3$, the required Mondt number will surely not be reached unless a moderate thermal conductivity exist. This result gives an indication of the conditions necessary for axial conduction to exist; it is not an ordinary occurrence.

To experience axial conduction when the wall aspect ratio is relatively large ($L^* > 1000$), the heat capacity must be small or the wall width must be large. These conditions require a fluid with a low specific heat (such as a gas), a creeping flow to provide the small mass flow rate, or a large heat transfer area with a correspondingly large wall width.

The wall thickness is present on both axis and produces opposite outcomes for each. As the wall thickness becomes smaller, the wall aspect ratio gets larger and the possibility of axial conduction decreases because the

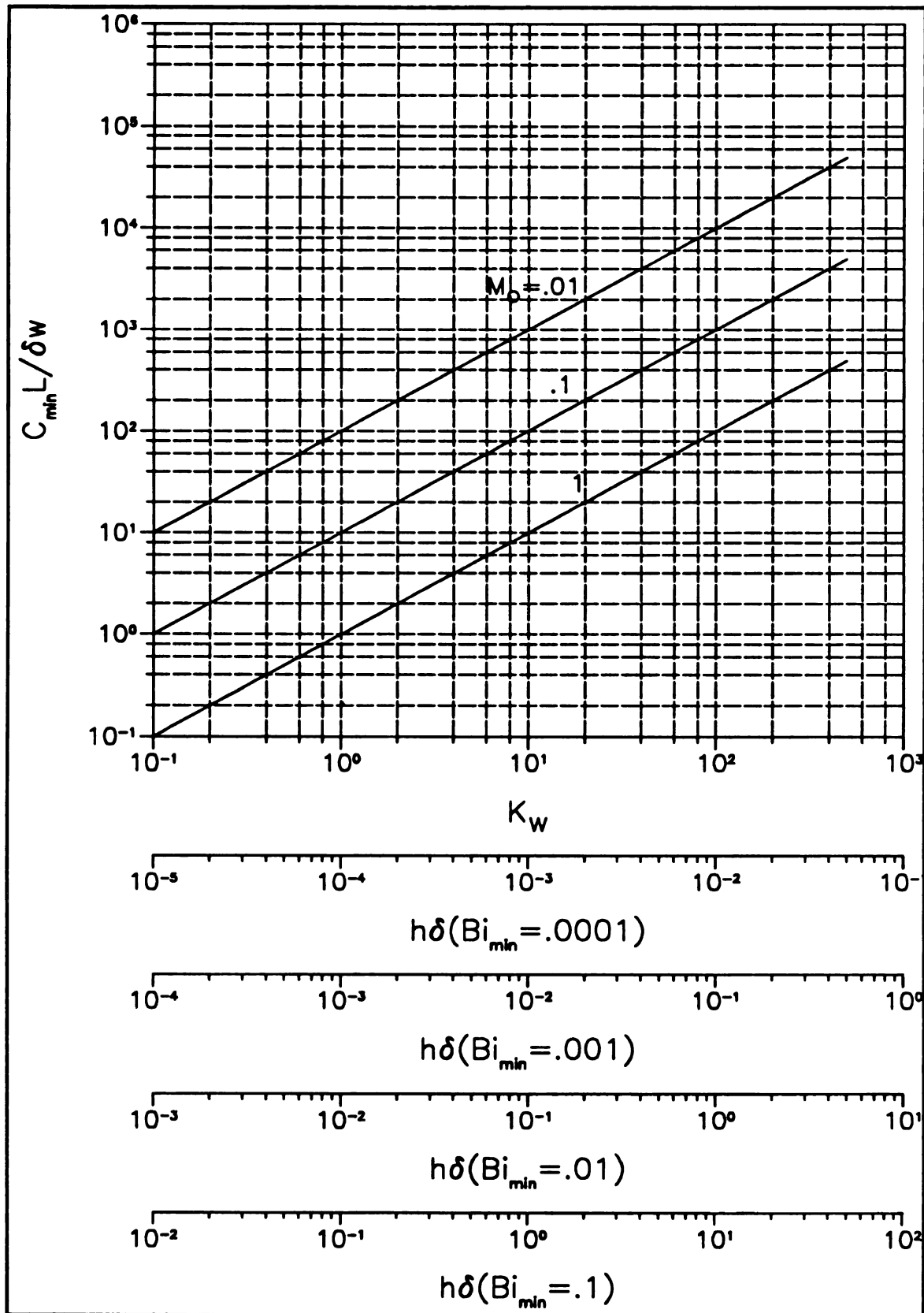


FIGURE 4.38. Magnitude of pertinent heat exchanger operating conditions as a function of the wall thermal conductivity, which is needed for axial conduction to exist

required minimum heat capacity is very small. However, the convective heat transfer coefficient on the horizontal axis becomes larger and more likely, which is due to the scaling scheme on the fluid Biot numbers while, the former effect of the wall thickness is due to its physical role.

From the previous discussion it is clear that to obtain the Mondt number necessary for axial conduction to exist requires one or more of the following conditions:

1. High wall thermal conductivity
2. Small ratio of wall length to thickness
3. Larger heat transfer area and corresponding wall width
4. Low specific heat fluids
5. Small mass flow rates

TABLE 4.7. Operating conditions for axial conduction to exist

	$\dot{m}L/w \text{ (kg/sec)}$			$h \text{ (W/m}^2\text{K)}$				Wall Material
	M_o			Bi_{min}				
	.01	.1	1	.0001	.001	.01	.1	
$\delta = .001$								
Air	1.5E-3	1.5E-4	1.5E-5	1.5	15	150	1500	Steel
Water	3.75E-4	3.75E-5	3.75E-6					
Air	4.0E-2	4.0E-3	4.0E-4	40	400	4000	40000	Copper
Water	1.0E-2	1.0E-3	1.0E-4					
$\delta = .01$								
Air	1.5E-2	1.5E-3	1.5E-4	.15	1.5	15	150	Steel
Water	3.75E-3	3.75E-4	3.75E-5					
Air	4.0E-1	4.0E-2	4.0E-3	4	40	400	4000	Copper
Water	1.0E-1	1.0E-2	1.0E-3					
$\delta = .1$								
Air	1.5E-1	1.5E-2	1.5E-3	.015	.15	1.5	15	Steel
Water	3.75E-2	3.75E-3	3.75E-4					
Air	4.0E+0	4.0E-1	4.0E-2	.4	4	40	400	Copper
Water	1.0E+0	1.0E-1	1.0E-2					

Consider the conditions needed for axial conduction in a wall material of steel ($K_w \approx 15$) or copper ($K_w \approx 400$) and fluids of water ($C_p \approx 4000$) or air ($C_p \approx 1000$). The possible combinations of wall material and fluid type are shown in Table 4.7 at various Mondt numbers and wall thicknesses. The results shown in Table 4.7 are the mass flow rate combined with the wall length and width and the convective heat transfer coefficient as a function of the fluid Biot number. The fluids, wall materials, and wall thicknesses were chosen to give a perspective over the range of the parameters that may be encountered for typical applications. Even though a wall thickness of .1 is quite extreme, it gives an indication of the magnitudes required for other parameters to become reasonable.

It was not possible to reduce to only the mass flow rate because the case would be too specialized. But noting that L/w is a minimum of one, and most likely larger than one; the magnitude of the mass flow rate is even smaller than the values shown for $\dot{m}L/w$ in Table 4.7.

It is apparent from the data presented in Table 4.7 that small mass flow rates and corresponding convection coefficients are required for axial conduction to exist. The required mass flow rate decreases as the Mondt number increases while the convection coefficient decreases as the minimum fluid Biot number decreases. Both trends demonstrate the requirement for axial conduction to become larger since large Mondt numbers and small fluid Biot numbers increase the effect of axial conduction on the performance of the heat exchanger.

Recalling that the results predicting axial conduction were based solely on the Mondt number, the results presented in Figure 4.38 and Table 4.7 do not particularly depend on the magnitude of the convective heat transfer coefficient. In essence, the magnitude of the convective heat transfer coefficient is arbitrary as long as the requirement on the Mondt number is met. But for a required Mondt number the magnitude of the convective heat transfer coefficient and wall dimensions will set the NTU . To obtain a particular NTU with a prescribed Mondt number and convective heat transfer coefficient may require unrealistic wall dimensions. Likewise, if the Mondt number and wall dimensions are prescribed, unrealistic convective heat transfer coefficients may be required. The magnitudes of the convective heat transfer coefficients are intended to represent the range that axial conduction was shown to exist

in physical situations. The range of the convective heat transfer coefficient, however, may not be physically realistic for the entire range of Mondt numbers shown.

4.5 Comparison to Published Results

All previous studies of the effect of axial conduction have been considerable less general than the present work. For this reason, there is only one specific case that can be compared to previously published results. This is the case of balanced symmetric flow in which the mass flow rates, heat capacities, and convective heat transfer coefficient between the fluid and wall are all equal for the two fluids. Therefore, the heat capacity ratio is one ($C_R = 1$) and the fluid Biot numbers will be equal ($Bi_{min} = Bi_{max}$).

For this case, Pan, Welch, and Head [15] derived a closed form expression for the effectiveness as a function of three variables

$$N_L = \frac{UA}{C} = NTU \quad (4.38)$$

$$N_K = \left(\frac{K_w A_w}{C}\right) \left(\frac{hA}{CL}\right) = \left(\frac{wK_w}{C}\right)^2 Bi \quad (4.39)$$

$$p = \left(1 + \frac{2}{N_K}\right)^{\frac{1}{2}} \quad (4.40)$$

which are related to the variables of the present study as shown. Note that the subscripts on heat capacity and Biot numbers have been dropped since the conditions are the same on both sides of the wall. The effectiveness is then given ([15] equation (34)) as

$$\varepsilon = \frac{N_L + (N_K/2p) \tanh(pN_L)}{N_L + (N_K/2p) \tanh(pN_L) + (N_K/2) + 1} \quad (4.41)$$

Using equation (4.41) the effectiveness (and ineffectiveness) was calculated and is shown in Figures 4.39-4.42 as a function of NTU at various minimum Biot numbers and wall aspect ratios. The results show excellent agreement with the present work. The results ($i - NTU$) differ only beyond the third decimal place, which can be attributed to computational round-off.

The same restrictive case was investigated by Rohsenow [17]. However, he proposed the effectiveness as a function of NTU and the Mondt number (M_o), which was earlier shown to be

$$M_o = \frac{K_w A_w}{LC} = \frac{K_w w}{CL^*} \quad (4.42)$$

and solved for the effectiveness at the extremes of the Mondt number, ([17] equations (32) and (34))

$$M_o = 0$$

$$\varepsilon = \frac{NTU}{1 + NTU} \quad (4.43)$$

$$M_o = \infty$$

$$\varepsilon = \frac{1}{2} (1 - e^{-2NTU}) \quad (4.44)$$

Obviously, with $M_o = 0$ the ineffectiveness is zero, since this is the case of neglecting axial conduction by allowing the wall thermal conductivity to shrink to zero; whereas, the wall conductivity becomes infinite for $M_o = \infty$. Both of these cases are shown also in Figures 4.39-4.42, and they provide bounds on the present results.

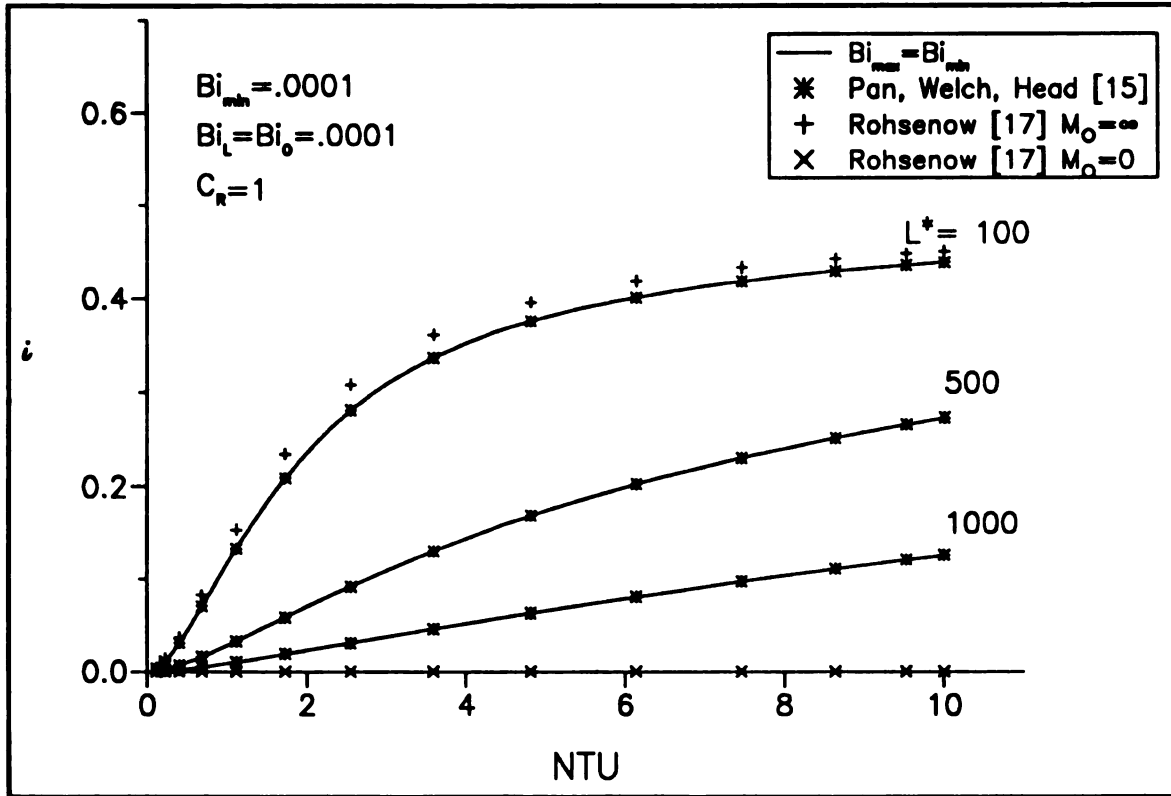


FIGURE 4.39. Comparison of present results to past result of Pan, Welch, and Head [15] and Rohsenow [17]. Ineffectiveness as a function of the NTU and wall aspect ratio for $Bi_{min} = 0.0001$ and $C_R = 1$.

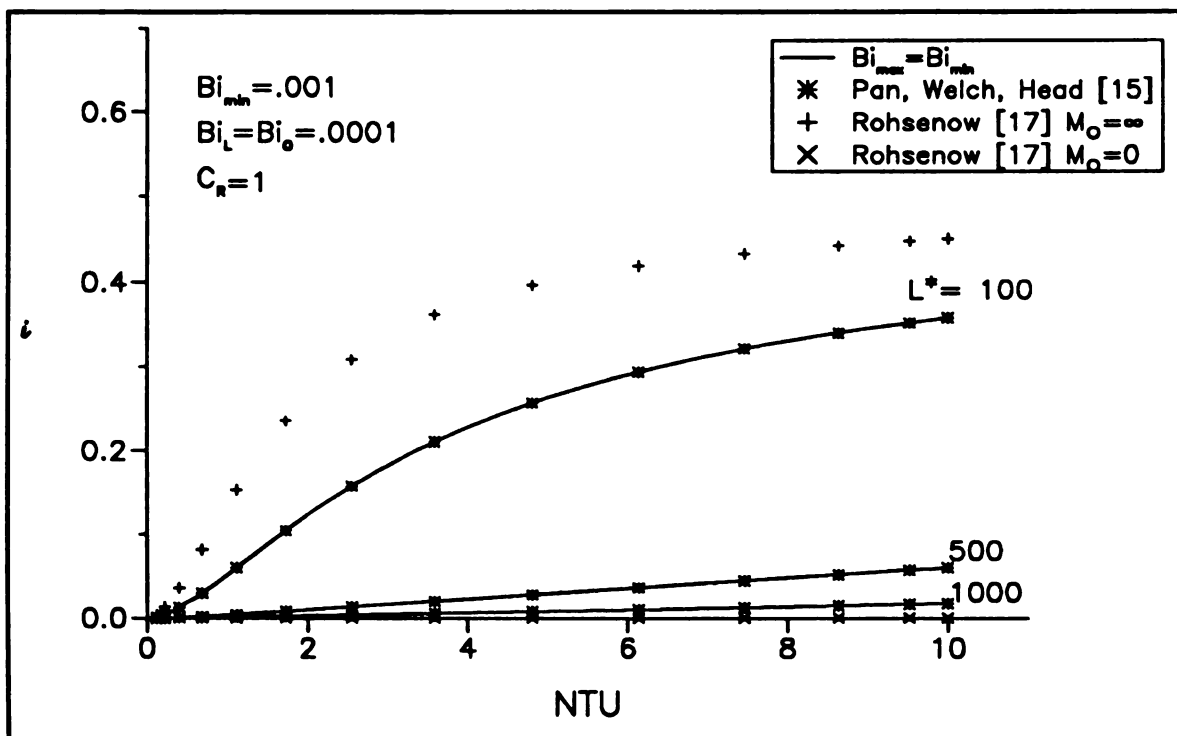


FIGURE 4.40. Comparison of present results to past result of Pan, Welch, and Head [15] and Rohsenow [17]. Ineffectiveness as a function of the NTU and wall aspect ratio for $Bi_{min} = 0.001$ and $C_R = 1$.

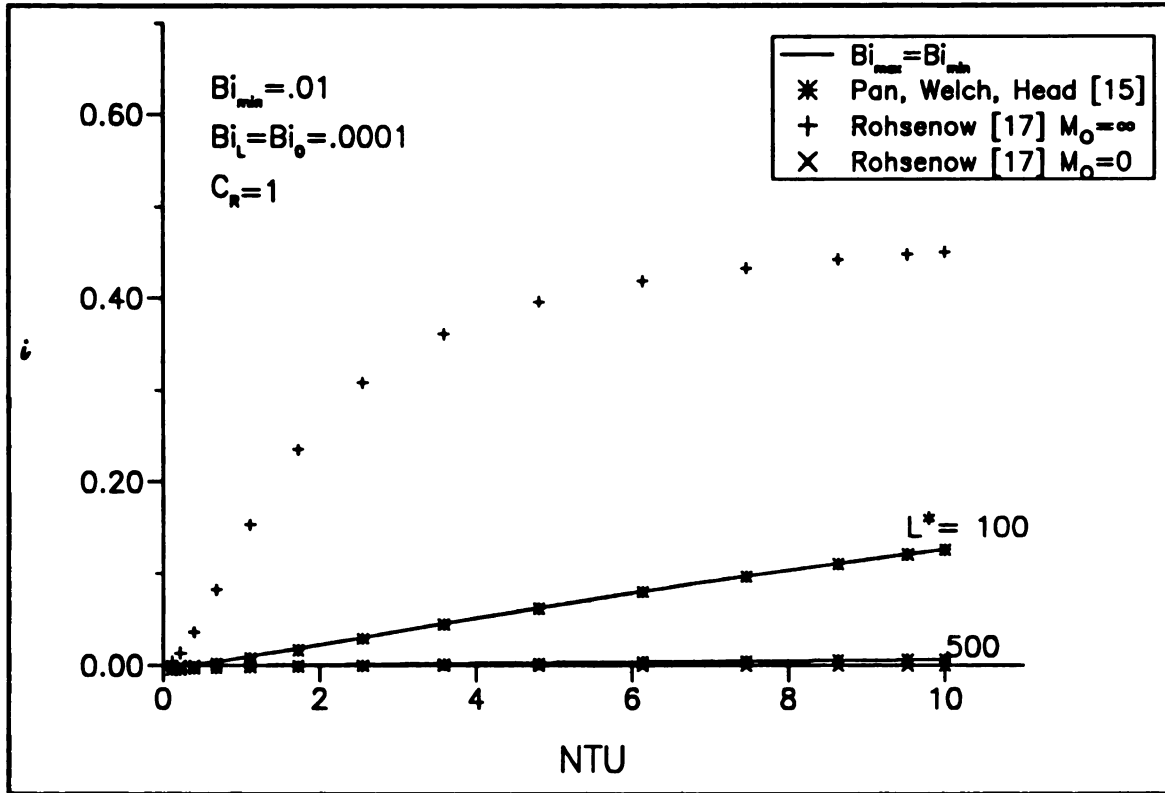


FIGURE 4.41. Comparison of present results to past result of Pan, Welch, and Head [15] and Rohsenow [17]. Ineffectiveness as a function of the NTU and wall aspect ratio for $Bi_{min} = 0.01$ and $C_R = 1$.

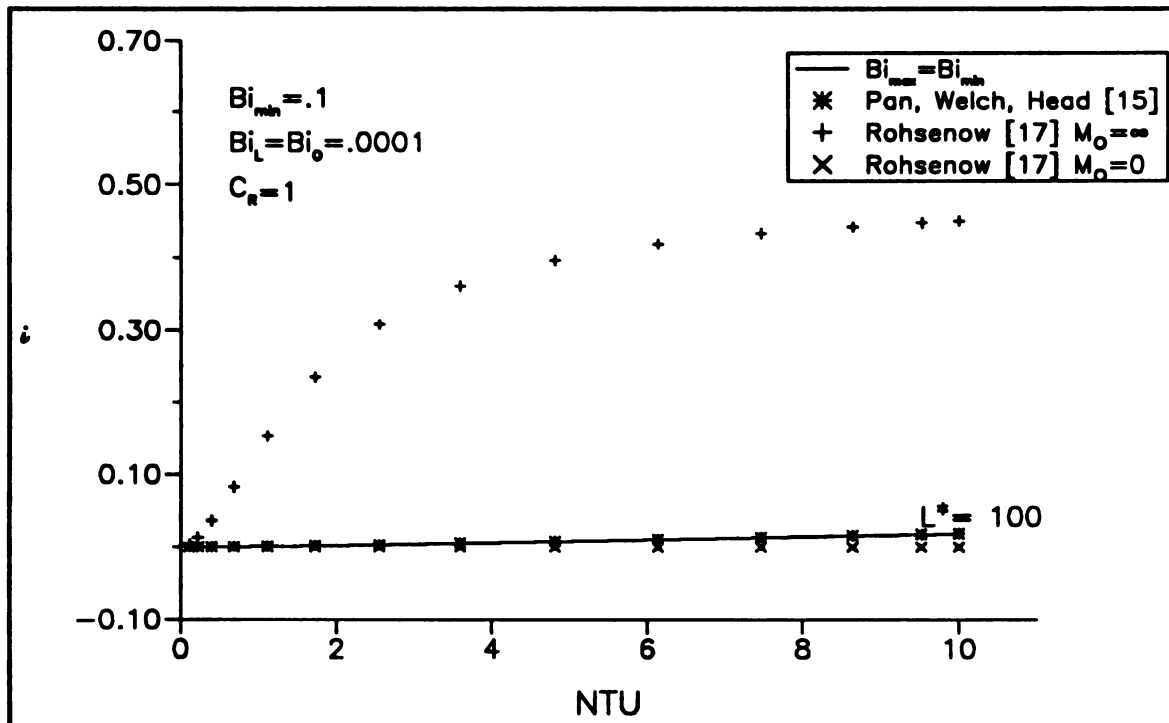


FIGURE 4.42. Comparison of present results to past result of Pan, Welch, and Head [15] and Rohsenow [17]. Ineffectiveness as a function of the NTU and wall aspect ratio for $Bi_{min} = 0.1$ and $C_R = 1$.

Chapter 5

Conclusions and Recommendations for Future Work

An exact solution for the analysis of the heat transfer occurring in a counterflow heat exchanger including the effect of axial conduction has been presented. In addition to the solution methodology a computer program to evaluate the numerical aspects of the exact solution was given. The program allowed for the investigation of the influential parameters in the solution and verification of the solution's validity. The role of all describing parameters was investigated to determine their importance in affecting axial conduction. The effect of axial conduction was quantified by the amount that the performance of the heat exchanger was degraded in comparison to the case of neglecting axial conduction.

The following results and conclusions are drawn from this investigation:

1. Axial conduction has less effect on the performance of the heat exchanger at larger wall aspect ratios.
2. Axial conduction has less effect on the performance of the heat exchanger at larger fluid Biot numbers.
3. Axial conduction is reduced at smaller heat capacity ratios.
4. The effect of the end Biot numbers on the performance of the heat exchanger is negligible for magnitudes less than or equal to the magnitude of the fluid Biot numbers.
5. Axial conduction is negligible for magnitudes of the Mondt number less than .01.
6. High wall thermal conductivity promotes axial conduction.
7. Axial conduction is more likely for large heat transfer areas.
8. Applications with low heat capacity fluids promote axial conduction.

The most obvious continuation of this work would be to experimentally verify the results presented herein. Although the effect requires some

atypical conditions, it was shown possible for common fluids. The applicability of this solution to an experimental set-up, which would typically be concentric tubes, will require the set-up to be approximated by the model, a plane dividing wall. Therefore, it must be possible to “cut and unroll” the concentric tubes and represent them as parallel plane walls without incurring an appreciable difference in the areas on opposite sides of the wall. In addition, the issue of identifying the type of boundary condition to model the physical problem at the ends of the wall will need to be addressed.

The computer program **AXCOND** could be coupled with existing thermal design software to predict the performance of a counterflow heat exchanger. Use of this program will be computationally expensive but will only need to be used when certain conditions exist, otherwise the traditional effectiveness-*NTU* relationships can be used. Incorporating the program into existing software will require conversion of the main program into a subroutine and consideration of the number of terms needed to produce a converged solution. Also, if the required analysis is a sizing problem, solving for the heat exchanger dimensions needed for a particular operating condition, an iterative scheme needs to be implemented.

The issue of the number of terms needed to obtain an accurate solution could also be further investigated. The outcome of this additional work may lead to possible simplifications if only a small number of terms are needed. Furthermore, simplified equations may result under certain conditions, which may allow for approximate solutions. In general, the complex solution presented may be studied for possible simplifying cases.

The solution presented could also be modified rather easily to determine the performance of a parallel flow heat exchanger. The formulation of the problem for the heat exchanger wall is exactly the same. The formulation of the fluid energy balance equations will differ by a sign and the location of the specified initial condition. The first difference will infiltrate the application of orthogonality to apply the nonhomogeneous boundary conditions on the wall and change one of the fluids temperature solution, but only by sign change(s). Whereas the initial condition will change the form of the integration constant on one of the fluid temperature solution. The conversion may be tedious, yet would require minimal computational effort or programming changes since the outline of the solution and program are given.

LIST OF REFERENCES

- [1] Beyer, W. H., CRC Standard Mathematical Tables, New York: CRC Press Inc., 1987
- [2] Campo, A., and J. C. Auguste, "Axial Conduction in Laminar Pipe Flows with Nonlinear Wall Heat Fluxes." International Journal of Heat and Mass Transfer, 1987, volume 21, p. 1957-1607
- [3] Chiou, J. P., "The Advancement of Compact Heat Exchanger Theory considering the Effects of Longitudinal Heat Conduction and Flow Nonuniformity." Compact Heat Exchangers,
- [4] Chiou, J. P., "Thermal Performance Deterioration in Crossflow Heat Exchangers Due to Longitudinal Heat Conduction in the Wall." ASME paper no. 76-Wa/HT-8
- [5] Chiou, J. P., "The Effect of Longitudinal Heat Conduction on Cross-flow Heat Exchangers." Journal of Heat Transfer, May 1978, volume 100, p.346-351
- [6] Edwards D. K., V. E. Denny, and A. F. Mills, Transfer Processes, New York: Hemisphere Publishing Corporation, 1979
- [7] Eisensmith, S. P., PlotIT User's Guide, September 1990
- [8] Hewitt, G. F., Hemisphere Handbook of Heat Exchanger Design, New York: Hemisphere Publishing Corporation, 1990
- [9] Incropera, F. P., and D. P. DeWitt, Introduction to Heat Transfer, New York: John Wiley and Sons, 1985
- [10] Kays W. M., and A. L. London, Compact Heat Exchangers, New York: McGraw Hill Book Company, 1984
- [11] Landau, H. G., and J. W. Hlinka, "Steady State Temperature Distribution in a Counterflow Heat Exchanger Including Longitudinal Conduction in the Wall." ASME paper no 60-Wa/HT-236
- [12] Mondt, J. R., Effects of Longitudinal Thermal Conduction in the Solid on Apparent Convection Behavior, with Data for Plate-Fin Surfaces." International Developments in Heat Transfer, 1960-61, p 614-621
- [13] Nyhoff, L., and S. Leestma, Fortran 77 for Engineers and Scientist, New York: Macmillan Publishing Company, 1988

- [14] Ozisik M. N., Heat Conduction, New York: John Wiley and Sons, 1980
- [15] Pan, C. L., N. E. Welch, and R. R. Head, "A New Concept to the General Understanding of the Effect of Longitudinal Conduction for Multi-stream Counter Flow Heat Exchanger." Proceedings of the 3rd International Heat Transfer Conference, 1966, volume I, p159-169
- [16] Pan, C. L., and N. E. Welch, "Exact Analytical Wall and Fluid Temperature Field for a Counterflow Heat Exchanger with the Effect of Longitudinal Heat Conduction." ASME paper no. 65-HT-63, 8th National Heat Transfer Conference, August 1965
- [17] Rohsenow, W. M., "Why Laminar Flow Heat Exchangers Can Perform Poorly." Heat Exchangers, New York: McGraw Hill Publishing Corporation, 1981, p. 1057-1072
- [18] Shah, R. K., "A Correlation for Longitudinal Heat Conduction Effects in Periodic-Flow Heat Exchangers." Journal of Engineering For Power, 1975, volume 97, p. 453-454
- [19] Somerton, C. W., Notes on Heat Exchanger Experiment, ME413 Course Notes, Michigan State University, 1990
- [20] Somerton, C. W., Personal Communication on Axial Conduction, 1990
- [21] Wark, K., Thermodynamics, New York: McGraw-Hill Book Company, 1983

APPENDICES

APPENDIX A

A.1 General Solution of the Wall Conduction Equation

Beginning with the partial differential equation for the wall and boundary conditions that were derived in Chapter 2

$$\frac{\partial^2 \theta_w}{\partial x^{*2}} + L^{*2} \frac{\partial^2 \theta_w}{\partial y^{*2}} = 0 \quad (\text{A.1})$$

$$-\frac{\partial \theta_w}{\partial x^*} \Big|_{x^*=0} + Bi_o \theta_w(0, y^*) = 0 \quad (\text{A.2a})$$

$$\frac{\partial \theta_w}{\partial x^*} \Big|_{x^*=1} + Bi_L \theta_w(1, y^*) = Bi_L (T_L - T_o) \quad (\text{A.2b})$$

$$-\frac{\partial \theta_w}{\partial y^*} \Big|_{y^*=0} + Bi_H \theta_w(x^*, 0) = Bi_H [T_H(x^*) - T_o] \quad (\text{A.2c})$$

$$\frac{\partial \theta_w}{\partial y^*} \Big|_{y^*=1} + Bi_C \theta_w(x^*, 1) = Bi_C [T_C(x^*) - T_o] \quad (\text{A.2d})$$

The problem is split into three simpler problems each with only one nonhomogeneous boundary condition.

Problem 1

$$\frac{\partial^2 \theta_1}{\partial x^{*2}} + L^{*2} \frac{\partial^2 \theta_1}{\partial y^{*2}} = 0 \quad (\text{A.3})$$

$$-\frac{\partial \theta_1}{\partial x^*} \Big|_{x^*=0} + Bi_o \theta_1(0, y^*) = 0 \quad (\text{A.4a})$$

$$\frac{\partial \theta_1}{\partial x^*} \Big|_{x^*=1} + Bi_L \theta_1(1, y^*) = Bi_L (T_L - T_o) \quad (\text{A.4b})$$

$$-\frac{\partial \theta_1}{\partial y^*} \Big|_{y^*=0} + Bi_H \theta_1(x^*, 0) = 0 \quad (\text{A.4c})$$

$$\left. \frac{\partial \theta_1}{\partial y^+} \right|_{y^+ = 1} + Bi_C \theta_1(x^+, 1) = 0 \quad (\text{A.4d})$$

Problem 2

$$\frac{\partial^2 \theta_2}{\partial x^{+2}} + L^{+2} \frac{\partial^2 \theta_2}{\partial y^{+2}} = 0 \quad (\text{A.5})$$

$$-\left. \frac{\partial \theta_2}{\partial x^+} \right|_{x^+ = 0} + Bi_o \theta_2(0, y^+) = 0 \quad (\text{A.6a})$$

$$\left. \frac{\partial \theta_2}{\partial x^+} \right|_{x^+ = 1} + Bi_L \theta_2(1, y^+) = 0 \quad (\text{A.6b})$$

$$-\left. \frac{\partial \theta_2}{\partial y^+} \right|_{y^+ = 0} + Bi_H \theta_2(x^+, 0) = Bi_H [T_H(x^+) - T_o] \quad (\text{A.6c})$$

$$\left. \frac{\partial \theta_2}{\partial y^+} \right|_{y^+ = 1} + Bi_C \theta_2(x^+, 1) = 0 \quad (\text{A.6d})$$

Problem 3

$$\frac{\partial^2 \theta_3}{\partial x^{+2}} + L^{+2} \frac{\partial^2 \theta_3}{\partial y^{+2}} = 0 \quad (\text{A.7})$$

$$-\left. \frac{\partial \theta_3}{\partial x^+} \right|_{x^+ = 0} + Bi_o \theta_3(0, y^+) = 0 \quad (\text{A.8a})$$

$$\left. \frac{\partial \theta_3}{\partial x^+} \right|_{x^+ = 1} + Bi_L \theta_3(1, y^+) = 0 \quad (\text{A.8b})$$

$$-\left. \frac{\partial \theta_3}{\partial y^+} \right|_{y^+ = 0} + Bi_H \theta_3(x^+, 0) = 0 \quad (\text{A.8c})$$

$$\left. \frac{\partial \theta_3}{\partial y^+} \right|_{y^+ = 1} + Bi_C \theta_3(x^+, 1) = Bi_C [T_C(x^+) - T_o] \quad (\text{A.8d})$$

It can be shown by adding the three problems in Eq. (A.3-8) that the original problem is obtained in Eq. (A.1-2). The solutions are related as follows:

$$\theta_w(x^+, y^+) = \theta_1(x^+, y^+) + \theta_2(x^+, y^+) + \theta_3(x^+, y^+) \quad (\text{A.9})$$

A.1.1 Solution for Nonhomogeneous Boundary Condition at $x^+ = 1$ (Problem 1)

Assuming a product solution for θ_1 of the form

$$\theta_1 = F(x^+) G(y^+) \quad (\text{A.10})$$

Substituting into the partial differential equation and boundary conditions, Eq. (A.3-4), gives

$$F_{x^+x^+}G + L^{*2}G_{y^+y^+}F = 0 \quad (\text{A.11})$$

$$-GF_{x^+}\big|_{x^+=0} + Bi_o GF(0) = 0 \quad (\text{A.12a})$$

$$GF_{x^+}\big|_{x^+=1} + Bi_o GF(1) = Bi_L(T_L - T_o) \quad (\text{A.12b})$$

$$-FG_{y^+}\big|_{y^+=0} + Bi_H FG(0) = 0 \quad (\text{A.12c})$$

$$FG_{y^+}\big|_{y^+=1} + Bi_H FG(1) = 0 \quad (\text{A.12d})$$

with the following convention for representing derivatives used:

$$\frac{\partial^2 F}{\partial x^{+2}} = F_{x^+x^+} \quad (\text{A.13})$$

Rearranging Eq. (A.11) to group similar variables and simplifying Eq. (A.12) gives

$$\frac{1}{L^{*2}} \frac{F_{x^+x^+}}{F} = -\frac{G_{y^+y^+}}{G} = \pm \mu^2 \quad (\text{A.14})$$

$$-F_{x^+}\big|_{x^+=0} + Bi_o F(0) = 0 \quad (\text{A.15a})$$

$$GF_{x^+}\big|_{x^+=1} + Bi_o GF(1) = Bi_L(T_L - T_o) \quad (\text{A.15b})$$

$$-G_{y^+}\big|_{y^+=0} + Bi_H G(0) = 0 \quad (\text{A.15c})$$

$$G_{y^+}\big|_{y^+=1} + Bi_H G(1) = 0 \quad (\text{A.15d})$$

where a constant, $\pm\mu^2$, was introduced in Eq. (A.14). With the left hand side only a function of x^* and the right hand side only a function of y^* for equality both sides must be equal to a constant, hence the introduction of the constant. This key result allows for separation of the variables, reducing the single partial differential equation to two ordinary differential equations. Before Eq. (A.14) can be separated however, a sign must be chosen for the constant. This sign is chosen to produce an eigenvalue problem for the function that has two homogenous boundary conditions to evaluate. The eigenvalue problem will have a general solution in terms of *sine* and *cosine* functions for this cartesian coordinate system. After choosing the sign, two ordinary differential equations can be written from Eq. (A.14) with the appropriate boundary conditions from Eq. (A.15)

$$F_{x^*x^*} - L^{*2}\mu^2 F = 0 \quad (\text{A.16})$$

$$-F_{x^*} \Big|_{x^*=0} + Bi_o F(0) = 0 \quad (\text{A.17a})$$

$$G_{y^*y^*} + \mu^2 G = 0 \quad (\text{A.18})$$

$$-G_{y^*} \Big|_{y^*=0} + Bi_H G(0) = 0 \quad (\text{A.19a})$$

$$G_{y^*} \Big|_{y^*=1} + Bi_H G(1) = 0 \quad (\text{A.19b})$$

Note that Eq. (A.16) only has one boundary condition, whereas Eq. (A.18) has two boundary conditions. The reason for this can be seen in Eq. (A.15b), which depends on both functions F and G and cannot be applied to either function singularly. Thus, this boundary condition must be applied after assembling the complete solution.

Eq. (A.16) and Eq. (A.18) have easily obtainable general solutions. The general solution for Eq. (A.16) is

$$F(x^*) = A_1 \cosh(\mu L^* x^*) + A_2 \sinh(\mu L^* x^*) \quad (\text{A.20})$$

Applying the boundary condition, Eq. (A.17a), gives a relationship for the two constants

$$A_2 = \frac{Bi_o}{\mu L^*} A_1 \quad (A.21)$$

which can be substituted into Eq. (A.20) and rearranged giving the solution

$$F(x^+) = A_4 [\mu L^* \cosh(\mu L^* x^+) + Bi_o \sinh(\mu L^* x^+)] \quad (A.22)$$

The solution of Eq. (A.18) is

$$G(y^+) = A_3 \cos(\mu y^+) + A_4 \sin(\mu y^+) \quad (A.23)$$

Applying the boundary conditions in Eq. (A.19a) solves for the relationship between the constants

$$A_4 = \frac{Bi_H A_3}{\mu} \quad (A.24)$$

Substituting into Eq. (A.23) and rearranging gives

$$G(y^+) = A_4 [\mu \cos(\mu y^+) + Bi_H \sin(\mu y^+)] \quad (A.25)$$

Applying the final boundary condition, Eq. (A.19b), does not provide any information about the constant A_4 because the constant cancels, it does provide information about the constant μ though, the equation simplifies to

$$\tan(\mu_n) = \frac{(Bi_H + Bi_C) \mu_n}{(\mu_n^2 - Bi_H Bi_C)} \quad (A.26)$$

To meet this boundary condition Eq. (A.26) must be satisfied for all values of μ_n . Eq. (A.26) is called a transcendental equation, it has an infinite number of solutions, hence the subscript on μ , and will be solved to determine the possible values of μ_n . The solution for the function G is then

$$G(\mu_n, y^+) = A_2 [\mu_n \cos(\mu_n y^+) + Bi_H \sin(\mu_n y^+)] \quad (A.27)$$

and μ_n is given by the solution of Eq. (A.26).

Putting Eq. (A.27) and Eq. (A.22) into Eq. (A.10) will give the solution. However, since there exist many solutions to Eq. (A.27) all possible solutions will be summed to obtain the final solution. Also, the undetermined constants, A_2 and A_4 , will be grouped into one constant that will be determined later by evaluating the last boundary condition, Eq. (A.4b), which was the boundary condition that did not separate and was not evaluated. The solution for problem one is

$$\theta_1(x^+, y^+) = \sum_{n=0}^{\infty} A_n [\mu_n L^* \cosh(\mu_n L^* x^+) + Bi_o \sinh(\mu_n L^* x^+)] * \\ [\mu_n \cos(\mu_n y^+) + Bi_H \sin(\mu_n y^+)] \quad (A.28)$$

and the eigenvalues are found from the solution of Eq. (A.26).

A.1.2 Solution for Nonhomogeneous Boundary Condition at $y^+ = 0$ (Problem 2)

Using similar methods problem two can be solved. Defining an assumed product solution

$$\theta_2 = F(x^+) G(y^+) \quad (A.29)$$

and substituting into the partial differential equation and boundary conditions and choosing a sign to make the proper eigenvalue problem allows the partial differential equation to be separated into two ordinary differential equations

$$F_{x^* x^*} + \alpha^2 F = 0 \quad (A.30)$$

$$-F_{x^*} \Big|_{x^*=0} + Bi_o F(0) = 0 \quad (A.31a)$$

$$F_{x^*} \Big|_{x^*=1} + Bi_L F(1) = 0 \quad (A.31b)$$

$$G_{y^* y^*} - \alpha^2 G = 0 \quad (A.32)$$

$$G_{y^*} \Big|_{y^*=1} + Bi_H G(1) = 0 \quad (A.33a)$$

The solutions are of the form, respectively

$$F(x^+) = B_1 \cos(\alpha x^+) + B_2 \sin(\alpha x^+) \quad (A.34)$$

$$G(y^+) = B_3 \cosh\left(\frac{\alpha}{L^*} y^+\right) + B_4 \sinh\left(\frac{\alpha}{L^*} y^+\right) \quad (A.35)$$

Applying the boundary conditions in Eq. (A.31a-b) to Eq. (A.33) gives

$$F(x^+) = B_1 [\alpha_n \cos(\alpha_n x^+) + Bi_o \sin(\alpha_n x^+)] \quad (A.36)$$

where the values of α_n are obtained from the solution of the transcendental equation

$$\tan(\alpha_n) = \frac{(Bi_o + Bi_L) \alpha_n}{(\alpha_n^2 + -Bi_L Bi_o)} \quad (A.37)$$

Applying the boundary condition given in Eq. (A.33a) to Eq. (A.35) gives

$$G(y^+) = B_3 \left[\cosh\left(\frac{\alpha}{L^*} y^+\right) - \zeta \sinh\left(\frac{\alpha}{L^*} y^+\right) \right] \quad (A.38)$$

where ζ is a constant, given by

$$\zeta = \frac{\frac{\alpha}{L^*} \sinh\left(\frac{\alpha}{L^*}\right) + Bi_C \cosh\left(\frac{\alpha}{L^*}\right)}{\frac{\alpha}{L^*} \cosh\left(\frac{\alpha}{L^*}\right) + Bi_C \sinh\left(\frac{\alpha}{L^*}\right)} \quad (A.39)$$

As before, putting the two solutions together and noting that the solution to Eq. (A.36) is the sum of all possible solution, and lumping undetermined constants together allows the solution to problem two to be written as

$$\theta_2(x^+, y^+) = \sum_{n=0}^{\infty} B_n \left[\cosh\left(\frac{\alpha_n}{L^*} y^+\right) - \zeta_n \sinh\left(\frac{\alpha_n}{L^*} y^+\right) \right] * \quad (A.40)$$

$$[\alpha_n \cos(\alpha_n x^+) + Bi_o \sin(\alpha_n x^+)]$$

and the values of α_n are obtained from the roots of Eq. (A.37).

A.1.3 Solution for Nonhomogeneous Boundary Condition at $y^+ = \delta$ (Problem 3)

Finally, applying the method again to solve problem three. Defining an assumed product solution

$$\theta_3 = F(x^+) G(y^+) \quad (A.41)$$

and substituting into the differential equation and boundary conditions and choosing a sign to make the proper eigenvalue problem allows the partial differential equation to be separated into two ordinary differential equations

$$F_{x^+ x^+} + \alpha^2 F = 0 \quad (A.42)$$

$$-F_{x^+} \Big|_{x^+=0} + Bi_o F(0) = 0 \quad (A.43a)$$

$$F_{x^+} \Big|_{x^+=1} + Bi_L F(1) = 0 \quad (A.43b)$$

$$G_{y^+y^+} - \alpha^2 G = 0 \quad (\text{A.44})$$

$$G_{y^+} \Big|_{y^+=0} + Bi_H G(0) = 0 \quad (\text{A.45a})$$

Realizing that Eq. (A.42-43) is exactly the same problem solved in the previous section, Eq. (A.30-31), the solution is

$$F(x^+) = C_1 [\alpha_n \cos(\alpha_n x^+) + Bi_o \sin(\alpha_n x^+)] \quad (\text{A.46})$$

where the values of α_n are obtained from the solution of the transcendental equation in Eq. (A.37). The solution to Eq. (A.44-45) is

$$G(y^+) = C_3 \left[\frac{\alpha_n}{L^*} \cosh\left(\frac{\alpha_n}{L^*} y^+\right) + Bi_H \sinh\left(\frac{\alpha_n}{L^*} y^+\right) \right] \quad (\text{A.47})$$

Putting the two solutions together and noting that the solution to Eq. (A.46) is the sum of all possible solution, and lumping undetermined constants together allows the solution to problem two to be written as

$$\theta_3(x^+, y^+) = \sum_{n=0}^{\infty} C_n \left[\frac{\alpha_n}{L^*} \cosh\left(\frac{\alpha_n}{L^*} y^+\right) + Bi_H \sinh\left(\frac{\alpha_n}{L^*} y^+\right) \right] * [\alpha_n \cos(\alpha_n x^+) + Bi_o \sin(\alpha_n x^+)] \quad (\text{A.48})$$

and the eigenvalues are given by the roots of Eq. (A.37)

A.1.4 Summary of the Solutions

The solutions for the three problems without applying the final (nonhomogeneous) boundary conditions are:

$$\theta_1(x^+, y^+) = \sum_{n=0}^{\infty} A_n [\mu_n L^* \cosh(\mu_n L^* x^+) + Bi_o \sinh(\mu_n L^* x^+)] * [\mu_n \cos(\mu_n y^+) + Bi_H \sin(\mu_n y^+)] \quad (\text{A.28})$$

$$\theta_2(x^+, y^+) = \sum_{n=0}^{\infty} B_n \left[\cosh\left(\frac{\alpha_n}{L^*} y^+\right) - \zeta_n \sinh\left(\frac{\alpha_n}{L^*} y^+\right) \right] * [\alpha_n \cos(\alpha_n x^+) + Bi_o \sin(\alpha_n x^+)] \quad (\text{A.39})$$

$$\theta_3(x^+, y^+) = \sum_{n=0}^{\infty} C_n \left[\frac{\alpha_n}{L^*} \cosh\left(\frac{\alpha_n}{L^*} y^+\right) + Bi_H \sinh\left(\frac{\alpha_n}{L^*} y^+\right) \right] * \\ [\alpha_n \cos(\alpha_n x^+) + Bi_o \sin(\alpha_n x^+)] \quad (A.47)$$

where the eigenvalues μ_n and α_n are given by the positive roots of the transcendental equations

$$\tan(\mu_n) = \frac{(Bi_H + Bi_C) \mu_n}{(\mu_n^2 - Bi_H Bi_C)} \quad (A.26)$$

$$\tan(\alpha_n) = \frac{(Bi_o + Bi_L) \alpha_n}{(\alpha_n^2 + -Bi_L Bi_o)} \quad (A.36)$$

The remaining boundary conditions to be applied to determine the constants A_n , B_n , and C_n , are Eq. (A.4b), Eq. (A.6c), and Eq. (A.8d) and they depend on the fluid temperatures for B_n and C_n , therefore all will be applied after the fluid temperatures are determined in Appendix B.

The solution for the wall conduction equation is given by Eq. (A.9) as the sum of the three solutions and the unscaled temperature (needed to solve for the fluid temperatures) is

$$T_w(x^+, y^+) = \theta_w(x^+, y^+) + T_o = \theta_1(x^+, y^+) + \theta_2(x^+, y^+) + \theta_3(x^+, y^+) + T_o \quad (A.48)$$

APPENDIX B

B.1 Solution of Hot Fluid Energy Balance

Taking the describing differential equation for the hot fluid that was derived in Chapter 2 and rearranging gives

$$\frac{dT_H}{dx^+} + N_H T_H = N_H T_w(x^+, 0) \quad (B.1)$$

$$T_H(0) = T_{H,in} \quad (B.2a)$$

The expression for the unscaled wall temperature (from Appendix A) is

$$\begin{aligned} T_w(x^+, 0) = T_o + \sum_{n=0}^{\infty} A_n \mu_n [\mu_n L^* \cosh(\mu_n L^* x^+) + Bi_o \sinh(\mu_n L^* x^+)] \\ + \sum_{n=0}^{\infty} \left(B_n + \frac{\alpha_n}{L^*} C_n \right) [\alpha_n \cos(\alpha_n x^+) + Bi_o \sin(\alpha_n x^+)] \end{aligned} \quad (B.3)$$

Putting this into the differential, Eq. (B.1), and arranging gives

$$\begin{aligned} \frac{dT_H}{dx^+} + N_H T_H = N_H \{ T_o + \sum_{n=0}^{\infty} A_n \mu_n [\mu_n L^* \cosh(\mu_n L^* x^+) + Bi_o \sinh(\mu_n L^* x^+)] \\ + \sum_{n=0}^{\infty} \left(B_n + \frac{\alpha_n}{L^*} C_n \right) [\alpha_n \cos(\alpha_n x^+) + Bi_o \sin(\alpha_n x^+)] \} \end{aligned} \quad (B.4)$$

To solve this problem it was first split into two problems, a homogeneous problem

$$\frac{dT_{H,h}}{dx^+} + N_H T_{H,h} = 0 \quad (B.5)$$

and a particular problem

$$\begin{aligned} \frac{dT_{H,p}}{dx^+} + N_H T_{H,p} = N_H \{ T_o + \sum_{n=0}^{\infty} A_n \mu_n [\mu_n L^* \cosh(\mu_n L^* x^+) + Bi_o \sinh(\mu_n L^* x^+)] \\ + \sum_{n=0}^{\infty} \left(B_n + \frac{\alpha_n}{L^*} C_n \right) [\alpha_n \cos(\alpha_n x^+) + Bi_o \sin(\alpha_n x^+)] \} \end{aligned} \quad (B.6)$$

The particular problem in Eq. (B.6) was further divided into three problems for each term on the right hand side of the equation. The general solution for Eq. (B.1) in terms of the simpler problem's solutions is

$$T_H(x^+) = T_{H,h}(x^+) + \sum_{i=1}^3 T_{H,pi}(x^+) \quad (B.7)$$

Where $T_{H,pi}$ is the solution to the problem

$$\begin{aligned} \frac{dT_{H,pi}}{dx^+} + N_H T_{H,pi} &= N_H \{ \delta_{1i} T_o \\ &+ \delta_{2i} \sum_{n=0}^{\infty} A_n \mu_n [\mu_n L^* \cosh(\mu_n L^* x^+) + Bi_o \sinh(\mu_n L^* x^+)] \\ &+ \delta_{3i} \sum_{n=0}^{\infty} \left(B_n + \frac{\alpha_n}{L^*} C_n \right) [\alpha_n \cos(\alpha_n x^+) + Bi_o \sin(\alpha_n x^+)] \} \end{aligned} \quad (B.8)$$

($i = 1, 2, 3$) and δ_{ji} is the kronecker delta function as defined in Eq. (3.7). Superposition of the problems in Eq. (B.8) and Eq. (B.5) will give the originally posed problem in Eq. (B.4).

B.1.1 Hot fluid Homogenous Solution

The homogenous problem in Eq. (B.5) is solved giving

$$T_{H,h}(x^+) = D_1 \exp(N_H x^+) \quad (B.9)$$

where D_1 is a constant to be determined after assembling the complete solution as shown in Eq. (B.7).

B.1.2 Hot fluid Particular Solution 1

Solution of the particular problem in Eq. (B.8) was obtained using standard variation of parameter techniques. This method substitutes a general solution of functional form similar to the nonhomogeneous term in the problem then solves for the unknown constants in this general solution. For the first particular solution ($i=1$) the general solution would be a constant,

$$T_{H,p1}(x^+) = f(T_o) = k = \text{constant} \quad (B.10)$$

Substituting this into the differential equation Eq. (B.8) yields

$$N_H k = N_H T_o \quad (\text{B.11})$$

and the solution is

$$T_{H,p1} = T_o \quad (\text{B.12})$$

B.1.3 Hot fluid Particular Solution 2

The functional form of the second particular solution ($i=2$) is

$$T_{H,p2} = \sum_{n=0}^{\infty} b_n \cosh(\mu_n L^* x^+) + c_n \sinh(\mu_n L^* x^+) \quad (\text{B.13})$$

Substituting into the differential equation, Eq. (B.8), (note the summations are not shown) gives

$$\begin{aligned} & b_n \mu_n L^* \sinh(\mu_n L^* x^+) + c_n \mu_n L^* \cosh(\mu_n L^* x^+) \\ & N_H [b_n \cosh(\mu_n L^* x^+) + c_n \sinh(\mu_n L^* x^+)] \\ & = N_H A_n \mu_n [\mu_n L^* \cosh(\mu_n L^* x^+) + Bi_o \sinh(\mu_n L^* x^+)] \end{aligned} \quad (\text{B.14})$$

For this particular solution to be correct equality must hold, which is accomplished through the constants b_n and c_n . Grouping all constants for the *sinh* and *cosh* terms separately into two equations produces

$$b_n \mu_n L^* + N_H c_n = N_H A_n \mu_n Bi_o \quad (\text{B.15})$$

for the *sinh* terms and

$$c_n \mu_n L^* + N_H b_n = N_H A_n \mu_n^2 L^* \quad (\text{B.16})$$

for the *cosh* terms. Solving these two equations for the unknown constants

$$b_n = A_n \mu_n^2 L^* \left[1 - \frac{(Bi_o N_H - \mu_n^2 L^{*2})}{(N_H^2 - \mu_n^2 L^{*2})} \right] \quad (\text{B.17})$$

$$c_n = A_n N_H \mu_n \left[\frac{(Bi_o N_H - \mu_n^2 L^{*2})}{(N_H^2 - \mu_n^2 L^{*2})} \right] \quad (\text{B.18})$$

and substituting into Eq. (B.13) gives the second particular solution

$$T_{H,p2}(x^+) = \sum_{n=0}^{\infty} A_n \left\{ \mu_n^2 L^* \left[1 - \frac{(Bi_o N_H - \mu_n^2 L^{*2})}{(N_H^2 - \mu_n^2 L^{*2})} \right] \cosh(\mu_n L^* x^+) \right. \\ \left. + N_H \mu_n \left[\frac{(Bi_o N_H - \mu_n^2 L^{*2})}{(N_H^2 - \mu_n^2 L^{*2})} \right] \sinh(\mu_n L^* x^+) \right\} \quad (B.19)$$

B.1.4 Hot fluid Particular Solution 3

The functional form of the third and final particular solution ($i=3$) is

$$T_{H,p3}(x^+) = \sum_{n=0}^{\infty} a_n \cos(\alpha_n x^+) + d_n \sin(\alpha_n x^+) \quad (B.20)$$

Substituting into the differential equation

$$-a_n \alpha_n \sin(\alpha_n x^+) + d_n \alpha_n \cos(\alpha_n x^+) + N_H [a_n \cos(\alpha_n x^+) + d_n \sin(\alpha_n x^+)] \\ = N_H \left(B_n + \frac{\alpha_n}{L^*} C_n \right) [\alpha_n \cos(\alpha_n x^+) + Bi_o \sin(\alpha_n x^+)] \quad (B.21)$$

then separating into two equations, the coefficients are

$$d_n \alpha_n + N_H a_n = N_H \left(B_n + \frac{\alpha_n}{L^*} C_n \right) \alpha_n \quad (B.22)$$

for the \cos terms and

$$-a_n \alpha_n + N_H d_n = N_H \left(B_n + \frac{\alpha_n}{L^*} C_n \right) Bi_o \quad (B.23)$$

for the \sin terms. Solving for the unknown constants

$$a_n = \left(B_n + \frac{\alpha_n}{L^*} C_n \right) \alpha_n \left[1 - \frac{(Bi_o N_H + \alpha_n^2)}{(N_H^2 + \alpha_n^2)} \right] \quad (B.24)$$

$$d_n = \left(B_n + \frac{\alpha_n}{L^*} C_n \right) N_H \left[\frac{Bi_o N_H + \alpha_n^2}{N_H^2 + \alpha_n^2} \right] \quad (B.25)$$

and substituting into Eq. (B.20) gives the particular solution

$$T_{H,p3}(x^+) = \sum_{n=0}^{\infty} \left(B_n + \frac{\alpha_n}{L^*} C_n \right) \left\{ \alpha_n \left[1 - \frac{(Bi_o N_H + \alpha_n^2)}{(N_H^2 + \alpha_n^2)} \right] \cos(\alpha_n x^+) \right. \\ \left. + N_H \left[\frac{Bi_o N_H + \alpha_n^2}{N_H^2 + \alpha_n^2} \right] \sin(\alpha_n x^+) \right\} \quad (B.26)$$

Assembling the solutions to the simpler problems, Eq. (B.9), Eq. (B.12), Eq. (B.19), and Eq. (B.26), using the relationship given in Eq. (B.7), the solution for the hot fluid energy balance is

$$T_H(x^+) = T_o + D_1 \exp(-N_H x^+) \\ + \sum_{n=0}^{\infty} A_n \left\{ \mu_n^2 L^* \left[1 - \frac{(Bi_o N_H - \mu_n^2 L^{*2})}{(N_H^2 - \mu_n^2 L^{*2})} \right] \cosh(\mu_n L^* x^+) \right. \\ \left. + N_H \mu_n \left[\frac{(Bi_o N_H - \mu_n^2 L^{*2})}{(N_H^2 - \mu_n^2 L^{*2})} \right] \sinh(\mu_n L^* x^+) \right\} \\ + \sum_{n=0}^{\infty} \left(B_n + \frac{\alpha_n}{L^*} C_n \right) \left\{ \alpha_n \left[1 - \frac{(Bi_o N_H + \alpha_n^2)}{(N_H^2 + \alpha_n^2)} \right] \cos(\alpha_n x^+) \right. \\ \left. + N_H \left[\frac{Bi_o N_H + \alpha_n^2}{N_H^2 + \alpha_n^2} \right] \sin(\alpha_n x^+) \right\} \quad (B.27)$$

Applying the boundary condition, Eq. (B.2a), the constant is

$$D_1 = T_{H,in} - T_o - \sum_{n=0}^{\infty} A_n \mu_n^2 L^* \left[1 - \frac{(Bi_o N_H - \mu_n^2 L^{*2})}{(N_H^2 - \mu_n^2 L^{*2})} \right] \\ - \sum_{n=0}^{\infty} \left(B_n + \frac{\alpha_n}{L^*} C_n \right) \alpha_n \left[1 - \frac{(Bi_o N_H + \alpha_n^2)}{(N_H^2 + \alpha_n^2)} \right] \quad (B.28)$$

B.2 Solution of Cold fluid Energy Balance

The differential equation that was derived in chapter 2 for the cold fluid, after rearranging is

$$-\frac{dT_C}{dx^+} + N_C T_C = N_C T_w(x^+, 1) \quad (\text{B.29})$$

$$T_C(1) = T_{C,in} \quad (\text{B.30a})$$

The wall temperature solution (from appendix A) is

$$\begin{aligned} T_w(x^+, 1) = T_0 + \sum_{n=0}^{\infty} A_n [\mu_n L^* \cosh(\mu_n L^* x^+) + Bi_o \sinh(\mu_n L^* x^+)] * \\ [\mu_n \cos(\mu_n) + Bi_H \sin(\mu_n)] \\ + \sum_{n=0}^{\infty} B_n \left[\cosh\left(\frac{\alpha_n}{L^*}\right) - \zeta_n \sinh\left(\frac{\alpha_n}{L^*}\right) \right] * \\ [\alpha_n \cos(\alpha_n x^+) + Bi_o \sin(\alpha_n x^+)] \\ + \sum_{n=0}^{\infty} C_n \left[\frac{\alpha_n}{L^*} \cosh\left(\frac{\alpha_n}{L^*}\right) + Bi_H \sinh\left(\frac{\alpha_n}{L^*}\right) \right] * \\ [\alpha_n \cos(\alpha_n x^+) + Bi_o \sin(\alpha_n x^+)] \quad (\text{B.31}) \end{aligned}$$

Defining the following constants:

$$A_n' = A_n [\mu_n \cos(\mu_n) + Bi_H \sin(\mu_n)] \quad (\text{B.32})$$

$$B_n' = B_n \left[\cosh\left(\frac{\alpha_n}{L^*}\right) - \zeta_n \sinh\left(\frac{\alpha_n}{L^*}\right) \right] \quad (\text{B.33})$$

$$C_n' = C_n \left[\frac{\alpha_n}{L^*} \cosh\left(\frac{\alpha_n}{L^*}\right) + Bi_H \sinh\left(\frac{\alpha_n}{L^*}\right) \right] \quad (\text{B.34})$$

simplifies the expression for $T_w(x^+, 1)$ to

$$\begin{aligned} T_w(x^+, 1) = T_0 + \sum_{n=0}^{\infty} A_n' [\mu_n L^* \cosh(\mu_n L^* x^+) + Bi_o \sinh(\mu_n L^* x^+)] \\ + \sum_{n=0}^{\infty} (B_n' + C_n') [\alpha_n \cos(\alpha_n x^+) + Bi_o \sin(\alpha_n x^+)] \quad (\text{B.35}) \end{aligned}$$

Putting this into the differential Eq. (B.29) and arranging gives

$$-\frac{dT_C}{dx^+} + N_C T_C = N_C \left\{ T_o + \sum_{n=0}^{\infty} A_n' [\mu_n L^* \cosh(\mu_n L^* x^+) + Bi_o \sinh(\mu_n L^* x^+)] \right. \\ \left. + \sum_{n=0}^{\infty} (B_n' + C_n') [\alpha_n \cos(\alpha_n x^+) + Bi_o \sin(\alpha_n x^+)] \right\} \quad (B.36)$$

To solve this problem it was first split into two simpler problems, a homogeneous problem

$$\frac{dT_{C,h}}{dx^+} + N_C T_{C,h} = 0 \quad (B.37)$$

and a particular problem

$$-\frac{dT_{C,p}}{dx^+} + N_C T_{C,p} = N_C \left\{ T_o + \sum_{n=0}^{\infty} A_n' [\mu_n L^* \cosh(\mu_n L^* x^+) + Bi_o \sinh(\mu_n L^* x^+)] \right. \\ \left. + \sum_{n=0}^{\infty} (B_n' + C_n') [\alpha_n \cos(\alpha_n x^+) + Bi_o \sin(\alpha_n x^+)] \right\} \quad (B.38)$$

The particular problem in Eq. (B.38) was further divided into three problems for each term on the right hand side of the equation. The general solution for Eq. (B.29) in terms of the simpler problem's solutions is

$$T_C(x^+) = T_{C,h}(x^+) + \sum_{i=1}^3 T_{C,pi}(x^+) \quad (B.39)$$

Where $T_{C,pi}$ is the solution to the problem given as

$$\frac{dT_{C,pi}}{dx^+} + N_C T_{C,pi} = N_C \left\{ \delta_{1i} T_o \right. \\ \left. + \delta_{2i} \sum_{n=0}^{\infty} A_n' [\mu_n L^* \cosh(\mu_n L^* x^+) + Bi_o \sinh(\mu_n L^* x^+)] \right. \\ \left. + \delta_{3i} \sum_{n=0}^{\infty} (B_n' + C_n') [\alpha_n \cos(\alpha_n x^+) + Bi_o \sin(\alpha_n x^+)] \right\} \quad (B.40)$$

($i = 1, 2, 3$) and δ_{ji} is the kronecker delta function as defined in Eq. (3.7)

B.2.1 Cold fluid Homogenous Solution

The solution to the homogeneous problem in Eq. (B.37) is

$$T_{C,h}(x^+) = E_1 \exp(N_C x^+) \quad (\text{B.41})$$

and E_1 is a constant to be determined, after assembling the complete solution. Superposition of the problems in Eq. (B.40) and Eq. (B.37) will give the originally posed problem in Eq. (B.36).

B.2.2 Cold fluid Particular Solution 1

Assuming the first particular solution ($i=1$) is a constant and substituting into the differential equation Eq. (B.40) and solving for the magnitude of the constant gives

$$T_{C,p1}(x^+) = T_o \quad (\text{B.42})$$

B.2.3 Cold fluid Particular Solution 2

The form of the second particular solution ($i=2$) is

$$T_{C,p2}(x^+) = \sum_{n=0}^{\infty} b_n \cosh(\mu_n L^* x^+) + c_n \sinh(\mu_n L^* x^+) \quad (\text{B.43})$$

substituting into the differential equation Eq. (B.40) (with summations not shown) gives

$$\begin{aligned} & b_n \mu_n L^* \sinh(\mu_n L^* x^+) + c_n \mu_n L^* \cosh(\mu_n L^* x^+) \\ & - N_C [b_n \cosh(\mu_n L^* x^+) + c_n \sinh(\mu_n L^* x^+)] \\ & = -N_C A_n' [\mu_n L^* \cosh(\mu_n L^* x^+) + Bi_o \sinh(\mu_n L^* x^+)] \quad (\text{B.44}) \end{aligned}$$

and the coefficients of the *sinh* terms and *cosh* terms are, respectively

$$b_n \mu_n L^* - N_C c_n = -N_C A_n' Bi_o \quad (\text{B.45})$$

$$c_n \mu_n L^* - N_C b_n = -N_C A_n' \mu_n L^* \quad (\text{B.46})$$

Solving for the unknown constants

$$b_n = A_n' \mu_n L^* \left[1 + \frac{N_C Bi_o + \mu_n^2 L^{*2}}{N_C^2 - \mu_n^2 L^{*2}} \right] \quad (B.47)$$

$$c_n = A_n' N_C \left[\frac{N_C Bi_o + \mu_n^2 L^{*2}}{N_C^2 - \mu_n^2 L^{*2}} \right] \quad (B.48)$$

and substituting into Eq. (B.43), the second particular solution is

$$T_{C,p2}(x^+) = \sum_{n=0}^{\infty} A_n' \left\{ \mu_n L^* \left[1 + \frac{N_C Bi_o + \mu_n^2 L^{*2}}{N_C^2 - \mu_n^2 L^{*2}} \right] \cosh(\mu_n L^* x^+) + \right. \\ \left. N_C \left[\frac{N_C Bi_o + \mu_n^2 L^{*2}}{N_C^2 - \mu_n^2 L^{*2}} \right] \sinh(\mu_n L^* x^+) \right\} \quad (B.49)$$

B.2.4 Cold fluid Particular Solution 3

The last particular solution is of functional form

$$T_{C,p3}(x^+) = \sum_{n=0}^{\infty} a_n \cos(\alpha_n x^+) + d_n \sin(\alpha_n x^+) \quad (B.50)$$

The resulting equation after substituting into the differential equation (without summations shown) is

$$(-a_n \alpha_n) \sin(\alpha_n x^+) + d_n \alpha_n \cos(\alpha_n x^+) - N_C [a_n \cos(\alpha_n x^+) + d_n \sin(\alpha_n x^+)] \\ = -N_C (B_n' + C_n') [\alpha_n \cos(\alpha_n x^+) + Bi_o \sin(\alpha_n x^+)] \quad (B.51)$$

Separating into coefficient equations for the *sin* and *cos* terms

$$-a_n \alpha_n - N_C d_n = -N_C (B_n' + C_n') Bi_o \quad (B.52)$$

$$d_n \alpha_n - N_C a_n = -N_C (B_n' + C_n') \alpha_n \quad (B.53)$$

and solving for the unknown constants

$$a_n = (B_n' + C_n') \alpha_n \left[1 + \frac{N_C Bi_o - \alpha_n^2}{N_C^2 + \alpha_n^2} \right] \quad (B.54)$$

$$d_n = (B_n' + C_n') N_C \left[\frac{N_C Bi_o - \alpha_n^2}{N_C^2 + \alpha_n^2} \right] \quad (B.55)$$

and substituting into Eq. (B.50) gives the final particular solution

$$T_{C,p3}(x^+) = \sum_{n=0}^{\infty} (B_n' + C_n') \left\{ \alpha_n \left[1 + \frac{N_C Bi_o - \alpha_n^2}{N_C^2 + \alpha_n^2} \right] \cos(\alpha_n x^+) \right. \\ \left. + N_C \left[\frac{N_C Bi_o - \alpha_n^2}{N_C^2 + \alpha_n^2} \right] \sin(\alpha_n x^+) \right\} \quad (B.56)$$

Assembling the simpler problem's solutions, Eq. (B.41) Eq. (B.42), Eq. (B.49), and Eq. (B.56), using Eq. (B.39) the solution for the temperature of the cold fluid can be written as

$$T_C(x^+) = T_o + E_1 \exp(N_C x^+) \\ + \sum_{n=0}^{\infty} A_n' \left\{ \mu_n L^* \left[1 + \frac{N_C Bi_o + \mu_n^2 L^{*2}}{N_C^2 - \mu_n^2 L^{*2}} \right] \cosh(\mu_n L^* x^+) \right. \\ \left. + N_C \left[\frac{N_C Bi_o + \mu_n^2 L^{*2}}{N_C^2 - \mu_n^2 L^{*2}} \right] \sinh(\mu_n L^* x^+) \right\} \\ + \sum_{n=0}^{\infty} (B_n' + C_n') \left\{ \alpha_n \left[1 + \frac{N_C Bi_o - \alpha_n^2}{N_C^2 + \alpha_n^2} \right] \cos(\alpha_n x^+) \right. \\ \left. + N_C \left[\frac{N_C Bi_o - \alpha_n^2}{N_C^2 + \alpha_n^2} \right] \sin(\alpha_n x^+) \right\} \quad (B.57)$$

By applying the boundary condition in Eq. (B.30a) the unknown constant E_1 can be determined

$$\begin{aligned}
E_1 = \exp(-N_C) & \left[(T_{C, in} - T_o) - \sum_{n=0}^{\infty} A_n' \left\{ \mu_n L^* \left[1 + \frac{N_C Bi_o + \mu_n^2 L^{*2}}{N_C^2 - \mu_n^2 L^{*2}} \right] \cosh(\mu_n L^*) \right. \right. \\
& \left. \left. + N_C \left[\frac{N_C Bi_o + \mu_n^2 L^{*2}}{N_C^2 - \mu_n^2 L^{*2}} \right] \sinh(\mu_n L^*) \right\} \right. \\
& - \sum_{n=0}^{\infty} (B_n' + C_n') \left\{ \alpha_n \left[1 + \frac{N_C Bi_o - \alpha_n^2}{N_C^2 + \alpha_n^2} \right] \cos(\alpha_n) \right. \\
& \left. \left. + N_C \left[\frac{N_C Bi_o - \alpha_n^2}{N_C^2 + \alpha_n^2} \right] \sin(\alpha_n) \right\} \right] \quad (B.58)
\end{aligned}$$

B.3 Summary Energy Balance Solutions

This section does not provide any new information it instead summarizes the solutions obtained in this appendix. The equation numbers will aid in locating the details of these solutions.

B.3.1 Hot Fluid Energy Balance Solution

Solution for the hot fluid temperature is

$$\begin{aligned}
 T_H(x^+) = & T_o + D_1 \exp(-N_H x^+) \\
 & + \sum_{n=0}^{\infty} A_n \left\{ \mu_n^2 L^* \left[1 - \frac{(Bi_o N_H - \mu_n^2 L^{*2})}{(N_H^2 - \mu_n^2 L^{*2})} \right] \cosh(\mu_n L^* x^+) \right. \\
 & \quad \left. + N_H \mu_n \left[\frac{(Bi_o N_H - \mu_n^2 L^{*2})}{(N_H^2 - \mu_n^2 L^{*2})} \right] \sinh(\mu_n L^* x^+) \right\} \\
 & + \sum_{n=0}^{\infty} \left(B_n + \frac{\alpha_n}{L^*} C_n \right) \left\{ \alpha_n \left[1 - \frac{(Bi_o N_H + \alpha_n^2)}{(N_H^2 + \alpha_n^2)} \right] \cos(\alpha_n x^+) \right. \\
 & \quad \left. + N_H \left[\frac{Bi_o N_H + \alpha_n^2}{N_H^2 + \alpha_n^2} \right] \sin(\alpha_n x^+) \right\} \quad (B.27)
 \end{aligned}$$

where

$$\begin{aligned}
 D_1 = & T_{H,in} - T_o - \sum_{n=0}^{\infty} A_n \mu_n^2 L^* \left[1 - \frac{(Bi_o N_H - \mu_n^2 L^{*2})}{(N_H^2 - \mu_n^2 L^{*2})} \right] \\
 & - \sum_{n=0}^{\infty} \left(B_n + \frac{\alpha_n}{L^*} C_n \right) \alpha_n \left[1 - \frac{(Bi_o N_H + \alpha_n^2)}{(N_H^2 + \alpha_n^2)} \right] \quad (B.28)
 \end{aligned}$$

B.3.2 Cold Fluid Energy Balance Solution

The solution for the cold fluid temperature is

$$\begin{aligned}
 T_C(x^+) = T_o + E_1 \exp(N_C x^+) & \\
 + \sum_{n=0}^{\infty} A_n' \left\{ \mu_n L^* \left[1 + \frac{N_C Bi_o + \mu_n^2 L^{*2}}{N_C^2 - \mu_n^2 L^{*2}} \right] \cosh(\mu_n L^* x^+) \right. & \\
 \left. + N_C \left[\frac{N_C Bi_o + \mu_n^2 L^{*2}}{N_C^2 - \mu_n^2 L^{*2}} \right] \sinh(\mu_n L^* x^+) \right\} & \\
 + \sum_{n=0}^{\infty} (B_n' + C_n') \left\{ \alpha_n \left[1 + \frac{N_C Bi_o - \alpha_n^2}{N_C^2 + \alpha_n^2} \right] \cos(\alpha_n x^+) \right. & \\
 \left. + N_C \left[\frac{N_C Bi_o - \alpha_n^2}{N_C^2 + \alpha_n^2} \right] \sin(\alpha_n x^+) \right\} & \quad (B.57)
 \end{aligned}$$

where

$$\begin{aligned}
 E_1 = \exp(-N_C) \left[(T_{C,in} - T_o) - \sum_{n=0}^{\infty} A_n' \left\{ \mu_n L^* \left[1 + \frac{N_C Bi_o + \mu_n^2 L^{*2}}{N_C^2 - \mu_n^2 L^{*2}} \right] \cosh(\mu_n L^*) \right. \right. & \\
 \left. \left. + N_C \left[\frac{N_C Bi_o + \mu_n^2 L^{*2}}{N_C^2 - \mu_n^2 L^{*2}} \right] \sinh(\mu_n L^*) \right\} \right. & \\
 - \sum_{n=0}^{\infty} (B_n' + C_n') \left\{ \alpha_n \left[1 + \frac{N_C Bi_o - \alpha_n^2}{N_C^2 + \alpha_n^2} \right] \cos(\alpha_n) \right. & \\
 \left. \left. + N_C \left[\frac{N_C Bi_o - \alpha_n^2}{N_C^2 + \alpha_n^2} \right] \sin(\alpha_n) \right\} \right] & \quad (B.58)
 \end{aligned}$$

APPENDIX C

C.1 Application of Nonhomogeneous Boundary Conditions

In Appendix A the solution of the wall conduction equation describing the temperature distribution in the wall was solved to the point of applying the nonhomogeneous boundary condition for the three simpler problems that the original problem was split into, because two of the three boundary conditions depended on the temperature of the fluids. With the solutions for the fluid temperatures complete (Appendix B) the final boundary conditions can be applied.

C.1.1 Application of Orthogonality at $x^+ = 1$

The solution for θ_1 up to the point of applying the nonhomogeneous boundary condition, and the boundary condition (Appendix A Eq. (A.28) and Eq. (A.4b)) are

$$\theta_1(x^+, y^+) = \sum_{n=0}^{\infty} A_n [\mu_n L^* \cosh(\mu_n L^* x^+) + Bi_o \sinh(\mu_n L^* x^+)] * [\mu_n \cos(\mu_n y^+) + Bi_H \sin(\mu_n y^+)] \quad (C.1)$$

$$\left. \frac{\partial \theta_1}{\partial x^+} \right|_{x^+=1} + Bi_L \theta_1(1, y^+) = Bi_L (T_L - T_o) \quad (C.2a)$$

Taking the derivative of Eq. (C.1) and evaluating the expression and its derivative at the boundary gives

$$\theta_1(1, y^+) = \sum_{n=0}^{\infty} A_n [\mu_n L^* \cosh(\mu_n L^*) + Bi_o \sinh(\mu_n L^*)] * [\mu_n \cos(\mu_n y^+) + Bi_H \sin(\mu_n y^+)] \quad (C.3)$$

$$\frac{\partial \theta_1}{\partial x^+}(1, y^+) = \sum_{n=0}^{\infty} A_n [\mu_n^2 L^{*2} \sinh(\mu_n L^*) + Bi_o \mu_n L^* \cosh(\mu_n L^*)] * [\mu_n \cos(\mu_n y^+) + Bi_H \sin(\mu_n y^+)] \quad (C.4)$$

Substituting these expressions into the boundary condition, Eq. (C.2a), produces

$$\begin{aligned}
 & \sum_{n=0}^{\infty} A_n [\mu_n^2 L^{*2} \sinh(\mu_n L^*) + Bi_o \mu_n L^* \cosh(\mu_n L^*)] * \\
 & \quad [\mu_n \cos(\mu_n y^+) + Bi_H \sin(\mu_n y^+)] \\
 & + Bi_L \sum_{n=0}^{\infty} A_n [\mu_n L^* \cosh(\mu_n L^*) + Bi_o \sinh(\mu_n L^*)] * \\
 & \quad [\mu_n \cos(\mu_n y^+) + Bi_H \sin(\mu_n y^+)] \\
 & = Bi_L (T_L - T_o) \tag{C.5}
 \end{aligned}$$

The orthogonality of the eigenfunctions was used to solve for the constants, A_n . The eigenfunction for this problem is

$$Y(\mu_n, y^+) = \mu_n \cos(\mu_n y^+) + Bi_H \sin(\mu_n y^+) \tag{C.6}$$

and these eigenfunctions have the property that

$$\int_0^1 w_{xy} Y(\mu_n, y^+) Y(\mu_m, y^+) dy^+ = \begin{cases} 0 & n \neq m \\ N(\mu_m) & n = m \end{cases} \tag{C.7}$$

where w_{xy} is a weighting constant and for the Cartesian coordinate system it is equal to one. Therefore, Eq. (C.5) will be multiplied by a second eigenfunction $Y(\mu_m, y^+)$ and integrated over the boundary. Because this integral is only nonzero for $m=n$ that is the only term that will remain from the summation. The integrals for each of the three terms in Eq. (C.5) are

$$\begin{aligned}
 & \int_0^1 \left\{ \sum_{n=0}^{\infty} A_n [\mu_n^2 L^{*2} \sinh(\mu_n L^*) + Bi_o \mu_n L^* \cosh(\mu_n L^*)] * \right. \\
 & \quad [\mu_n \cos(\mu_n y^+) + Bi_H \sin(\mu_n y^+)] [\mu_m \cos(\mu_m y^+) + Bi_H \sin(\mu_m y^+)] \left. \right\} dy^+ = \\
 & \quad A_m [\mu_m^2 L^{*2} \sinh(\mu_m L^*) + Bi_o \mu_m L^* \cosh(\mu_m L^*)] N(\mu_m) \tag{C.8}
 \end{aligned}$$

$$\int_0^1 \left\{ Bi_L \sum_{n=0}^{\infty} A_n [\mu_n L^* \cosh(\mu_n L^*) + Bi_o \sinh(\mu_n L^*)] * \right. \\ \left. [\mu_n \cos(\mu_n y^+) + Bi_H \sin(\mu_n y^+)] [\mu_m \cos(\mu_m y^+) + Bi_H \sin(\mu_m y^+)] dy^+ \right\} = \\ A_m Bi_L [\mu_m L^* \cosh(\mu_m L^*) + Bi_o \sinh(\mu_m L^*)] N(\mu_m) \quad (C.9)$$

$$Bi_L (T_L - T_o) \int_0^1 [\mu_m \cos(\mu_m y^+) + Bi_H \sin(\mu_m y^+)] dy^+ = \\ Bi_L (T_L - T_o) \left[\sin(\mu_m) - \frac{Bi_H}{\mu_m} \cos(\mu_m) + \frac{Bi_H}{\mu_m} \right] \quad (C.10)$$

After applying orthogonality Eq. (C.5) is

$$A_m [\mu_m^2 L^{*2} \sinh(\mu_m L^*) + Bi_o \mu_m L^* \cosh(\mu_m L^*)] N(\mu_m) + \\ A_m Bi_L [\mu_m L^* \cosh(\mu_m L^*) + Bi_o \sinh(\mu_m L^*)] N(\mu_m) = \\ Bi_L (T_L - T_o) \left[\sin(\mu_m) - \frac{Bi_H}{\mu_m} \cos(\mu_m) + \frac{Bi_H}{\mu_m} \right] \quad (C.11)$$

which can be solved for the unknown constant A_m

$$A_m = \frac{Bi_L (T_L - T_o) \left[\sin(\mu_m) - \frac{Bi_H}{\mu_m} \cos(\mu_m) + \frac{Bi_H}{\mu_m} \right]}{[(\mu_m^2 L^{*2} + Bi_o Bi_L) \sinh(\mu_m L^*) + (Bi_o + Bi_L) \mu_m L^* \cosh(\mu_m L^*)] N(\mu_m)} \quad (C.12)$$

The functional relationship for $N(\mu_m)$ is

$$N(\mu_m) = \frac{1}{2} \left[(\mu_m^2 + Bi_o^2) \left(1 + \frac{Bi_L}{(\mu_m^2 + Bi_L^2)} \right) + Bi_o \right] \quad (C.13)$$

Having this information everything is completely known for evaluating θ_1 . It would be possible to substitute Eq. (C.13) into Eq. (C.12) and this result into Eq. (C.1) to obtain a closed form solution for θ_1 , but because the expression would be algebraically cumbersome this will not be done.

C.1.2 Application of Orthogonality at $y^+ = 0$

The equation and boundary condition to be applied for determination of the unknown constants (Appendix A Eq. (A.40) and Eq. (A.6c)) are

$$\theta_2(x^+, y^+) = \sum_{n=0}^{\infty} B_n \left[\cosh\left(\frac{\alpha_n}{L^*} y^+\right) - \zeta_n \sinh\left(\frac{\alpha_n}{L^*} y^+\right) \right] + [\alpha_n \cos(\alpha_n x^+) + Bi_o \sin(\alpha_n x^+)] \quad (C.14)$$

$$-\frac{\partial \theta_2}{\partial y^+} \Big|_{y^+=0} + Bi_H \theta_2(x^+, 0) = Bi_H [T_H(x^+) - T_o] \quad (C.15a)$$

The difficulty in applying this boundary condition is recognized by noting the right hand side contains the temperature of the hot fluid. The needed temperature expressions for evaluating Eq. (C.15a) are:

$$\theta_2(x^+, 0) = \sum_{n=0}^{\infty} B_n [\alpha_n \cos(\alpha_n x^+) + Bi_o \sin(\alpha_n x^+)] \quad (C.16)$$

$$\frac{\partial \theta_2}{\partial y^+}(x^+, 0) = - \sum_{n=0}^{\infty} B_n \frac{\alpha_n}{L^*} \zeta_n [\alpha_n \cos(\alpha_n x^+) + Bi_o \sin(\alpha_n x^+)] \quad (C.17)$$

$$T_H(x^+) = T_o + D_1 \exp(-N_H x^+)$$

$$\begin{aligned} & + \sum_{n=0}^{\infty} A_n \left\{ \mu_n^2 L^* \left[1 - \frac{(Bi_o N_H - \mu_n^2 L^{*2})}{(N_H^2 - \mu_n^2 L^{*2})} \right] \cosh(\mu_n L^* x^+) \right. \\ & \quad \left. + N_H \mu_n \left[\frac{(Bi_o N_H - \mu_n^2 L^{*2})}{(N_H^2 - \mu_n^2 L^{*2})} \right] \sinh(\mu_n L^* x^+) \right\} \\ & + \sum_{n=0}^{\infty} \left(B_n + \frac{\alpha_n}{L^*} C_n \right) \left\{ \alpha_n \left[1 - \frac{(Bi_o N_H + \alpha_n^2)}{(N_H^2 + \alpha_n^2)} \right] \cos(\alpha_n x^+) \right. \\ & \quad \left. + N_H \left[\frac{Bi_o N_H + \alpha_n^2}{N_H^2 + \alpha_n^2} \right] \sin(\alpha_n x^+) \right\} \quad (C.18) \end{aligned}$$

Putting these expressions into Eq. (C.15a)

$$\begin{aligned}
& \sum_{n=0}^{\infty} B_n \frac{\alpha_n}{L^*} \zeta_n [\alpha_n \cos(\alpha_n x^+) + Bi_o \sin(\alpha_n x^+)] \\
& + Bi_H \sum_{n=0}^{\infty} B_n [\alpha_n \cos(\alpha_n x^+) + Bi_o \sin(\alpha_n x^+)] = \\
& Bi_H [D_1 \exp(-N_H x^+)] \\
& + \sum_{n=0}^{\infty} A_n \left\{ \mu_n^2 L^* \left[1 - \frac{(Bi_o N_H - \mu_n^2 L^{*2})}{(N_H^2 - \mu_n^2 L^{*2})} \right] \cosh(\mu_n L^* x^+) \right. \\
& \quad \left. + N_H \mu_n \left[\frac{(Bi_o N_H - \mu_n^2 L^{*2})}{(N_H^2 - \mu_n^2 L^{*2})} \right] \sinh(\mu_n L^* x^+) \right\} \\
& + \sum_{n=0}^{\infty} \left(B_n + \frac{\alpha_n}{L^*} C_n \right) \left\{ \alpha_n \left[1 - \frac{(Bi_o N_H + \alpha_n^2)}{(N_H^2 + \alpha_n^2)} \right] \cos(\alpha_n x^+) \right. \\
& \quad \left. + N_H \left[\frac{Bi_o N_H + \alpha_n^2}{N_H^2 + \alpha_n^2} \right] \sin(\alpha_n x^+) \right\} \quad (C.19)
\end{aligned}$$

for which orthogonality will be applied. Each term in Eq. (C.19) will be multiplied by the eigenfunction

$$X(\alpha_n, x^+) = \alpha_n \cos(\alpha_n x^+) + Bi_o \sin(\alpha_n x^+) \quad (C.20)$$

evaluated at term m and integrated over the boundary. The eigenfunction has the same property as discussed earlier, which is given in Eq. (C.7). Each of the integral will be listed separately and evaluated starting with the first term in Eq. (C.19) and proceeding to the last term.

$$\begin{aligned}
& \int_0^1 \left\{ \sum_{n=0}^{\infty} B_n \frac{\alpha_n}{L^*} \zeta_n [\alpha_n \cos(\alpha_n x^+) + Bi_o \sin(\alpha_n x^+)] * \right. \\
& \quad \left. [\alpha_m \cos(\alpha_m x^+) + Bi_o \sin(\alpha_m x^+)] \right\} dx^+ = B_m \frac{\alpha_m}{L^*} \zeta_m N(\alpha_m) \quad (C.21)
\end{aligned}$$

$$\int_0^1 \{ Bi_H \sum_{n=0}^{\infty} B_n [\alpha_n \cos(\alpha_n x^+) + Bi_o \sin(\alpha_n x^+)]^* \\ [\alpha_m \cos(\alpha_m x^+) + Bi_o \sin(\alpha_m x^+)] \} dx^+ = Bi_H B_m N(\alpha_m) \quad (C.22)$$

$$Bi_H D_1 \int_0^1 \{ \exp(-N_H x^+) [\alpha_m \cos(\alpha_m x^+) + Bi_o \sin(\alpha_m x^+)] \} dx^+ = \\ \frac{Bi_H D_1}{(N_H^2 + \alpha_m^2)} \{ (N_H + Bi_o) \alpha_m + e^{-N_H} [- (N_H + Bi_o) \alpha_m \cos(\alpha_m) + \\ (\alpha_m^2 - N_H Bi_o) \sin(\alpha_m)] \} \quad (C.23)$$

$$\int_0^1 \{ Bi_H \sum_{n=0}^{\infty} A_n \mu_n^2 L^* \left[1 - \frac{(Bi_o N_H - \mu_n^2 L^{*2})}{(N_H^2 - \mu_n^2 L^{*2})} \right] \cosh(\mu_n L^* x^+)^* \\ [\alpha_m \cos(\alpha_m x^+) + Bi_o \sin(\alpha_m x^+)] \} dx^+ = \\ \sum_{n=0}^{\infty} \frac{A_n Bi_H \alpha_m}{(\mu_n^2 L^{*2} + \alpha_m^2)} \mu_n^2 L^* \left[1 - \frac{N_H Bi_o - \mu_n^2 L^{*2}}{N_H^2 - \mu_n^2 L^{*2}} \right] \{ \sinh(\mu_n L^*) \mu_n L^* \cos(\alpha_m) \\ + \cosh(\mu_n L^*) \alpha_m \sin(\alpha_m) \} \\ + \sum_{n=0}^{\infty} \frac{A_n Bi_H Bi_o}{(\mu_n^2 L^{*2} + \alpha_m^2)} \mu_n^2 L^* \left[1 - \frac{N_H Bi_o - \mu_n^2 L^{*2}}{N_H^2 - \mu_n^2 L^{*2}} \right] \{ \sinh(\mu_n L^*) \mu_n L^* \sin(\alpha_m) \\ - \cosh(\mu_n L^*) \alpha_m \cos(\alpha_m) + \alpha_m \} \quad (C.24)$$

$$\begin{aligned}
& \int_0^1 \{ B i_H \sum_{n=0}^{\infty} A_n \mu_n N_H \left[\frac{(Bi_o N_H - \mu_n^2 L^{*2})}{(N_H^2 - \mu_n^2 L^{*2})} \right] \sinh(\mu_n L^* x^+) * \\
& \quad [\alpha_m \cos(\alpha_m x^+) + Bi_o \sin(\alpha_m x^+)] \} dx^+ = \\
& \quad \sum_{n=0}^{\infty} \frac{A_n Bi_H \alpha_m}{(\mu_n^2 L^{*2} + \alpha_m^2)} \mu_n N_H \left[\frac{N_H Bi_o - \mu_n^2 L^{*2}}{N_H^2 - \mu_n^2 L^{*2}} \right] \{ \cosh(\mu_n L^*) \mu_n L^* \cos(\alpha_m) \\
& \quad + \sinh(\mu_n L^*) \alpha_m \sin(\alpha_m) - \mu_n L^* \} \\
& \quad + \sum_{n=0}^{\infty} \frac{A_n Bi_H Bi_o}{(\mu_n^2 L^{*2} + \alpha_m^2)} \mu_n N_H \left[\frac{N_H Bi_o - \mu_n^2 L^{*2}}{N_H^2 - \mu_n^2 L^{*2}} \right] \{ \cosh(\mu_n L^*) \mu_n L^* \sin(\alpha_m) \\
& \quad - \sinh(\mu_n L^*) \alpha_m \cos(\alpha_m) \} \quad (C.25)
\end{aligned}$$

The remaining integrals depend on whether $n=m$.

$$\begin{aligned}
& \int_0^1 \{ B i_H \sum_{n=0}^{\infty} \left(B_n + \frac{\alpha_n}{L^*} C_n \right) \alpha_n \left[1 - \frac{(Bi_o N_H + \alpha_n^2)}{(N_H^2 + \alpha_n^2)} \right] \cos(\alpha_n x^+) * \\
& \quad [\alpha_m \cos(\alpha_m x^+) + Bi_o \sin(\alpha_m x^+)] \} dx^+ =
\end{aligned}$$

For $n=m$

$$\begin{aligned}
& Bi_H \sum_{n=0}^{\infty} \left(B_n + \frac{\alpha_n}{L^*} C_n \right) \alpha_n \left[1 - \frac{(Bi_o N_H + \alpha_n^2)}{(N_H^2 + \alpha_n^2)} \right] * \\
& \quad \left[\frac{\alpha_m}{2} + \frac{1}{4} \sin(2\alpha_m) + \frac{Bi_o}{2\alpha_m} \sin^2(\alpha_m) \right] \quad (C.26)
\end{aligned}$$

For $n \neq m$

$$\begin{aligned}
& Bi_H \sum_{n=0}^{\infty} \left(B_n + \frac{\alpha_n}{L^*} C_n \right) \alpha_n \left[1 - \frac{(Bi_o N_H + \alpha_n^2)}{(N_H^2 + \alpha_n^2)} \right] \left\{ \alpha_m \left[\frac{\sin(\alpha_m - \alpha_n)}{2(\alpha_m - \alpha_n)} + \frac{\sin(\alpha_m + \alpha_n)}{2(\alpha_m + \alpha_n)} \right] \right. \\
& \quad \left. + Bi_o \left[\frac{1 - \cos(\alpha_m - \alpha_n)}{2(\alpha_m - \alpha_n)} + \frac{1 - \cos(\alpha_m + \alpha_n)}{2(\alpha_m + \alpha_n)} \right] \right\} \quad (C.27)
\end{aligned}$$

$$\int_0^1 \left\{ Bi_H \sum_{n=0}^{\infty} \left(B_n + \frac{\alpha_n}{L^*} C_n \right) N_H \left[\frac{(Bi_o N_H + \alpha_n^2)}{(N_H^2 + \alpha_n^2)} \right] \sin(\alpha_n x^+) + \right. \\ \left. [\alpha_m \cos(\alpha_m x^+) + Bi_o \sin(\alpha_m x^+)] \right\} dx^+ =$$

For $n=m$

$$Bi_H \sum_{n=0}^{\infty} \left(B_n + \frac{\alpha_n}{L^*} C_n \right) N_H \left[\frac{(Bi_o N_H + \alpha_n^2)}{(N_H^2 + \alpha_n^2)} \right] \left[\frac{Bi_o}{2} - \frac{Bi_o}{4\alpha_m} \sin(2\alpha_m) + \frac{1}{2} \sin^2(\alpha_m) \right] \quad (C.28)$$

For $n \neq m$

$$Bi_H \sum_{n=0}^{\infty} \left(B_n + \frac{\alpha_n}{L^*} C_n \right) N_H \left[\frac{(Bi_o N_H + \alpha_n^2)}{(N_H^2 + \alpha_n^2)} \right] \left\{ Bi_o \left[\frac{\sin(\alpha_m - \alpha_n)}{2(\alpha_m - \alpha_n)} - \frac{\sin(\alpha_m + \alpha_n)}{2(\alpha_m + \alpha_n)} \right] \right. \\ \left. + \alpha_m \left[\frac{1 - \cos(\alpha_m - \alpha_n)}{2(\alpha_m - \alpha_n)} + \frac{1 - \cos(\alpha_m + \alpha_n)}{2(\alpha_m + \alpha_n)} \right] \right\} \quad (C.29)$$

Instead of substituting these large expression into the Eq. (C.19) some new variables are defined. For Eq. (C.23) let

$$\omega_m \equiv \frac{Bi_H}{N_H^2 + \alpha_m} \left\{ (N_H + Bi_o) \alpha_m + e^{-N_H} [-(N_H + Bi_o) \alpha_m \cos(\alpha_m) \right. \\ \left. + (\alpha_m^2 - N_H Bi_o) \sin(\alpha_m)] \right\} \quad (C.30)$$

In Eq. (C.24-25) define:

$$\rho_{mn,1} \equiv \frac{Bi_H \alpha_m}{(\mu_n^2 L^{*2} + \alpha_m^2)} \mu_n^2 L^* \left[1 - \frac{N_H Bi_o - \mu_n^2 L^{*2}}{N_H^2 - \mu_n^2 L^{*2}} \right] \left\{ \sinh(\mu_n L^*) \mu_n L^* \cos(\alpha_m) \right. \\ \left. + \cosh(\mu_n L^*) \alpha_m \sin(\alpha_m) \right\} \quad (C.31)$$

$$\rho_{mn,2} \equiv \frac{Bi_H Bi_o}{(\mu_n^2 L^{*2} + \alpha_m^2)} \mu_n^2 L^* \left[1 - \frac{N_H Bi_o - \mu_n^2 L^{*2}}{N_H^2 - \mu_n^2 L^{*2}} \right] \left\{ \sinh(\mu_n L^*) \mu_n L^* \sin(\alpha_m) \right. \\ \left. - \cosh(\mu_n L^*) \alpha_m \cos(\alpha_m) + \alpha_m \right\} \quad (C.32)$$

$$\rho_{mn,3} \equiv \frac{Bi_H \alpha_m}{(\mu_n^2 L^{*2} + \alpha_m^2)} \mu_n N_H \left[\frac{N_H Bi_o - \mu_n^2 L^{*2}}{N_H^2 - \mu_n^2 L^{*2}} \right] \{ \cosh(\mu_n L^*) \mu_n L^* \cos(\alpha_m) \\ + \sinh(\mu_n L^*) \alpha_m \sin(\alpha_m) - \mu_n L^* \} \quad (C.33)$$

$$\rho_{mn,4} \equiv \frac{Bi_H Bi_o}{(\mu_n^2 L^{*2} + \alpha_m^2)} \mu_n N_H \left[\frac{N_H Bi_o - \mu_n^2 L^{*2}}{N_H^2 - \mu_n^2 L^{*2}} \right] \{ \cosh(\mu_n L^*) \mu_n L^* \sin(\alpha_m) \\ - \sinh(\mu_n L^*) \alpha_m \cos(\alpha_m) \} \quad (C.34)$$

and for Eq. (C.26-29), for $m=n$

$$\psi_{mn} \equiv Bi_H \alpha_n \left[1 - \frac{(Bi_o N_H + \alpha_n^2)}{(N_H^2 + \alpha_n^2)} \right] \left[\frac{\alpha_m}{2} + \frac{1}{4} \sin(2\alpha_m) + \frac{Bi_o}{2\alpha_m} \sin^2(\alpha_m) \right] \\ + N_H \left[\frac{(Bi_o N_H + \alpha_n^2)}{(N_H^2 + \alpha_n^2)} \right] \left[\frac{Bi_o}{2} - \frac{Bi_o}{4\alpha_m} \sin(2\alpha_m) + \frac{1}{2} \sin^2(\alpha_m) \right] \quad (C.35)$$

and for $m \neq n$

$$\psi_{mn} \equiv Bi_H \alpha_n \left[1 - \frac{(Bi_o N_H + \alpha_n^2)}{(N_H^2 + \alpha_n^2)} \right] \left\{ \alpha_m \left[\frac{\sin(\alpha_m - \alpha_n)}{2(\alpha_m - \alpha_n)} + \frac{\sin(\alpha_m + \alpha_n)}{2(\alpha_m + \alpha_n)} \right] \right. \\ \left. + Bi_o \left[\frac{1 - \cos(\alpha_m - \alpha_n)}{2(\alpha_m - \alpha_n)} + \frac{1 - \cos(\alpha_m + \alpha_n)}{2(\alpha_m + \alpha_n)} \right] \right\} \\ + N_H \left[\frac{(Bi_o N_H + \alpha_n^2)}{(N_H^2 + \alpha_n^2)} \right] \left\{ Bi_o \left[\frac{\sin(\alpha_m - \alpha_n)}{2(\alpha_m - \alpha_n)} - \frac{\sin(\alpha_m + \alpha_n)}{2(\alpha_m + \alpha_n)} \right] \right. \\ \left. + \alpha_m \left[\frac{1 - \cos(\alpha_m - \alpha_n)}{2(\alpha_m - \alpha_n)} + \frac{1 - \cos(\alpha_m + \alpha_n)}{2(\alpha_m + \alpha_n)} \right] \right\} \quad (C.36)$$

Using the newly defined variables given in Eq. (C.30-36) in the integrals of Eq. (C.21-29); Eq. (C.19) after applying orthogonality, can be written as

$$B_m \frac{\alpha_m}{L^*} \zeta_m N(\alpha_m) + B_m Bi_H N(\alpha_m) = \omega_m D_1 + \sum_{n=0}^{\infty} A_n (\rho_{mn,1} + \rho_{mn,2} + \rho_{mn,3} + \rho_{mn,4}) + \sum_{n=0}^{\infty} \left(B_n + C_n \frac{\alpha_n}{L^*} \right) \psi_{mn} \quad (C.37)$$

where the orthogonality relationship is

$$N(\alpha_m) = \frac{1}{2} \left[(\alpha_m^2 + Bi_H^2) \left(1 + \frac{Bi_C}{\alpha_m^2 + Bi_C^2} \right) + Bi_H \right] \quad (C.38)$$

Defining one last variable

$$\lambda_m = - \left[\frac{\alpha_m}{L^*} \zeta_m + Bi_H \right] N(\alpha_m) \quad (C.39)$$

and rearranging the equation gives

$$B_m \lambda_m + \sum_{n=0}^{\infty} \left(B_n + C_n \frac{\alpha_n}{L^*} \right) \psi_{mn} + \omega_m D_1 = - \sum_{n=0}^{\infty} A_n (\rho_{mn,1} + \rho_{mn,2} + \rho_{mn,3} + \rho_{mn,4}) \quad (C.40)$$

where the sign changes were introduced (in λ_m and Eq. (C.40)) so that the variables are exactly as programmed in the computer program used to evaluate the problem (in Appendix F).

C.1.3 Application of Orthogonality at $y^+ = 1$

The equation and boundary condition to be applied for determination of the unknown constants (Appendix A Eq. (A.48) and Eq. (A.8d)) are

$$\theta_3(x^+, y^+) = \sum_{n=0}^{\infty} C_n \left[\frac{\alpha_n}{L^*} \cosh\left(\frac{\alpha_n}{L^*} y^+\right) + Bi_H \sinh\left(\frac{\alpha_n}{L^*} y^+\right) \right]^* \\ [\alpha_n \cos(\alpha_n x^+) + Bi_o \sin(\alpha_n x^+)] \quad (C.41)$$

$$\left. \frac{\partial \theta_3}{\partial y^+} \right|_{y^+=1} + Bi_C \theta_3(x^+, 1) = Bi_C [T_C(x^+) - T_o] \quad (C.42a)$$

The evaluation of this boundary condition is very similar to the previously discussed method for θ_2 , except the algebra is a little more involved because the boundary condition is evaluated at $y^+ = 1$ instead of 0. The needed temperature expressions for evaluating Eq. (C.42a) are

$$\theta_3(x^+, 1) = \sum_{n=0}^{\infty} C_n \left[\frac{\alpha_n}{L^*} \cosh\left(\frac{\alpha_n}{L^*}\right) + Bi_H \sinh\left(\frac{\alpha_n}{L^*}\right) \right]^* \\ [\alpha_n \cos(\alpha_n x^+) + Bi_o \sin(\alpha_n x^+)] \quad (C.43)$$

$$\frac{\partial \theta_3}{\partial y^+}(x^+, 1) = \sum_{n=0}^{\infty} C_n \frac{\alpha_n}{L^*} \left[\frac{\alpha_n}{L^*} \sinh\left(\frac{\alpha_n}{L^*}\right) + Bi_H \cosh\left(\frac{\alpha_n}{L^*}\right) \right]^* \\ [\alpha_n \cos(\alpha_n x^+) + Bi_o \sin(\alpha_n x^+)] \quad (C.44)$$

$$\begin{aligned}
T_C(x^+) &= T_o + E_1 \exp(N_C x^+) \\
&+ \sum_{n=0}^{\infty} A_n' \left\{ \mu_n L^* \left[1 + \frac{(Bi_o N_C + \mu_n^2 L^{*2})}{(N_C^2 - \mu_n^2 L^{*2})} \right] \cosh(\mu_n L^* x^+) \right. \\
&\quad \left. + N_C \left[\frac{(Bi_o N_C + \mu_n^2 L^{*2})}{(N_C^2 - \mu_n^2 L^{*2})} \right] \sinh(\mu_n L^* x^+) \right\} \\
&+ \sum_{n=0}^{\infty} (B_n' + C_n') \left\{ \alpha_n \left[1 + \frac{(Bi_o N_C - \alpha_n^2)}{(N_C^2 + \alpha_n^2)} \right] \cos(\alpha_n x^+) \right. \\
&\quad \left. + N_C \left[\frac{Bi_o N_C - \alpha_n^2}{N_C^2 + \alpha_n^2} \right] \sin(\alpha_n x^+) \right\} \quad (C.45)
\end{aligned}$$

Putting these expressions into Eq. (C.42a) gives

$$\begin{aligned}
&\sum_{n=0}^{\infty} C_n \frac{\alpha_n}{L^*} \left[\frac{\alpha_n}{L^*} \sinh\left(\frac{\alpha_n}{L^*}\right) + Bi_H \cosh\left(\frac{\alpha_n}{L^*}\right) \right] [\alpha_n \cos(\alpha_n x^+) + Bi_o \sin(\alpha_n x^+)] \\
&+ Bi_C \sum_{n=0}^{\infty} C_n \left[\frac{\alpha_n}{L^*} \cosh\left(\frac{\alpha_n}{L^*}\right) + Bi_H \sinh\left(\frac{\alpha_n}{L^*}\right) \right] * \\
&\quad [\alpha_n \cos(\alpha_n x^+) + Bi_o \sin(\alpha_n x^+)] =
\end{aligned}$$

$$Bi_C [E_1 \exp(N_C x^+)]$$

$$\begin{aligned}
&+ \sum_{n=0}^{\infty} A_n' \left\{ \mu_n L^* \left[1 + \frac{(Bi_o N_C + \mu_n^2 L^{*2})}{(N_C^2 - \mu_n^2 L^{*2})} \right] \cosh(\mu_n L^* x^+) \right. \\
&\quad \left. + N_C \left[\frac{(Bi_o N_C + \mu_n^2 L^{*2})}{(N_C^2 - \mu_n^2 L^{*2})} \right] \sinh(\mu_n L^* x^+) \right\} \\
&+ \sum_{n=0}^{\infty} (B_n' + C_n') \left\{ \alpha_n \left[1 + \frac{(Bi_o N_C - \alpha_n^2)}{(N_C^2 + \alpha_n^2)} \right] \cos(\alpha_n x^+) \right. \\
&\quad \left. + N_C \left[\frac{(Bi_o N_C - \alpha_n^2)}{(N_C^2 + \alpha_n^2)} \right] \sin(\alpha_n x^+) \right\} \quad (C.46)
\end{aligned}$$

for which orthogonality will be applied. Each term in Eq. (C.46) will be multiplied by the eigenfunction

$$X(\alpha_n, x^+) = \alpha_n \cos(\alpha_n x^+) + Bi_o \sin(\alpha_n x^+) \quad (C.47)$$

evaluated at term m and integrated over the boundary. The eigenfunction has the same property as discussed earlier, which is given in Eq. (C.7). Each of the integral will be listed separately and evaluated starting with the first term in Eq. (C.46) and proceeding to the last term.

$$\begin{aligned} \int_0^1 \left\{ \sum_{n=0}^{\infty} C_n \frac{\alpha_n}{L^*} \left[\frac{\alpha_n}{L^*} \sinh\left(\frac{\alpha_n}{L^*}\right) + Bi_H \cosh\left(\frac{\alpha_n}{L^*}\right) \right] [\alpha_n \cos(\alpha_n x^+) + Bi_o \sin(\alpha_n x^+)]^* \right. \\ \left. [\alpha_m \cos(\alpha_m x^+) + Bi_o \sin(\alpha_m x^+)] \right\} dx^+ = \\ C_m \frac{\alpha_m}{L^*} \left[\frac{\alpha_m}{L^*} \sinh\left(\frac{\alpha_m}{L^*}\right) + Bi_H \cosh\left(\frac{\alpha_m}{L^*}\right) \right] N(\alpha_m) \end{aligned} \quad (C.48)$$

$$\begin{aligned} \int_0^1 \left\{ Bi_C \sum_{n=0}^{\infty} C_n \left[\frac{\alpha_n}{L^*} \cosh\left(\frac{\alpha_n}{L^*}\right) + Bi_H \sinh\left(\frac{\alpha_n}{L^*}\right) \right] [\alpha_n \cos(\alpha_n x^+) + Bi_o \sin(\alpha_n x^+)]^* \right. \\ \left. [\alpha_m \cos(\alpha_m x^+) + Bi_o \sin(\alpha_m x^+)] \right\} dx^+ = \\ Bi_C C_m \left[\frac{\alpha_m}{L^*} \cosh\left(\frac{\alpha_m}{L^*}\right) + Bi_H \sinh\left(\frac{\alpha_m}{L^*}\right) \right] N(\alpha_m) \end{aligned} \quad (C.49)$$

$$\begin{aligned} Bi_C E_1 \int_0^1 \{ \exp(N_C x^+) [\alpha_m \cos(\alpha_m x^+) + Bi_o \sin(\alpha_m x^+)] \} dx^+ = \\ \frac{Bi_C E_1}{N_C^2 + \alpha_m^2} \{ (Bi_o - N_C) \alpha_m + e^{N_C} [(N_C - Bi_o) \alpha_m \cos(\alpha_m) + \\ (\alpha_m^2 + N_C Bi_o) \sin(\alpha_m)] \} \end{aligned} \quad (C.50)$$

$$\begin{aligned}
& \int_0^1 \{ B i_C \sum_{n=0}^{\infty} A_n' \mu_n L^* \left[1 + \frac{(B i_o N_C + \mu_n^2 L^{*2})}{(N_c^2 - \mu_n^2 L^{*2})} \right] \cosh(\mu_n L^* x^+) * \\
& \quad [\alpha_m \cos(\alpha_m x^+) + B i_o \sin(\alpha_m x^+)] \} dx^+ = \\
& \quad \sum_{n=0}^{\infty} \frac{A_n' B i_C \alpha_m \mu_n L^*}{(\mu_n^2 L^{*2} + \alpha_m^2)} \left[1 + \frac{(B i_o N_C + \mu_n^2 L^{*2})}{(N_c^2 - \mu_n^2 L^{*2})} \right] \{ \sinh(\mu_n L^*) \mu_n L^* \cos(\alpha_m) \\
& \quad + \cosh(\mu_n L^*) \alpha_m \sin(\alpha_m) \} \\
& \quad + \sum_{n=0}^{\infty} \frac{A_n' B i_C B i_o \mu_n L^*}{(\mu_n^2 L^{*2} + \alpha_m^2)} \left[1 + \frac{(B i_o N_C + \mu_n^2 L^{*2})}{(N_c^2 - \mu_n^2 L^{*2})} \right] \{ \sinh(\mu_n L^*) \mu_n L^* \sin(\alpha_m) \\
& \quad - \cosh(\mu_n L^*) \alpha_m \cos(\alpha_m) + \alpha_m \} \quad (C.51)
\end{aligned}$$

$$\begin{aligned}
& \int_0^1 \{ B i_C \sum_{n=0}^{\infty} A_n' N_C \left[\frac{(B i_o N_C + \mu_n^2 L^{*2})}{(N_c^2 - \mu_n^2 L^{*2})} \right] \sinh(\mu_n L^* x^+) * \\
& \quad [\alpha_m \cos(\alpha_m x^+) + B i_o \sin(\alpha_m x^+)] \} dx^+ = \\
& \quad \sum_{n=0}^{\infty} \frac{A_n' B i_C \alpha_m N_C}{(\mu_n^2 L^{*2} + \alpha_m^2)} \left[\frac{(B i_o N_C + \mu_n^2 L^{*2})}{(N_c^2 - \mu_n^2 L^{*2})} \right] \{ \cosh(\mu_n L^*) \mu_n L^* \cos(\alpha_m) \\
& \quad + \sinh(\mu_n L^*) \alpha_m \sin(\alpha_m) - \mu_n L^* \} \\
& \quad + \sum_{n=0}^{\infty} \frac{A_n' B i_C B i_o N_C}{(\mu_n^2 L^{*2} + \alpha_m^2)} \left[\frac{(B i_o N_C + \mu_n^2 L^{*2})}{(N_c^2 - \mu_n^2 L^{*2})} \right] \{ \cosh(\mu_n L^*) \mu_n L^* \sin(\alpha_m) \\
& \quad - \sinh(\mu_n L^*) \alpha_m \cos(\alpha_m) \} \quad (C.52)
\end{aligned}$$

The remaining integrals depend on whether $n=m$

$$\int_0^1 \left\{ Bi_C \sum_{n=0}^{\infty} (B_n' + C_n') \alpha_n \left[1 + \frac{(Bi_o N_C - \alpha_n^2)}{(N_C^2 + \alpha_n^2)} \right] \cos(\alpha_n x^+) + \right. \\ \left. [\alpha_m \cos(\alpha_m x^+) + Bi_o \sin(\alpha_m x^+)] \right\} dx^+ =$$

for $n=m$

$$Bi_C \sum_{n=0}^{\infty} (B_n' + C_n') \alpha_n \left[1 + \frac{(Bi_o N_C - \alpha_n^2)}{(N_C^2 + \alpha_n^2)} \right] \left[\frac{\alpha_m}{2} + \frac{1}{4} \sin(2\alpha_m) + \frac{Bi_o}{2\alpha_m} \sin^2(\alpha_m) \right] \quad (C.53)$$

for $n \neq m$

$$Bi_C \sum_{n=0}^{\infty} (B_n' + C_n') \alpha_n \left[1 + \frac{(Bi_o N_C - \alpha_n^2)}{(N_C^2 + \alpha_n^2)} \right] \left\{ \alpha_m \left[\frac{\sin(\alpha_m - \alpha_n)}{2(\alpha_m - \alpha_n)} + \frac{\sin(\alpha_m + \alpha_n)}{2(\alpha_m + \alpha_n)} \right] \right. \\ \left. + Bi_o \left[\frac{1 - \cos(\alpha_m - \alpha_n)}{2(\alpha_m - \alpha_n)} + \frac{1 - \cos(\alpha_m + \alpha_n)}{2(\alpha_m + \alpha_n)} \right] \right\} \quad (C.54)$$

$$\int_0^1 \left\{ Bi_C \sum_{n=0}^{\infty} (B_n' + C_n') N_C \left[\frac{(Bi_o N_C - \alpha_n^2)}{(N_C^2 + \alpha_n^2)} \right] \sin(\alpha_n x^+) + \right. \\ \left. [\alpha_m \cos(\alpha_m x^+) + Bi_o \sin(\alpha_m x^+)] \right\} dx^+ =$$

for $n=m$

$$Bi_C \sum_{n=0}^{\infty} (B_n' + C_n') N_C \left[\frac{(Bi_o N_C - \alpha_n^2)}{(N_C^2 + \alpha_n^2)} \right] \left[\frac{Bi_o}{2} - \frac{Bi_o}{4\alpha_m} \sin(2\alpha_m) + \frac{1}{2} \sin^2(\alpha_m) \right] \quad (C.55)$$

for $n \neq m$

$$Bi_C \sum_{n=0}^{\infty} (B_n' + C_n') N_C \left[\frac{(Bi_o N_C - \alpha_n^2)}{(N_C^2 + \alpha_n^2)} \right] \left\{ Bi_o \left[\frac{\sin(\alpha_m - \alpha_n)}{2(\alpha_m - \alpha_n)} - \frac{\sin(\alpha_m + \alpha_n)}{2(\alpha_m + \alpha_n)} \right] \right. \\ \left. + \alpha_m \left[\frac{1 - \cos(\alpha_m - \alpha_n)}{2(\alpha_m - \alpha_n)} + \frac{1 - \cos(\alpha_m + \alpha_n)}{2(\alpha_m + \alpha_n)} \right] \right\} \quad (C.56)$$

Instead of substituting these large expression into the Eq. (C.46) some new variables are defined. For Eq. (C.50) let

$$\Omega_m \equiv \frac{Bi_C}{N_C^2 + \alpha_m^2} \{ (Bi_o - N_C) \alpha_m + e^{N_C} [(N_C - Bi_o) \alpha_m \cos(\alpha_m) + (\alpha_m^2 - N_H Bi_o) \sin(\alpha_m)] \} \quad (C.57)$$

In Eq. (C.51-52) define:

$$P_{mn,1} \equiv \frac{Bi_C \alpha_m \mu_n L^*}{(\mu_n^2 L^{*2} + \alpha_m^2)} \left[1 + \frac{(Bi_o N_C + \mu_n^2 L^{*2})}{(N_C^2 - \mu_n^2 L^{*2})} \right] \{ \sinh(\mu_n L^*) \mu_n L^* \cos(\alpha_m) + \cosh(\mu_n L^*) \alpha_m \sin(\alpha_m) \} \quad (C.58)$$

$$P_{mn,2} \equiv \frac{Bi_C Bi_o \mu_n L^*}{(\mu_n^2 L^{*2} + \alpha_m^2)} \left[1 + \frac{(Bi_o N_C + \mu_n^2 L^{*2})}{(N_C^2 - \mu_n^2 L^{*2})} \right] \{ \sinh(\mu_n L^*) \mu_n L^* \sin(\alpha_m) - \cosh(\mu_n L^*) \alpha_m \cos(\alpha_m) + \alpha_m \} \quad (C.59)$$

$$P_{mn,3} \equiv \frac{Bi_C \alpha_m N_C}{(\mu_n^2 L^{*2} + \alpha_m^2)} \left[\frac{(Bi_o N_C + \mu_n^2 L^{*2})}{(N_C^2 - \mu_n^2 L^{*2})} \right] \{ \cosh(\mu_n L^*) \mu_n L^* \cos(\alpha_m) + \sinh(\mu_n L^*) \alpha_m \sin(\alpha_m) - \mu_n L^* \} \quad (C.60)$$

$$P_{mn,4} \equiv \frac{Bi_C Bi_o N_C}{(\mu_n^2 L^{*2} + \alpha_m^2)} \left[\frac{(Bi_o N_C + \mu_n^2 L^{*2})}{(N_C^2 - \mu_n^2 L^{*2})} \right] \{ \cosh(\mu_n L^*) \mu_n L^* \sin(\alpha_m) - \sinh(\mu_n L^*) \alpha_m \cos(\alpha_m) \} \quad (C.61)$$

and for Eq. (C.53-56) define

for $m=n$

$$\begin{aligned} \Psi_{mn} = & Bi_C \alpha_n \left[1 + \frac{(Bi_o N_C - \alpha_n^2)}{(N_H^2 + \alpha_n^2)} \right] \left[\frac{\alpha_m}{2} + \frac{1}{4} \sin(2\alpha_m) + \frac{Bi_o}{2\alpha_m} \sin^2(\alpha_m) \right] \\ & + N_C \left[\frac{(Bi_o N_C - \alpha_n^2)}{(N_H^2 + \alpha_n^2)} \right] \left[\frac{Bi_o}{2} - \frac{Bi_o}{4\alpha_m} \sin(2\alpha_m) + \frac{1}{2} \sin^2(\alpha_m) \right] \quad (C.62) \end{aligned}$$

for $m \neq n$

$$\begin{aligned} \Psi_{mn} = & Bi_C \alpha_n \left[1 + \frac{(Bi_o N_C - \alpha_n^2)}{(N_H^2 + \alpha_n^2)} \right] \left\{ \alpha_m \left[\frac{\sin(\alpha_m - \alpha_n)}{2(\alpha_m - \alpha_n)} + \frac{\sin(\alpha_m + \alpha_n)}{2(\alpha_m + \alpha_n)} \right] \right. \\ & \left. + Bi_o \left[\frac{1 - \cos(\alpha_m - \alpha_n)}{2(\alpha_m - \alpha_n)} + \frac{1 - \cos(\alpha_m + \alpha_n)}{2(\alpha_m + \alpha_n)} \right] \right\} \\ & + N_C \left[\frac{(Bi_o N_C - \alpha_n^2)}{(N_H^2 + \alpha_n^2)} \right] \left\{ Bi_o \left[\frac{\sin(\alpha_m - \alpha_n)}{2(\alpha_m - \alpha_n)} - \frac{\sin(\alpha_m + \alpha_n)}{2(\alpha_m + \alpha_n)} \right] \right. \\ & \left. + \alpha_m \left[\frac{1 - \cos(\alpha_m - \alpha_n)}{2(\alpha_m - \alpha_n)} + \frac{1 - \cos(\alpha_m + \alpha_n)}{2(\alpha_m + \alpha_n)} \right] \right\} \quad (C.63) \end{aligned}$$

Using the newly defined variables in the expressions for the integrals, Eq. (C.46) after applying orthogonality is

$$\begin{aligned} C_m \frac{\alpha_m}{L^*} \left[\frac{\alpha_m}{L^*} \sinh\left(\frac{\alpha_m}{L^*}\right) + Bi_H \cosh\frac{\alpha_m}{L^*} \right] N(\alpha_m) \\ + Bi_C C_m \left[\frac{\alpha_m}{L^*} \cosh\left(\frac{\alpha_m}{L^*}\right) + Bi_H \sinh\frac{\alpha_m}{L^*} \right] N(\alpha_m) = \\ \Omega_m E_1 + \sum_{n=0}^{\infty} A_n' (P_{mn,1} + P_{mn,2} + P_{mn,3} + P_{mn,4}) + \sum_{n=0}^{\infty} (B_n' + C_n') \Psi_{mn} \quad (C.64) \end{aligned}$$

Defining a final variable

$$\Phi_m = \left[\left(\frac{\alpha_m^2}{L^{*2}} + Bi_C Bi_H \right) \sinh\left(\frac{\alpha_m}{L^*}\right) + (Bi_H + Bi_C) \cosh\left(\frac{\alpha_m}{L^*}\right) \right] N(\alpha_m) \quad (C.65)$$

and substituting into Eq. (C.64) and rearranging gives

$$C_m \Phi_m - \sum_n (B_n' + C_n') \Psi_{mn} - \Omega_m E_1 = \sum_n A_n' (P_{mn,1} + P_{mn,2} + P_{mn,3} + P_{mn,4}) \quad (\text{C.66})$$

C.2 Summary of Applying Nonhomogen. Boundary Conditions

The final boundary conditions were applied and simplified using the orthogonality of the eigenfunctions. This procedure produced a close form solution for the constant A_n in θ_1 since the nonhomogeneous term in the boundary condition was a constant

$$A_m = \frac{Bi_L (T_L - T_o) \left[\sin(\mu_m) - \frac{Bi_H}{\mu_m} \cos(\mu_m) + \frac{Bi_H}{\mu_m} \right]}{[(\mu_m^2 L^{*2} + Bi_o Bi_L) \sinh(\mu_m L^*) + (Bi_o + Bi_L) \mu_m L^* \cosh(\mu_m L^*)] N(\mu_m)} \quad (C.12)$$

where

$$N(\mu_m) = \frac{1}{2} \left[(\mu_m^2 + Bi_o^2) \left(1 + \frac{Bi_L}{(\mu_m^2 + Bi_L^2)} \right) + Bi_o \right] \quad (C.13)$$

However, for the constants B_n in θ_2 and C_n in θ_3 the boundary conditions to be applied have nonhomogeneous terms that are functions containing the unknown constants B_n and C_n . These functions are contained in the solutions for the fluid temperatures. Thus, in applying the boundary conditions and orthogonality the resulting equation is simplified, yet still contains summations and is a function of both unknown constants B_n and C_n . The equations to be solved to determine these constants are

$$B_m \lambda_m + \sum_{n=0}^{\infty} \left(B_n + C_n \frac{\alpha_n}{L^*} \right) \Psi_{mn} + \omega_m D_1 = - \sum_{n=0}^{\infty} A_n (\rho_{mn,1} + \rho_{mn,2} + \rho_{mn,3} + \rho_{mn,4}) \quad (C.40)$$

$$C_m \Phi_m - \sum_{n=0}^{\infty} (B_n' + C_n') \Psi_{mn} - \Omega_m E_1 = \sum_{n=0}^{\infty} A_n' (P_{mn,1} + P_{mn,2} + P_{mn,3} + P_{mn,4}) \quad (C.41)$$

These two equations represent a set of simultaneous equations that need to be solved for the unknown constants B_n and C_n ($n=1,2,\dots,N$). The terms on the left hand side contain unknown constants and the right hand side contains all known information for two equations. The solution of these equations is given and discussed in Appendix D.

APPENDIX D

D.1 Solution for Constants B_n and C_n

After evaluating the final nonhomogeneous boundary conditions and applying orthogonality two equations were derived to solve for B_n and C_n , (Appendix C Eq. (C.40) and Eq. (C.66), which are

$$B_m \lambda_m + \sum_{n=0}^{\infty} \left(B_n + C_n \frac{\alpha_n}{L^*} \right) \Psi_{mn} + \omega_m D_1 = - \sum_{n=0}^{\infty} A_n (\rho_{mn,1} + \rho_{mn,2} + \rho_{mn,3} + \rho_{mn,4}) \quad (D.1)$$

$$C_m \Phi_m - \sum_{n=0}^{\infty} (B_n' + C_n') \Psi_{mn} - \Omega_m E_1 = \sum_{n=0}^{\infty} A_n' (P_{mn,1} + P_{mn,2} + P_{mn,3} + P_{mn,4}) \quad (D.2)$$

where all the greek variables are defined in Appendix C and the expressions for E_1 and D_1 are (from Appendix B Eq. (B.25) and Eq. (B.52))

$$D_1 = T_{H,in} - T_o - \sum_{n=0}^{\infty} A_n \mu_n^2 L^* \left[1 - \frac{(Bi_o N_H - \mu_n^2 L^{*2})}{N_H^2 - \mu_n^2 L^{*2}} \right] - \sum_{n=0}^{\infty} \left(B_n + \frac{\alpha_n}{L^*} C_n \right) \alpha_n \left[1 - \frac{(Bi_o N_H + \alpha_n^2)}{N_H^2 + \alpha_n^2} \right] \quad (D.3)$$

$$E_1 = \exp(-N_C) \left[(T_{C,in} - T_o) - \sum_{n=0}^{\infty} A_n' \left\{ \mu_n L^* \left[1 + \frac{(Bi_o N_C + \mu_n^2 L^{*2})}{N_C^2 - \mu_n^2 L^{*2}} \right] \cosh(\mu_n L^*) + N_C \left[\frac{(Bi_o N_C + \mu_n^2 L^{*2})}{N_C^2 - \mu_n^2 L^{*2}} \right] \sinh(\mu_n L^*) \right\} - \sum_{n=0}^{\infty} (B_n' + C_n') \left\{ \alpha_n \left[1 + \frac{Bi_o N_C - \alpha_n^2}{N_C^2 + \alpha_n^2} \right] \cos(\alpha_n) + N_C \left[\frac{(Bi_o N_C - \alpha_n^2)}{N_C^2 + \alpha_n^2} \right] \sin(\alpha_n) \right\} \right] \quad (D.4)$$

Defining the following variables:

$$\beta_n \equiv (\mu_n^2 L^*) \left[1 - \frac{(Bi_o N_H - \mu_n^2 L^{*2})}{N_H^2 - \mu_n^2 L^{*2}} \right] \quad (D.5)$$

$$\gamma_n \equiv \alpha_n \left[1 - \frac{(Bi_o N_H + \alpha_n^2)}{N_H^2 + \alpha_n^2} \right] \quad (D.6)$$

$$\begin{aligned} v_n \equiv e^{-N_C} \{ \mu_n L^* \left[1 + \frac{(Bi_o N_C + \mu_n^2 L^{*2})}{N_C^2 - \mu_n^2 L^{*2}} \right] \cosh(\mu_n L^*) \\ + N_C \left[\frac{(Bi_o N_C + \mu_n^2 L^{*2})}{N_C^2 - \mu_n^2 L^{*2}} \right] \sinh(\mu_n L^*) \} \end{aligned} \quad (D.7)$$

$$\begin{aligned} \sigma_n \equiv e^{-N_C} \left[\cosh\left(\frac{\alpha_n}{L^*}\right) - \zeta_n \sinh\left(\frac{\alpha_n}{L^*}\right) \right] \left\{ \alpha_n \left[1 + \frac{(Bi_o N_C - \alpha_n^2)}{N_C^2 + \alpha_n^2} \right] \cos(\alpha_n) \right. \\ \left. + N_C \left[\frac{(Bi_o N_C - \alpha_n^2)}{N_C^2 + \alpha_n^2} \right] \sin(\alpha_n) \right\} \end{aligned} \quad (D.8)$$

$$\begin{aligned} \tau_n \equiv e^{-N_C} \left[\frac{\alpha_n}{L^*} \cosh\left(\frac{\alpha_n}{L^*}\right) + Bi_H \sinh\left(\frac{\alpha_n}{L^*}\right) \right] \left\{ \alpha_n \left[1 + \frac{(Bi_o N_C - \alpha_n^2)}{N_C^2 + \alpha_n^2} \right] \cos(\alpha_n) \right. \\ \left. + N_C \left[\frac{(Bi_o N_C - \alpha_n^2)}{N_C^2 + \alpha_n^2} \right] \sin(\alpha_n) \right\} \end{aligned} \quad (D.9)$$

and substituting into Eq. (D.3-4) gives

$$D_1 = (T_{H,in} - T_o) - \sum_{n=0}^{\infty} A_n \beta_n - \sum_{n=0}^{\infty} \left(B_n + C_n \frac{\alpha_n}{L^*} \right) \gamma_n \quad (D.10)$$

$$E_1 = \exp(-N_C) (T_{C,in} - T_o) - \sum_{n=0}^{\infty} A_n' v_n - \sum_{n=0}^{\infty} (B_n \sigma_n + C_n \tau_n) \quad (D.11)$$

where Eq. (D.8-9) contain the necessary constants to convert B_n' and C_n' to B_n and C_n . Defining two last variables, to convert all unknown constants to a form without a superscript prime

$$(\Psi B)_{nn} = \Psi_{nn} \left[\cosh\left(\frac{\alpha_n}{L^*}\right) - \zeta_n \sinh\left(\frac{\alpha_n}{L^*}\right) \right] \quad (D.12)$$

$$(\Psi C)_{mn} = \Psi_{mn} \left[\frac{\alpha_n}{L^*} \cosh \left(\frac{\alpha_n}{L^*} \right) + Bi_h \sinh \left(\frac{\alpha_n}{L^*} \right) \right] \quad (D.13)$$

Introducing Eq. (D.10-13) into Eq. (D.1-2) and rearranging gives

$$B_m \lambda_m + \sum_{n=0}^{\infty} B_n (\Psi_{mn} - \gamma_n \omega_m) + \sum_{n=0}^{\infty} C_n \frac{\alpha_n}{L^*} (\Psi_{mn} - \gamma_n \omega_m) =$$

$$- \omega_m (T_{H, in} - T_o) - \sum_{n=0}^{\infty} A_n (\rho_{mn, 1} + \rho_{mn, 2} + \rho_{mn, 3} + \rho_{mn, 4} - \omega_m \beta_n) \quad (D.14)$$

$$\sum_n [\Omega_m \sigma_n - (\Psi B)_{mn}] B_n + C_m \Phi_m + \sum_{n=0}^{\infty} [\Omega_m \tau_n - (\Psi C)_{mn}] C_n =$$

$$\Omega_m \exp(-N_C) (T_{C, in} - T_o) + \sum_{n=0}^{\infty} A_n' (P_{mn, 1} + P_{mn, 2} + P_{mn, 3} + P_{mn, 4} - \Omega_m v_n) \quad (D.15)$$

These two equations represent a set of simultaneous equations to be solved for the constants B_n and C_n . To accomplish this the series must be truncated at a value $n=N$ giving $2N$ constants to solve for (B_i and C_i $i = 1, 2, \dots, N$). There are only two equations, however these equations can be written for each eigenvalue; hence the subscript m denotes the eigenvalue considered. Therefore, since there are $m=N$ eigenvalues and two equations for each eigenvalue the total number of equations are $2N$ to solve for the same amount of constants.

For illustrative purposes consider a matrix representation of the equations

$$[K] \begin{bmatrix} B \\ C \end{bmatrix} = [F] \quad (D.16)$$

where $[K]$ is the coefficient matrix of order $(2N \times 2N)$ and $[F]$ is the forcing vector $(2N \times 1)$ and the unknown constant vectors given as

1

$$[B] = \begin{bmatrix} B_1 \\ B_2 \\ \cdot \\ \cdot \\ \cdot \\ B_N \end{bmatrix} \quad [C] = \begin{bmatrix} C_1 \\ C_2 \\ \cdot \\ \cdot \\ \cdot \\ C_N \end{bmatrix} \quad (D.17)$$

Further, the coefficients matrix can be quartered and the forcing vector halved

$$[K] = \begin{bmatrix} K_1 & K_2 \\ K_3 & K_4 \end{bmatrix} \quad (D.18)$$

$$[F] = \begin{bmatrix} F_1 \\ F_2 \end{bmatrix} \quad (D.19)$$

Each quarter of the coefficient matrix is a square matrix of order ($N \times N$) and half the forcing vector is of length ($N \times 1$). Referring to Eq. (D.16) the simultaneous equations can be represented as

$$\begin{bmatrix} K_1 & K_2 \\ K_3 & K_4 \end{bmatrix} \begin{bmatrix} B \\ C \end{bmatrix} = \begin{bmatrix} F_1 \\ F_2 \end{bmatrix} \quad (D.20)$$

This shows where the terms that need to be put into the coefficient matrix and forcing vector will come from. The rows in the coefficient matrix in Eq. (D.20) represent the coefficients of B_n and C_n for each equation. Row one corresponds to Eq. (D.14) and row two to Eq. (D.15). Similarly, the entries in the forcing vector correspond to Eq. (D.14) for row one and Eq. (D.15) for row two. Presenting the equations in this form, Eq. (D.20), makes it possible to write out some of the terms of the matrices to show the developing pattern and indicate where these terms originate. The individual matrices and forcing vectors that form Eq. (D.18) and Eq. (D.19) are listed below.

$$[K_1] = \begin{bmatrix} (\lambda_1 + \psi_{11} - \gamma_1 \omega_1) & (\psi_{12} - \gamma_2 \omega_1) & \dots & (\psi_{1N} - \gamma_N \omega_1) \\ (\psi_{21} - \gamma_1 \omega_2) & (\lambda_2 + \psi_{22} - \gamma_2 \omega_2) & \dots & (\psi_{2N} - \gamma_N \omega_2) \\ \vdots & \vdots & \ddots & \vdots \\ (\psi_{N1} - \gamma_1 \omega_N) & (\psi_{N2} - \gamma_2 \omega_N) & \dots & (\lambda_N + \psi_{NN} - \gamma_N \omega_N) \end{bmatrix} \quad (D.21)$$

$$[K_2] = \begin{bmatrix} \left((\psi_{11} - \gamma_1 \omega_1) \frac{\alpha_1}{L^*} \right) & \left((\psi_{12} - \gamma_2 \omega_1) \frac{\alpha_2}{L^*} \right) & \dots & \left((\psi_{1N} - \gamma_N \omega_1) \frac{\alpha_N}{L^*} \right) \\ \left((\psi_{21} - \gamma_1 \omega_2) \frac{\alpha_1}{L^*} \right) & \left((\psi_{22} - \gamma_2 \omega_2) \frac{\alpha_2}{L^*} \right) & \dots & \left((\psi_{2N} - \gamma_N \omega_2) \frac{\alpha_N}{L^*} \right) \\ \vdots & \vdots & \ddots & \vdots \\ \left((\psi_{N1} - \gamma_1 \omega_N) \frac{\alpha_1}{L^*} \right) & \left((\psi_{N2} - \gamma_2 \omega_N) \frac{\alpha_2}{L^*} \right) & \dots & \left((\psi_{NN} - \gamma_N \omega_N) \frac{\alpha_N}{L^*} \right) \end{bmatrix} \quad (D.22)$$

$$[K_3] = \begin{bmatrix} (\Omega_1 \sigma_1 - (\Psi B)_{11}) & (\Omega_1 \sigma_2 - (\Psi B)_{12}) & \dots & (\Omega_1 \sigma_N - (\Psi B)_{1N}) \\ (\Omega_2 \sigma_1 - (\Psi B)_{21}) & (\Omega_2 \sigma_2 - (\Psi B)_{22}) & \dots & (\Omega_2 \sigma_N - (\Psi B)_{2N}) \\ \vdots & \vdots & \ddots & \vdots \\ (\Omega_N \sigma_1 - (\Psi B)_{N1}) & (\Omega_N \sigma_2 - (\Psi B)_{N2}) & \dots & (\Omega_N \sigma_N - (\Psi B)_{NN}) \end{bmatrix} \quad (D.23)$$

$$[K_4] = \begin{bmatrix} (\Phi_1 + \Omega_1 \tau_1 - (\Psi C)_{11}) & \Omega_1 \tau_2 - (\Psi C)_{12} & \dots & \Omega_1 \tau_N - (\Psi C)_{1N} \\ \Omega_2 \tau_1 - (\Psi C)_{21} & (\Phi_2 + \Omega_2 \tau_2 - (\Psi C)_{22}) & \dots & \Omega_2 \tau_N - (\Psi C)_{2N} \\ \vdots & \vdots & \ddots & \vdots \\ \Omega_N \tau_1 - (\Psi C)_{N1} & \Omega_N \tau_2 - (\Psi C)_{N2} & \dots & (\Phi_N + \Omega_N \tau_N - (\Psi C)_{NN}) \end{bmatrix} \quad (D.24)$$

$$[F_1] = \begin{bmatrix} -\omega_1 (T_{H,in} - T_o) - \sum_n A_n (\rho_{1n,1} + \rho_{1n,2} + \rho_{1n,3} + \rho_{1n,4}) \\ -\omega_2 (T_{H,in} - T_o) - \sum_n A_n (\rho_{2n,1} + \rho_{2n,2} + \rho_{2n,3} + \rho_{2n,4}) \\ \vdots \\ -\omega_N (T_{H,in} - T_o) - \sum_n A_n (\rho_{Nn,1} + \rho_{Nn,2} + \rho_{Nn,3} + \rho_{Nn,4}) \end{bmatrix} \quad (D.25)$$

$$[F_2] = \begin{bmatrix} e^{-N_c} \Omega_1 (T_{C,in} - T_o) + \sum_n A_n' (P_{1n,1} + P_{1n,2} + P_{1n,3} + P_{1n,4} - \Omega_1 v_n) \\ e^{-N_c} \Omega_2 (T_{C,in} - T_o) + \sum_n A_n' (P_{2n,1} + P_{2n,2} + P_{2n,3} + P_{2n,4} - \Omega_2 v_n) \\ \vdots \\ e^{-N_c} \Omega_N (T_{C,in} - T_o) + \sum_n A_n' (P_{Nn,1} + P_{Nn,2} + P_{Nn,3} + P_{Nn,4} - \Omega_N v_n) \end{bmatrix} \quad (D.26)$$

The indices, row- i and column- j , of the coefficient matrix can be interpreted as the coefficient of the constant B_j (or C_j) for the i^{th} eigenvalue. That is, a row corresponds to a single eigenvalue and a column to a single constant.

APPENDIX E

E.1 Derivation of Effectiveness-NTU Relationship for a Counterflow Heat Exchanger Neglecting Axial Conduction

Consider a double pipe heat exchanger geometry as shown in Figure E.1, with the energy balances on the fluids as shown. For the fluids, the energy balances give

$$(\dot{m}C_p)_C T_C|_x = (\dot{m}C_p)_C T_C|_{x+\Delta x} + dq \quad (\text{E.1})$$

$$(\dot{m}C_p)_H T_H|_x = (\dot{m}C_p)_H T_H|_{x+\Delta x} + dq \quad (\text{E.2})$$

In addition to the fluid energy balances over the differential length a thermal circuit can be analyzed for the heat exchanger wall. The thermal circuit for this heat exchanger is shown in Figure E.2, neglecting any fouling. The heat transfer over a differential element of length Δx is

$$dq = UP(T_H - T_C)\Delta x \quad (\text{E.3})$$

where

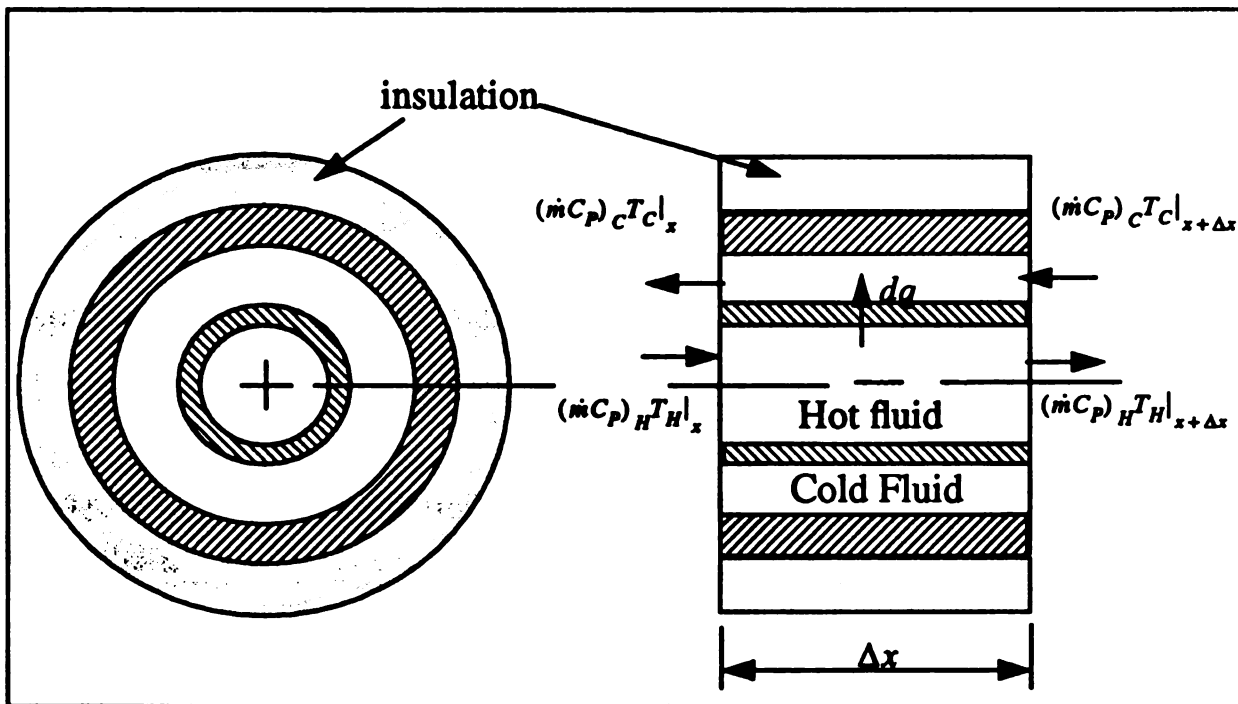


Figure E.1. Double pipe heat exchanger geometry and the energy balance for a differential element of length Δx

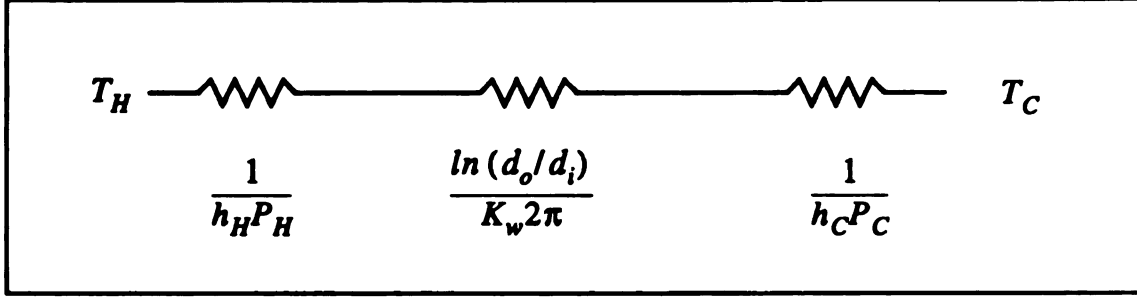


Figure E.2. Thermal circuit for heat exchanger wall

$$UP = \left[\frac{1}{h_H P_H} + \frac{\ln(d_o/d_i)}{2\pi k_w} + \frac{1}{h_C P_C} \right] \quad (\text{E.4})$$

Substituting Eq(E.3) into Eq(E.2) and Eq. (E.1) gives

$$-\frac{[(mC_p)_C T_C|_{x+\Delta x} - (mC_p)_C T_C|_x]}{\Delta x} = UP(T_H - T_C) \quad (\text{E.5})$$

$$-\frac{[(mC_p)_H T_H|_{x+\Delta x} - (mC_p)_H T_H|_x]}{\Delta x} = UP(T_H - T_C) \quad (\text{E.6})$$

Introducing the heat capacity

$$C \equiv mC_p \quad (\text{E.7})$$

and taking the limit as $\Delta x \rightarrow 0$, Eq. (E.5) and Eq. (E.6) can be written as

$$-\frac{dT_C}{dx} = \frac{UP}{C_C} (T_H - T_C) \quad (\text{E.8})$$

$$-\frac{dT_H}{dx} = \frac{UP}{C_H} (T_H - T_C) \quad (\text{E.9})$$

Subtracting Eq. (E.9) from Eq. (E.8) gives

$$\frac{d}{dx} (T_H - T_C) = -UP \left(\frac{1}{C_H} - \frac{1}{C_C} \right) (T_H - T_C) \quad (\text{E.10})$$

This equation can be separated and integrated over the length of the heat exchanger

$$\int_0^L \frac{d(T_H - T_C)}{(T_H - T_C)} = -UP \left(\frac{1}{C_H} - \frac{1}{C_C} \right) \int_0^L dx \quad (\text{E.11})$$

giving

$$\ln (T_H - T_C) \Big|_0^L = -UP \left(\frac{1}{C_H} - \frac{1}{C_C} \right) x \Big|_0^L \quad (\text{E.12})$$

Evaluating the terms and rearranging Eq. (E.12), provides a solution in terms of the operating conditions of the fluids and the heat exchanger wall design

$$\frac{(T_{H, out} - T_{C, in})}{(T_{H, in} - T_{C, out})} = \exp \left[-UA \left(\frac{1}{C_H} - \frac{1}{C_C} \right) \right] \quad (\text{E.13})$$

The transformation of Eq. (E.13) into a dimensionless form will begin by subtracting and adding the inlet temperatures of the fluids to the numerator and denominator on the left hand side of the equation

$$\frac{(T_{H, in} - T_{C, in}) - (T_{H, in} - T_{H, out})}{(T_{H, in} - T_{C, in}) - (T_{C, out} - T_{C, in})} = \exp \left[-UA \left(\frac{1}{C_H} - \frac{1}{C_C} \right) \right] \quad (\text{E.14})$$

Next, each term of on the left hand side will be divided by the temperature difference at the fluid inlets, $(T_{H, in} - T_{C, in})$, and the numerator multiplied by (C_H/C_H) and denominator by (C_C/C_C)

$$\frac{\left[1 - \frac{C_H (T_{H, in} - T_{H, out})}{C_H (T_{H, in} - T_{C, in})} \right]}{\left[1 - \frac{C_C (T_{C, out} - T_{C, in})}{C_C (T_{H, in} - T_{C, in})} \right]} = \exp \left[-UA \left(\frac{1}{C_H} - \frac{1}{C_C} \right) \right] \quad (\text{E.15})$$

Defining the effectiveness as

$$\varepsilon = \frac{q}{C_{min} (T_{H, in} - T_{C, in})} \quad (\text{E.16})$$

where

$$C_{min} = \min (C_C, C_H) \quad (\text{E.17})$$

and q is the actual heat transfer that occurs over the length of the heat exchanger, which was derived in chapter 1 using an energy balance on the fluid, and is written as

$$q = C_C (T_{C, out} - T_{C, in}) = C_H (T_{H, in} - T_{H, out}) \quad (\text{E.18})$$

The effectiveness could be substituted into Eq. (E.15) if it was know which fluid had the minimum heat capacity, for the sake of generality all possibilities will be considered. Two of three possible expressions for Eq. (E.15) can be written as follows, the third will be addressed later:

For $C_{min} = C_H$

$$\frac{1 - \varepsilon}{1 - \left(\frac{C_H}{C_C}\right)\varepsilon} = \exp\left[-\frac{UA}{C_H}\left(1 - \frac{C_H}{C_C}\right)\right] \quad (E.19)$$

For $C_{min} = C_C$

$$\frac{1 - \left(\frac{C_C}{C_H}\right)\varepsilon}{1 - \varepsilon} = \exp\left[\frac{UA}{C_C}\left(1 - \frac{C_C}{C_H}\right)\right] \quad (E.20)$$

Solving Eq. (E.19) and (E.20) for the effectiveness, after introducing the number of transfer units

$$NTU = \frac{UA}{C_{min}} \quad (E.21)$$

and the heat capacity ratio

$$C_R = \frac{C_{min}}{C_{max}} \quad (E.22)$$

into the equations gives the same solution for both Eq. (E.19) and Eq. (E.20), which is

$$\varepsilon = \frac{1 - \exp[-NTU(1 - C_R)]}{1 - C_R \exp[-NTU(1 - C_R)]} \quad (E.23)$$

This provides results for $C_H \neq C_C$, however, if the heat capacity ratios are equal, which is the third possibility that was mentioned previously, Eq. (E.23) is indefinite ($\frac{0}{0}$). For this case L'Hospital's rule can be applied to determine the limit as the heat capacity ratio goes to 1 giving

$$\varepsilon = \frac{1 + NTU}{NTU} \quad (E.24)$$

for $C_H = C_C$.

E.2 Solution of Fluid Temperatures for a Counterflow Heat Exchanger Neglecting Axial Conduction

E.2.1 Unequal Heat Capacities ($C_H \neq C_C$)

Solving for the general solution of the differential equation in Eq. (E.10) for the temperature difference between the hot and cold fluid gives

$$T_H - T_C = C_1 \exp \left[-UP \left(\frac{1}{C_H} - \frac{1}{C_C} \right) x \right] \quad (\text{E.25})$$

where C_1 is a constant. Substituting Eq. (E.25) into the individual differential equations for the fluids, in Eq. (E.8) and (E.9), gives the equations to be solved for the temperatures of the fluid, with appropriate initial conditions

$$\frac{dT_H}{dx} = -\frac{UP}{C_H} C_1 \exp \left[-UP \left(\frac{1}{C_H} - \frac{1}{C_C} \right) x \right] \quad (\text{E.26})$$

$$T_H(0) = T_{H,in} \quad (\text{E.26a})$$

$$\frac{dT_C}{dx} = -\frac{UP}{C_C} C_1 \exp \left[-UP \left(\frac{1}{C_H} - \frac{1}{C_C} \right) x \right] \quad (\text{E.27})$$

$$T_C(L) = T_{C,in} \quad (\text{E.27a})$$

These two equations, Eq. (E.26) and (E.27), are easily solved for the temperatures of the hot and cold fluids

$$T_H = \frac{C_1}{C_H \left(\frac{1}{C_H} - \frac{1}{C_C} \right)} \exp \left[-UP \left(\frac{1}{C_H} - \frac{1}{C_C} \right) x \right] + C_2 \quad (\text{E.28})$$

$$T_C = \frac{C_1}{C_C \left(\frac{1}{C_H} - \frac{1}{C_C} \right)} \exp \left[-UP \left(\frac{1}{C_H} - \frac{1}{C_C} \right) x \right] + C_3 \quad (\text{E.29})$$

where C_2 and C_3 are constants, but noting that Eq. (E.25) must hold gives

$$C_4 \equiv C_2 = C_3 \quad (\text{E.30})$$

Incorporating Eq. (E.30) and rearranging Eq. (E.28) and (E.29) gives

$$T_H(x) = C_4 + \frac{C_1}{(1 - C_H/C_C)} \exp \left[-UP \left(\frac{1}{C_H} - \frac{1}{C_C} \right) x \right] \quad (\text{E.31})$$

$$T_C(x) = C_4 - \frac{C_1}{(1 - C_C/C_H)} \exp\left[-UP\left(\frac{1}{C_H} - \frac{1}{C_C}\right)x\right] \quad (\text{E.32})$$

which can be solved for the unknown constants using the initial conditions in Eq. (E.26a) and (E.27a). Applying these conditions to the equations for the hot and cold fluids produces

$$T_{H,in} = C_4 + \frac{C_1}{(1 - C_H/C_C)} \quad (\text{E.33})$$

$$T_{C,in} = C_4 - \frac{C_1}{(1 - C_C/C_H)} \exp\left[-UP\left(\frac{1}{C_H} - \frac{1}{C_C}\right)L\right] \quad (\text{E.34})$$

a set of two equations with two unknowns. Solving, the two unknown constants are

$$C_1 = \frac{(T_{H,in} - T_{C,in})(C_C - C_H)}{C_C - C_H \exp\left[-UP\left(\frac{1}{C_H} - \frac{1}{C_C}\right)L\right]} \quad (\text{E.35})$$

$$C_4 = \frac{C_C T_{C,in} - T_{H,in} C_H \exp\left[-UP\left(\frac{1}{C_H} - \frac{1}{C_C}\right)L\right]}{C_C - C_H \exp\left[-UP\left(\frac{1}{C_H} - \frac{1}{C_C}\right)L\right]} \quad (\text{E.36})$$

If $C_H > C_C$ and the heat capacity ratio is used $C_R = C_C/C_H$, Eq (E.35) and Eq. (E.36) become

$$C_1 = \frac{(T_{H,in} - T_{C,in})(C_R - 1)}{C_R - \exp[-UP/C_C(C_R - 1)L]} \quad (\text{E.37})$$

$$C_4 = \frac{C_R T_{C,in} - T_{H,in} \exp[-UP(C_R - 1)L]}{C_R - \exp[-UP/C_C(C_R - 1)L]} \quad (\text{E.38})$$

Substituting Eq (E.35) and (E.36) into the solutions for the hot and cold fluids, Eq. (E.31) and (E.32), gives

$$T_H(x) = \frac{C_C T_{C,in} - T_{H,in} C_H \exp\left[-UP\left(\frac{1}{C_H} - \frac{1}{C_C}\right)L\right]}{C_C - C_H \exp\left[-UP\left(\frac{1}{C_H} - \frac{1}{C_C}\right)L\right]} + \frac{(T_{H,in} - T_{C,in})(C_C - C_H)}{(1 - C_H/C_C) \{C_C - C_H \exp\left[-UP\left(\frac{1}{C_H} - \frac{1}{C_C}\right)L\right]\}} \exp\left[-UP\left(\frac{1}{C_H} - \frac{1}{C_C}\right)x\right] \quad (\text{E.39})$$

$$T_C(x) = \frac{C_C T_{C,in} - T_{H,in} C_H \exp\left[-UP\left(\frac{1}{C_H} - \frac{1}{C_C}\right)L\right]}{C_C - C_H \exp\left[-UP\left(\frac{1}{C_H} - \frac{1}{C_C}\right)L\right]} - \frac{(T_{H,in} - T_{C,in})(C_C - C_H)}{(1 - C_C/C_H) \{C_C - C_H \exp\left[-UP\left(\frac{1}{C_H} - \frac{1}{C_C}\right)L\right]\}} \exp\left[-UP\left(\frac{1}{C_H} - \frac{1}{C_C}\right)x\right] \quad (\text{E.40})$$

For the case of $C_H > C_C$ Eq. (E.37) and (E.38) can be used in place of Eq. (E.35) and (E.36) giving the following expression for the hot and cold fluid temperatures:

$$T_H(x^+) = \frac{C_R T_{C,in} - T_{H,in} \exp[-UP/C_C(C_R - 1)L]}{C_R - \exp[-UP/C_C(C_R - 1)L]} + \frac{(T_{H,in} - T_{C,in}) C_R}{C_R - \exp[-UP/C_C(C_R - 1)L]} \exp[-UP(C_R - 1)x] \quad (\text{E.41})$$

$$T_C(x^+) = \frac{C_R T_{C,in} - T_{H,in} \exp[-UP/C_C(C_R - 1)L]}{C_R - \exp[-UP/C_C(C_R - 1)L]} - \frac{(T_{H,in} - T_{C,in})}{C_R - \exp[-UP/C_C(C_R - 1)L]} \exp[-UP(C_R - 1)x] \quad (\text{E.42})$$

Nondimensionalizing the length scales by the total length of the heat exchanger

$$x^+ = \frac{x}{L} \quad (\text{E.43})$$

and introducing the number of transfer units (NTU)

$$NTU = \frac{UPL}{C_{min}} \quad (E.44)$$

the final equations for the hot and cold temperatures become

$$T_H = \frac{C_R T_{C,in} - T_{H,in} \exp[-NTU(C_R - 1)]}{C_R - \exp[-NTU(C_R - 1)L]} + \frac{(T_{H,in} - T_{C,in}) C_R}{C_R - \exp[-NTU(C_R - 1)]} \exp[-NTU(C_R - 1)x^+] \quad (E.45)$$

$$T_C = \frac{C_R T_{C,in} - T_{H,in} \exp[-NTU(C_R - 1)]}{C_R - \exp[-NTU(C_R - 1)]} + \frac{(T_{H,in} - T_{C,in})}{C_R - \exp[-NTU(C_R - 1)]} \exp[-NTU(C_R - 1)x^+] \quad (E.46)$$

Note that Eq. (E.45) and (E.46) apply for $C_H > C_C$, which could easily be converted if the opposite were true.

E.2.2 Equal Heat Capacities ($C_H = C_C$)

If the heat capacity ratio of the two fluids are equal the solution of the differential equation, in Eq. (E.10), for the temperature difference between the fluids is a constants.

$$T_H - T_C = C_1 \quad (E.47)$$

Which upon substituting into Eq. (E.8) and (E.9) give the following differential equations and initial conditions for the temperatures of the hot and cold fluids, respectively.

$$\frac{dT_H}{dx} = \frac{-UP}{C_H} C_1 \quad (E.48)$$

$$T_H(0) = T_{H,in} \quad (E.48a)$$

$$\frac{dT_C}{dx} = \frac{-UP}{C_C} C_1 \quad (E.49)$$

$$T_C(L) = T_{C,in} \quad (E.49a)$$

The general solution of these differential equations is

$$T_H(x) = \frac{-UP}{C_H} C_1 x + C_2 \quad (\text{E.50})$$

$$T_C(x) = \frac{-UP}{C_C} C_1 x + C_3 \quad (\text{E.51})$$

where C_2 and C_3 are constants, giving a total of three constants to be determined. The initial conditions in Eq. (E.48a) and (E.49a) provide two conditions and the third condition comes from Eq. (E.25). Applying these three conditions gives the following set of equations to be solved for the unknown constants.

$$T_{H, in} = C_2 \quad (\text{E.52})$$

$$T_{C, in} = -\frac{UP}{C_C} C_1 L + C_3 \quad (\text{E.53})$$

$$T_H - T_C = C_1 = \frac{-UP}{C_H} C_1 x + \frac{-UP}{C_C} C_1 x + (C_2 - C_3) \quad (\text{E.54})$$

The solution for C_2 is obvious, solving for the other constants gives

$$C_1 = \frac{(T_{H, in} - T_{C, in})}{(1 + \frac{UPL}{C_C})} \quad (\text{E.55})$$

$$C_3 = \frac{T_{C, in} + T_{H, in} \frac{UPL}{C_C}}{(1 + \frac{UPL}{C_C})} \quad (\text{E.56})$$

which can be rewritten using Eq. (E.44) as

$$C_1 = \frac{(T_{H, in} - T_{C, in})}{1 + NTU} \quad (\text{E.57})$$

$$C_3 = \frac{T_{C, in} + T_{H, in} NTU}{1 + NTU} \quad (\text{E.58})$$

Substituting Eq. (E.57) and (E.58) into the general solutions, Eq. (E.50) and (E.51), the expressions for temperature of the hot and cold fluids are

$$T_H(x) = -\frac{UP(T_{H, in} - T_{C, in})}{C_H(1 + NTU)} x + T_{H, in} \quad (\text{E.59})$$

$$T_C(x) = \frac{UP(T_{H,in} - T_{C,in})}{C_C(1 + NTU)}x + \frac{(T_{C,in} + T_{H,in}NTU)}{1 + NTU} \quad (\text{E.60})$$

If length dimensions are scaled according to Eq. (E.43), expressions for temperature become

$$T_H(x) = -\frac{NTU(T_{H,in} - T_{C,in})}{(1 + NTU)}x^+ + T_{H,in} \quad (\text{E.61})$$

$$T_C(x) = \frac{NTU(T_{H,in} - T_{C,in})}{(1 + NTU)}x^+ + \frac{(T_{C,in} + T_{H,in}NTU)}{1 + NTU} \quad (\text{E.62})$$

APPENDIX F

```

*
*
*   Program AXCOND
*
*   BOUNDARY CONDITIONS OF THE THIRD KIND
*   ORTHOGONALITY APPLIED WITH COSINE AND SINE FUNCTION
*
*   ASSUMING  $T_0 = T_1$  (CONSTANT AMB TEMP)
*
*
*   LAST MODIFIED 4/27/92
*
implicit double precision (a-h,o-z)
character para*10,runfil*60
integer size,size2
double precision len,Nc,Nh,Kw,Lstr,mu,NTU
parameter (size=200,size2=50)
dimension coeff(size,size+1),BC(size),A(size),
+ Tcold(size2),Thot(size2),Twall(size2,size2),
+ mu(size),alph(size),
+ dTcold(size2),dTthot(size),dTdx0(size2),dTdx1(size2),
+ dTdy0(size2),dTdy1(size2)

common delta,len,Lstr,Nc,Nh,Bic,Bih,Bio,Bil,Tcin,Thin,To,Tl

**
**   INPUT DATA
**
**   delta - wall thickness (m)
**   len   - total length (m)
**   Cc    - heat capacity cold stream (W/K)
**   Ch    - heat capacity hot stream (W/K)
**   hc    - convection coeff cold side (W/m**2 K)
**   hh    - convection coeff hot side (W/m**2 K)
**   Kw    - thermal conductivity of wall (W/m K)
**   ho    - convection coeff to ambient at x=0 (W/m**2 K)
**   h1    - convection coeff to ambient at x=L (W/m**2 K)
**   To    - Temp of ambient at x=0 (C)
**   T1    - Temp of ambient at x=L (C)
**   Tcin  - temp of cold fluid at x=L
**   Thin  - temp of hot fluid at x=0
**   Lx(L) - scale length for x-direction

```



```

**      Ly(delta)- scale length for y-direction
**
**
**      CALCULATED DATA
**
**
**      Lstr  -  $L_x/L_y$ 
**      Nc    -  $h_c P_c L_x / C_c$ 
**      Nh    -  $h_h P_h L_x / C_h$ 
**      Bio   -  $h_o L_x / K_w$       all variables dimensionless
**      Bil   -  $h_l L_x / K_w$ 
**      Bic   -  $h_c L_y / K_w$ 
**      Bih   -  $h_h L_y / K_w$ 
**
**
**
**      read the input data in and define looping method
**      iopt - 0 -input raw data (dimensional)
**            1 -input Non-dimensional data
**
      iloop = 0
      irun = 1
50    continue
*
*      READ IN NEXT RUN FILE NAME AND BEGIN CALCULATIONS
*
*      if(irun.eq.1)runfil='[dowding.thesis.rundata]Bih.one'
*      if(irun.eq.2)runfil='[dowding.thesis.rundata]Bih.low'
*      if(irun.eq.3)runfil='[dowding.thesis.rundata]Bio.one'
*      if(irun.eq.4)runfil='[dowding.thesis.rundata]Bil.one'
*      if(irun.eq.5)runfil='[dowding.thesis.rundata]BihBic.one'
*      if(irun.eq.6)runfil='[dowding.thesis.rundata]BioBil.one'
*      if(irun.eq.7)runfil='[dowding.thesis.rundata]Lstr.one'
*      if(irun.eq.1)runfil='[dowding.thesis.rundata]cr1.low'
*      if(irun.eq.2)runfil='[dowding.thesis.rundata]cr75.low'
*      if(irun.eq.3)runfil='[dowding.thesis.rundata]cr50.low'
*      if(irun.eq.4)runfil='[dowding.thesis.rundata]cr25.low'
*      if(irun.eq.12)runfil='[dowding.thesis.rundata]nterm.one'
*      if(irun.eq.5)go to 300

      print *, 'running data set ', irun

*      open(20,status='unknown',file=runfil)
*      read(20,'(i10)')iopt
      print *, 'enter ioption 0-single run 1-vary parameter 2-stop'
      read(*,'(i1)')iopt

```

```

        if(iopt.eq.2)go to 300

100    continue

        if(iopt.eq.0)then
            call input0(Cc,Ch,Kw,wid,nterm,ibound,ifluid,iwall,ider,
+            deltax,deltay,istop)
        elseif(iopt.eq.1)then
            iloop=iloop + 1
            call input1(Cc,Ch,Kw,wid,nterm,ibound,ifluid,iwall,ider,
+            deltax,deltay,istop,iloop,para,ipara,del,parmax)
        endif
            Nc = Bic*Kw*Lstr*wid/Cc
            Nh = Bih*Kw*Lstr*wid/Ch
*    print *, '  read in input'
        if(istop.eq.1)go to 200
*
*    SOLVE FOR THE EIGENVALUES
*
*    print *, 'going to calculate eigenvalues'
*    SOLVE FOR ALPHA AND MU
        call root(alph,size,Bio,Bil,nterm)
        call root(mu,size,Bic,Bih,nterm)
        if(alph(1).gt.3.141592654)then
            write(10,*)alph(1),' eigen troubles'
            go to 300
        endif
        if(mu(1).gt.3.141592654)then
            write(10,*)mu(1),' eigen troubles'
            go to 200
        endif

*    print *, '  calculated eigenvalues'
*
*    BUILD MATRIX OF UNKNOWN COEFFICIENTS
*
        call build(mu,alph,coeff,nterm,size,A)
*    print *, '  built matrix '
*
*    SOLVE THE COEFF MATRIX FOR THE NEEDED CONSTANTS
*
        call gauss(coeff,size,nterm,BC)
*    print *, '  solved matrix '
*
*    CALCULATE THE FLUID AND WALL TEMPERATURES
*
        call profil(BC,A,size,size2,nterm,deltax,deltay,Thot,

```

```

+      Tcold,Twall,dTcold,dThot,mu,alph,dTdx0,dTdx1,
+      dTdy0,dTdy1,qx0,qx1)
*      print *, ' solved for temperatures '
*
*      CALCULATE THE EFFECTIVNESS AND NUMBER OF TRANSFER UNITS
*      WITH AND WITHOUT AXIAL CONDUCTION INCLUDED
*
      n = nint(1/deltax) + 1
      m = nint(1/deltay) + 1

      if(Cc.le.Ch)then
        Cmin = Cc
        Cr = Cc/Ch
      else
        Cmin = Ch
        Cr = Ch/Cc
      endif

      NTU = (Bic*Bih*Kw*Lstr*wid)/(Cmin*(Bih+Bic*Bih+Bic))
      effc = Cc*(Tcold(1) - Tcold(n))/(Cmin*(Thot(1)-Tcold(n)))
      effh = Ch*(Thot(1) - Thot(n))/(Cmin*(Thot(1)-Tcold(n)))
*      write(*,*)'NTU ',NTU

      if(Cr.eq.1)then
        eff = NTU/(1.0 + NTU)
      else
        eff = (1-exp(-NTU*(1-Cr)))/(1-Cr*exp(-NTU*(1-Cr)))
      endif
*      print *, ' calculated Effect and NTU '
*
*
*      CALCULATE THE HEAT FLUXED AND INSURE THAT ENERGY IS CONSERVED
*

      qhot = Ch * (Thot(1) - Thot(n))
      qcold = Cc * (Tcold(1) - Tcold(n))

      qx0 = -wid*Kw/Lstr*qx0
      qx1 = -wid*Kw/Lstr*qx1

*write(10,*)'heat fluxes'
*write(10,*)'qx0 =' ,qx0
*write(10,*)'qx1 =' ,qx1
*write(10,*)'qhot =' ,qhot
*write(10,*)'qcold =' ,qcold

```

```

      qtot = (qhot - qcold + qx0 - qx1)/(min(qhot,qcold))
*      print *, '      calculated heat fluxes '
*
*
*      GENERATE THE OUTPUT FILE OF THE TEMPERATURE DISTRIBUTIONS OF THE
*      FLUIDS AND WALL AND CHECK THAT THE BOUNDARY CONDITIONS ARE MET
*
      if(iopt.eq.0)then
        call output(deltax,deltay,size2,dTdx0,dTdx1,dTdy0,
+          dTdy1,Thot,Tcold,Twall,iwall,ifluid,ibound,
+          ilder,p0x,p1x,p0y,p1y)
        call out0(NTU,eff,effc,effh,nterm,Kw,Cc,Ch,qtot,p0x,p1x,
+          p0y,p1y)
      else
        call output(deltax,deltay,size2,dTdx0,dTdx1,dTdy0,
+          dTdy1,Thot,Tcold,Twall,iwall,ifluid,ibound,
+          ilder,p0x,p1x,p0y,p1y)
        call out1(NTU,eff,effc,effh,nterm,Kw,Cc,Ch,para,qtot,p0x,p1x,
+          p0y,p1y,iloop,ipara)
      endif
*      print *, '      Generated output files '

      if(iopt.eq.0)close(10)

      go to 100

200  continue

      if(iopt.eq.1)then
        close(10)
        close(40)
        irun=irun+1
        istop=0
        iloop=0
        go to 50
      endif

300  continue

      stop
      end

*      DATE  3/05/92
*
*      SUBROUTINE TO GENERATE THE OUTPUT FILE FOR OPTION 0

```

* - SINGLE DATA FILE OPTION VARYING SOME PARAMETER

*
*

```
subroutine out0(NTU,eff,effc,effh,nterm,Kw,Cc,Ch,qtot,
+      p0x,p1x,p0y,p1y)
implicit double precision(a-h,o-z)
double Precision NTU,Nc,Nh,len,Lstr,Kw
```

```
common delta,len,Lstr,Nc,Nh,Bic,Bih,Bio,Bil,Tcin,Thin,To,Tl
```

*
*
*

WRITE THE NONDIM DATA AND INLET PARAMETERS USED IN CALCULATION

```
write(10,*)' '
write(10,*)' Nondimensional Data'
write(10,'(a,f12.5)') L*      ='Lstr
write(10,'(a,f12.5)') Hot side(Bih)  ='Bih
write(10,'(a,f12.5)') Cold side(Bic) ='Bic
write(10,'(a,f12.5)') Wall End(Bio)  ='Bio
write(10,'(a,f12.5)') Wall End(Bil)  ='Bil
write(10,'(a,f12.5)') "ntu" hot (Nh)  ='Nh
write(10,'(a,f12.5)') "ntu" cold(Nc)  ='Nc
write(10,*)' '
write(10,*)' Fluid and Wall conditions '
write(10,'(a,f12.5,a)') Wall Conductivity(Kw)  ='Kw,' W/m^2K'
write(10,'(a,f12.5,a)') Heat Cap cold (Cc)      ='Ch,' W/K'
write(10,'(a,f12.5,a)') Heat Cap hot (Ch)       ='Cc,' W/K'
write(10,'(a,f12.5,a)') Inlet Temp cold (Tcin)  ='Tcin,' C'
write(10,'(a,f12.5,a)') Inlet Temp hot (Thin)   ='Thin,' C'
write(10,*)' '
write(10,*)' Ambient Temperatures '
write(10,'(a,f12.5)') At x=L (Tl)  ='Tl
write(10,'(a,f12.5)') At x=0 (To)  ='To
write(10,*)' '
write(10,'(a,i2,a)') Summations terminated at 'nterm,' terms'
write(10,*)' '
write(10,'(17x,a,5x,a,4x,a,4x,a)')Hot','Cold',
+ 'Negl','Eng  Boundry Condition err Bi'
write(10,'(5x,a,8x,a,6x,a,5x,a,5x,a)')NTU','Eff','Eff','Eff',
+ 'Bal Bio Bil Bih Bic'
write(10,'(2x,f7.4,2x,3f9.4,1x,e8.2,4f7.4)')NTU,effh,
+      effc,eff,qtot,p0x,p1x,p0y,p1y

return
end
```

* DATE 3/05/92

```

*
* SUBROUTINE TO GENERATE THE OUTPUT FILE FOR OPTION 1
* - OPTION VARYING SOME PARAMETER
*
*
      subroutine out1(NTU,eff,effc,effh,nterm,Kw,Cc,Ch,para,qtot,
+      p0x,p1x,p0y,p1y,iloop,ipara)
      implicit double precision(a-h,o-z)
      double Precision NTU,NTUlam,Nc,Nh,len,Lstr,Kw
      character para*10

      common delta,len,Lstr,Nc,Nh,Bic,Bih,Bio,Bil,Tcin,Thin,To,Tl

*
* WRITE THE NONDIM DATA AND INLET PARAMETERS USED IN CALCULATION
*
      if(iloop.eq.1)then

        write(10,*)' '
        write(10,*)' Nondimensional Data'
        write(10,'(a,f12.5)') L*      =' ,Lstr
        write(10,'(a,f12.5)') Hot side(Bih)  =' ,Bih
        write(10,'(a,f12.5)') Cold side(Bic)  =' ,Bic
        write(10,'(a,f12.5)') Wall End(Bio)   =' ,Bio
        write(10,'(a,f12.5)') Wall End(Bil)   =' ,Bil
        write(10,'(a,f12.5)') "ntu" hot (Nh)   =' ,Nh
        write(10,'(a,f12.5)') "ntu" cold(Nc)   =' ,Nc
        write(10,*)' '
        write(10,*)' Fluid and Wall conditions '
        write(10,'(a,f12.5,a)') Wall Conductivity(Kw)  =' ,Kw,' W/m^2K'
        write(10,'(a,f12.5,a)') Heat Cap cold (Cc)     =' ,Cc,' W/K'
        write(10,'(a,f12.5,a)') Heat Cap hot (Ch)      =' ,Ch,' W/K'
        write(10,'(a,f12.5,a)') Inlet Temp cold (Tcin) =' ,Tcin,' C'
        write(10,'(a,f12.5,a)') Inlet Temp hot (Thin)  =' ,Thin,' C'
        write(10,*)' '
        write(10,*)' Ambient Temperatures '
        write(10,'(a,f12.5)') At x=L (Tl)  =' ,Tl
        write(10,'(a,f12.5)') At x=0 (To)  =' ,To
        write(10,*)' '
        write(10,'(a,i3,a)') Summations terminated at ' ,nterm,' terms'
        write(10,*)' '
        write(10,'(a,a)') varying parameter ' ,para
        write(10,*)' '
        write(10,'(3x,a9,16x,a,5x,a,4x,a,4x,a)') para,'Hot','Cold',
+      'Negl','Eng  Boundry Condition'
        write(10,'(19x,a,6x,a,5x,a,5x,a,5x,a)') 'NTU',
+      'Eff','Eff','Eff','Bal  max error'
      endif

```

```

BCerr = max(p0x,p1x,p0y,p1y)

uneff = (eff - (effh+effc)/2)/eff
Cmin = min(Ch,Cc)
Cmax = max(Ch,Cc)
NTUlam = Kw*Lstr/Cmin
if(ipara.eq.1)then
  write(10,'(3x,f7.2,5x,f8.3,1x,3f8.5,1x,e8.2,3x,f7.5)')
+   Lstr,NTU,effh,effc,eff,qtot,BCerr
  write(40,'(1x,f10.3,1x,f4.2,2f10.6,2x,4f9.5)')Lstr,Cmin/Cmax,
+   Cmin,NTU,effh,effc,eff,uneff
  return

elseif(ipara.eq.2)then
  write(10,'(3x,f7.4,5x,f8.3,1x,3f8.5,1x,e8.2,3x,f7.5)')Bih,NTU,
+   effh,effc,eff,qtot,BCerr
  write(40,'(1x,f10.6,1x,f4.2,2f10.6,2x,4f9.5)')Bih,Cmin/Cmax,
+   Cmin,NTU,effh,effc,eff,uneff
  return
elseif(ipara.eq.3)then
  write(10,'(3x,f7.4,5x,f8.3,1x,3f8.5,1x,e8.2,3x,f7.5)')Bic,NTU,
+   effh,effc,eff,qtot,BCerr

  write(40,'(1x,f10.6,1x,f4.2,2f10.6,2x,4f9.5)')Bic,Cmin/Cmax,
+   Cmin,NTU,effh,effc,eff,uneff
  return
elseif(ipara.eq.4)then
  write(10,'(3x,f7.4,5x,f8.3,1x,3f8.5,1x,e8.2,3x,f7.5)')Bio,NTU,
+   effh,effc,eff,qtot,BCerr
  write(40,'(1x,f10.6,1x,f4.2,2f10.6,2x,4f9.5)')Bio,Cmin/Cmax,
+   Cmin,NTU,effh,effc,eff,uneff
  return
elseif(ipara.eq.5)then
  write(10,'(3x,f7.4,5x,f8.3,1x,3f8.5,1x,e8.2,3x,f7.5)')Bil,NTU,
+   effh,effc,eff,qtot,BCerr
  write(40,'(1x,f10.6,1x,f4.2,2f10.6,2x,4f9.5)')Bil,Cmin/Cmax,
+   Cmin,NTU,effh,effc,eff,uneff
  return
elseif(ipara.eq.6.and.Ch.lt.Cc)then
  write(10,'(3x,f7.4,5x,f8.3,1x,3f8.4,1x,e8.2,3x,f7.5)')Ch/Cc,NTU,
+   effh,effc,eff,qtot,BCerr
  write(40,'(1x,f4.2,1x,2f10.6,2x,4f9.5)')Cmin/Cmax,Cmin,NTU,effh,
+   effc,eff,uneff
  return
elseif(ipara.eq.6.and.Cc.le.Ch)then
  write(10,'(3x,f7.4,5x,f8.3,1x,3f8.5,1x,e8.2,3x,f7.5)')Cc/Ch,NTU,

```

```

+      effh,effc,eff,qtot,BCerr
      write(40,'(1x,f4.2,1x,2f10.6,2x,4f9.5)')Cmin/Cmax,Cmin,NTU,effh,
+      effc,eff,uneff
      return
      elseif(ipara.eq.16.and.Cc.le.Ch)then
      write(10,'(f7.4,f8.2,f8.3,1x,3f8.5,1x,e8.2,3x,f7.5)')Cc/Ch,Lstr,NTU,
+      effh,effc,eff,qtot,BCerr
      return
      elseif(ipara.eq.16.and.Ch.lt.Cc)then
      write(10,'(f7.4,f8.2,f8.3,1x,3f8.5,1x,e8.2,3x,f7.5)')Ch/Cc,Lstr,NTU,
+      effh,effc,eff,qtot,BCerr
      return
      elseif(ipara.eq.23)then
      write(10,'(3x,f7.5,5x,f8.3,1x,3f8.5,1x,e8.2,3x,f7.5)')Bih,NTU,
+      effh,effc,eff,qtot,BCerr
      write(40,'(1x,2f8.5,1x,f4.2,1x,f8.4,1x,f5.2,4f8.5)')Bic,Bih,
+      Cmin/Cmax,Cmin,NTU,effh,effc,eff,uneff
      return

      elseif(ipara.eq.45)then
      write(10,'(1x,f7.5,1x,f7.5,f8.3,1x,3f8.5,1x,e8.2,3x,f7.5)')Bio,
+      Bil,NTU,effh,effc,eff,qtot,BCerr
      write(40,'(1x,2f8.5,1x,f4.2,1x,f8.4,1x,f5.2,4f8.5)')Bio,Bil,
+      Cmin/Cmax,Cmin,NTU,effh,effc,eff,uneff
      return

      elseif(ipara.eq.8)then
      write(10,'(3x,i5,7x,f8.3,1x,3f8.5,1x,e8.2,3x,f7.4)')nterm,NTU,effh,
+      effc,eff,qtot,BCerr
      write(40,'(1x,3i,f10.6,2x,4f9.5)')N,NTU,effh,
+      effc,eff,uneff
      return
      endif
      end

```

```

*      DATE 2/17/92

```

```

*

```

```

*      SUBROUTINE TO OPEN FILE AND READ IN RAW DATA

```

```

*

```

```

      subroutine input0(Cc,Ch,Kw,wid,nterm,ibound,ifluid,iwall,ider,
+      deltax,deltay,istop)

```

```

      implicit double precision (a-h,o-z)
      double precision len,Lx,Ly,Kw,Nc,Nh,Lstr

```



```
character outfil*60,infil*60
```

```
common delta,len,Lstr,Nc,Nh,Bic,Bih,Bio,Bil,Tcin,Thin,To,Tl
```

```
print *, 'Enter the input file'
```

```
read(*, '(a)')infil
```

```
print *, 'Enter the output file'
```

```
read(*, '(a)')outfil
```

```
*
```

```
*
```

```
CHECK IF EOF FLAG TO TERMINATE THE PROGRAM HAS BEEN READ IN
```

```
*
```

```
if(outfil.eq.'eof')then
```

```
*
```

```
close(20)
```

```
istop = 1
```

```
return
```

```
else
```

```
istop=0
```

```
endif
```

```
*
```

```
*
```

```
READ IN THE RAW DATA
```

```
*
```

```
open(10,status='new',file=outfil)
```

```
open(40,status='new',file=outfil)
```

```
open(50,status='new',file=outfil)
```

```
open(30,status='unknown',file=infil)
```

```
read(30,'(17x,f20.0)')Lstr
```

```
read(30,'(17x,f20.0)')Bih
```

```
read(30,'(17x,f20.0)')Bic
```

```
read(30,'(17x,f20.0)')Bio
```

```
read(30,'(17x,f20.0)')Bil
```

```
read(30,'(17x,f20.0)')Kw
```

```
read(30,'(17x,f20.0)')Ch
```

```
read(30,'(17x,f20.0)')Cc
```

```
read(30,'(17x,f20.0)')Thin
```

```
read(30,'(17x,f20.0)')Tcin
```

```
read(30,'(17x,f20.0)')To
```

```
read(30,'(17x,f20.0)')Tl
```

```
read(30,'(17x,f20.0)')wid
```

```
read(30,'(17x,i20)')nterm
```

```
read(30,'(17x,i20)')ibound
```

```
read(30,'(17x,i20)')ifluid
```

```
read(30,'(17x,i20)')iwall
```

```
read(30,'(17x,i20)')ider
```

```
read(30,'(17x,f20.0)')deltax
```

```
read(30,'(17x,f20.0)')deltay
```

```
close(30)
```

```

return
end
*
*
*      DATA 3/05/92
*
*      SUBROUTINE TO OPEN FILE AND READ IN RAW DATA
*

      subroutine input1(Cc,Ch,Kw,wid,nterm,ibound,ifluid,iwall,ider,
+          deltax,deltay,istop,iloop,para,ipara,del,parmax)

      implicit double precision (a-h,o-z)
      double precision len,Lstr,Nc,Nh,Kw
      character outfil*60,para*10,infil*60

      common delta,len,Lstr,Nc,Nh,Bic,Bih,Bio,Bil,Tcin,Thin,To,Tl

      if(iloop.eq.1)then

*
*      READ IN PARAMETER TO VARY, INCREMENT, AND MAX VALUE. THEN THE RAW
*      DATA FILE NAME AND PERTINENT DATA
          print *,'enter the para to vary'
          read(*,'(i10)')ipara
          print *,'enter the del'
          read(*,'(f20.0)')del
          print*,'enter the max value'
          read(*,'(f20.0)')parmax
          print *,'enter the input file name'
          read(*,'(a)')infil
          print *,'enter the output file name'
          read(*,'(a)')outfil

          open(40,status='new',file=outfil)
          open(10,status='new',file=outfil)
          open(30,status='unknown',file=infil)

          read(30,'(17x,f20.0)')Lstr
          read(30,'(17x,f20.0)')Bih
          read(30,'(17x,f20.0)')Bic
          read(30,'(17x,f20.0)')Bio
          read(30,'(17x,f20.0)')Bil
          read(30,'(17x,f20.0)')Kw
          read(30,'(17x,f20.0)')Ch
          read(30,'(17x,f20.0)')Cc

```

```

read(30,'(17x,f20.0)')Thin
read(30,'(17x,f20.0)')Tcin
read(30,'(17x,f20.0)')To
read(30,'(17x,f20.0)')Tl
read(30,'(17x,f20.0)')wid
read(30,'(17x,i20)')nterm
read(30,'(17x,i20)')ibound
read(30,'(17x,i20)')ifluid
read(30,'(17x,i20)')iwall
read(30,'(17x,i20)')ider
read(30,'(17x,f20.0)')deltax
read(30,'(17x,f20.0)')deltay

*      close(20)
      close(30)
*
*      OTHERWISE INCREMENT THE PARAMETER THAT IS BEING VARIED AND SEND
*      DATA BACK TO PROGRAM
*
endif
  if(ipara.eq.1)then
    para = 'Lstr'
    if(iloop.eq.1)then
      Cmin = min(Cc,Ch)
      Cr = Cc/Ch
      ratio = Lstr/Cmin
    else
      Lstr = Lstr + del
      *      write(*,*)'Lstr ',Lstr
      Cmin = Lstr/ratio
      if(Cc.le.Ch)then
        Cc = Cmin
        Ch = Cc/Cr
      else
        Ch = Cmin
        Cc = Cr * Ch
      endif
    endif
  endif
  istop = 0
  if(Lstr.gt.parmax)istop=1
  return
elseif(ipara.eq.2)then
  para = 'Bih'
  istop = 0
  if(iloop.eq.1)then
    Cmin = min(Cc,Ch)
    Cr = Cc/Ch

```

```

      ratioi = Lstr/Cmin*(Bih*Bic*Kw*wid/
+      (Bih + Bic*Bih + Bic))
    else
      Bih = Bih * del
      ratio = Lstr *(Bih*Bic*Kw*wid/
+      (Bih + Bic*Bih + Bic))
      Cmin = ratio/ratioi
      if(Cc.le.Ch)then
        Cc = Cmin
        Ch = Cc/Cr
      else
        Ch = Cmin
        Cc = Cr * Ch
      endif
    endif
    if(Bih.gt.parmax)istop=1
    return
  elseif(ipara.eq.3)then
    para = 'Bic'
    istop = 0
    if(iloop.eq.1)then
      Cmin = min(Cc,Ch)
      Cr = Cc/Ch
      ratioi = Lstr/Cmin*(Bih*Bic*Kw*wid/
+      (Bih + Bic*Bih + Bic))
    else
      Bic = Bic * del
      ratio = Lstr *(Bih*Bic*Kw*wid/
+      (Bih + Bic*Bih + Bic))
      Cmin = ratio/ratioi
      if(Cc.le.Ch)then
        Cc = Cmin
        Ch = Cc/Cr
      else
        Ch = Cmin
        Cc = Cr * Ch
      endif
    endif
    if(Bic.gt.parmax)istop=1
    return
  elseif(ipara.eq.4)then
    para = 'Bio'
    istop = 0
    if(iloop.gt.1)Bio = Bio * del
    if(Bio.gt.parmax)istop=1
    return
  elseif(ipara.eq.5)then

```

```

para = 'Bil'
istop = 0
if(iloop.gt.1)Bil = Bil * del
if(Bil.gt.parmax)istop=1
return
elseif(ipara.eq.6)then
para = 'Cr'
istop = 0
Cr = Ch/Cc
if(iloop.gt.1)Ch = Ch + del
if(iloop.gt.1)Cc = Ch/Cr
if(Cc.gt.parmax)istop=1
return
* elseif(ipara.eq.16)then
* para = 'Cr & L*'
* istop = 0
* Cmax = max(Cc,Ch)
* Cmin = min(Cc,Ch)
* if(iloop.eq.1)then
* ratio = Lstr/Cmin
* deLstr = del * (parmax-Lstr)
* delCr = del * ratio/(Cmax - Cmin)
* write(*,*)'delCr delLstr =',delCr,deLstr
* else
* if(Ch.le.Cc)then
* Lstr = Lstr + deLstr
* Ch = Ch + delCr
* else
* Lstr = Lstr + deLstr
* Cc = Cc + delCr
* endif
* endif
* if(Lstr.gt.parmax)istop = 1
* return
elseif(ipara.eq.23)then
para = 'Bih & Bic'
istop = 0
if(iloop.eq.1)then
Cmin = min(Cc,Ch)
Cr = Cc/Ch
ratioi = Lstr/Cmin*(Bih*Bic*Kw*wid/
+ (Bih + Bic*Bih + Bic))

else
Bih = Bih + del
Bic = Bic + del
ratio = Lstr *(Bih*Bic*Kw*wid/

```

```

+      (Bih + Bic*Bih + Bic))
      Cmin = ratio/ratioi
      if(Cc.le.Ch)then
        Cc = Cmin
        Ch = Cc/Cr
      else
        Ch = Cmin
        Cc = Cr * Ch
      endif
    endif
    if(Bih.gt.parmax)istop = 1
    return
  elseif(ipara.eq.45)then
    para = 'Bio & Bil'
    istop = 0
    if(iloop.eq.1)then
      Bioi=Bio
      Bili=Bil
    else
      Bio = Bioi * del
      Bil = Bili * del
    Bioi = Bio
    Bili = Bil
  endif
    if(Bio.gt.parmax)istop = 1
    return
  elseif(ipara.eq.8)then
    para = 'N'
    istop = 0
    if(iloop.gt.1)nterm = nterm * del
    if(nterm.gt.parmax)istop=1
    return
  endif
end

*
*   date 2/09/92
*
*
*   SUBROUTINE TO BUILD THE MATRIX OF UNKNOWN COEFF
*
*
*
subroutine build(mu,alph,coeff,nterm,size,A)

implicit double precision (a-h,o-z)
integer size

```

```
double precision len,Nc,Nh,mu,mulsq,mul,Lstr,Ncsq,Nhsq,lam,musq
common delta,len,Lstr,Nc,Nh,Bic,Bih,Bio,Bil,Tcin,Thin,To,Tl
```

```
dimension coeff(size,size+1),mu(size),alph(size)
dimension A(size)
```

```
*
```

```
* GENERATION OF THE MATRIX, ORDER WILL BE (2*NTERM X 2*NTERM +1)
```

```
*
```

```
* SET CONSTANTS AND INITIALIZE THE PARAMETERS
```

```
pi = 3.141592654
```

```
Ncsq = Nc * Nc
```

```
Nhsq = Nh * Nh
```

```
rhs1 = 0.0
```

```
rhs2 = 0.0
```

```
rhs3 = 0.0
```

```
rhs4 = 0.0
```

```
expNc = dexp(-Nc)
```

```
*
```

```
* BEGIN COMPUTTIN MATRIX -i CORRESPONDS TO ROW NUMBER
```

```
*
```

```
do 10 i=1,nterm
```

```
mul = mu(i)*Lstr
```

```
mulsq = mul * mul
```

```
musq = mu(i) * mu(i)
```

```
alpl = alph(i) / Lstr
```

```
alphsq = alph(i) * alph(i)
```

```
alplsq = alpl * alpl
```

```
hsin = sinh(alpl)
```

```
hcos = cosh(alpl)
```

```
sine = sin(alph(i))
```

```
cosin = cos(alph(i))
```

```
zeta = (alpl*hsin + Bic*hcos)/(Bic*hsin + alpl*hcos)
```

```
orth = ((alphsq+Bio**2.0)*(1.+Bil/(alphsq+Bil**2.))+Bio)/2.0
```

```
orthmu = ((musq+Bih**2.0)*(1.0+Bic/(musq+Bic**2.0))+Bih)/2.0
```

```
lam = -(alpl*zeta + Bih) * orth
```

```
if(Nh.lt.100)then
```

```
omg = Bih/(Nhsq+alphsq)*((Nh+Bio)*alph(i)+dexp(-Nh)*
```

```
+ ((alphsq-Nh*Bio)*sine - (Bio+Nh)*alph(i)*cosin))
```

```
else
```

```
omg = Bih/(Nhsq+alphsq)*(Nh+Bio)*alph(i)
```

```
endif
```

$cphi = ((alpsq+Bic*Bih)*hsin+(Bic+Bih)*alpl*hcoss)*orth$

*

* **ABSORBED EXP(-NC) INTO COMG FROM LOADING OF THE MATRIX**

*

if(Nc.lt.100)then

comg = Bic/(Ncsq+alpsq)*(expNc*(Bio-Nc)*alph(i)+

+ ((alpsq+Bio*Nc)*sine + (Nc-Bio)*alph(i)*cosin))

else

comg = Bic/(Ncsq+alpsq)*((alpsq+Bio*Nc)*sine +

+ (Nc-Bio)*alph(i)*cosin)

endif

*

* **j CORRESPONDS TO COLUMN NUMBER**

*

do 20 j=1,nterm

alphi = alph(i)

alpl = alph(j)/Lstr

alpsq = alph(j) * alph(j)

musq = mu(j) * mu(j)

mul = mu(j)*Lstr

mulsq = mul*mul

*

hsinmu = sinh(mul)

*

hcosmu = cosh(mul)

hsinal = sinh(alpl)

hcosal = cosh(alpl)

sinal = sin(alph(j))

cosal = cos(alph(j))

sinmu = sin(mu(j))

cosmu = cos(mu(j))

ch1 = (Nh*Bio-mulsq)/(Nhsq-mulsq)

ch2 = (Nh*Bio+alpsq)/(Nhsq+alpsq)

cc1 = (Nc*Bio+mulsq)/(Ncsq-mulsq)

cc2 = (Nc*Bio-alpsq)/(Ncsq+alpsq)

*

* **CONSTANTS c1,c2,c3,c4 AND eps HAVE A COSH FACTORED OUT OF THEN WHICH**

* **CANCELS WITH THE COSH FACTORED OUT OF THE CONST A(j) WHEN MULT**

* **TOGETHER WITH rho AND crho IN RHS CONSTANTS AS COMPARED TO SOLUTION**

*

c1 = tanh(mul)*mul*cos(alphi)

+ + alphi*sin(alphi)

c2 = tanh(mul)*mul*sin(alphi)

+ - alphi*cos(alphi) + alphi


```

c3    = mul*cos(alphi)
+      + tanh(mul)*alphi*sin(alphi) - mul
c4    = mul*sin(alphi)
+      - tanh(mul)*alphi*cos(alphi)

denom1 = mulsq + alphi*alphi
zeta   = (alpl*hsinal + Bic*hcosal)/
+       (Bic*hsinal + alpl*hcosal)

rho1   = Bih*alphi/denom1*musq*Lstr*(1-ch1)*c1
rho2   = Bih*Bio/denom1*musq*Lstr*(1-ch1)*c2
rho3   = Bih*Nh/denom1*mu(j)*alphi*ch1*c3
rho4   = Bih*Nh*Bio/denom1*mu(j)*ch1*c4

crho1  = Bic*alphi/denom1*mul*(1+cc1)*c1
crho2  = Bic*Bio/denom1*mul*(1+cc1)*c2
crho3  = Bic*Nc/denom1*alphi*cc1*c3
crho4  = Bic*Nc*Bio/denom1*cc1*c4

beta   = (1-ch1)*musq*Lstr
gam    = (1-ch2)*alph(j)
eps    = (1+cc1)*mul+ Nc*cc1*tanh(mul)
sig    = (hcosal-zeta*hsinal)*((1+cc2)*alph(j)*cosal
+       + Nc*cc2*sinal)
tau    = (alpl*hcosal+Bih*hsinal)*((1+cc2)*alph(j)*cosal
+       + Nc*cc2*sinal)

ammn   = alphi - alph(j)
ampn   = alphi + alph(j)
anmm   = alph(j) - alphi
anpm   = alph(j) + alphi

if(i.eq.j)then

psi    = (.5+1/(4*alphi)*sin(2*alphi))*(1-ch2)*alphsq
+       + ((Bio*(1-ch2) + Nh*ch2)/2) *(sin(alphi))**2
+       + (.5-1/(4*alphi)*sin(2*alphi))*Nh*Bio*ch2

cpsi   = (.5+1/(4*alphi)*sin(2*alphi))*(1+cc2)*alphsq
+       + ((Bio*(1+cc2) + Nc*cc2)/2) *(sin(alphi))**2
+       + (.5-1/(4*alphi)*sin(2*alphi))*Nc*Bio*cc2

```

```

else
  sin1m = sin(ammn)/(2*ammn)
  sin1p = sin(ampn)/(2*ampn)
  cos2m = cos(ammn)/(2*ammn)
  cos2p = cos(ampn)/(2*ampn)
  cos3m = cos(anmm)/(2*anmm)
  cos3p = cos(anpm)/(2*anpm)

  arg1 = sin1m + sin1p
  arg2 = -cos2m - cos2p + 1/(2*ammn) + 1/(2*ampn)
  arg3 = -cos3m - cos3p + 1/(2*anmm) + 1/(2*anpm)
  arg4 = sin1m - sin1p

  psi = arg1*alph(j)*alphi*(1-ch2)
+    + arg2*alph(j)*(1-ch2)*Bio
+    + arg3*ch2*Nh*alphi + arg4*ch2*Nh*Bio

  cpsi = arg1*alph(j)*alphi*(1+cc2)
+    + arg2*alph(j)*(1+cc2)*Bio
+    + arg3*cc2*Nc*alphi + arg4*cc2*Nc*Bio

endif

psiB = psi * Bih
psiC = psi * Bih * alpl

cpsiB = cpsi * Bic * (hcosal - zeta * hsinal)
cpsic = cpsi * Bic * (alpl*hcosal + Bih*hsinal)

*
*   LOAD THE MATRIX, LOADING IS DONE IN QUARTERS(i.e.TOP LEFT,
*   top right, bottom left.....) but concurrently
*
*   1ST EQUATION LOADING - TOP LEFT AND TOP RIGHT
coeff(i,j) = -omg*gam + psiB
coeff(i,j+nterm) = -omg*gam*alpl + psiC

*   2ND EQUATION LOADING - BOTTOM LEFT AND BOTTOM RIGHT
coeff(i+nterm,j) = comg*sig - cpsiB
coeff(i+nterm,j+nterm) = comg*tau - cpsiC

if(i.eq.j)then
  coeff(i,j) = coeff(i,j) + lam
  coeff(i+nterm,j+nterm) = coeff(i+nterm,j+nterm) + cphi

```

```

endif
*
*   CONSTANT A(j) HAS A COSH FACTORED OUT OF THE DENOMINATOR THAT
*   IS CANCELLED BY THE COSH FROM C1..C4 WHEN MULTIPLIED BY rho AND
*   crho IN THE RHS CONSTANTS CALCULATIONS
*

      if((Tl-To).ne.0)then
        A(j) = (Bil*(Tl-To)*(sin(mu(j))-Bih/mu(j)*cos(mu(j))
+          +Bih/mu(j))) /(orthmu*
+          ((mulsq+Bil*Bio)*tanh(mul)+(Bil+Bio)*mul))
        Aprm = A(j)*(mu(j)*cosmu + Bih*sinmu)
      else
        A(j) = 0.0
        Aprm = 0.0
      endif

      rhs1 = (rho1+rho2+rho3+rho4)*A(j) + rhs1
      rhs2 = (crho1+crho2+crho3+crho4)*Aprm + rhs2
      rhs3 = beta*A(j) + rhs3
      rhs4 = eps*Aprm + rhs4
*
*
*   LOADING THE RHS CONSTANTS - DONE FOR EQUATION 1 THEN EQ 2
*

      if(j.eq.nterm)then
        coeff(i,2*nterm+1) = -rhs1 + omg*rhs3 - omg*(Thin-To)

        coeff(i+nterm,2*nterm+1)=rhs2 - comg*rhs4
+          + comg*(Tcin-To)
      endif

20      continue

      rhs1 = 0.0
      rhs2 = 0.0
      rhs3 = 0.0
      rhs4 = 0.0

10      continue

      return
end
*
*
*   DATE 5/12/92
*

```

* SUBROUTINE TO CALCULATE EIGENVALUES FROM THE TRANSCENDENTAL
 * EQUATIONS. USING A SCHEME THAT MARCHES OUT UNTIL THE FUNCTION
 * CHANGES SIGN THEN BACKSTEPS TO THE ROOT
 *

subroutine root(eigen,size,B1,B2,nterm)

implicit double precision(a-h,o-z)

integer size

double precision Nc,Nh,len,Lstr

common delta,len,Lstr,Nc,Nh,Bic,Bih,Bio,Bil,Tcin,Thin,To,Tl

dimension eigen(size)

func(x) = tan(x) - (x*(B1+B2))/(x**2-B1*B2)

irep = 0

delin = .5d+0

ndel = 2

pi = 4.0d+0*atan(1.0d+0)

eps = 1d-8

ep = 1d-10

del = delin/ndel

K = 0

arg =sqrt(B1*B2)

idenom = 0

*
 * CHECK IF FUNCTION CHANGES SIGN DUE TO CHANGE OF SIGN IN DENOM-
 * INATOR OF THE FUNCTION. (X<B1B2 ON THE INTEVAL) IDENOM
 * SIGNALS LEG WHERE DENOM CHANGES SIGN HAS BEEN PASSED
 *

5 continue

if(arg.lt.(k+1)*pi .and. idenom.eq.0)then

if(arg.lt.(2*(k+1)-1)*pi/2)then

x = arg + ep

del = ((2d+0*(k+1d+0)-1d+0)*pi/2d+0 - x)/ndel

ileg = 1

else

x = (2d+0*(k+1d+0)-1d+0)*pi/2d+0 + ep

del = (arg -(2d+0*(k+1d+0)-1d+0)*pi/2d+0)/ndel

ileg = 1

endif

idenom = 1

else

```

*
* IF DENOMINATOR DOESN'T CHANGE SIGN OD INTERVAL [K*PI,(K+1)*PI]
* SEARCH FOR ROOT ON THE PROPER LEG OF FUNCTION
*
  ileg = 0
  if(idenom.eq.0)then
    x = (2d+0*(k+1d+0)-1d+0)*pi/2d+0 + ep
    del = delin/ndel
  else
    x = k * pi + ep
    del = delin/ndel
  endif
endif
10  continue
   if(irep.gt.10)go to 100
   fx = func(x)

*   CHECK SIGN OF THE FUNCTION

12  if(fx)13,13,15
13  n=0
   i=n
   go to 20
15  n=1
   i=n

*   INDEX X AND MARCH FORWARD

20  x = x + del
   hx = func(x)

*
*   CHECK SIGN AT NEXT STEP
*
   if(hx)23,23,25
23  n=0
   go to 30
25  n=1

*
*   CHECK IF SIGN CHANGED. IF NO SIGN CHANGE CONTINUE MARCHING
*   IF CHANGED GO BACK AND TAKE A SMALLER STEP FORWARD.
*

30  if(i-n)40,20,40
*
*   CHECK FOR CONVERGENCE

```

```

*
40  if(eps-del)45,51,51
45  x = x - del
    del = del/2d+0
    go to 20
51  k = k + 1
    eigen(k)=x
*
*  CHECK IF EIGENVALUE WAS MISSED _ IF SO DECREASE STEP SIZE AND REPEAT
*
  if(k.gt.1)then
    if((eigen(k)-eigen(k-1)).gt.pi)then
      ndel = 2*ndel
      ep  = ep/2.0d+0
      k   = k-1
      if(ileg.eq.1)idenom=0
      irep = irep + 1
      go to 5
    endif
  else
    if(eigen(k).gt.pi)then
      ndel = 2*ndel
      ep  = ep / 2.0d+0
      k   = k-1
      idenom = 0
      irep = irep + 1
      go to 5
    endif
  endif
*
*  CHECK IF NEED TO COMPUTE MORE ROOTS
*
  if(k-nterm)5,60,60
100 continue
  write(10,*)'eigentroubles; irep =' ,irep
  write(10,*)'eigen funct =' ,x,fx
60  continue
  return
end
*
*  date 2/09/92
*
*  SOLVES THE MATRIX USING A PARTIAL PIVOTING SCHEME
*
  SUBROUTINE GAUSS(A,SIZE,N,X)
*
*  A  - SQUARE MATRIX TO SOLVE WIHT ADDITIONAL RHS CONSTANTS

```

* N - NUMBER OF TERMS IN THE SERIES (A IS ORDER $(2N \times 2N+1)$)
 * SIZE - DECLARED MAX SIZE OF A IN MAIN PROGRAM
 * X - SOLUTION
 *
 *

implicit double precision (a-h,o-z)
 double precision MULT
 INTEGER SIZE,PIVOT
 DIMENSION A(SIZE,SIZE+1),X(SIZE)

N=2*N

*
 * GAUSSIAN ELIMINATION USING PARTIAL PIVOTING
 *

DO 70 I=1,N

IF(A(I,I).EQ.0) THEN
 PIVOT=0
 J=J+1
 30 IF((PIVOT.EQ.0). AND .(J.LE.N)) THEN
 IF(A(J,I).NE.0) PIVOT = J
 J=J+1
 GO TO 30
 ENDIF
 IF(PIVOT.EQ.0) THEN
 STOP 'SINGULAR MATRIX'
 ELSE

*
 * INTERCHANGE ROWS
 *

DO 40 J=1,N+1
 TEMP = A(I,J)
 A(I,J) = A(PIVOT,J)
 A(PIVOT,J) = TEMP
 40 CONTINUE
 ENDIF
 ENDIF

*
 * ELIMINATE THE ITH UNKNOWN
 *

DO 60 J= I + 1, N

MULT = -A(J,I)/A(I,I)

DO 50 K=I,N+1
 A(J,K) = A(J,K) + MULT * A(I,K)

50 CONTINUE

60 CONTINUE

70 CONTINUE

*

* FIND SOLUTION

*

$X(N) = A(N,N+1)/A(N,N)$

 DO 90 J=N-1,1,-1

$X(J) = A(J,N+1)$

 DO 80 K = J+1,N

$X(J) = X(J) - A(J,K) * X(K)$

80 CONTINUE

$X(J) = X(J) / A(J,J)$

90 CONTINUE

 N=N/2

 RETURN

 END

*

*

* date 2/16/92

*

* SUBROUTINE TO CALCULATE THE FLUID TEMPERATURES

* AND WALL TEMPERATURES ALONG WITH THEIR DERIVATIVES

 subroutine profil(BC,A,size,size2,nterm,deltax,deltay,

+ Thot,Tcold,Twall,dTcold,dThot,mu,alph,dTdx0,

+ dTdx1,dTdy0,dTdy1,qx0,qx1)

 implicit double precision (a-h,o-z)

 double precision len,Nc,Nh,mu,musq,mulsq,mulx,Ncsq,Nhsq,Lstr,

+ muy,mul

 integer size,size2

 common delta,len,Lstr,Nc,Nh,Bic,Bih,Bio,Bil,Tcin,Thin,To,Tl

 dimension BC(size),A(size),Tcold(size2),Thot(size2),

+ dTcold(size2),dThot(size2),Twall(size2,size2),

+ mu(size),alph(size),dTdx0(size2),dTdx1(size2),dTdy0(size2),

+ dTdy1(size2)

 pi = 3.1415926535


```

n  = nint(1/deltax) + 1
m  = nint(1/deltay) + 1
Nhsq = Nh * Nh
Ncsq = Nc * Nc

```

```

*

```

```

*   CALCULATING FLUID TEMPERATURES

```

```

*

```

```

*   NOTE: ONLY A FUNCTION OF X

```

```

do 10 i=1,n

```

```

sumh1 = 0.0
sumh2 = 0.0
sumc1 = 0.0
sumc2 = 0.0
sumdh1 = 0.0
sumdh2 = 0.0
sumdc1 = 0.0
sumdc2 = 0.0

```

```

if(i.eq.1)sumD1=0.0

```

```

if(i.eq.1)sumE1=0.0

```

```

do 20 j=1,nterm
mul  = mu(j)*Lstr
musq = mu(j)*mu(j)
mulsq = mul*mul
mulx  = mu(j)*Lstr*(i-1)*deltax
alphl = alph(j)/Lstr
alphx = alph(j)*(i-1)*deltax
alphsq = alph(j)*alph(j)

```

```

ch1  = (Nh*Bio-mulsq)/(Nhsq-mulsq)
ch2  = (Nh*Bio+alphsq)/(Nhsq+alphsq)
cc1  = (Nc*Bio+mulsq)/(Ncsq-mulsq)
cc2  = (Nc*Bio-alphsq)/(Ncsq+alphsq)

```

```

      zeta = (alphl*sinh(alphl)+Bic*cosh(alphl))/
+      (Bic*sinh(alphl) + alphl*cosh(alphl))
      if(A(j).ne.0)then
Apr = A(j)/cosh(mul)*(mu(j)*cos(mu(j))+Bih*sin(mu(j)))
      else
Apr = 0.0
      endif
Bpr = BC(j)*(cosh(alphl)-zeta*sinh(alphl))
Cpr = BC(j+nterm)*(alphl*cosh(alphl)+Bih*sinh(alphl))

```

```

if(i.eq.1)then
  if(A(j).ne.0)then
    sumD1 = A(j)/cosh(mul)*musq*Lstr*(1-ch1)+(BC(j)+
+      BC(j+nterm)*alphl)*(1-ch2)*alph(j) + sumD1
  else
    sumD1 = (BC(j)+
+      BC(j+nterm)*alphl)*(1-ch2)*alph(j) + sumD1
  endif
  if(A(j).ne.0)then
    sumE1 = Apr*(mul*(1+cc1)*cosh(mul)+Nc*cc1*sinh(mul))
+      + (Bpr+Cpr)*((1+cc2)*alph(j)*cos(alph(j))
+      + Nc*cc2*sin(alph(j))) + sumE1
  else
    sumE1 = (Bpr+Cpr)*((1+cc2)*alph(j)*cos(alph(j))
+      + Nc*cc2*sin(alph(j))) + sumE1
  endif
endif
  if(A(j).ne.0)then
    sumh1 = A(j)/cosh(mul)*((1-ch1)*musq*Lstr*cosh(mulx)
+      + Nh*mu(j)*ch1*sinh(mulx)) + sumh1
  else
    sumh1 = 0.0
+
  endif
  hot2 = (1-ch2)*alph(j)*cos(alphx)
+      + Nh*ch2*sin(alphx)

  sumh2 = (BC(j)+BC(j+nterm)*alphl)*hot2 + sumh2

  if(A(j).ne.0)then
    sumc1 = Apr*((1+cc1)*mul*cosh(mulx)
+      + Nc*cc1*sinh(mulx)) + sumc1
  else
    sumc1 = 0.0
  endif

  sumc2 = ((1+cc2)*alph(j)*cos(alphx)+Nc*cc2*sin(alphx))
+      *(Bpr + Cpr) + sumc2

  if(A(j).ne.0)then
    sumdh1 = A(j)/cosh(mul)*((1-ch1)*musq*mul*Lstr
+      *sinh(mulx) + Nh*musq*Lstr*ch1*cosh(mulx)) +sumdh1
  else
    sumdh1 = 0.0
  endif

  dhot2 =(-1+ch2)*alphsq*sin(alphx)

```

```

+           + Nh*ch2*alph(j)*cos(alphx)

      sumdh2 = (BC(j)+BC(j+nterm)*alph1)*dhot2 + sumdh2

      if(A(j).ne.0)then
      sumdc1 = Apr*((1+cc1)*mulsq*sinh(mulx)
+           +Nc*cc1*mul*cosh(mulx)) + sumdc1
      else
      sumdc1 = 0.0
      endif

      sumdc2 = (- (cc2+1)*alphsq*sin(alphx)
+           +Nc*cc2*alph(j)*cos(alphx))*(Bpr+Cpr)+sumdc2

20      continue

      if(i.eq.1)then
      D1 = (Thin-To) - sumD1
      E1 = (Tcin-To-sumE1)
      endif

      if((Nh*(i-1)*deltax).lt.100)then
      Thot(i) = D1*Dexp(-Nh*(i-1)*deltax) + To + sumh1 + sumh2
      dThot(i) = -D1*Nh*dexp(-Nh*(i-1)*deltax) +sumdh1 +sumdh2
      else
      Thot(i) = To + sumh1 + sumh2
      dThot(i) = sumdh1 + sumdh2
      endif

      if((-Nc*(1-(i-1)*deltax)).lt.100)then
      Tcold(i) = E1*Dexp(-Nc*(1-(i-1)*deltax)) + To + sumc1 + sumc2
      dTcold(i) = E1*Nc*Dexp(-Nc*(1-(i-1)*deltax)) + sumdc1 + sumdc2
      else
      Tcold(i) = To + sumc1 + sumc2
      dTcold(i) = sumdc1 + sumdc2
      endif

10      continue

*
*      COMPUTE TEMPERATURES IN THE WALL
*      SUMW1-THETA1 SUMW2-THETA2 SUMW3-THETA3
*
*      TWALL= THETA1 + THETA2 + THETA3 + To
*
*      if(iwall.eq.0)go to 100

```

```

dTdx1=0.0
dTdx2=0.0
dTdx3=0.0
dTdy1=0.0
dTdy2=0.0
dTdy3=0.0
Q1 =0.0
Q2 =0.0
Q3 =0.0

```

```

*
```

```

*   i  X-DIRECTION MARCHING
*
```

```

*
```

```

do 30 i=1,n

```

```

*
```

```

j  Y-DIRECTION MARCHING

```

```

do 40 j=1,m

```

```

sumw1 = 0.0

```

```

sumw2 = 0.0

```

```

sumw3 = 0.0

```

```

*
```

```

k SUMMATION OVER THE N-TERMS

```

```

do 50 k=1,nterm

```

```

alphl = alph(k)/Lstr

```

```

mul   = mu(k)*Lstr

```

```

mulx  = mul*(i-1)*deltax

```

```

alphx = alph(k)*(i-1)*deltax

```

```

muy   = mu(k)*(j-1)*deltay

```

```

alphy = alphl*(j-1)*deltay

```

```

zeta  =(alphl*sinh(alphl)+Bic*cosh(alphl))

```

```

+      /(Bic*sinh(alphl)+alphl*cosh(alphl))

```

```

if(A(j).ne.0)then

```

```

sumw1 = A(k)/cosh(mul)*(mul*cosh(mulx)+Bio

```

```

+      *sinh(mulx))*(mu(k)*cos(muy)+Bih*sin(muy))+ sumw1

```

```

else

```

```

sumw1 = 0.0

```

```

endif

```

```

sumw2 = BC(k)*(cosh(alphy)-zeta*sinh(alphy))*

```

```

+      (alph(k)*cos(alphx)+Bio*sin(alphx)) + sumw2

```

```

sumw3 = BC(k+nterm)*(alphl*cosh(alphy)+Bih

```

```

+      *sinh(alphy))*(alph(k)*cos(alphx)+Bio*

```

```

+      sin(alphx)) + sumw3

```

```

if(i.eq.1.or.i.eq.n)then
if(A(j).ne.0)then
  dTdx1 = A(k)/cosh(mul)*mul*(mul*sinh(mulx)+Bio*
+   cosh(mulx))*(mu(k)*cos(muy)+Bih*sin(muy))+ dTdx1
else
  dTdx1 = 0.0
endif

  dTdx2 = BC(k)*(cosh(alphy)-zeta*sinh(alphy))*
+   (-alph(k)*sin(alphx)+Bio*cos(alphx))*alph(k)
+   + dTdx2

  dTdx3 = BC(k+nterm)*(alphl*cosh(alphy)+Bih
+   *sinh(alphy))*(-alph(k)*sin(alphx)+Bio*
+   cos(alphx))*alph(k) + dTdx3
if(A(j).ne.0)then
  Q1 = A(k)/cosh(mul)*mul*(mul*sinh(mulx)+Bio*
+   cosh(mulx))*(sin(mu(k))-Bih/mu(k)*cos(mu(k))+
+   Bih/mu(k)) + Q1
else
  Q1 = 0.0
endif

  Q2 = BC(k)*Lstr*(sinh(alphl)-zeta*cosh(alphl)+zeta)*
+   (-alph(k)*sin(alphx)+Bio*cos(alphx))
+   + Q2

  Q3 = BC(k+nterm)*Lstr*(alphl*sinh(alphl)+Bih
+   *cosh(alphl) -Bih)*(-alph(k)*sin(alphx)+Bio*
+   cos(alphx)) + Q3
endif

if(j.eq.1.or.j.eq.m)then
if(A(j).ne.0)then
  dTdy1 = A(k)/cosh(mul)*(mul*cosh(mulx)+Bio*
+   sinh(mulx))*(-mu(k)*sin(muy)+Bih*cos(muy))*mu(k) + dTdy1
else
  dTdy1 = 0.0
endif

  dTdy2 = BC(k)*alphl*(sinh(alphy)-zeta*cosh(alphy))*
+   (alph(k)*cos(alphx)+Bio*sin(alphx)) + dTdy2

  dTdy3 = BC(k+nterm)*(alphl*sinh(alphy)+Bih
+   *cosh(alphy))*alphl*(alph(k)*cos(alphx)+Bio

```

```

+          *sin(alphx))  + dTdy3

```

```

endif

```

```

50      continue

```

```

Twall(i,j) = sumw1 + sumw2 + sumw3 + To

```

```

if(i.eq.1)then
dTdx0(j)= dTdx1+dTdx2+dTdx3
dTdx1=0.0
dTdx2=0.0
dTdx3=0.0
qx0 = Q1 + Q2 + Q3
Q1 = 0.0
Q2 = 0.0
Q3 = 0.0
endif

```

```

if(i.eq.n)then
dTdx1(j)= dTdx1+dTdx2+dTdx3
dTdx1=0.0
dTdx2=0.0
dTdx3=0.0
qx1 = Q1 + Q2 + Q3
Q1 = 0.0
Q2 = 0.0
Q3 = 0.0
endif

```

```

if(j.eq.1)then
dTdy0(i)=dTdy1+dTdy2+dTdy3
dTdy1=0.0
dTdy2=0.0
dTdy3=0.0
endif

```

```

if(j.eq.m)then
dTdy1(i)= dTdy1+dTdy2+dTdy3
dTdy1=0.0
dTdy2=0.0
dTdy3=0.0
endif

```

```

40      continue

```

```

30  continue

100  continue
    return
    end
*
*
*      date 3/05/92
*
*      SUBROUTINE TO GENERATE THE OUTPUT OF THE RUN
*
    subroutine output(deltax,deltay,size2,dTdx0,dTdx1,dTdy0,
+      dTdy1,Thot,Tcold,Twall,iwall,ifluid,ibound,
+      nder,p0x,p1x,p0y,p1y)
    implicit double precision(a-h,o-z)
    integer size2
    double precision Nc,Nh,len,Lstr
    common delta,len,Lstr,Nc,Nh,Bic,Bih,Bio,Bil,Tcin,Thin,To,Tl
    dimension dTdx0(size2),dTdx1(size2),dTdy0(size2),
+  dTdy1(size2),Thot(size2),Tcold(size2),Twall(size2,size2)

    n = nint(1/deltax) + 1
    m = nint(1/deltay) + 1
    k = m/5

    if(ifluid.eq.0) go to 100
*
*      WRITE OUT THE FLUID TEMPERATURES - IF IFLUID=1
*
*
    write(10,*)''
    write(10,*)''
    do 10 i=1,n
        x=(i-1)*deltax

        if(i.gt.1) go to 15
        write(10,*)' x*      Tc*      Th* '
15  write(10,'(f4.2,3x,2f15.8)')x,Tcold(i),
+      Thot(i)
        write(40,'(f4.2,3x,2f15.8)')x,(Tcold(i)-Tcin)/(Thin-Tcin),
+      (Thot(i)-Tcin)/(Thin-Tcin)
10  continue

    write(10,*)''
    write(10,*)''

```

```

100  continue

      if(iwall.eq.0)go to 200
*    WRITE OUT THE WALL TEMPERATURE - IF IWALL=1
*
      write(10,*)'Wall temperatutes '
      do 20 i=1,k
        y=(i-1)*deltay*5
        write(10,*)'                y*'
        write(10, '(a,5f12.3)')' x',y,y+deltay,y+2*deltay,y+3*deltay,
+ y+4*deltay

        do 25 ii=1,n
          x=(ii-1)*deltax
          write(10, '(1x,f5.2,5f12.7)')x,((Twall(ii,j+(k-1)*5)-Tcin)
+ /(Thin-Tcin),j=1,5)
          write(50, '(1x,f5.2,5f12.7)')x,((Twall(ii,j+(k-1)*5)-Tcin)
+ /(Thin-Tcin),j=1,5)
25    continue
      write(10,*)' '
20    continue
200  continue

*    PRINT THE DERIVATTIVES AT THE WALL ENDS. IF IDER=1

      if(ider.eq.0)go to 250

      write(10,*)' '
      write(10,*)'dTw/dx*(x*=0)'
      write(10,*)' '
      x=0.0
      write(10, '(1x,f4.2,3x,6f11.6)')x,(dTdx0(j),j=1,m)
      write(10,*)' '

      write(10,*)' '
      write(10,*)'dTw/dx*(x*=1) '
      write(10,*)' '
      x=(n-1)*deltax
      write(10, '(1x,f4.2,3x,6f11.6)')x,(dTdx1(j),j=1,m)
      write(10,*)' '

250  continue

      if(ibound.eq.0)go to 300
*
*
```



```

*   CHECK BOUNDRY CONDITIONS- IF IBOUND= 1 OR 2
*
*    $\frac{dT}{dx}(0,y^*) = Bi_o (Tw(0,y^*) - T_o)$ 
*    $-\frac{dT}{dx}(1,y^*) = Bi_L (Tw(1,y^*) - T_L)$ 
*    $-\frac{dT}{dy}(x^*,0) = Bi_h (Th(x^*) - Tw(x^*,0))$ 
*    $-\frac{dT}{dy}(x^*,1) = Bi_c (Tw(x^*,1) - T_c(x^*))$ 
*
dif1m = 0.0
dif2m = 0.0
dif3m = 0.0
dif4m = 0.0

if(ibound.eq.2)then
write(10,*)' '
write(10,*)' '
write(10,*)' Check of Boundry Conditions'
write(10,*)' In the Y-direction BCy0 - y*=0 BCy1 - y*=1'
write(10,*)' x*          BCy0          BCy1 '
endif

do 30 i=2,n-1
  x=(i-1)*deltax
  dif1 = -dTdy0(i)/(Thot(i)-Twall(i,1))
  dif2 = -dTdy1(i)/(Twall(i,m)-Tcold(i))
  if(abs(dif1-Bih).ge.abs(dif1m))then
    dif1m=dif1-Bih
    im1 = i
  endif
  if(abs(dif2-Bic).ge.abs(dif2m))then
    dif2m=dif2-Bic
    im2 = i
  endif
  if(ibound.eq.2)write(10,'(1x,f4.2,3x,2f18.9)')x,dif1,dif2
30 continue

if(ibound.eq.2)then
write(10,*)' '
write(10,*)' '
write(10,*)' In the X-direction BCx0 - x*=0 BCx1 - x*=1'
write(10,*)' y*          BCx0          BCx1 '
endif

do 40 j=2,m-1
  y=(j-1)*deltay
  dif1 = dTdx0(j)/(Twall(1,j)-To)
  dif2 = -dTdx1(j)/(Twall(n,j)-Tl)

```

```

    if(abs(dif1-Bio).ge.abs(dif3m))then
        dif3m=dif1-Bio
        jm3 = j
    endif
    if(abs(dif2-Bil).ge.abs(dif4m))then
        dif4m=dif2-Bil
        jm4 = j
    endif
    if(ibound.eq.2)write(10,'(1x,f4.2,3x,2f18.9)'y,dif1,dif2
40    continue

    p0y = dif1m/Bih
    p1y = dif2m/Bic
    p0x = dif3m/Bio
    p1x = dif4m/Bil

*    if(ibound.eq.1)then
*    write(10,*)' '
*    write(10,*)' '
*    write(10,*)'Max Errors in the boundry conditions and locations '
*    write(10,'(a,f5.2,f12.6)')x* = 0  y* = ',(jm3-1)*deltay,p0x
*    write(10,'(a,f5.2,f12.6)')x* = 1  y* = ',(jm4-1)*deltay,p1x
*    write(10,'(a,f5.2,f12.6)')y* = 0  x* = ',(im1-1)*deltax,p0y
*    write(10,'(a,f5.2,f12.6)')y* = 1  x* = ',(im2-1)*deltax,p1y
*    endif

300    continue
    return
end

```

MICHIGAN STATE UNIV. LIBRARIES



31293008975074